

## Durham E-Theses

---

*Sedimentology and geochemistry of the upper Triassic mercia mudstone group and marginal deposits, southwest Britain*

Alick Bruce Leslie

### How to cite:

---

Leslie, Alick Bruce (1989) Sedimentology and geochemistry of the upper Triassic mercia mudstone group and marginal deposits, southwest Britain. Doctoral thesis, Durham University.

### Use policy

---

The full-text may be used and/or reproduced, and given to third parties in any format or medium, without prior permission or charge, for personal research or study, educational, or not-for-profit purposes provided that:

- a full bibliographic reference is made to the original source
- a <https://etheses.durham.ac.uk/id/eprint/6747/> is made to the metadata record in Durham E-Theses
- the full-text is not changed in any way

The full-text must not be sold in any format or medium without the formal permission of the copyright holders.

Please consult the [full Durham E-Theses policy](#) for further details.

**Sedimentology and Geochemistry of the Upper Triassic  
Mercia Mudstone Group and Marginal Deposits,  
Southwest Britain**

Alick Bruce Leslie

A thesis submitted to the University of Durham for the degree of  
Doctor of Philosophy

The copyright of this thesis rests with the author.  
No quotation from it should be published without  
his prior written consent and information derived  
from it should be acknowledged.

Department of Geological Sciences

October, 1989



2 AUG 1990

## **Declaration**

The content of this thesis is the original work of the author and has not previously been submitted for a degree at this or any other university. Other people's work is acknowledged by reference.

Alick Bruce Leslie  
Department of Geological Sciences,  
University of Durham.

## **Copyright**

The copyright of this thesis rests with the author. No quotation from it should be published without his prior written consent, and information derived from it should be acknowledged.

## **Sedimentology and Geochemistry of the Upper Triassic Mercia Mudstone Group and Marginal Deposits, Southwest Britain.**

During the Upper Triassic red dolomitic mudstones of the Mercia Mudstone Group overlapped a folded and eroded Palaeozoic basement. In Southwest Britain deposition occurred in elongate basins whose orientations were controlled by an earlier rift valley system. In the basins, marginal coarse clastic deposits underlie and are laterally equivalent to the mudstones which contain horizons of sulphate and halite. At Sully Island in South Wales, a series of marginal lacustrine deposits formed within a small basin overlying alluvial and shoreline clastics. The marginal deposits comprise dolomites containing replaced evaporites and perilittoral freshwater limestones which are overlain by red mudstones of the Mercia Mudstone Group. The replaced evaporite nodules are composed of quartz and carbonate, some of which show textures characteristic of sabkha environments. The limestones are fenestral intrapelsparites which contain abundant calcrete horizons. Stromatolites are common in finely laminated beds and travertines are locally developed. At Dinas Powys, 3 kilometres to the north, stromatolites and travertines overly a fluvial conglomerate in a palaeovalley. The limestones and travertines are depleted in both oxygen and carbon isotopes, indicating formation in meteoric waters unaffected by evaporation. The stable isotopic composition of the replaced evaporites suggests replacement in meteoric waters. The dolomites do not appear to contain any primary geochemical signatures, although the enrichment in sodium in the dolomites may be an indication of variation in palaeosalinity between the two units. Changes in the hydrological environment can thus be inferred for the Sully Island sequence, with the limestones being deposited during resurgence of fresh/meteoric waters while the dolomites and marls formed in hypersaline waters more typical of the Mercia Mudstone Group.

The Mercia Mudstone Group deposits themselves were laid down in a distal playa-alluvial environment with periods of more permanent lacustrine conditions alternating with times of desiccation and calcretisation. The topmost 30 metres of the Mercia Mudstone Group consists of interbedded green dolomites and marls laid down in a less arid climate ( the Blue Anchor Formation ). Data from boreholes have allowed the subdivision of the Mercia Mudstone Group into six units on the basis of gamma-ray and sonic velocity logs. In this study a portable gamma-ray spectrometer was used to identify these unit boundaries at outcrop in Devon, Somerset and South Wales. There is no surface expression of these boundaries at outcrop but clay mineralogical and stable isotopic analyses were carried out in order to correlate changes in gamma-ray values with geochemical variations in the mudstones. The gamma-ray variations are the result of changes in clay mineralogy caused by the influx of marine-derived waters into the Upper Triassic basins which gave rise to a different suite of clay minerals. The clay mineralogy variations can be correlated with changes in stable isotopic composition of the carbonate component of the mudstones which is also indicative of changes in the chemistry of the depositional waters. Thus a subtle lithostratigraphic correlation of the upper Mercia Mudstone Group has been established which can be applied over a large area of southern Britain.

## Acknowledgements

Thanks are firstly due to my supervisor, Dr. Maurice Tucker for his constant help and numerous discussions during the past three years. Financial support was provided by NERC grant number GT/86/GS/27 . I am indebted to Mike Leeder ( University of Leeds ) and Colin North ( University of Bristol ) for advice on certain aspects of field work. Jonathon Henton ( University of Durham ) provided the statistical programme for the calculation of trace elemental values, and Ian Billing gave much help in the adaptation of the programme for the reduction of field gamma-ray data, for which many thanks. Stuart Arnott read the completed document and made many helpful comments.

Technical facilities were made available at the University of Durham, Department of Geological Sciences ( XRD, XRF, AAS, cathodoluminescence and NA ), Department of Engineering ( SEM ); University of Newcastle ( AAS ); Royal Holloway and Bedford New College ( ICP-AES ); Open University ( gamma-ray spectrometer ) and at the British Geological Survey Isotope Geology Section, London ( stable isotopes ).

Technical assistance was provided by Ron Hardy, Paul Laverick and Phil Leat ( University of Durham ); Pete Oakley ( University of Newcastle ); Alison Warren ( Royal Holloway and Bedford New College ); Jill Eyers and Geoff Brown ( Open University ) and Baruch Spiro and Pete Greenwood ( British Geological Survey ).

Thanks are also due to Ron Lambert and George Randall for the preparation of numerous thin sections; to Gerry Dresser and Alan Carr for photography; to Karen Gittins for draughting; to Dave Asbery for just about everything else and finally to Carole Blair and Jeanette Finn for secretarial work above and beyond...

Destruction of brain cells and other distractions were accomplished by the 'lads' in particular room-mates Ian, Neville, Abdul-Kader, Ian and Shafea. Advice on financial matters by Steve, Ken and Chris is much appreciated.

## FREEDOM COME-ALL-YE

Roch the wind in the claer day's dawin  
Blaws the clouds heelster-gowdie ow'r the bay,  
But there's mair nor a roch wind blawin  
Through the great glen o' the warld the day.  
It's a thocht that will gar oor rattans  
- A' they rogues that gang gallus, fresh and gay -  
Tak the road, and seek ither loanins  
For their ill ploys, tae sport and play.

Nae mair will the bonnie callants  
Maich tae war when oor braggarts crousley craw,  
Nor wee wains frae pit-heid and clachan  
Mourn the ships sailin' doon the Broomielaw.  
Broken faimlies in lands we've herriet  
Will curse Scotland the Brave nae mair, nae mair;  
Black and white, ane till ither mairriet,  
Mak the vile barracks o' their maisters bare.

So come all ye at hame wi' Freedom,  
Never heed what the hoodies croak for doom.  
In your hoose a' the bairns o' Adam  
Can find breid, barley-bree and painted room.  
When Maclean meets wi' his friens in Springburn,  
A' the roses and geans will turn tae bloom,  
And a boy frae yont Nyanga  
Dings the fell gallows o' the burghers doon.

Hamish Henderson

## Contents

## Contents

<b>Declaration &amp; Copyright</b>	ii
<b>Abstract</b>	iii
<b>Acknowledgements</b>	iv
<b>Contents</b>	vi
<b>Chapter 1 The Mercia Mudstone Group and Marginal Deposits in Southwest Britain: Introduction</b>	1
1.1 The Upper Triassic in Britain	1
1.2 Research Objectives	4
1.3 Thesis Outline	5
<b>Chapter 2 Upper Triassic Marginal Deposits, South Wales: Introduction</b>	7
2.1 Introduction	7
2.2 Previous Work	10
2.3 Marginal Deposits in South Wales	12
2.3.1 Introduction	12
2.3.2 Continental Marginal Deposits	12
2.3.3 Lacustrine Marginal Deposits	13
2.3.3a The Sully Island succession	14
2.3.3b Dinas Powys	18
2.4 Aims of the Present Study	19

<b>Chapter 3</b>	<b>Sedimentology of the Evaporitic Dolomite Unit, Sully Island</b>	20
3.1	Introduction	20
3.2	Sedimentology of the Evaporitic Dolomite Unit	20
3.2.1	The Basal Dolomite	20
3.2.2	The Main Evaporitic Dolomite Unit	27
3.2.3	The Nodular Dolomite Horizon	32
3.2.4	Evaporitic Dolomite Beds, Bendrick Rock	35
3.3	Replaced Sulphates	36
3.3.1	Introduction	36
3.3.2	Carbonate-replaced Nodules	36
3.3.2a	'Sabkha' Nodules	36
3.3.2b	Other Carbonate-replaced Nodules	41
3.3.3	Quartz-replaced Nodules	43
3.4	Conclusions	45
<b>Chapter 4</b>	<b>Sedimentology of the Lacustrine Limestones, South Wales</b>	51
4.1	Introduction	51
4.1.1	The Limestone Unit, Sully Island	51
4.1.2	The Limestones Exposed at Dinas Powys	56
4.1.3	Previous Work	56
4.2	Depositional Environment of the Limestones	56
4.2.1	Introduction	56
4.2.1a	Fenestral Intrasparites	57
4.2.1b	Laminated Limestones	61

4.3 Calcretes	68
4.3.1 Introduction	68
4.3.2 The Basal Calcrete	68
4.3.3 Nodular Calcretes	72
4.3.4 Blocky Calcrete	74
4.4 Microbial Laminated Carbonates	77
4.4.1 Introduction	77
4.4.2 Columnar Stromatolites and Oncoids	77
4.4.3 Laminar Stromatolites	79
4.4.4 Microbial Mounds	83
4.5 Travertine Deposits	83
4.5.1 Introduction	83
4.5.2 Flowstones	86
4.5.3 Minor Forms of Travertine	93
4.5.3a Travertine Pisoids	93
4.5.3b Flöe Calcite	95
4.5.3c Spherulitic Structures	97
4.6 Tepee-like Structures	100
4.6.1 Introduction	100
4.6.2 Tepees in the Laminated Limestones	102
4.6.3 Megapolygonal Structures	102
4.6.3a Tepee and Saucer Structures	102
4.6.3b Polygonal Fissures as Groundwater Conduits	104
4.7 Vadose Diagenesis of the Limestones	111
4.7.1 Introduction	111
4.7.2 Vadose Cavities in the Limestones	111
4.7.3 Vadose Diagenetic Sediments and Cements	115

4.7.4 Late Spar Cementation	119
4.8 Analogous Depositional Environments to the Sully Island Succession	123
4.8.1 Introduction	123
4.8.2 Australian Coastal Salinas	124
4.9 Conclusions	129
4.9.1 Sully Island	129
4.9.2 Dinas Powys	130
<b>Chapter 5 Geochemistry of the Sully Island and Dinas Powys Carbonates</b>	<b>131</b>
5.1 Introduction	131
5.1.1 Reasons for Geochemical Sampling	131
5.1.2 Sampling	131
5.1.3 Methods of Preparation	132
5.2 Stable Isotopic Analysis, Results	132
5.2.1 Introduction	132
5.2.2 Evaporitic Dolomite Unit, Sully Island	133
5.2.3 Limestone Unit, Sully Island and Dinas Powys	138
5.2.3a Introduction	138
5.2.3b Intraclastic Limestones, Sully Island	138
5.2.3c Travertine Deposits, Sully Island and Dinas Powys	142
5.3 Trace Elemental Analyses, Results	149
5.3.1 Introduction	149
5.3.2 Evaporitic Dolomite Unit	149
5.3.3 Limestone Unit, Sully Island and Dinas Powys	153
5.4 Conclusions	156

<b>Chapter 6</b>	<b>Marginal Lacustrine Deposits</b>	
	<b>in South Wales: Conclusions</b>	159
6.1	Introduction	159
6.2	The Evaporitic Dolomite Unit	159
6.3	The Limestone Unit, Sully Island and Dinas Powys	161
6.3.1	Sully Island	161
6.3.2	Dinas Powys	164
6.4	The Sully Island Sequence	165
6.5	Summary	166
<b>Chapter 7</b>	<b>Mercia Mudstone Group:</b>	
	<b>Introduction and Petrography</b>	167
7.1	Introduction	167
7.1.1	The Mercia Mudstone Group in Southwest Britain	167
7.1.2	Problems of Correlation of the Mercia Mudstone Group	169
7.1.3	Previous Work	171
7.1.4	Depositional Environment of the Mercia Mudstone Group	173
7.1.5	Aims of the Present Study	174
7.2	Petrography of the Upper Mercia Mudstone Group	175
7.2.1	General Petrography and Mineralogy	175
7.2.2	Dolomitic Beds	179
7.2.3	Shoreline Deposits	187
7.2.4	Calcretes	190
7.2.5	Aeolian Beds	192
7.3	Conclusions	196
<b>Chapter 8</b>	<b>Clay Mineralogy of the Mercia Mudstone Group</b>	198
8.1	Introduction	198

8.1.1 Uses of Clay Mineralogy	198
8.1.2 Sampling	198
8.1.3 Methods and Interpretation	200
8.1.4 Previous Work	208
8.2 Clay Mineralogy, This Study	212
8.2.1 Introduction	212
8.2.2 Clay Assemblages, South Devon	212
8.2.3 Clay Assemblages, North Somerset	216
8.2.4 Clay Assemblages, South Wales	219
8.2.5 Clay Assemblages, Blue Anchor Formation	221
8.3 Scanning Electron Microscopy	223
8.4 Conclusions	223
<b>Chapter 9 Gamma-Ray Spectrometry of the Mercia Mudstone Group</b>	226
9.1 Gamma-Ray Spectrometry, Introduction	226
9.1.1 Background	226
9.1.2 Field Methods	227
9.1.3 Gamma-Ray Sources	229
9.1.4 Gamma-Ray Correlation with Borehole Data	229
9.2 Gamma Ray Total Count Results	230
9.2.1 Introduction	230
9.2.2 Total Count Results, South Devon	232
9.2.3 Total Count Results, North Somerset	236
9.2.4 Total Count Results, South Wales	238
9.3 Gamma-Ray Elemental Analyses	240
9.3.1 Introduction	240

9.3.2 Correlation of Gamma-Ray Spectrometry Results	240
9.3.3 Potassium	242
9.3.4 Uranium / Thorium	246
9.4 Conclusions	249
<b>Chapter 10 Geochemistry of the Mercia Mudstone Group</b>	<b>251</b>
10.1 Introduction	251
10.1.1 Reasons for Analysis of the Carbonate	251
10.1.2 Sampling	251
10.1.3 Methods	252
10.2 Carbonate in the Mercia Mudstone Group	252
10.2.1 Origin of the Carbonate	252
10.2.2 Dolomite - Calcite Cogenesis	256
10.3 Stable Isotopic Analysis, Results	262
10.3.1 Introduction and Previous Work	262
10.3.2 Stable Isotopic Results, Devon	263
10.3.3 Stable Isotopic Results, Somerset	268
10.3.3a General Trends	268
10.3.3b Lithological Variations	271
10.3.4 Stable Isotopic Results, South Wales	273
10.3.5 Discussion	275
10.4 Trace Elemental Analysis, Results	277
10.4.1 Introduction and Previous Work	277
10.4.2 Trace Elemental Results, Devon	279
10.4.3 Trace Elemental Results, Somerset	283
10.4.4 Trace Elemental results, South Wales	283
10.4.5 Trace Elemental Correlations	288

10.5 Conclusions	291
<b>Chapter 11 The Mercia Mudstone Group in Southwest Britain: Conclusions</b>	295
11.1 Problems of the Mercia Mudstone Group	295
11.2 Clay Mineralogy	296
11.3 Gamma-Ray Correlations	298
11.4 Geochemical Variations	300
11.5 Conclusions	301
<b>Chapter 12 The Upper Triassic Mercia Mudstone Group in Southwest Britain: Conclusions</b>	303
12.1 The Sully Island Succession	303
12.2 Correlation of the Mercia Mudstone Group	305
12.3 The Depositional Environment in South Wales	306
<b>References</b>	308
<b>Appendices</b>	325

## **Chapter 1**

### **The Mercia Mudstone Group and Marginal Deposits in Southwest Britain: Introduction**

## Chapter 1

### The Mercia Mudstone Group and Marginal Deposits in Southwest Britain: Introduction

#### 1.1 The Upper Triassic in Britain

The Triassic rocks in the United Kingdom have been subdivided into a lower coarse clastic unit ( Sherwood Sandstone Group ) and an upper mudstone unit ( Mercia Mudstone Group ). Marginal to the Mercia Mudstone Group and occurring around the fringes of all of the Upper Triassic basins are coarse clastic beds which formed as fluvial / alluvial detritus surrounding basement highs ( Warrington et al., 1980 ). The Triassic beds were laid down in graben and half-graben structures ( Chadwick, 1985 ) in which the normal faulting appears to be the result of reactivation of deep-seated thrusts, possibly of Varsican age. In general, active faulting in the grabens was greatest in the early Permian and early Triassic, when the maximum crustal extension took place. In the later Triassic active faulting was of relatively low intensity and deposition took place in passively subsiding basins with consequent onlap of the basin margins ( Figs. 1.1, 1.2 ), ( Chadwick, 1985 ).

In this study Upper Triassic beds from the South West of Britain were examined along with their laterally equivalent marginal deposits. The beds studied lie entirely within the Norian and Rhaetian Stages. The Norian Mercia Mudstone Group consists of over 150 metres of red and green mudstones containing sulphate horizons but few sedimentary structures. In the more basinal areas containing the thickest successions halite horizons are present. Thick salt deposits were laid down in the Cheshire, Worcester, Somerset and Dorset Basins in Carnian times, before deposition of the beds covered by this study. During the Norian no extensive deposition of salt took place although scattered individual salt crystals do occur on bedding planes. Sulphate beds are relatively common in the Norian and Rhaetian mudstones.

In the Norian the mudstones onlapped a complex basement topography. There is



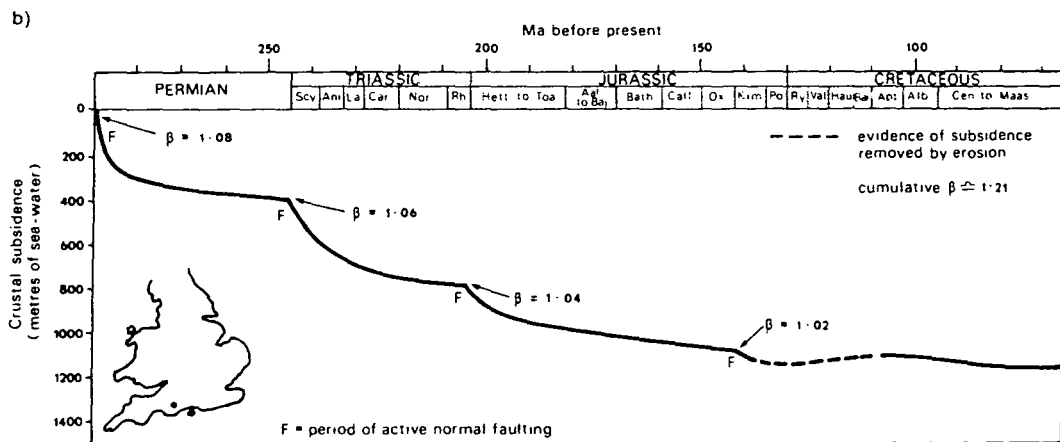
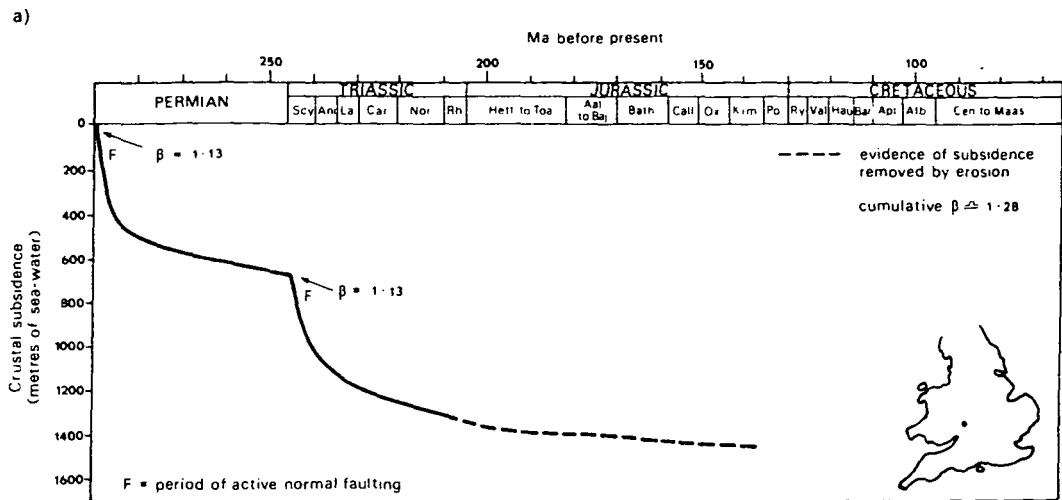


**Fig. 1.1** Crustal subsidence curves for the Permian to Triassic for a) Worcester Basin and b) Dorset / Devon Basins. Note the lack of subsidence in the Upper Triassic ( From Chadwick, 1985 ).

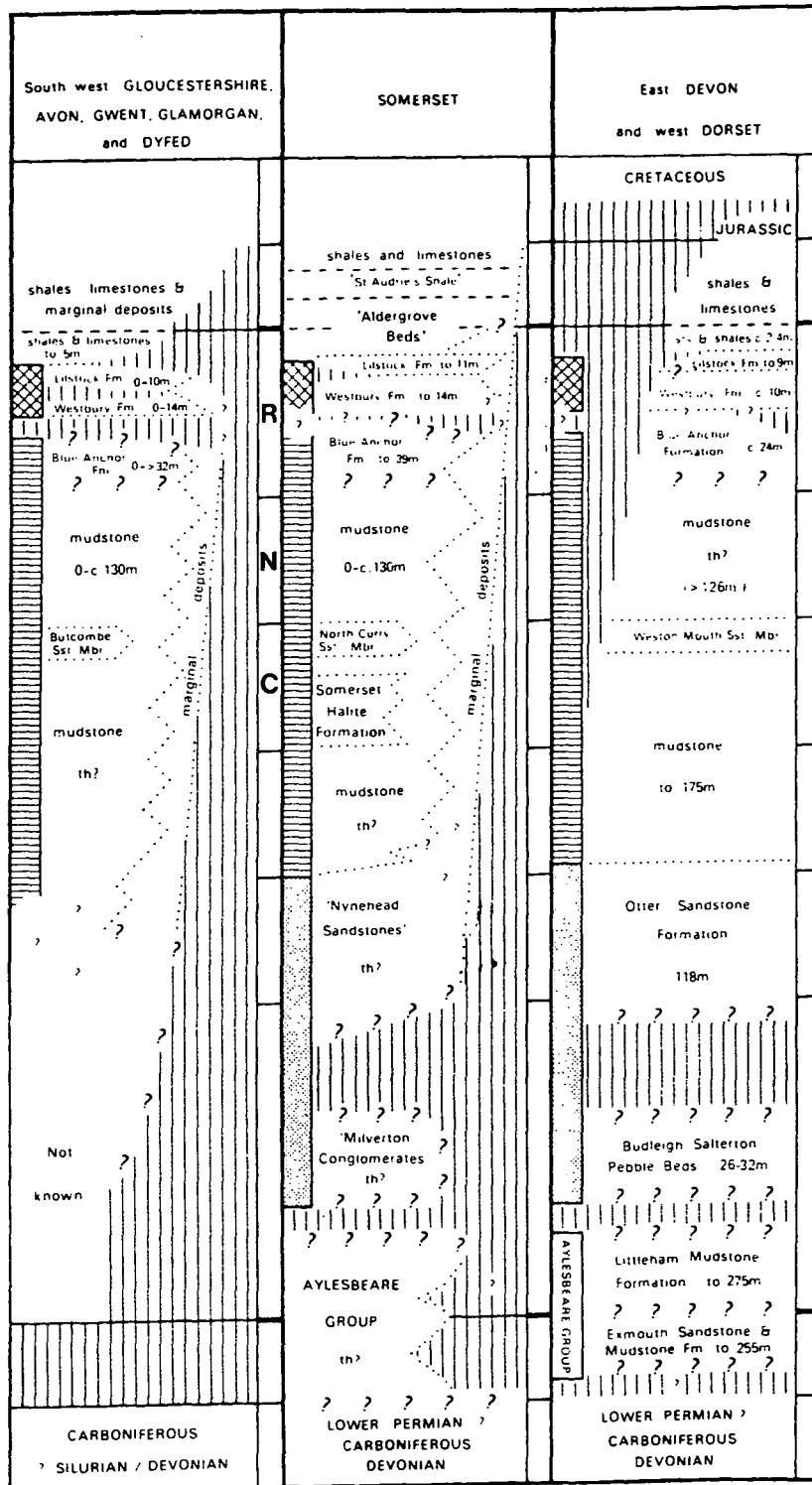


Fig. 1.2 Sketch logs for the Triassic of South West Britain. R - Rhaetian. N - Norian. C - Carnian. Cross-hatching - Penarth Group. Horizontal stripe - Mercia Mudstone Group. Stipple - Sherwood Sandstone Group. ( From Warrington et al., 1980 ).

evidence for the filling of river valleys or 'wadi' systems. The marginal deposits consist of coarse detritus derived from the surrounding basement and are of variable thickness. In South Wales the marginal deposits have been subdivided further into fluvial and marginal lacustrine subfacies.

## 1.2 Research Objectives

The main aims of this study are twofold and represent essentially two distinct but related sub-projects.

The first part of this project involved the study of the marginal lacustrine carbonates in South Wales. These rocks have been described by Tucker in several papers in the 1970's but detailed petrographic studies had not been undertaken. In view of the unique sedimentology of these beds and the rarity of equivalent depositional environments in the geological record, it was felt necessary to carry out a detailed petrographic and geochemical study. In total, 7 weeks field work were spent studying the marginal carbonates in South Wales.

The second part of the project was concerned with a petrographic and, more importantly, geochemical study of the mudstones and siltstones of the Mercia Mudstone Group in Southwest Britain. The Mercia Mudstone Group at outcrop is essentially undivided apart from the uppermost 30 metres which consist of green mudstones and dolomites ( Blue Anchor Formation ) and some sandstone beds of Carnian age ( Warrington et al., 1980 ). The red mudstones between the Blue Anchor Formation and the sandstones are indivisible at outcrop using normal field methods. In borehole records this series of mudstones has been subdivided on the basis of gamma-ray and sonic logs ( Lott et al., 1984 ). In this study a portable gamma-ray spectrometer was used to correlate outcrop sections with borehole records. The petrographic and geochemical data were then used to apply lithological constraints to the variations observed in the borehole data. Six weeks were spent studying the Mercia Mudstone Group deposits exposed in Devon, Somerset and South Wales. In view of the rarity of sedimentary structures, detailed logging was not carried out.

### 1.3 Thesis Outline

As has been stated, this thesis comprises two sections which are essentially separate pieces of research. Chapters 2-6 contain the study of the marginal lacustrine carbonates exposed in South Wales. Chapter 2 is an introduction to the study and includes a summary of the depositional environments in which the marginal deposits were laid down as well as a description of the palaeogeography of the South Wales area. Chapter 3 describes the sedimentology of the Evaporitic Dolomite Unit in Sully Island, South Wales, which consists of a unit of recrystallised dolomites containing some sedimentary structures and replaced sulphate nodules. Chapter 4 describes the petrography of the Limestone Unit which overlies the dolomites at Sully Island, and of a smaller outcrop which is exposed inland at Dinas Powys. In the limestones, preservation of sedimentary structures is very good and the depositional environment of the Limestone Unit is described in detail. The environment in which the limestones were laid down is compared to similar modern examples. Chapter 5 includes the results of the stable isotopic and trace elemental analyses of the marginal lacustrine deposits. Variations in the geochemical composition of the carbonates are related to changes in both depositional and diagenetic environments. Chapter 6 summarises the findings of the study of the marginal carbonates in Sully Island and Dinas Powys.

Chapters 7-11 deal with the research into the geochemical correlations of the mudstones of the Mercia Mudstone Group in Southwest Britain. Chapter 7 summarises the problems of correlation of a structureless mudstone sequence and describes the petrography of the mudstones which can be seen at outcrop. Chapter 8 gives a detailed description of the outcrops which were sampled. The clay mineralogy of the mudstones is described along with a discussion of the reasons for changes in the clay mineral assemblage. Chapter 9 provides a short summary of the principles of gamma-ray spectrometry and describes the changes in gamma-ray values seen in the sections of Mercia Mudstone Group examined. Correlation of the outcrop measurements with nearby borehole data is attempted along with a regional correlation of the Mercia Mudstone Group in Southwest Britain on the basis of gamma-ray variations. Chapter 10 summarises the geochemical ( stable isotopic and trace elemental ) analyses which were carried out on the carbonate in

the mudstones and relates geochemical variations with changes in gamma-ray intensity and clay mineralogy. Chapter 11 correlates the variations observed in the mudstones and attempts to fit these changes into a depositional and diagenetic framework.

The final chapter provides a brief summary of the conclusions of each section of the research and brings together the two sections to describe the depositional environment of the Upper Triassic Mercia Mudstone Group in the South Wales area.

## **Chapter 2**

### **Upper Triassic Marginal Deposits, South Wales: Introduction**

## Chapter 2

### Upper Triassic Marginal Deposits, South Wales: Introduction

#### 2.1 Introduction

In South Wales up to 110 metres of red mudstones of the Mercia Mudstone Group were laid down in the Upper Triassic ( Waters & Lawrence, 1987 ). The South Wales area is marginal to the main Triassic Bristol Channel and Somerset Basins and the Palaeozoic basement was only covered in Norian ( Upper Triassic ) times ( Fig. 2.1 ). The marginal deposits underlie and are laterally equivalent to the mudstones and are composed of red and yellow conglomerates and sandstones. In South Wales marginal deposits are exposed over a large area surrounding Cardiff ( Fig. 2.2 ). The maximum thickness of mudstones is in the Cardiff area where an embayment of the Upper Triassic shoreline was present. In the area to the south and west of Cardiff, alluvial and fluvial clastic sediments are exposed, overlain and laterally equivalent to mudstones.

In the Upper Triassic the marginal deposits onlapped the Palaeozoic basement. Basement topography in the South Wales area was complex and at present several palaeohills of Carboniferous Limestone are flanked by a thin cover of conglomerates and sandstones, which are themselves overlain by mudstones ( Fig. 2.2 ). There is no evidence for any major fault activity in the Upper Triassic. Topographic relief appears to have been formed in Permian and Lower Triassic times, after which the basement was passively onlapped as can be seen in coastal exposures between Barry and Sully Island south of Cardiff. The marginal deposits are the products of ephemeral streams which drained the upland areas to the north and west of Cardiff. North of Cardiff, there is evidence for the existence of large alluvial canyons whose rivers drained the South West Coalfield uplands ( Fig. 2.3 ). These marginal deposits pass laterally into the red mudstones which formed in distal playa-alluvial depositional environment. There is evidence in the South Wales area in particular to suggest that the Mercia Mudstone Group formed in a relatively permanent lake ( Tucker, 1977 ). Although evidence for the presence of a lacustrine shoreline is present in several exposures west of Cardiff

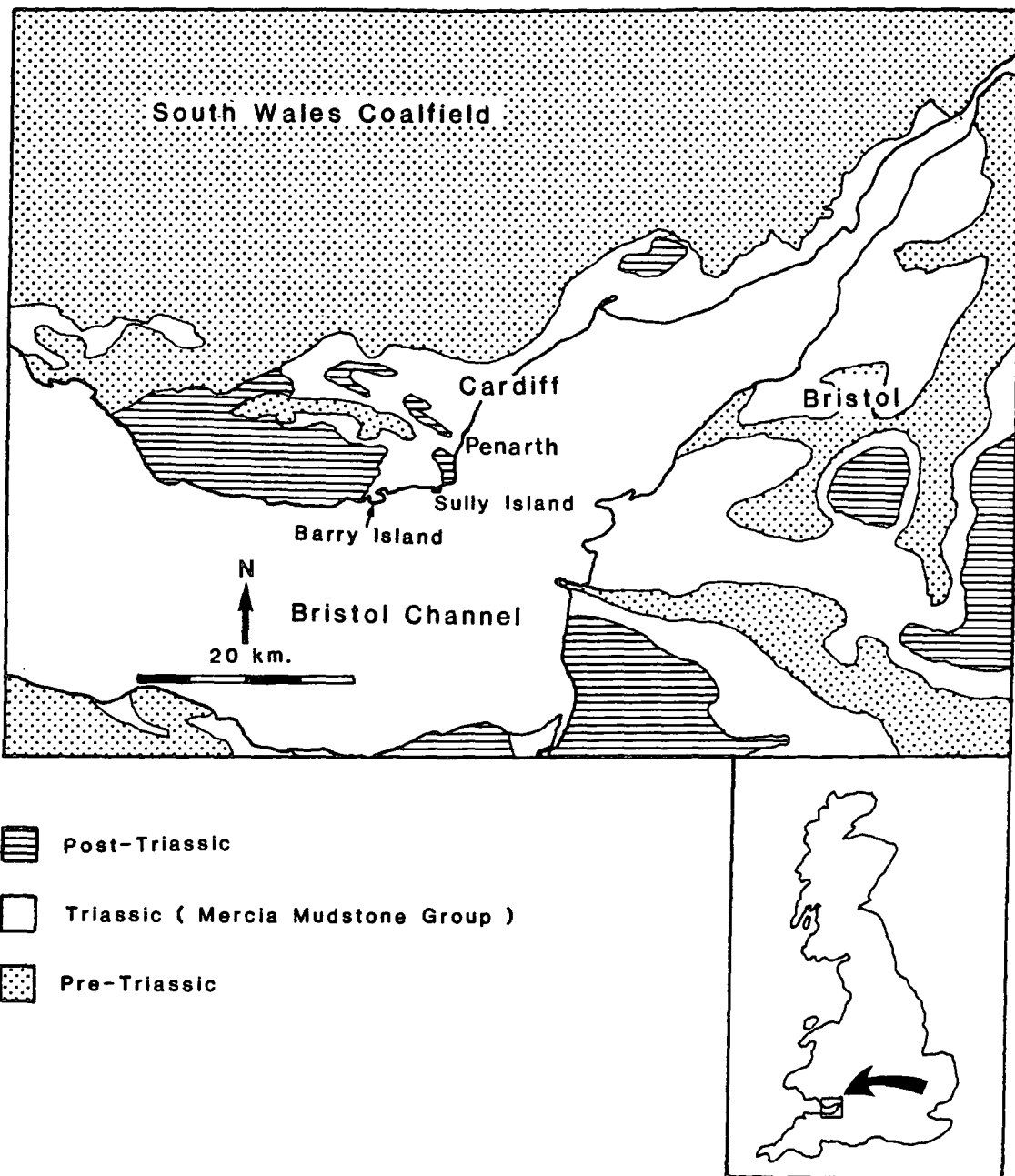
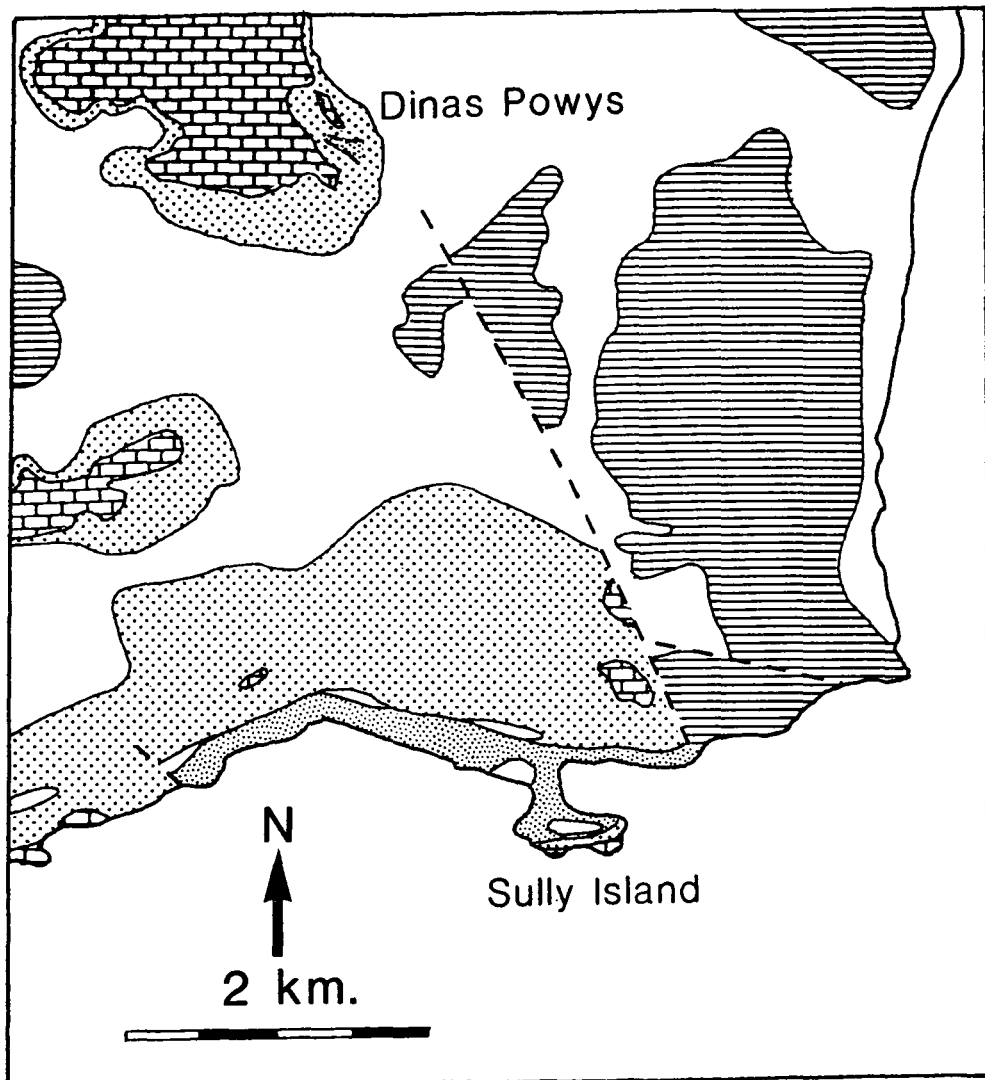


**Fig. 2.1** Summary geological map of South Wales and adjacent areas. The Palaeozoic basement is overlain by marginal deposits and mudstones of the Mercia Mudstone Group which is partly obscured by Jurassic cover. The inset gives the location of the main map.








-  Rhaetian and Post-Triassic
-  Mercia Mudstone Group
-  Lacustrine Marginal Deposits
-  Continental Marginal Deposits
-  Pre-Triassic ( Carboniferous Limestone )

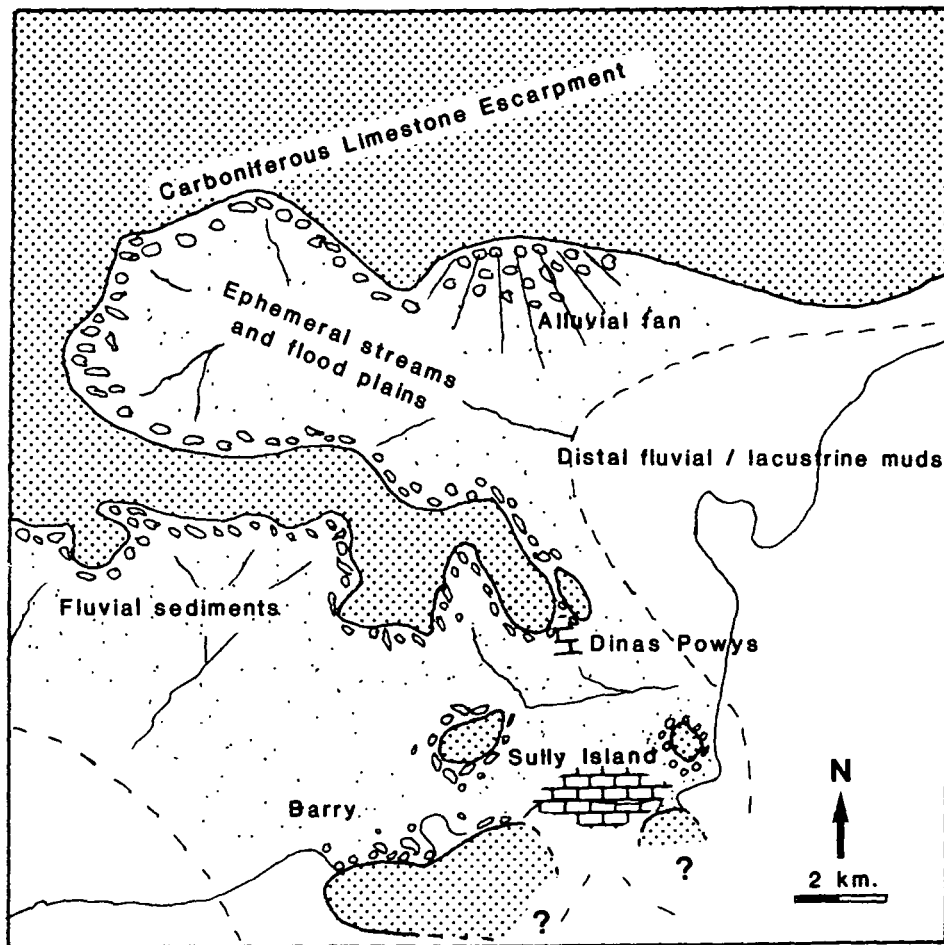
Fig. 2.2 Geological map of the area of South Wales around Sully Island and Dinas Powys.




( Waters & Lawrence, 1987 ), the transition between coarse clastic beds and the more distal mudstones through shoreline carbonates is best seen in the Sully Island area 9 kilometres south of Cardiff. In this section up to 16 metres of evaporitic dolomites and limestones are exposed which are laterally equivalent to mudstones in the Bristol Channel Basin to the south. The limestones at Sully Island and a similar outcrop at Dinas Powys, 6 kilometres to the north are the only such marginal lacustrine deposits exposed in the British Triassic.

The Sully Island succession lies in the topmost 50 metres of the red mudstones below the Blue Anchor Formation. Since only 30 metres of red mudstones are exposed in cliff sections at Penarth and Barry ( Fig. 2.1 ), the Sully Island succession may not be the lateral equivalent of any outcropping mudstones. The lateral extent of the limestones at Sully Island is not known, although there is no evidence for a similar sequence of rock types in any boreholes. The number of outliers of Carboniferous Limestone around the Sully Island area suggests that the limestones were not extensive. The exposure of limestone at Dinas Powys represents a more localised depositional environment. The limestones crop out between two outliers of Carboniferous Limestone and was laid down in a steep-sided palaeovalley.

## **2.2 Previous Work**

The Mercia Mudstone Group and marginal deposits of South Wales have been described by several authors, most of whom have incorporated the area into larger studies of the Upper Triassic in Southern Britain ( Audley-Charles, 1970b; Warrington et al., 1980; Taylor, 1983 ). Relatively little has been published on the South Wales area itself or on the Sully Island deposits in particular. The Memoir of the Geological Society covering the area ( Strahan & Cantrill, 1912 ) has recently been rewritten by Waters & Lawrence ( 1987 ). The Mercia Mudstone Group in South Wales and other areas was described by Klein ( 1962 ) who provided a list of sedimentary structures in the mudstones and in the Sully Island limestones. The Mercia Mudstone Group distribution offshore in the Bristol Channel has been described by Banner et al. ( 1971 ) and Lloyd et al. ( 1973 ). Triassic marginal deposits have been covered by Thomas ( 1952, 1968 ), who



-  Upper Triassic Lacustrine Limestones
-  Palaeozoic Basement
-  Palaeoshoreline

**Fig. 2.3** Sketch map of the Upper Triassic palaeogeography of the area around Cardiff showing the embayment of the palaeoshoreline in the Sully Island area. ( Adapted from Tucker, 1978 ).

described a number of cave fills and conglomerates in the area to the west of Cardiff; and by Bluck ( 1965 ), who described in detail individual alluvial fans at Ogmere, 20 kilometres west of Cardiff.

In a series of papers Tucker and others have described both the clastic marginal deposits around Cardiff ( Tucker, 1974, 1977; Tucker & Burchette, 1977 ) and the sequence of dolomites and limestones exposed at Sully Island and Dinas Powys ( Tucker, 1975, 1978; Tucker & Leslie, in press ). These papers formed the background to this part of the project and contain much of the basic interpretations which are expanded in this first part of the thesis.

## **2.3 Marginal Deposits in South Wales**

### **2.3.1 Introduction**

The marginal deposits in the South Wales area around Cardiff consist of up to 35 metres of coarse clastics with rare finer interbeds ( Tucker, 1977 ). The marginal deposits have been subdivided into continental and lacustrine shore-zone subfacies by Waters & Lawrence ( 1987 ). The lacustrine shore-zone deposits were of most interest in this study. The continental subfacies deposits will be described briefly.

### **2.3.2 Continental Marginal Deposits**

The continental subfacies rocks of the marginal deposits are overlain and laterally equivalent to the mudstones of the Mercia Mudstone Group and consist of conglomerates and sandstones with local fine intercalations. These beds are termed clastic and are thus distinguished from the dolomites and limestones in the Sully Island area. In fact much of the clastic material is derived from the Carboniferous Limestone and is itself carbonate.

The coarse clastic marginal deposits consist of well sorted and cross bedded fluvial conglomerates and sandstones with some marginal siltstones. These are the result of ephemeral streams whose deposits flank the outliers of Carboniferous Limestone exposed in the area ( Fig. 2.3 ). Sheet flood deposits are also common

( Tucker, 1977 ), and in areas of greatest topographic relief, poorly sorted scree are developed. It is likely that to the northwest of Cardiff the ephemeral streams were part of a larger drainage system whose watershed took in part of the South Wales Coalfield upland. The presence of large alluvial fans draining the upland area has been postulated by Tucker ( 1977 ). This fan passes eastwards and interdigitates with red mudstones. There is no evidence for the presence of shore-zone carbonates ( Waters & Lawrence, 1987 ). Stream and sheet flood deposits also interdigitate with red mudstones in the coastal exposures at Bendrick Rock, 3 kilometres west of Sully Island. The distribution of the continental marginal deposits is thus controlled by the basement topography at the time of deposition. Large alluvial fans coming off the high land to the north drained into an area of ephemeral streams which grades into the evaporitic mudstones of the Mercia Mudstone Group ( Fig. 2.3 ).

### **2.3.3 Lacustrine Marginal Deposits**

Lacustrine shore-zone deposits are exposed over a wide area west and south of Cardiff, and can themselves be subdivided into clastic and carbonate types. The majority of the beds ascribed to the lacustrine shore-zone subfacies by Waters & Lawrence ( 1987 ) consist of clastic sediments which have been reworked at a lake shoreline, becoming better sorted and containing laminar fenestrae. The beds which are of interest in this study are the marginal lacustrine limestones and associated evaporitic beds exposed at Sully Island and Dinas Powys ( Fig. 2.2 ). These beds contain abundant sedimentary structures which indicate carbonate precipitation as opposed to the reworked carbonate clastic shoreline deposits. The only other bed of interest to this study is exposed at Tinkinswood, 9 kilometres north west of Sully Island where a bed of pisoids up to 20 centimetres in thickness is interbedded with coarse breccias and sandstones. The pisoids are a reworked deposit and were probably formed in a fluvial depositional environment in which carbonate was being precipitated from saturated waters. The limestones exposed at Dinas Powys represent an analogous environment of deposition to that in which the pisoliths at Tinkinswood were formed. Other than this one bed, marginal lacustrine limestones are only exposed in the area around Sully Island and at Dinas Powys.

### 2.3.3a The Sully Island Succession

The area of limestones exposed around Sully Island extends from Ball Rock ( ST17456749 ) in the east to Hayes Point ( ST14086728 ) in the west ( Fig. 2.4 ). At Hayes Point the limestones are predominantly clastic in nature, with conglomerates interbedded with finer limestones. Coarse beds become less common to the east and at the centre of Sully Bay ( ST15006780 ) there are no coarse clastic beds within the limestones. The limestones at Ball Rock are cut by the St. Mary's Well Bay Fault which downthrows to the east ( Fig. 2.4 ).

The limestones are exposed in two ways. From Hayes Point to Swanbridge and on the northwest side of Sully Island, the limestone is exposed in a continuous wave-cut platform 200 metres in width. In practise the higher 100 metres of limestone provide good outcrop. This wave-cut platform is roughly parallel to bedding along most of its length and exposes part of the upper limestone unit. The overlying evaporitic mudstones and siltstones of the Mercia Mudstone Group are exposed in discontinuous low cliffs above the platform. On the south and east sides of Sully Island, and from Swanbridge to Ball Rock, the limestones and surrounding beds are exposed in cliff sections. The best section through the limestones and underlying dolomites is exposed at the southeast corner of Sully Island ( ST16916686 ), ( Figs. 2.5, 2.6 ). The Carboniferous Limestone basement is exposed on both the southeast and southwest corners of Sully Island. On the southwest corner the contact with the overlying Triassic rocks lies in the intertidal zone whilst in the southeast corner the nature of the unconformity can be more clearly seen ( Fig. 2.5 ). The Carboniferous Limestone itself ( Friars Point Limestone ) dips at approximately 50 degrees to the east. On the southeast corner of Sully Island it has been eroded into a planar surface which dips at between 5 and 10 degrees to the northwest relative to the overlying Triassic beds which have been slightly folded.

The Carboniferous Limestone is overlain by a wedge of clastic sedimentary rocks which belong to the clastic shore-zone subfacies ( Tucker, 1978 ). This wedge thins to the southeast and on the corner of Sully Island the clastic beds are not present. The wedge thickens and becomes finer rapidly to the west and 3 to 4 metres of clastic beds overlie the basement on the southwest corner of Sully

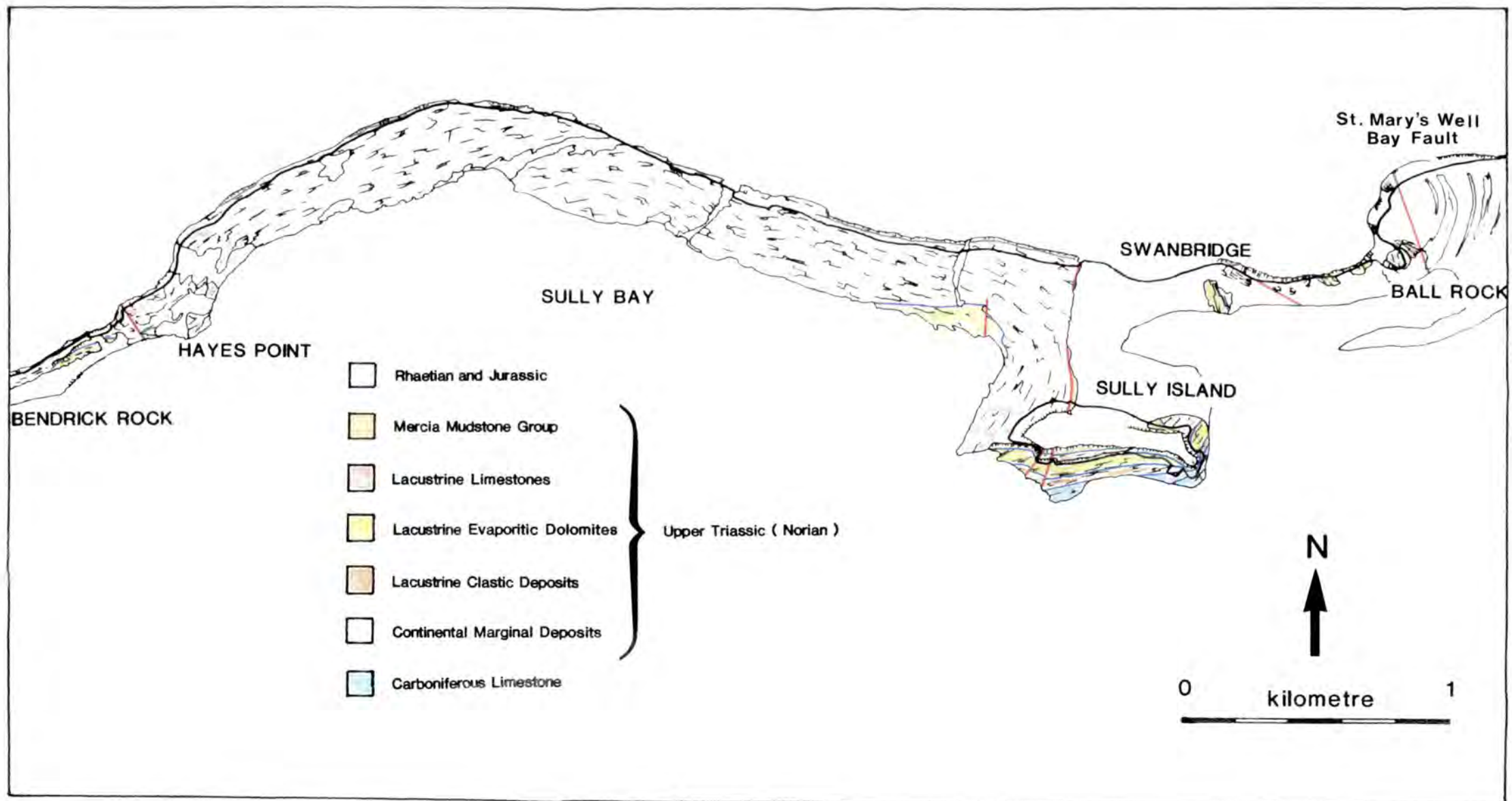


Fig. 2.4 Geological map of the Sully Island area.

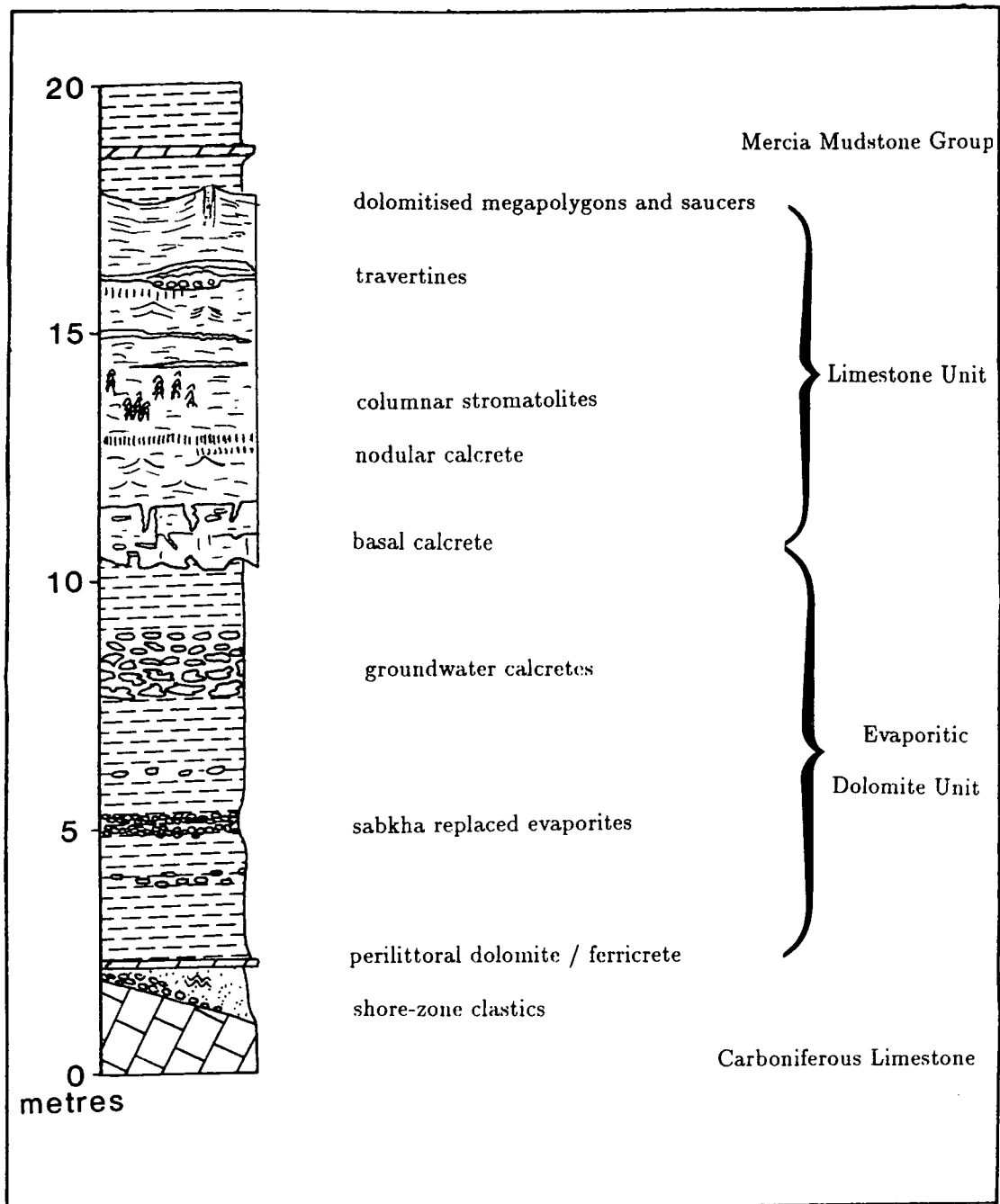


Fig. 2.6 Sketch log of the succession of marginal lacustrine deposits on Sully Island.



**Fig. 2.5** The succession on the south-east corner of Sully Island. A plained-off surface of Carboniferous Limestone ( A ) is overlain by beach-type clastics and 8 metres of dolomites containing replaced sulphate nodules and calcretes. The red dolomites are overlain by white and yellow limestones ( B ) in the topmost part of the cliff. The upper part of the Limestone Unit is not shown.



**Fig. 2.7** Outcrop of stromatolitic limestones and travertines at Dinas Powys. Length of hammer 40 centimetres. The limestones overlie a fluvial conglomerate.

Island. The thin end of the wedge is composed of well sorted angular breccias of Carboniferous Limestone clasts ( Tucker, 1978 ). These are the result of wave-sorting of beach gravels at the shoreline of the Upper Triassic lake during a time when there was a relatively permanent water body in the South Wales area. Further evidence for the presence of this water body is presented in Chapters 7 to 11 in the second part of this thesis. The beach gravels grade rapidly ( in 10 metres ) into rippled and laminated red sandstones and siltstones in the thickest part of the clastic wedge. These beds formed in shallow sublittoral conditions and contain local graded storm beds ( Tucker, 1978 ).

The clastic wedge is overlain by a thin fenestral dolomite which on the southeast corner of Sully Island rests directly on the Carboniferous Limestone basement. This bed marks the lower horizon of the limestone and dolomite sequence which is described in detail in the following four chapters. Up to 10 metres of evaporitic dolomites are exposed in the area around Sully Island. This unit underlies the limestones and is thus only exposed in the cliff sections on Sully Island and in the area east of Swanbridge ( Fig. 2.4 ). The dolomite unit is predominantly composed of red dolomitic micropar and contains a number of nodular beds in which quartz and carbonate have replaced the original sulphate. The limestones are up to 8 metres in thickness and have been partially dolomitised. The limestones are composed of intraclasts of Carboniferous Limestone and peloids and contain calcretes, stromatolites and locally travertine ( spring ) deposits. The topmost surface of the limestones has been deformed into a series of tepee and saucer structures up to 5 metres in diameter ( Fig. 2.6 ). The limestones are overlain by red dolomitic siltstones and mudstones with some massive yellow dolomitic beds. These are more typical of the deposits of the Upper Triassic and represent the onlap of the Sully Island area by the hypersaline mudstones of the Bristol Channel Basin.

### **2.3.3b Dinas Powys**

Although there are a number of exposures of clastic shoreline deposits in the Dinas Powys area, limestones crop out in one small roadside exposure in the centre of Dinas Powys itself ( ST15357133 ), ( Fig. 2.7 ). In this exposure a

fluvial conglomerate is overlain by 1.5 metres of stromatolitic and laminated fine limestones containing abundant travertine deposits.

#### **2.4 Aims of the Present Study**

In the South Wales area the marginal fluvial and clastic shoreline deposits have been adequately described in the literature. The main area of interest in this study was the sequence of dolomites and limestones in the Sully Island area which has not been described in the literature and which is unique in the British Triassic. The main aims of this part of the project are set out as follows:

- 1) To describe the sedimentology of the Evaporitic Dolomite Unit which underlies the limestones in the Sully Island area and to define the depositional environment in which the beds formed.
- 2) To define the depositional or diagenetic environment in which the nodules within the dolomites formed and to describe the sequence of replacements which have taken place.
- 3) To describe in detail the sedimentology of the limestones at Sully Island and Dinas Powys, in particular the travertine deposits and related structures.
- 4) To describe the geochemistry of the dolomite and limestone units in Sully Island in terms of changes in the hydrological environment.
- 5) To derive an overall depositional environment for the Sully Island succession and to incorporate the Sully Island and Dinas Powys areas into a general palaeoenvironmental model for the Upper Triassic of South Wales.

## **Chapter 3**

### **Sedimentology of the Evaporitic Dolomitic Unit, Sully Island**

## Chapter 3

### Sedimentology of the Evaporitic Dolomite Unit, Sully Island

#### 3.1 Introduction

Horizons of nodular sulphate are common within the Upper Triassic Mercia Mudstone Group. The Evaporitic Dolomite Unit exposed on Sully Island, however, differs in several respects from the majority of sulphates present in the red mudstones. The dolomite unit is exposed in the cliff sections on the south side of Sully Island and east of Swanbridge. The unit varies in thickness between 9.2 and 6.0 metres and is thickest on the southeast corner of Sully Island. Over much of the area of exposure the lower part of the unit is covered by fallen blocks on the foreshore. A complete log of the unit was made in three places: opposite Ball Rock ( Fig. 3.1 ) and at the southeast and southwest corners of Sully Island ( Fig.3.2 ). In all the sections the sequence of nodular horizons is basically similar. The following descriptions are mostly taken from the section in the southeast corner of Sully Island where the unit is thickest.

The majority of the unit is composed of structureless red sandy or silty dolomite ( Fig. 3.1 ). Although sedimentary structures are rarely preserved, the structures which can be seen within the dolomite and in the replaced sulphate nodules suggest that the replaced evaporites on Sully Island formed in a marginal lacustrine depositional environment.

#### 3.2 Sedimentology of the Evaporitic Dolomite Unit

##### 3.2.1 The Basal Dolomite

The Basal Dolomite forms a convenient marker bed between the shoreline clastic deposits and the overlying dolomites. It is best exposed on the southeast corner of Sully Island and can be followed westwards along the southern shore where it forms a prominent bed on the wave-cut platform due to its resistance to erosion.



**Fig. 3.1** The Evaporitic Dolomitic Unit, Swanbridge Cliffs opposite Ball Rock. The unit is here 5.7 metres in thickness. A - basal iron-rich calcrete. B - 'sabkha' band of replaced sulphate nodules. C - base of groundwater calcretes. D - top of Evaporitic Dolomitic Unit.

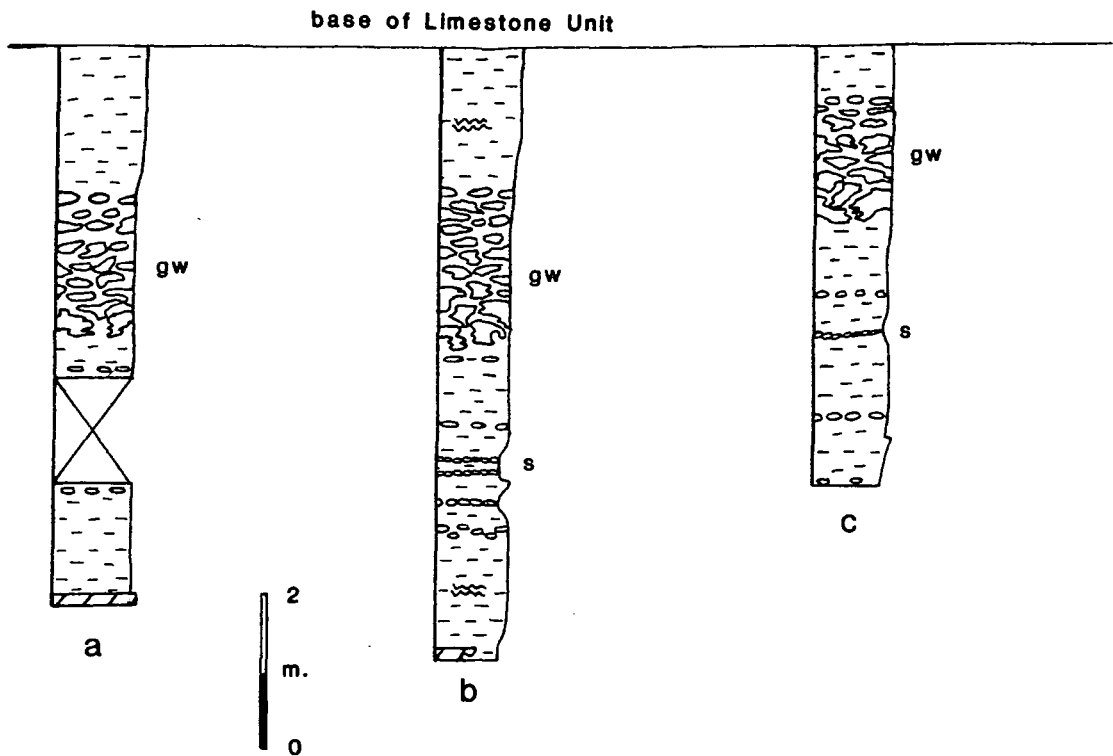


**Fig. 3.2** Sketch log of the Evaporitic Dolomite Unit in a) South West Sully Island, b) South East Sully Island, c) the cliffs opposite Ball Rock. In Section c the basal dolomite has been completely replaced by ferricrete. In sections a and b the topmost 1 metre of the unit has been recrystallised to a coarse array of rhombic dolomite. s - sabkha nodular bands. gw - groundwater calcrete.

On the southwest of Sully Island the dolomite separates fine dolomitic clastic deposits from very similar beds in the Evaporitic Dolomitic Unit. As such it is an arbitrary boundary within a sequence of beds laid down in a similar depositional environment.

Along the south side of Sully Island the bed is 20 centimetres in thickness although the base of the bed becomes very irregular to the east. The bed is best developed in the west of Sully Island where it is yellow in colour and has a crystalline form. The base of the bed is gradational into the red dolomitic marl of the distal shoreline clastic deposits while the top forms a sharp contact with the overlying dolomites. The bed contains laminar fenestrae and is itself poorly laminated. The dolomite is composed of an array of zoned rhombic crystals up to 300  $\mu m$  in length. The fenestrae are filled with partially dolomitised calcite spar. There is a patchy red colouration. The rhombs consist of a central, yellow inclusion rich zone and a clear outer rim. The inclusions are in places oriented parallel to the rhomb faces. Dolomitisation has obliterated all detailed sedimentary structures and only the lamination and fenestral fabric are present.

Towards the eastern end of Sully Island the character of the bed changes markedly. The rhombic dolomite is more ferroan and haematite cement becomes common and is patchily abundant. Parts of the bed have been dissolved and fractured. The vuggy cavities are filled by ferroan calcite spar ( Fig. 3.4 ). Farther to the east the rhombic dolomite is replaced by a haematite-rich, clastic form more akin to the underlying clastic sediments than the well crystallised bed to the west ( Fig. 3.4 ). In the dolomite the iron staining is more pronounced than in the surrounding red beds. On the southeast corner of Sully Island the dolomitic bed lies directly on the Carboniferous Limestone basement. In the cliffs east of Swanbridge and opposite Ball Rock the bed contains some irregular quartz nodules and is distinguished by the greater amount of iron staining rather than the crystalline nature of the dolomite.

There is thus a distinctive change in the form of the bed which is clearly seen on the south side of Sully Island. The array of intergrown dolomite rhombs is progressively replaced by a haematite rich bed in which the dolomite is more clastic in form and contains abundant quartz clasts. In thin section the dolomite appears

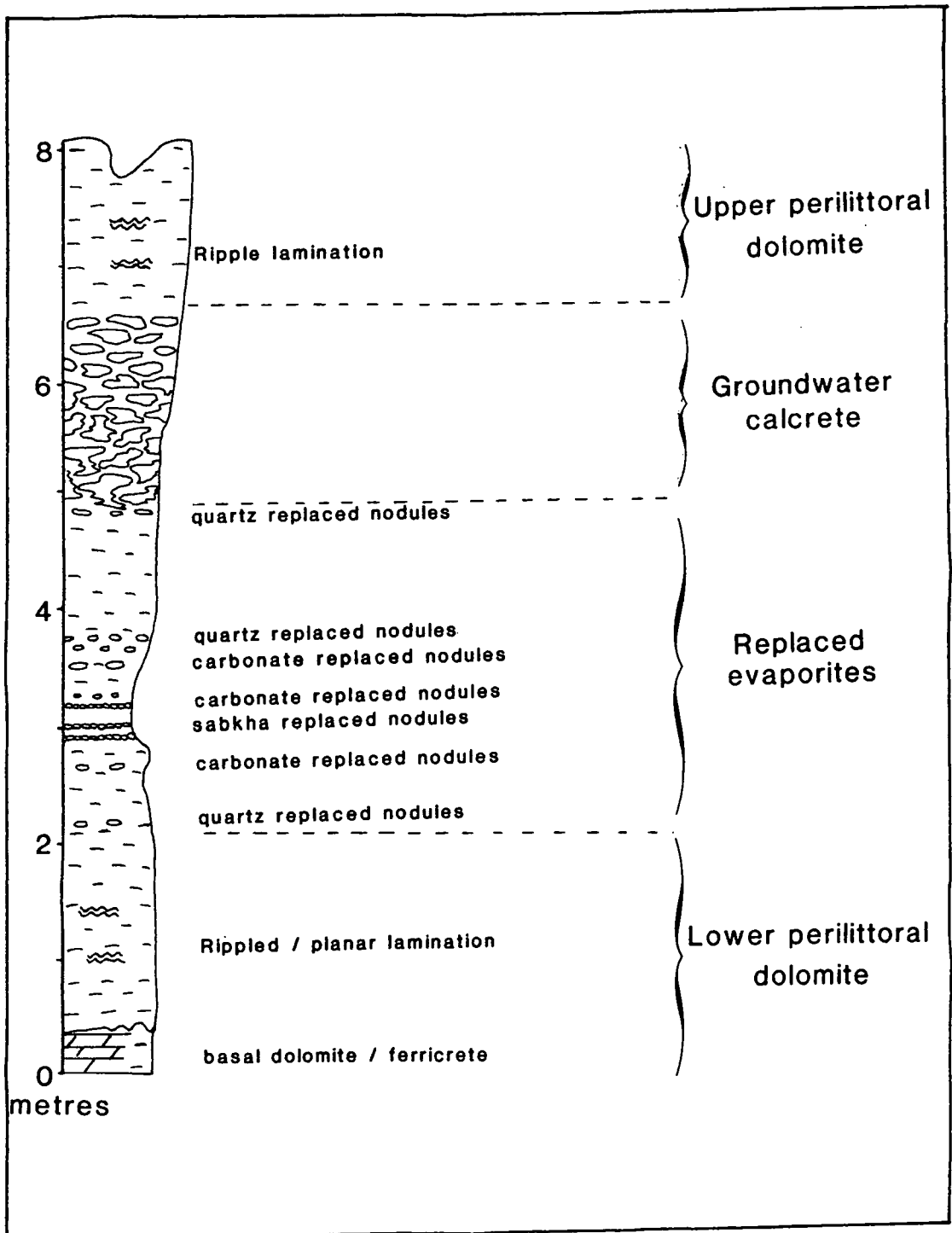


**Fig. 3.3** Log of the Evaporitic Dolomite Unit at the South East corner of Sully Island.

to have replaced a calcitic precursor and is itself replaced by a haematite rich sediment which contains irregular laminae or stringers composed of haematite with a residue of quartz grains ( Fig. 3.5 ). Individual dolomite rhombs appear to have been corroded around the areas of haematite.

The relict laminae and the fenestral fabric in the dolomite indicates that the bed was formed in a perilittoral environment. Dolomitisation has obscured any evidence for the nature of the original carbonate although by analogy with other beds in the Sully Island succession the lamination might be of microbial origin. The bed was subject to progressively more exposure to the east where partial dissolution of the bed took place. The cavities in the bed are filled by a haematite rich sandy dolomite. On the southeast corner of Sully Island the rhombic dolomite has been entirely replaced by the haematite-rich sediment. This haematite-rich bed can be followed from Sully Island to the cliff section opposite Ball Rock where it serves to separate the clastic beds from the similar overlying Evaporitic Dolomitic Unit.

The dolomite bed has been interpreted as the result of the removal of relief at the lake shoreline and the formation of a perilittoral mud-flat environment ( Tucker, 1978 ), during which the fenestral dolomites formed. The dissolution and replacement of the fenestral bed by the haematite-rich dolomite is indicative of exposure and some pedogenesis at the lake shoreline. This bed has been termed a ferricrete by Tucker ( 1978 ). The fact that the fenestral dolomite has only been partially replaced is an indication that there was some relief at the margin of the lake and that the shoreline had not regressed a great distance. The presence of a ferricrete resting on the Carboniferous Limestone and of haematite rich material filling fractures in the basement on Sully Island suggests that only the more proximal areas of dolomite, to the east of the area, were exposed.

The dolomite bed serves as a useful boundary between the deposition of clastic material and the establishment of a more marginal perilittoral environment. The palaeogeography of the Sully Island area relative to deposition of the the South Wales Mercia Mudstone Group will be discussed further in Chapter 6 .

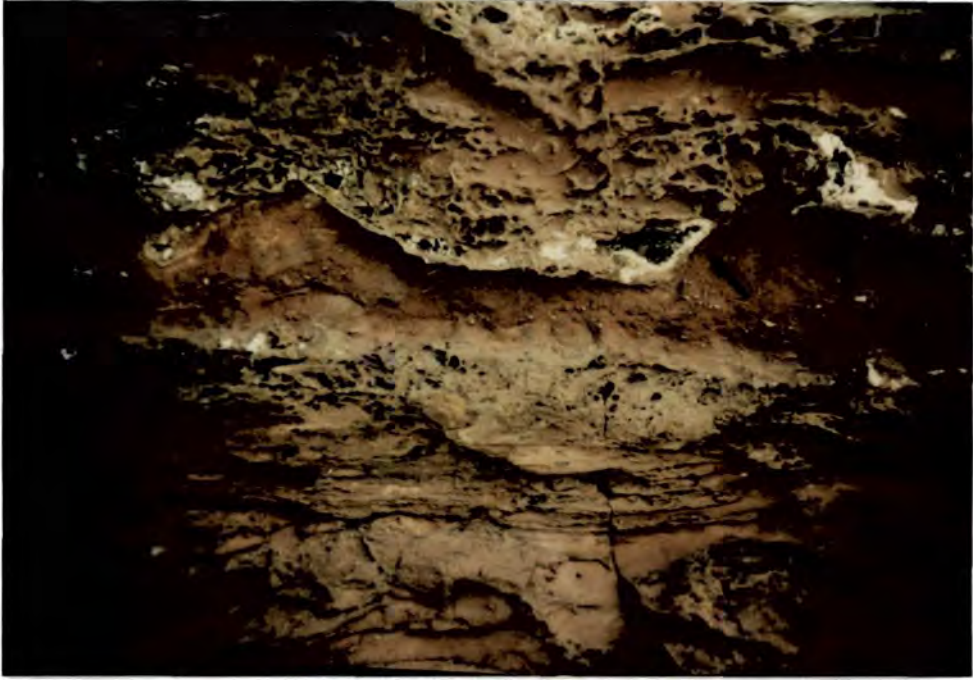


**Fig. 3.4** Iron-rich calcrite ( ferricrete ) at the base of the Evaporitic Dolomitic Unit. Fenestral dolomite has been completely replaced by haematitic dolomite containing vugs of calcite spar. (arrowed)  
Field of view 1.2 metres in width.

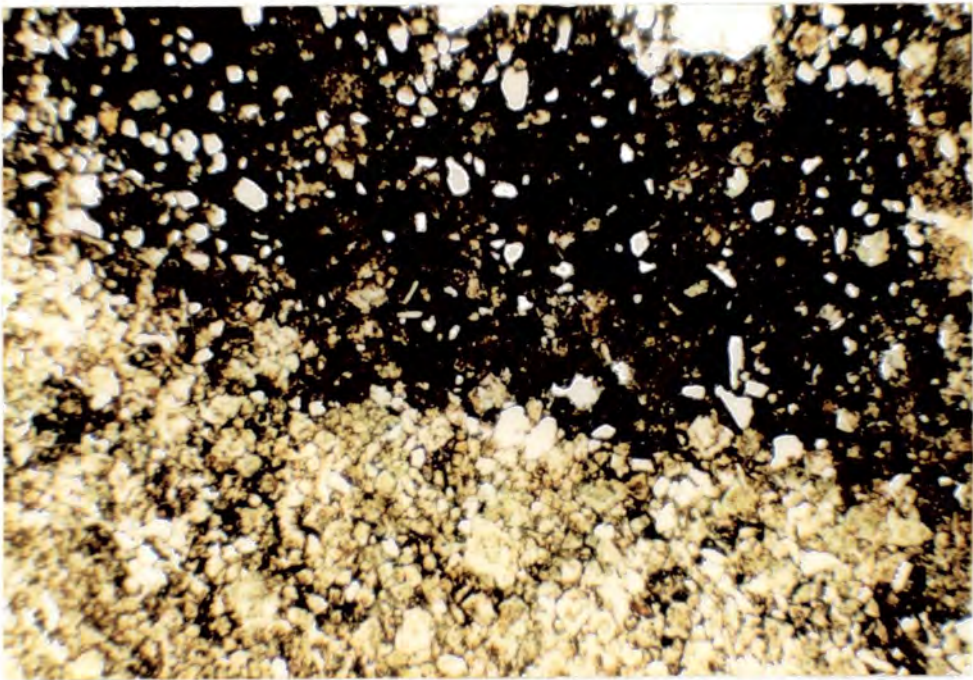


**Fig. 3.5** Photomicrograph of iron-rich calcrite. Rhombic dolomite is being replaced by haematite-rich anhedra dolomite. Field of view 4.1 millimetres. Plane polars. ( In all of the photomicrographs in the thesis the field of view is 4.1 millimetres unless otherwise stated ).

the dolomites are similar in composition to the peritidal dolomicrites of Hird ( 1985 ) which were not recrystallised during burial. The association of poorly calcian dolomites with evaporitic beds ( Morrow, 1982 ) has now been questioned ( Rosen et al., 1988 ). Although in this case the relationship described in Morrow ( 1982 ) appears to be upheld the range of dolomite stoichiometeries reported from evaporitic units in the Coorong region of South Australia is such that the association of evaporites with calcian ( 52 to 54%  $\text{CaCO}_3$  ) dolomites does not appear to be definitive. On the basis of stoichiometry alone the depositional environment of the dolomites cannot therefore be identified and interpretations must rely upon the petrographic analyses of the rocks.

The dolomite in the Evaporitic Dolomite Unit was most likely formed during deposition and early diagenesis of the sequence. The formation of peritidal dolomite albeit in a poorly ordered form has been described by numerous authors ( Bush, 1973; papers in Zenger et al. ( eds. ), 1980; Rosen et al., 1988 ). There was undoubtedly some carbonate input into the beds during deposition but the Carboniferous Limestone in the Sully Island area is mostly undolomitised. The majority of the clastic carbonate will have been dolomitised during formation of the unit. The original mineralogy of the beds has been obscured by the dolomitisation. It is possible that the original carbonate phase was not a protodolomite but a mixture of minerals. Rosen et al. ( 1988 ) described primary assemblages containing aragonite, high and low magnesium calcite, hydromagnesite and magnesite in the Coorong region of South Australia, along with penecontemporaneous dolomite. In the Sully Island dolomites there is no evidence for the original presence of other carbonate phases. This does not preclude their early diagenetic replacement by a more stable dolomite phase. The dolomite in the Sully Island succession most probably formed during early burial, almost certainly while in contact with surface waters.

Apart from a poorly developed lamination which is preserved throughout the unit there are few sedimentary structures preserved. In the upper and lowermost dolomites, some symmetrical ripples are preserved. This is indicative of periodic shallow sublittoral conditions. It is noticeable that these rippled beds do not occur in the central part of the Evaporitic Dolomite Unit where the sulphate nodules are present. The ripples are poorly preserved but crest orientations trend

in a northeast / southwest direction. This is a similar orientation to those in the underlying shoreline clastics whose average trend is 074-254 degrees which is an indication of the orientation of the shoreline during deposition of the Evaporitic Dolomitic Unit.

In one exposure of the dolomites east of Swanbridge there is evidence for the preservation of original lamination ( Fig. 3.9 ). In this case an area several centimetres in thickness and 0.5 metres in length contains an undulose parallel lamination in which individual laminae are under one millimetre in thickness. The laminae are not of constant thickness and tend to thin over raised parts of the underlying bed. This can be taken as evidence against a microbial origin for the laminae ( Aitken, 1967 ). The undulose character of the laminae, however, is suggestive of a microbial origin for the bed. Unfortunately there are no other patches of well preserved sedimentary structures which could be used to clarify the origin of the lamination. In thin section the origins of the laminae are obscured by later dolomitisation.

### **3.2.3 The Nodular Dolomite Horizon (Groundwater Calcrete)**

The nodular dolomite horizon is up to 2 metres in thickness and consists of large vertically flattened structures whose margins are commonly irregular in a matrix of red silty dolomite which is similar in form to the overlying sublittoral beds ( Fig.3.1 ).

The nodules are between 0.1 and 1.5 metres in diameter, with an average of 0.5 metres. Individual nodules tend to coalesce giving irregular forms. This has happened most markedly at the base of the unit, where the nodules form a solid band one metre in thickness ( Fig. 3.10 ). Above the basal one metre the size of the nodules does not change but the packing decreases and individual nodules are surrounded by matrix material.

The nodules are distinguished from the surrounding matrix by their lack of iron staining, less fissile nature and more crystalline appearance. In thin section the boundary between the nodules and matrix is shown by the red colouration of the latter. There are no other observable differences between the two. Using XRD analysis the nodules contain less quartz and more dolomite, as well as some

calcite. There is some evidence in thin section for the original presence of sparry calcite in the nodules, now almost entirely replaced by dolomite. The resistance of the nodules to weathering is indicative of greater cementation relative to the surrounding matrix. The oblate shape of the nodules is commonly contorted around the margins into folds and crenulations. This folding is most noticeable at the base of the horizon where the nodules have coalesced. Some of the folds are reminiscent of overturning or slumping ( Fig. 3.10 ). The nodules in the upper beds are more regular in their distribution and in plan view appear to be regularly spaced ( Fig. 3.11 ), almost forming a polygonal pattern. On the foreshore at Swanbridge the nodules are exposed on the wave-cut platform and again have a deformed nature. The nodules are arranged in pipe-like structures, 0.3 metres wide and several metres long ( Fig. 3.12 ). These pipes are identical in composition to those seen on Sully Island. The elongate nodules occur in the topmost one metre of the horizon. The thickness of the bed cannot be estimated but the area of elongate nodules is 20 by 70 metres. The elongate nodules are cut by thin spar filled fractures which are perpendicular to the axis of elongation.

The origin of these nodular structures is not certain. In terms of size and distribution within the bed they are similar in form to the sulphate horizons developed within the Mercia Mudstone Group ( Fig. 7.3 ). There is no evidence, however, for the original presence of sulphate in these nodules. Furthermore, the style of deformation of the nodules does not suggest an evaporitic origin. Similar structures have been described from Recent alluvial systems in central and eastern Australia ( Mann & Horowitz, 1979 ). These structures, termed groundwater calcretes, form from the non-pedogenic precipitation of carbonate below the water table in arid drainage systems. During times of high evaporation, growth of the calcrete is almost continuous, and carbonate precipitated at the water table displaces and deforms earlier calcrete. In the Sully Island area the deformation is concentrated in the lowest one metre of the bed. This may indicate that growth of the calcrete took place at the top of the unit in response to a rising water table. There is some evidence that the nodules were originally composed of calcite and have been subsequently dolomitised, as is the case with the Recent examples from Australia ( Mann & Horowitz, 1979 ). The calcretes in Sully Island did not reach the mature stage during which beds are deformed upwards and can form anticlinal structures at the surface. The upper surface of



**Fig. 3.10** Deformed groundwater calcrite nodules at the base of the calcrite section, south side, Sully Island. The deformed nodule which has been pushed into the underlying dolomites is 0.7 metres in width.



**Fig. 3.11** Plan view of undeformed nodules in the upper groundwater calcrite, south side, Sully Island. Length of hammer 40 centimetres.

the horizon in Sully Island is undeformed and probably represents the last phase of carbonate precipitation. The formation of the elongate nodules is more problematic, since they are assumed to have formed at or just below the water table. Their elongate shape compared to the normal polygonally arranged nodules is similar to structures of various types which form under the influence of a slope such as periglacial stone stripes and fractures in halite which form due to thermal contraction ( Tucker & Tucker, 1981 ). It is possible that near the margin of the basin during periods of excessive desiccation, the water table could be drawn down in the basin centre, creating a gradient which would allow the formation of pipe-like nodules. The presence of rippled beds overlying this nodular horizon is evidence that a sub-perilittoral environment similar to that seen in the lower dolomite was re-established in the upper beds as the water table continued to rise.

#### **3.2.4 Evaporitic Dolomite Beds, Bendrick Rock**

Three kilometres west of Sully Island between Hayes Point and Bendrick Rock a number of dolomitic beds are exposed which contain evidence for the former presence of evaporites ( Fig. 3.13 ). There are ten cycles of massive dolomites interbedded with rippled clay-rich beds. Three of the dolomite beds are nodular and are cut by polygonal fractures up to 1.5 metres in diameter. The other dolomite beds are more regularly bedded and contain small nodules which are now composed of quartz but which were originally sulphate. These dolomitic horizons have been interpreted by Tucker ( 1977, 1978 ) as deposits of a perilittoral saline mudflat. The nodular dolomites were interpreted as replacements of crusts of sulphate similar to those which are forming at present in playas in the western U.S.A. ( Hunt & Washburn, 1966 ). It is possible that the three nodular dolomitic beds represent replacement of a surficial crust, although Hunt & Washburn did not describe such structures in the sulphate zone. In the less nodular dolomites there is evidence for the original presence of sulphates within the sediment. The nodular dolomites may have contained sulphate disseminated within the sediment as well as in a surficial crust. The polygonal structures on the surface of the dolomite may represent a pattern which was superimposed on the underlying sediment after dissolution of the evaporite crust. In the distal fluvial



**Fig. 3.12** Elongate groundwater calcrite nodules, trending from top left to bottom right of the photograph. East of Swanbridge. Length of hammer 40 centimetres.

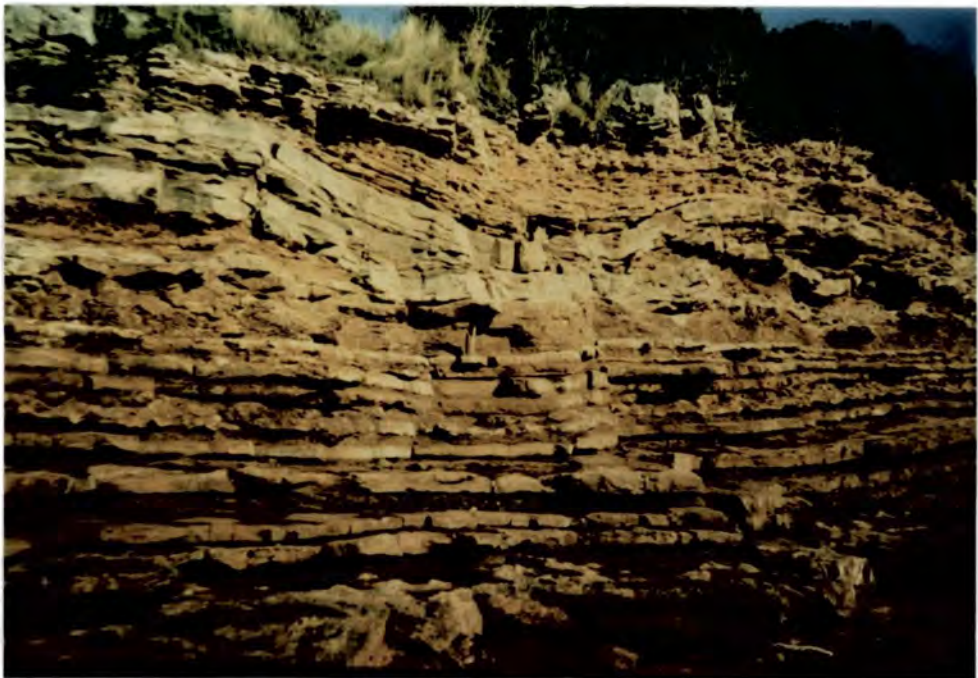


**Fig. 3.13** Evaporitic and nodular dolomites interbedded with clay-rich peritidal deposits, West of Hayes Point. The hammer rests on the topmost nodular dolomitic bed. Downwarping of the overlying sandstone is the result of solution of sulphates in the underlying beds, probably accentuating an original erosive surface. Length of hammer 40 centimetres.

environment of the Bendrick Rock area it is unlikely that a surface crust will have been preserved for any length of time or that a crust the thickness of the nodular dolomite beds would have accumulated. Dissolution of sulphate present within the dolomite could give rise to the irregular form of some of the dolomitic beds. There is abundant evidence for the dissolution of sulphate within the section at Bendrick Rock. Both small collapse structures 0.5 metres in diameter and larger depressions involving saucer-shaped structures up to 3.0 metres in diameter are present within the section.

The presence of the interbedded siltstones and dolomites is indicative of a marginal mudflat environment in which periods of clastic input into a shallow sublittoral setting alternated with times of exposure and sulphate precipitation. The sequence between Bendrick Rock and Hayes Point may be the lateral equivalent of the evaporitic beds in the Evaporitic Dolomitic Unit. This cannot be proved since the two sequences are not directly correlatable, but it is possible that the dolomitic interbeds formed synchronously with the replaced evaporites in the Sully Island succession.

### **3.3 Replaced Sulphates**

#### **3.3.1 Introduction**

In total there are eight horizons of replaced sulphate nodules in the 3 metres in the centre of the Evaporitic Dolomitic Unit. The sulphate has been replaced in several ways and the nodules themselves occur in two distinct forms. Quartzose nodules are relatively large ( up to 0.5 metres across ) discrete forms spaced along horizons. Carbonate replaced nodules occur both in distinct horizons and also in less regular beds, packed together.

#### **3.3.2 Carbonate-replaced Nodules**

##### **3.3.2a 'Sabkha' Nodules**

The sabkha type of carbonate-replaced sulphate nodules occurs in two double bands in the centre of the replaced evaporite section of the dolomite unit

( Fig. 3.14 ). The uppermost of the two bands is the best developed and consists of two irregular but parallel bands of white sub-spherical nodules between 4 and 9 centimetres in diameter separated by 5 to 10 centimetres of red siltstone and mudstone. The packed nature of both double bands of nodules is similar to the 'chicken-wire' texture of sulphate in Recent sabkhas from the Trucial Coast, ( Shearman, 1966; Butler, 1969; papers in: Purser ( ed. ), 1973 ). In this environment anhydrite replaces gypsum and also precipitates from hypersaline solutions, forming displacive nodules which coalesce to form the chicken-wire texture. The two double bands in the Sully Island dolomites are thus interpreted as having formed in a sabkha-type environment on a supralittoral mud flat. The two sets of sabkha nodules may have formed in response to a regression-transgression pair similar to but on a smaller scale than the sequence caused by sea-level fluctuations in the Trucial Coast ( Bush, 1973 ).

In thin section the sabkha nodules are composed of strongly ferroan equant calcite spar which has been partially replaced by dolomite microspar ( Fig. 3.15 ). The calcite spar contains abundant inclusions of anhydrite up to 100  $\mu m$  in length, indicating that the nodules were originally composed of sulphate. The calcite itself does not appear to have pseudomorphed individual sulphate crystals. Within the calcite spar, individual laths of anhydrite are arranged in packets or groups. Under cathodoluminescence areas of brightly luminescing spar surrounded by duller material can be seen ( Fig. 3.16 ). These areas are not related to patterns of inclusions within the spar and do not coincide with crystal boundaries. They appear to be related to structures for which there is now no direct evidence in the nodules. There are a number of these brightly luminescent areas in the spar, roughly lenticular in shape and 1 to 2 millimetres in length. The shape of these brightly luminescent zones is similar to those of gypsum crystals which form during early burial.

A number of phases of mineralisation can thus be inferred for the sabkha-type nodules from the initial precipitation as gypsum or as mixed gypsum-anhydrite which has been described from the Trucial Coast by Bush ( 1973 ), through a partial recrystallisation to lath-like anhydrite, to a replacement by calcite spar and finally dolomite.

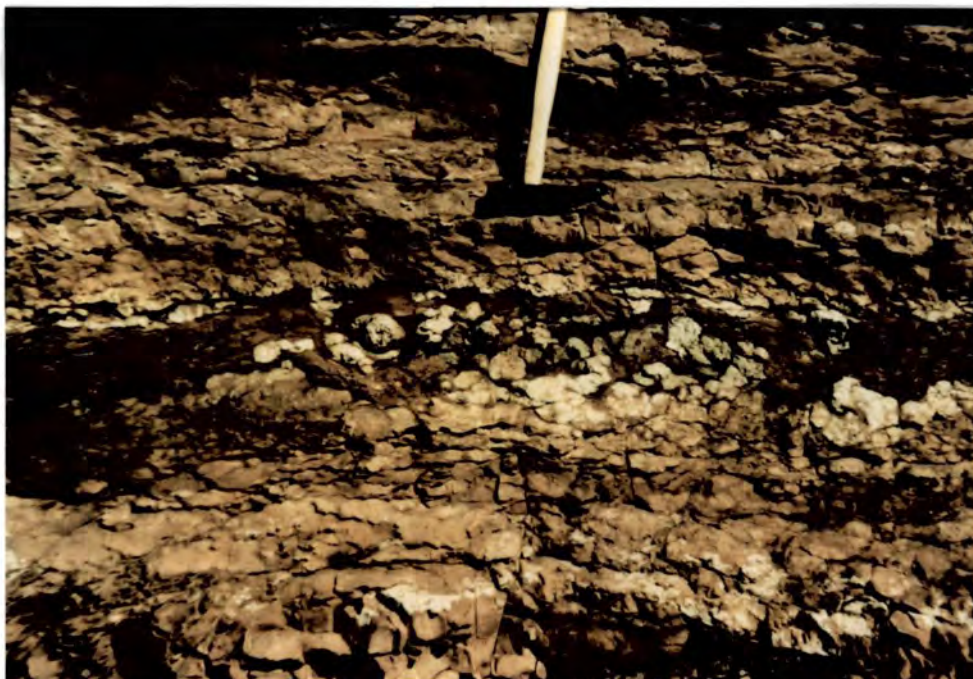


**Fig. 3.14** Upper sabkha nodule band, south-east corner of Sully Island. the two bands of nodules are separated by an iron-rich, pedogenetically altered sediment. Length of hammer head 19 centimetres.

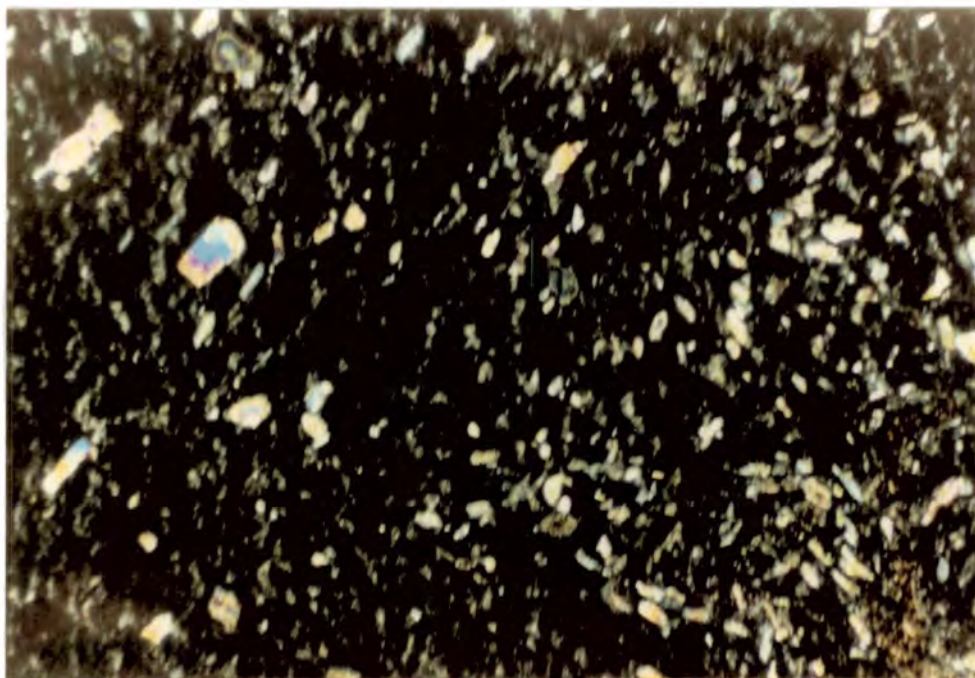


**Fig. 3.15** Photomicrograph of calcite spar which has replaced sulphate in the sabkha nodules. The high birefringence, lath-shaped inclusions are anhydrite. The calcite crystal is in extinction. Width of view 2.1 millimetres. Crossed-polars.

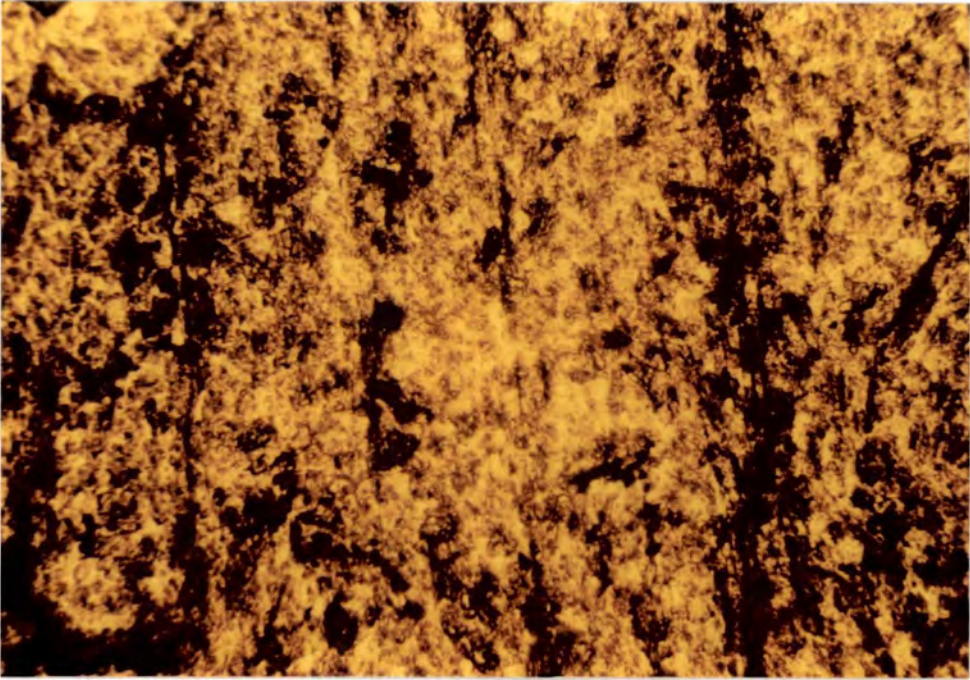


**Fig. 3.16A** Photomicrograph of a single crystal of calcite spar in a sabkha nodule. Plane polars.

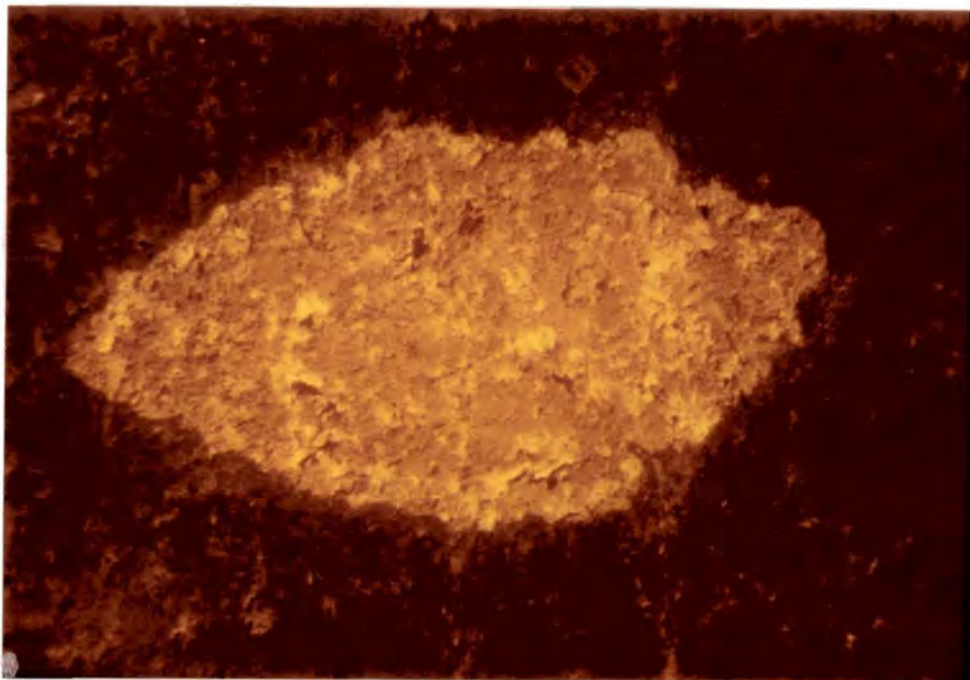


**Fig. 3.16B** Cathodoluminescence view of Fig. 3.16A showing a brightly luminescent lenticular zone - the only evidence for the original presence of gypsum in the sabkha band.

### 3.3.2b Other Carbonate-replaced Nodules

As well as the two sabkha bands there are several other horizons which contain carbonate replaced nodules. The nodules within these bands are larger, between 5 and 10 centimetres in diameter, and are more irregular in shape, often having a knobby surface. These are composed of white, friable carbonate and boundaries with the surrounding dolomites are commonly diffuse. The nodules occur in single horizons and are usually spaced along the bed, with no evidence of coalescence. They can occur in the same horizons as the quartzose nodules.

In thin section the nodules can be seen to be composed of calcite spar within a matrix of fine dolomite ( Fig. 3.17 ). Lath-shaped inclusions of anhydrite are present within the spar. In this case the diffuse nodule margins contains numerous needle shaped partially replaced anhydrite crystals which formed as the anhydrite replaced the original gypsum nodules. The original lenticular shape of the gypsum can be seen in some of the nodules ( Fig. 3.17 ). The anhydrite relics in the centre of the replaced nodules are larger than the marginal needles and suggest that the size of the anhydrite crystals in the centre of the fibrous masses was larger. The fact that these sulphates have been replaced by calcite spar indicates that they underwent a similar diagenetic sequence to the sabkha-type nodules. There is no evidence in the nodules for relict lenticular gypsum as shown by cathodoluminescence, although the general shape of the nodules is similar to anhydrite nodules from the Triassic of Northwest England which were originally gypsum ( Tucker, 1981 ). This suggests that these nodules were also initially composed of gypsum before recrystallisation to anhydrite and then carbonate.

These less well developed sulphate horizons display the same diagenetic history as the sabkha-type nodules. They do not, however, form a band of coalescing nodules but are more widely spaced. In this case the sulphate may have formed as a smaller band within the sediment or even as a surface crust which was later recrystallised during early burial. The lateral discontinuity of these bands is an indication that they were not as well developed as the sabkha horizons.

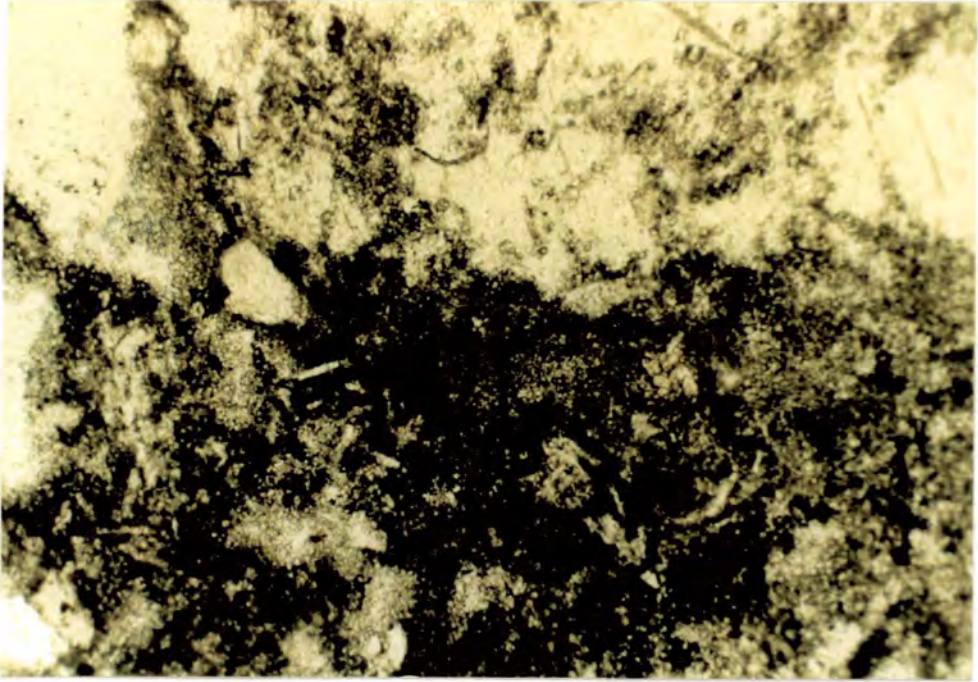


**Fig. 3.17** Photomicrograph showing the margin of a carbonate-replaced nodule with several lath-shaped anhydrite crystals ( now replaced by calcite ) in the sediment marginal to the nodule. Field of view 2.1 millimetres. Plane polars.



**Fig. 3.18** Photograph of cut face of quartz-replaced sulphate nodule from a horizon above the sabkha band. Several nodules have amalgamated to form a larger structure. Note the sucrosic nature of the quartz and the interstitial calcite.

### 3.3.3 Quartz-replaced Nodules

Three bands of quartz-replaced nodules occur in the replaced evaporite section of the dolomite unit. These are variable in size but are generally larger than the carbonate nodules and can be up to 25 centimetres in diameter. On average the nodules are 10 centimetres in diameter and are more regular in shape than the carbonate nodules. In cross section individual nodules can be seen to be composed of a number of smaller forms ( Fig. 3.18 ). The nodules contain few cavities and no well developed crystal terminations were seen. The majority of the quartz is sucrosic in texture with a grain size of between 0.1 and 1.0 millimetres. In some nodules there is a clearer outer zone and an inner more milky zone which appears to contain more inclusions ( Fig. 3.18 ).

In thin section the nodules are composed of either lath-shaped or equant megaquartz which ranges in size between sucrosic crystals one millimetre in diameter and, more rarely, microquartz 10  $\mu m$  in diameter. Chalcedonic quartz was not observed within these nodules, nor were any length-slow fibrous crystals seen, although such forms have been reported from similar Triassic silica-replaced nodules near Bristol ( Tucker, 1976 ). All of the nodules contain evidence for the original presence of sulphates in the form of laths of anhydrite. As in the carbonate-replaced nodules the laths tend to occur in groups which are crystallographically orientated in the same direction.

The nodules composed of lath or tabular megaquartz contain a greater amount of interstitial calcite. The laths are between 0.3 and 1.0 millimetres in length and 0.2 to 0.5 millimetres wide. In any one area the laths have a similar orientation, which is generally parallel to the orientation of the anhydrite relics. On a larger scale the laths can form a radial pattern ( Fig. 3.19 ). This is most clearly seen in areas where the laths are separated by interstitial calcite. Where laths are interlocking the radial pattern becomes less clear but in some parts of the nodules laths are folded. This pattern of megaquartz orientation appears to be the result of the original orientation of the anhydrite crystals. In places the megaquartz is being replaced by or is associated with equant microquartz. This occurs interstitially to the laths but also appears to be replacing laths along intercrystalline boundaries ( Fig. 3.20 ).

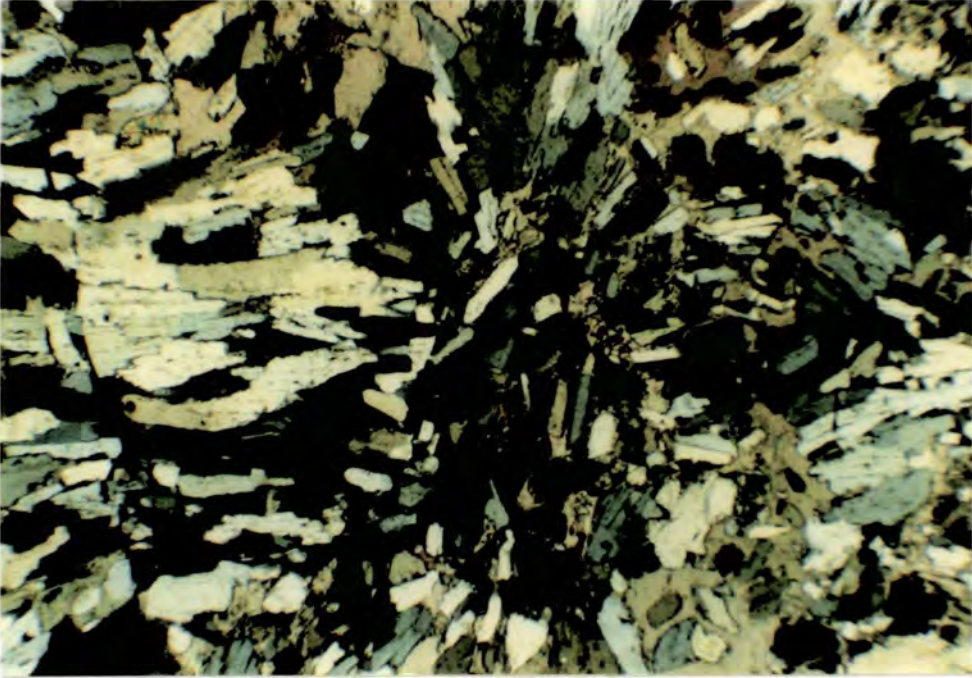


**Fig. 3.19** Photomicrograph of quartz-replaced sulphate nodule showing a faint radial pattern in the arrangement of the quartz laths. Crossed polars.

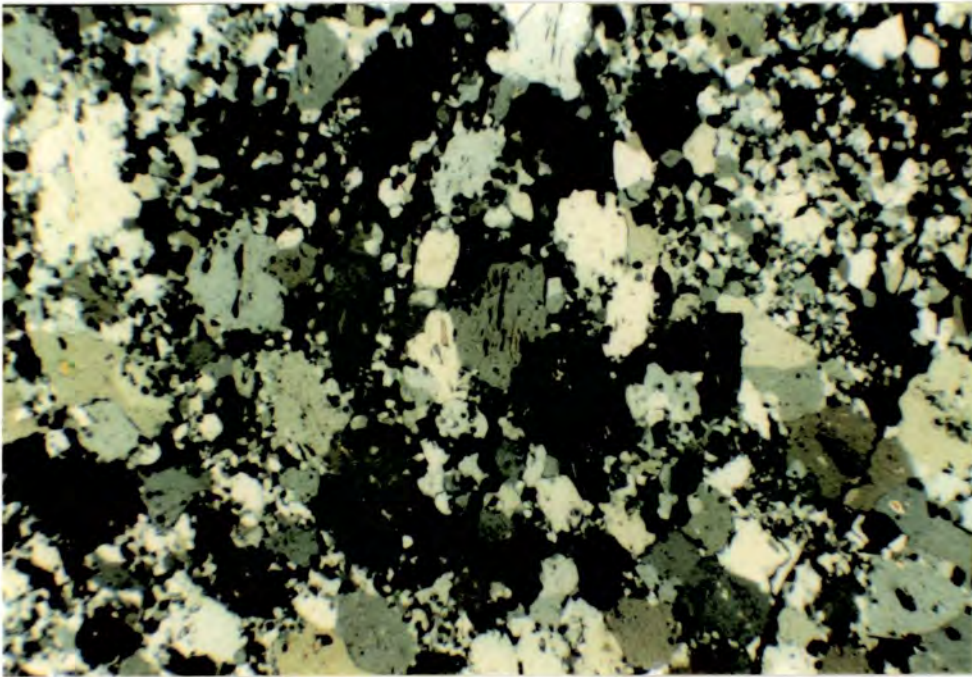


**Fig. 3.20** Photomicrograph showing recrystallisation of megaquartz to inclusion-free microquartz, particularly along crystal boundaries. Replacement has proceeded from the crystal margin which lies towards the top of the photograph. Crossed polars.

Equant mega and microcrystalline quartz nodules also contain inclusions of anhydrite but the crystal form of the quartz itself is not related to the orientation of the original sulphate crystals. In the centre of these nodules the quartz forms an interlocking array of crystals between 0.3 and 1.0 millimetres in diameter ( Fig. 3.21 ). Towards the outer margins of these nodules the grain size of the quartz becomes smaller and the inclusions of anhydrite are less abundant. The smaller crystals around the nodule margin again appear to be replacing the megaquartz and the smaller crystals do not contain anhydrite inclusions. At the nodule margin some fibrous anhydrite crystals have been partially replaced by quartz ( Fig. 3.22 ). The form of the sulphate which has been replaced by quartz does not appear to differ from that which has been replaced by carbonate. One nodule is composed entirely of equant quartz of varying grain size between 5 and 100  $\mu m$  in diameter. This nodule contains no anhydrite inclusions but is associated with inclusion rich carbonate which is itself being dolomitised. This nodule appears to have been partially silicified after the sulphate was replaced by carbonate. This texture was found in one nodular horizon which is itself very friable and appears to have consisted of disseminated sulphate rather than a distinct nodule.

The silicified nodules in the replaced evaporite section appear to have been originally basically similar to those which are now carbonate. The replacement of sulphate by quartz or silica has been related to the passage of meteoric groundwaters through the rock ( Tucker, 1976; Milliken, 1979 ). The megaquartz and in one case a carbonate-replaced nodule have been partially replaced by inclusion-free microquartz which represents the final phase of the diagenesis of the nodules. Although it cannot be proved the final phase of silicification is possibly related to the dolomitisation of the carbonate nodules, which also represents the final phase of diagenesis of the majority of the Evaporitic Dolomitic Unit.

### 3.4 Conclusions

The Evaporitic Dolomite Unit consists of between 6 and 9 metres of red dolomite deposited in an arid perilittoral environment. The dolomitic unit is separated from the underlying clastic shoreline deposits by a fenestral dolomite which to the east has been calcretised and consists of a haematite rich dolocrete. This

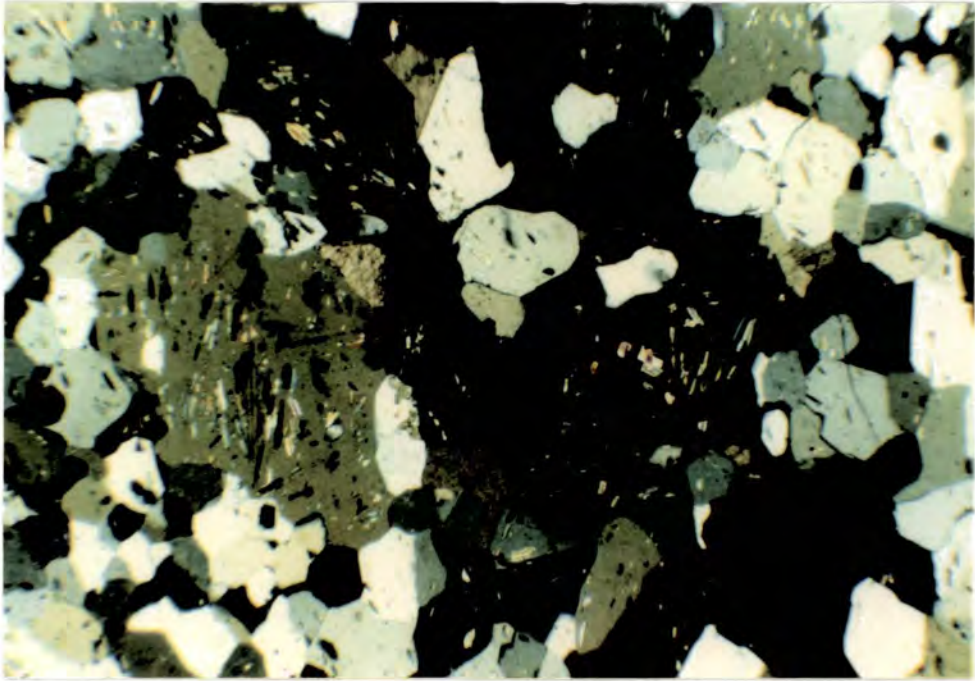


**Fig. 3.21** Photomicrograph of quartz-replaced nodule with some interstitial calcite. The relict laths of anhydrite occur in groups which have similar orientation. Crossed polars.

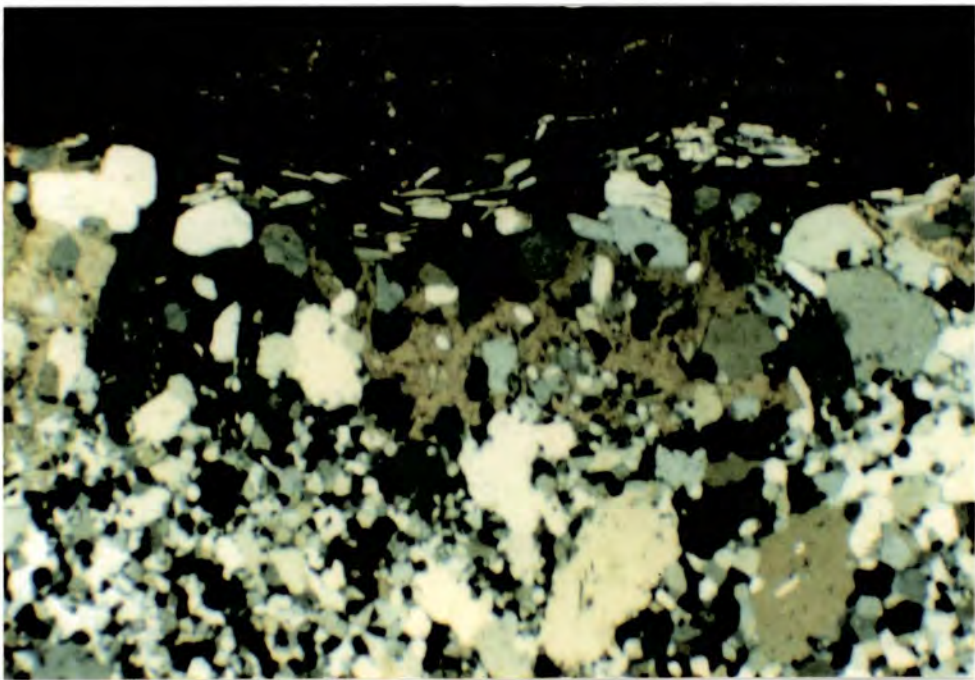


**Fig. 3.22** Photomicrograph of margin of quartz-replaced nodule showing elongate quartz crystals which are the replacements of individual anhydrite crystals. The nodule has been partially recrystallised to microquartz. Crossed polars.

dolomite represents the point at which most of the relief at the lake shoreline was removed and a mud flat was established. The top of the dolomite unit is sharply overlain by a calcitic calcrete with an irregular base which represents the base of the limestone unit.

The Dolomite Unit has been subdivided into four sections on the basis of sedimentary structures and mineralogy ( Fig. 3.23 ). The lower and upper sections of the dolomite unit are composed of laminated and rippled dolomite, which were formed in a shallow sublittoral environment. The dolomite itself is calcian and relatively poorly ordered, which is analogous to peritidal dolomicrites described from the Carboniferous by Hird ( 1985 ). There is some evidence for pedogenesis within the dolomite, indicating periods of exposure, and microbial lamination is preserved in one exposure. Most of the sedimentary structures have been lost due to the recrystallisation of the beds, possibly from a mixed-carbonate precursor. The topmost few metres of the unit have been recrystallised to an array of coarse rhombic dolomite, most likely the effects of the calcretisation of the overlying limestones.

Underlying the upper perilittoral dolomites 2 metres of large dolomitic nodules which have been deformed and folded in the lower part and which are arranged in a polygonal pattern in the upper part. These are the result of the non-pedogenic precipitation of carbonate at or just below the water table. Each phase of precipitation can deform previously formed calcrete and displace it upwards or downwards, depending on the stability of the water table. In this case precipitation appears to have taken place on the top of the unit in response to a slowly rising water table. The topmost nodules in the section are undeformed whereas the lower nodules show evidence of some compression after formation. Deformation is ductile rather than brittle in form, indicating that the cementation of the nodules was not complete during their initial formation. The rise in the water table appears to have continued to the point where precipitation of carbonate ceased ( Fig.3.23 ). The overlying rippled dolomites may be the result of this water table rise although it cannot be discounted that the calcrete formed after deposition of these beds and before formation of the basal calcrete of the limestone unit.

The section underlying the groundwater calcretes is composed of 3 metres of

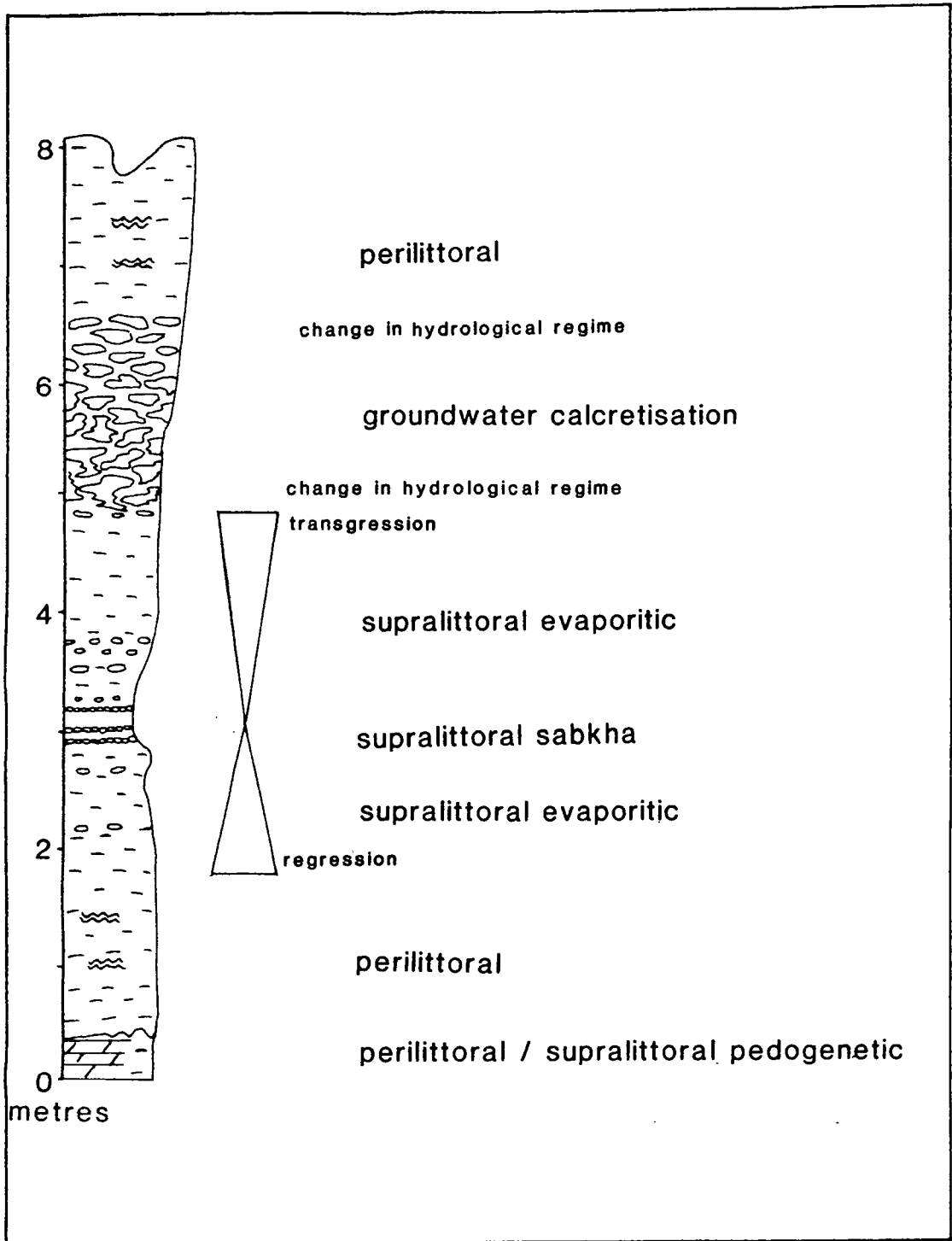


**Fig. 3.23** Summary sketch log of the depositional environments in the Evaporitic Dolomitic Unit.

dolomites containing replaced evaporite nodules. There are eight horizons of nodules, two of which are analogous to sulphates formed in sabkha-type peritidal environments in the present day ( Butler, 1969 ). The sabkha nodules are composed of calcite spar which contains abundant inclusions of anhydrite and which has been partially dolomitised. There is also evidence for the nodules having originally consisted of gypsum. The other beds of nodules contain either carbonate or quartz-replaced sulphate nodules which are more regularly spaced and generally larger. In both cases the replacement minerals contain inclusions of anhydrite and partially replaced needle like anhydrite crystals can be seen at the margins of the nodules. The six horizons of spaced nodules formed in a similar manner to the sabkha beds but represent less well developed sulphate horizons. The two sabkha beds may represent a transgression-regression cycle similar to but on a smaller scale than that seen in the Trucial Coast ( Bush, 1973 ). The reason for the selective silicification of certain beds in the replaced evaporite section is not known. In some of the quartz nodules there is evidence of replacement of a nodule which is already composed of carbonate. The replacement of the sulphate by calcite may possibly be related to the formation of the groundwater calcrete. The exact timing of the silicification is not certain but the passage of meteoric groundwaters through the dolomites will have taken place over a relatively long period of time during which the limestones were laid down even if the basal calcrete acted as a partial aquiclude. The two phases of silicification can be assumed to have taken place at this time, during which the upper dolomites may have formed in waters of mixed origin.

Three kilometres to the east of Sully Island several cycles of evaporitic dolomite are interbedded with sublittoral clastic beds. These dolomites are the result of the precipitation of sulphate on a supralittoral mudflat which was periodically covered by distal clastic beds. Some of the dolomite may have replaced surficial sulphate crusts as well as replacing evaporites within the sediment itself. The cyclic interbeds are the lateral equivalent of the Evaporitic Dolomite Unit at Sully Island indicating that a perilittoral environment with greater clastic input existed in the western part of the Sully Island subbasin.

The Evaporitic Dolomite Unit can thus be represented as a perilittoral deposit in which there is a regression in the lower part of the unit leading to calcretisation

and the formation of sulphates and a transgression in the upper part leading to the return of sublittoral conditions in the uppermost dolomite ( Fig. 3.23 ). The base of the overlying limestones is composed of a mature calcrete which indicates a long period of exposure, presumably as a result of further regression of the lake shoreline after deposition of the dolomite unit.

## **Chapter 4**

### **Sedimentology of the Lacustrine Limestones, South Wales**

## Chapter 4

### Sedimentology of the Lacustrine Limestones, South Wales

#### 4.1 Introduction

##### 4.1.1 The Limestone Unit, Sully Island

The Limestone Unit is exposed in the Sully Island area along the shoreline from Ball Rock ( ST17426760 ) in the east to Hayes Point ( ST 14006728 ) in the west ( Fig. 4.1 ). It is also exposed on the causeway at Swanbridge and on Sully Island itself. At Ball Rock a total of 4 metres of limestone are present whereas on the south side of Sully Island up to 8 metres are exposed. To the west of Sully Island, where the limestones are exposed on a wave-cut platform which is parallel to bedding, only topmost few metres of limestone are exposed and the total thickness of the unit is not known. From the centre of Sully Bay westwards the limestones are progressively more clastic and conglomerates units become more common. At Hayes Point the limestones are mostly composed of clastic material. There is a small fault at Hayes Point which downthrows to the northwest. From this point westwards the beds are classed as part of the marginal clastic deposits and are not included in this study.

The limestones have been partially dolomitised over most of the area. At Ball Rock, the entire limestone unit is dolomitic, obscuring the majority of the sedimentary structures. By contrast in the east of Sully Bay only the topmost metre of the limestone has been replaced by dolomite and sedimentary structures are excellently preserved. The limestones can be subdivided into three parts on the basis of original sedimentary structures ( Fig. 4.2 ).

The basal part of the limestone is composed of a micritic calccrete between 1.0 and 1.5 metres in thickness. This calccrete overlies the Evaporitic Dolomites with a very irregular contact which has a relief of up to 0.5 metres. This calccrete is usually calcitic and is commonly the only part of the Limestone Unit which has not been dolomitised. The central part of the limestones comprises the majority

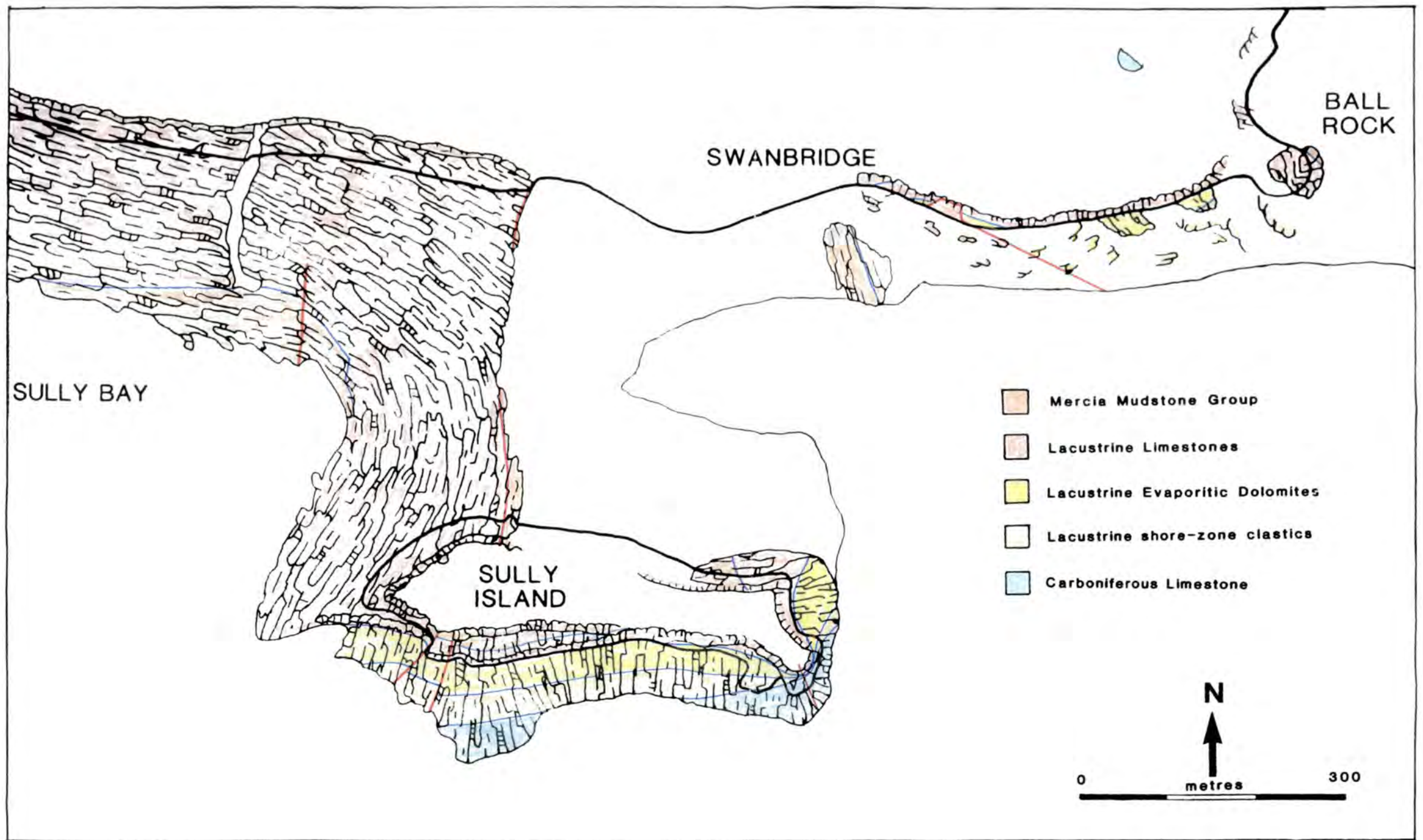


Fig. 4.1 Geological map of Sully Island and adjacent areas.

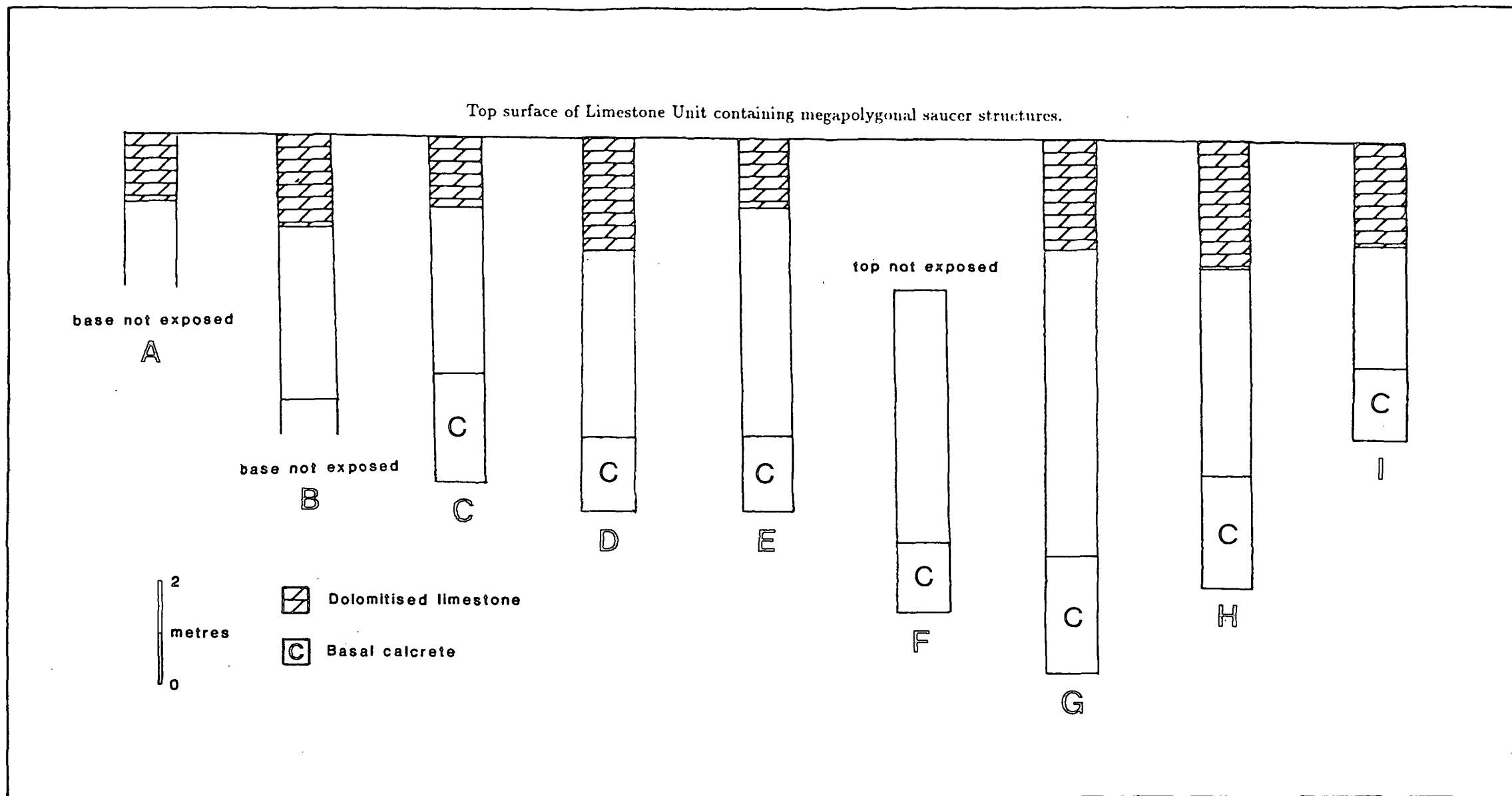
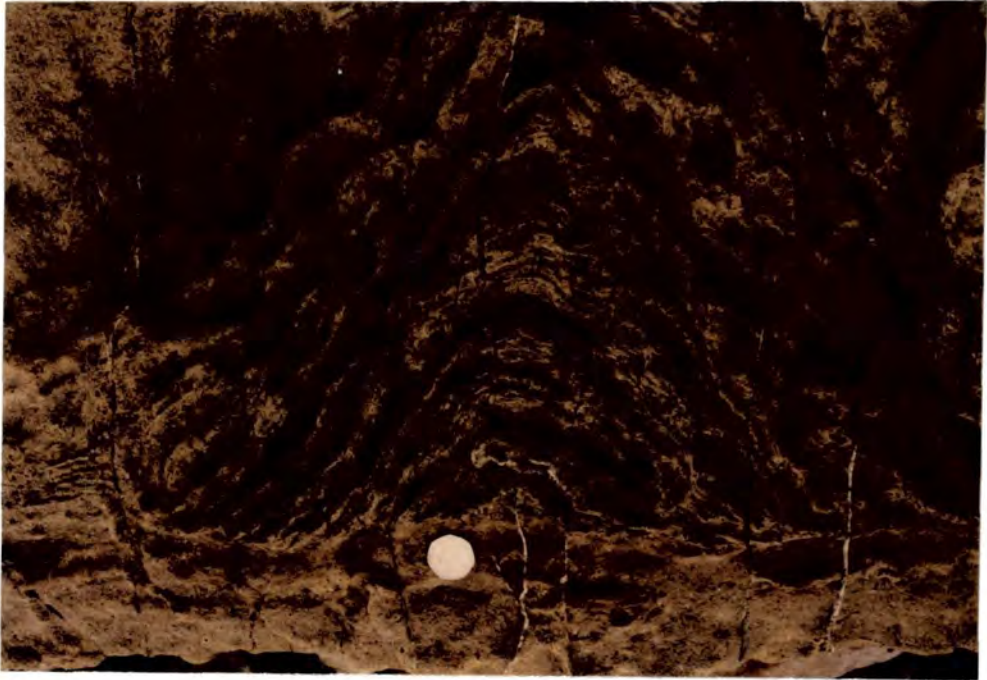


Fig. 4.2 Sketch logs showing thickness changes in the Limestone Unit in the Sully Island area. A - Central Sully Bay. B - Eastern Sully Bay C - West Sully Island. D - South West Sully Island. E - South Sully Island. F - South East Sully Island. G - East Sully Island. H - East Swanbridge. I - Ball Rock.

of the section and is composed of between 2.5 and 5.0 metres of fenestral intra-clastic limestone. These beds contain the majority of the sedimentary structures which are described in this chapter, such as nodular calcretes, microbial beds and travertines ( spring deposits ). The wave-cut platform exposed in Sully Island provides excellent exposure of these structures, as do the cliffs on the south side of Sully Island which provide good vertical exposures. This central part of the limestones has been partially dolomitised on Sully Island and almost completely replaced in the cliffs to the east of Swanbridge where few sedimentary structures are preserved ( Fig. 4.2 ). The upper section of the limestones is 0.5 metres in thickness and is dolomitised over all of the area. This upper part of the Limestone Unit is composed of faintly laminated coarse dolomite. The topmost surface of this dolomitised limestone has been deformed into large tepee and saucer structures up to 5 metres in diameter. Other than these structures nothing has survived the dolomitisation. In general the limestones are thickest in the Sully Island area, indicating the local depocentre of the subbasin.

The limestones are overlain by silty and sandy red dolomites interbedded with several white crystalline dolomites which contain evidence of microbial lamination ( Fig. 4.3 ). The red silty dolomites contain a detrital clay assemblage of illite and chlorite as well as quartz. There are no sedimentary structures in the red dolomites although small quartz nodules are present locally within certain horizons. These are the result of the replacement of sulphate nodules and are similar to those described from the replaced evaporite section of the Evaporitic Dolomite Unit ( Section 3.3 ). These beds represent the onlapping of the Sully Island succession by the evaporitic playa-lacustrine mudstones which form the majority of the Mercia Mudstone Group. The three dolomitic beds contain few sedimentary structures other than the relict microbial lamination which is best preserved in the thickest of the dolomites ( Fig. 4.3 ). These beds are composed of an array of rhombic dolomite with rhombs up to 5 millimetres in length. Some poorly preserved fenestrae can also be seen and coarse clasts of Carboniferous Limestone up to 3 millimetres in diameter occur. These dolomites are similar to the dolomitised upper limestone and contain some small tepees although these are not large and were not the result of upwelling groundwaters. It is likely that they represent the temporary return to a more marginal lacustrine environment when the climate was less arid. The fenestrae indicate a perilittoral environment.



**Fig. 4.3** Microbial mound in fenestral dolomite overlying the Limestone Unit on Sully Island.



**Fig. 4.4** Outcrop of stromatolitic limestones and travertines at Dinas Powys. Length of hammer 40 centimetres.

There is evidence elsewhere in the Mercia Mudstone Group of South Wales for the migration of the palaeoshoreline ( Chapter 7.2 ). In this case there was an interbedding of the meteoric water perilittoral carbonate and hypersaline lacustrine mudstone environments before the red mudstone of the Mercia Mudstone Group became fully established.

#### **4.1.2 The Limestones Exposed at Dinas Powys**

At Dinas Powys a much smaller section of limestone is exposed as part of a garden wall in the centre of the village ( ST15351733 ), ( Fig. 4.4 ). Two metres of limestone overlie a fluvial conglomerate ( Tucker, 1978 ). The limestones have not been dolomitised and preservation of the sedimentary structures is excellent. Columnar and laminar stromatolites are present, interbedded with laminated fine limestones and travertines ( spring deposits ).

#### **4.1.3 Previous Work**

The Sully Island area has surprisingly received little attention in the literature. It is specifically mentioned in Klein ( 1962 ) who considered the limestones to be part of the distal Mercia Mudstone Group. The only other papers to cover the Sully Island sequence were by Tucker ( 1974, 1975, 1977, 1978 ) who briefly described the sedimentology of the limestones as part of a larger study of the marginal deposits of South Wales.

### **4.2 Depositional Environment of the Limestones**

#### **4.2.1 Introduction**

The limestones exposed at Sully Island and Dinas Powys were laid down in a complex depositional environment in which a number of processes were operating at any one time. Section 4.2 covers the original source of sediment into the Sully Island area and its deposition. Processes occurring after deposition are covered in the following sections. The majority of the limestones are composed of two types: fenestral intrasparite and laminated silty limestones. The fenestral limestone is the more common of the two types, making up the majority of the Sully Island

area, while the laminated limestones are exposed in the cliffs east of Swanbridge and are more common in the Dinas Powys limestones.

#### 4.2.1a Fenestral Intrasparites

Although the unit described in this section is referred to as a limestone, much of the rock itself is composed of detrital ( intraclastic ) material. Intraclasts of Carboniferous Limestone are abundant in the coarser beds at Hayes Point. Recognisable clasts of Carboniferous Limestone become rarer to the east. East of the centre of Sully Bay the intraclasts are between 0.2 and 0.5 millimetres in diameter. The variation in average clast size and the percentage of intraclasts within the limestones in the Sully Island area are given in Fig. 4.5 . In areas where it was not possible to sample non-dolomitised beds an estimate of the original grain size was made by measuring the sizes of the quartz clasts. The size of the intraclasts and the percentage of intraclastic material within the rock decreases to the east, with the most coarse material at Hayes Point ( Fig. 4.5 ). From the centre of Sully Bay, the change in size of the intraclasts is less marked although there is still a reduction in grain size to the east of Sully Island. There is also a slight increase in grain size on the southwest corner of Sully Island ( Fig. 4.5 ).

There would appear to have been only one source of clastic sediment into the Sully Island subbasin, from the west. This is in agreement with Tucker ( 1977 ) who described palaeocurrent directions from the west and northwest in the clastic beds between Hayes Point and Bendrick Rock which are the lateral equivalents of the limestones. There is no indication of a second source of clastic input into the basin which has some implications for the palaeogeography of the Sully Island subbasin. The Carboniferous Limestone basement is exposed to the north of Sully Bay and Swanbridge ( Fig. 4.1 ), and there is almost no evidence for the southerly transport of clastics into the basin other than in one exposure of a matrix supported conglomerate north of Ball Rock ( Tucker, 1977 ). This conglomerate was derived from the local basement which is exposed 200 metres to the west, and is in fact separated from the limestone by a number of faults. It may therefore not be a lateral equivalent of the limestones, although the faults do not represent a large amount of displacement. There is no evidence that

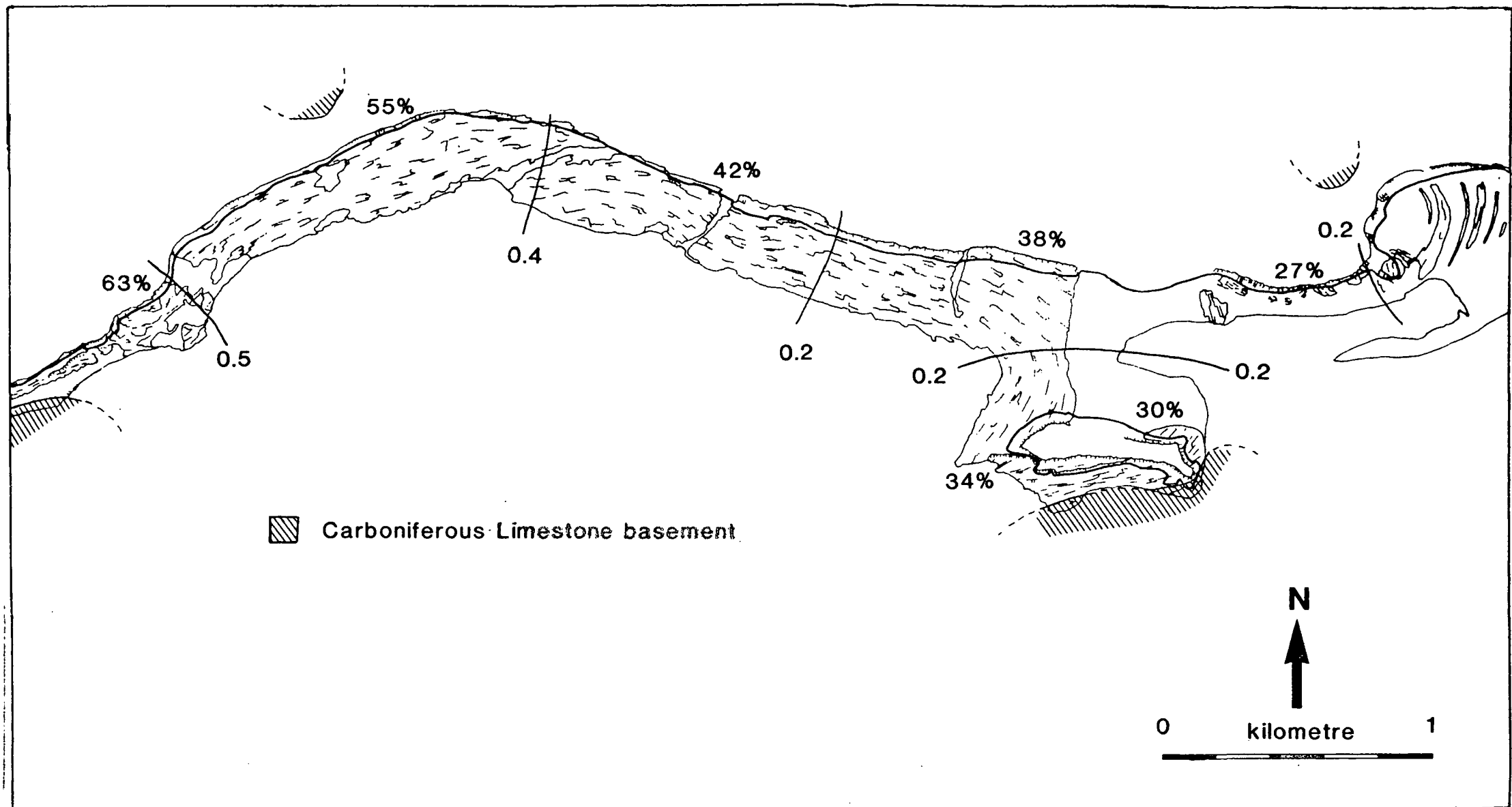


**Fig. 4.5** Average clast size ( contours in 0.1 millimetre gradations ) and average % clastic material in the limestones in the Sully Island area. Taken from 42 samples from approximately the same horizon within the upper limestones.

this basement was a source of coarse clastic material into the Sully Island basin. The limestones containing slightly coarser clasts on the southwest side of Sully Island could be interpreted as an indication of the presence of a source of clastic material to the southwest. This is very unlikely given the palaeogeography of the area. There is no other evidence for the presence of basement offshore to the southwest. Banner et al. ( 1971 ) and Lloyd et al. ( 1973 ) both sampled the sea bed to the south of Sully Island and no Carboniferous Limestone was found to the southwest. The coarser clastic limestones on Sully Island are more likely to be the result of a local influx of coarse material, possibly sorted at the lake shoreline.

Micritic sediment is ubiquitous in the limestones and serves as part of the matrix for much of the intraclastic material. In several areas of Sully Bay the intraclasts have been coated in micrite or microspar forming a pelleted sediment ( Fig. 4.6 ) which is commonly laminated. These superficial peloids in places make up the majority of the limestone. True peloids, which are generally smaller ( under 0.5 millimetres in diameter ) also occur in the limestones. These peloids and the larger superficial forms, probably formed by the same process. It is most likely that the peloids formed by precipitation of micrite which incorporated coarser microspar during growth ( Macintyre, 1985 ). It is not likely that algae were directly involved in the formation of the peloids although some of the micrite in the limestones is of microbial origin.

The fenestrae which are present throughout much of the Limestone Unit and which are commonly the only sedimentary structures which are recognisable after dolomitisation are also indicative of a perilittoral environment. The fenestrae can be equant, akin to the 'bird's-eye' shape or laminar in form. In the intraclastic limestones fenestrae are more commonly equant. On the northwest side of Sully Island there is a regular increase in the size of the fenestrae between 2 and 4 to 5 millimetres in length over a distance of 100 metres. A study of variations in fenestra size was made over the area of outcrop of the limestones. No regular pattern in fenestra size or form was seen. The size and shape of fenestrae can be related to the morphology of overlying algal mat in the Recent peritidal environment of Shark Bay, Western Australia ( Logan et al. ( eds. ), 1974 ). In the limestones around Sully Island the lack of any regular spacial variation may be

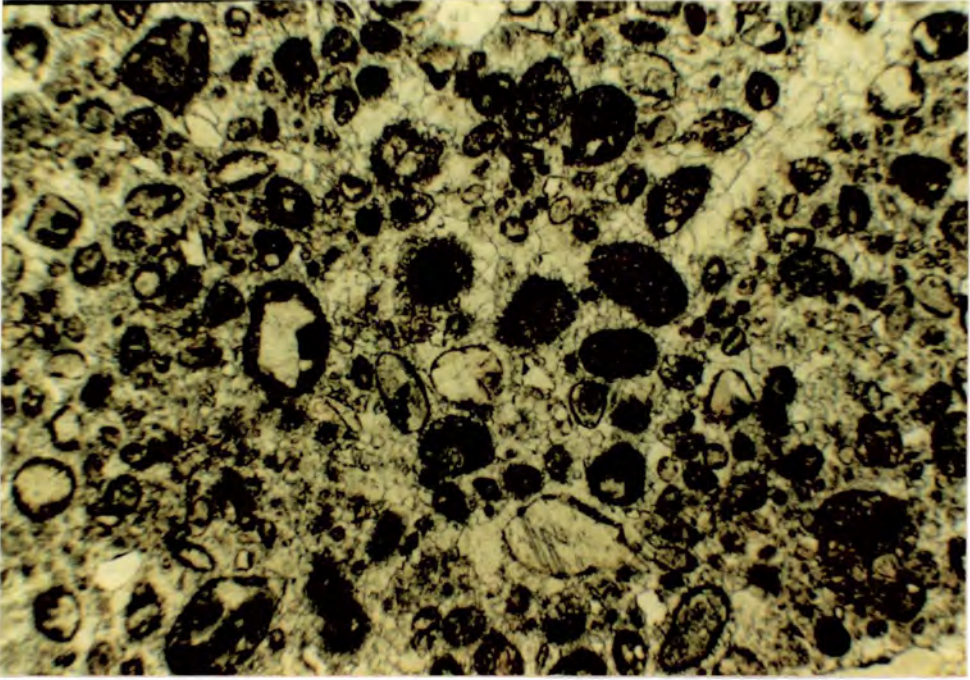


**Fig. 4.6** Photomicrograph of intrasparite consisting of subangular clasts of quartz, Carboniferous Limestone and reworked limestone. Some clasts have been coated by micritic sediment, forming superficial peloids. Plane polars.

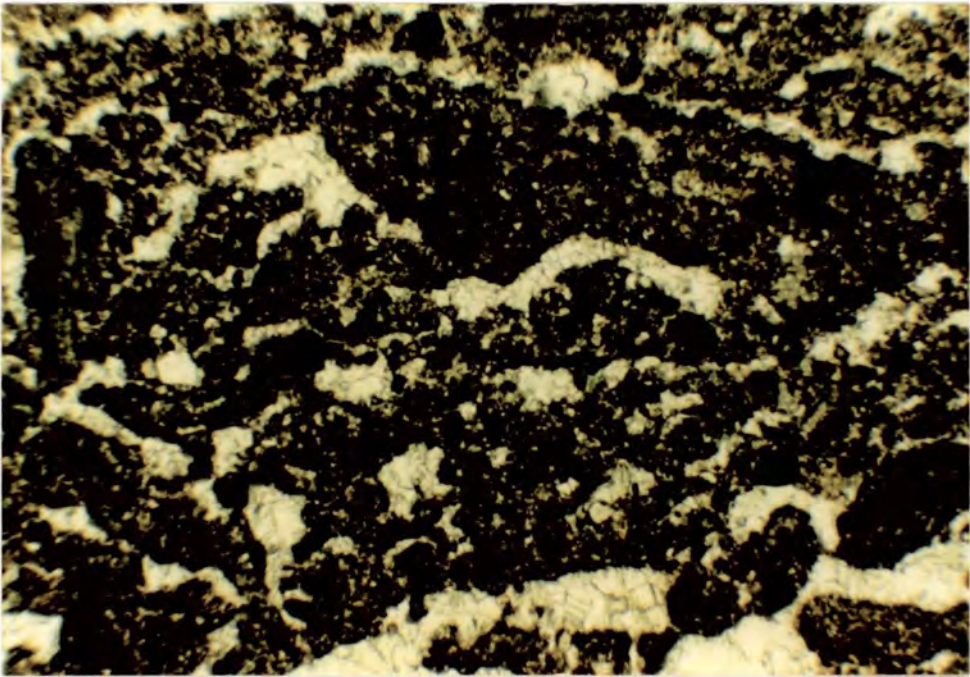


**Fig. 4.7** Photomicrograph of fenestral intrapelsparite. Equant fenestrae are developed in a fine limestone. This lithology is typical of much of the Limestone Unit in the Sully Island area. Plane polars.

due to changes in algal mat morphology or to other controlling factors for which there is no evidence preserved within the sediment. The fenestrae themselves commonly contain internal sediment which is composed of crystal silt or locally peloids.

Further evidence for the perilittoral depositional environment of the limestones is the presence of asymmetric ripples on bedding planes. The ripples are commonly slightly sinuous but parallel and some bifurcations are seen. On large rippled bedding planes the orientations of the ripples do not vary by more than 10 degrees. The results of measurements of the orientations of the ripple crests are shown in Fig. 4.8 . The ripple crest orientations reveal one prominent trend of 055 degrees and one locally developed trend which is perpendicular to the first. The main trend indicates a northeast-southwest trending shoreline which is consistent with the palaeogeography of the South Wales area. The presence of Carboniferous Limestone in the south and southeast of Sully Island, however, suggests that the limestones may have formed in a more restricted environment than a simple southwest facing shoreline. The detailed palaeogeography of the Sully Island area will be discussed in detail in Section 4.8 . If the ripple orientations are plotted individually at each outcrop, the secondary trend in the data is shown to be confined to one area in Sully Bay ( Fig. 4.9 ). It is possible that this local disruption in the pattern of ripple orientations is the result of slight relief at the lake margin such that water and wave movements were refracted around the obstacle giving rise to a local change in the ripple orientations.

As well as rippled surfaces the limestones are commonly desiccated and contain polygonal fractures up to 10 centimetres in diameter. In one bed a rippled surface has been covered by desiccation cracks ( Fig. 4.10 ). The alternation of rippling and desiccation of the beds is indicative of the fluctuation of the water table in the Sully Island area causing rapid changes from supra to sublittoral deposition.

#### **4.2.1b Laminated Limestones**

Laminated silty and micritic limestones form a minor part of the succession in the cliffs east of Swanbridge, but are well developed in the Dinas Powys area where they constitute the major part of the limestone exposed. In both areas

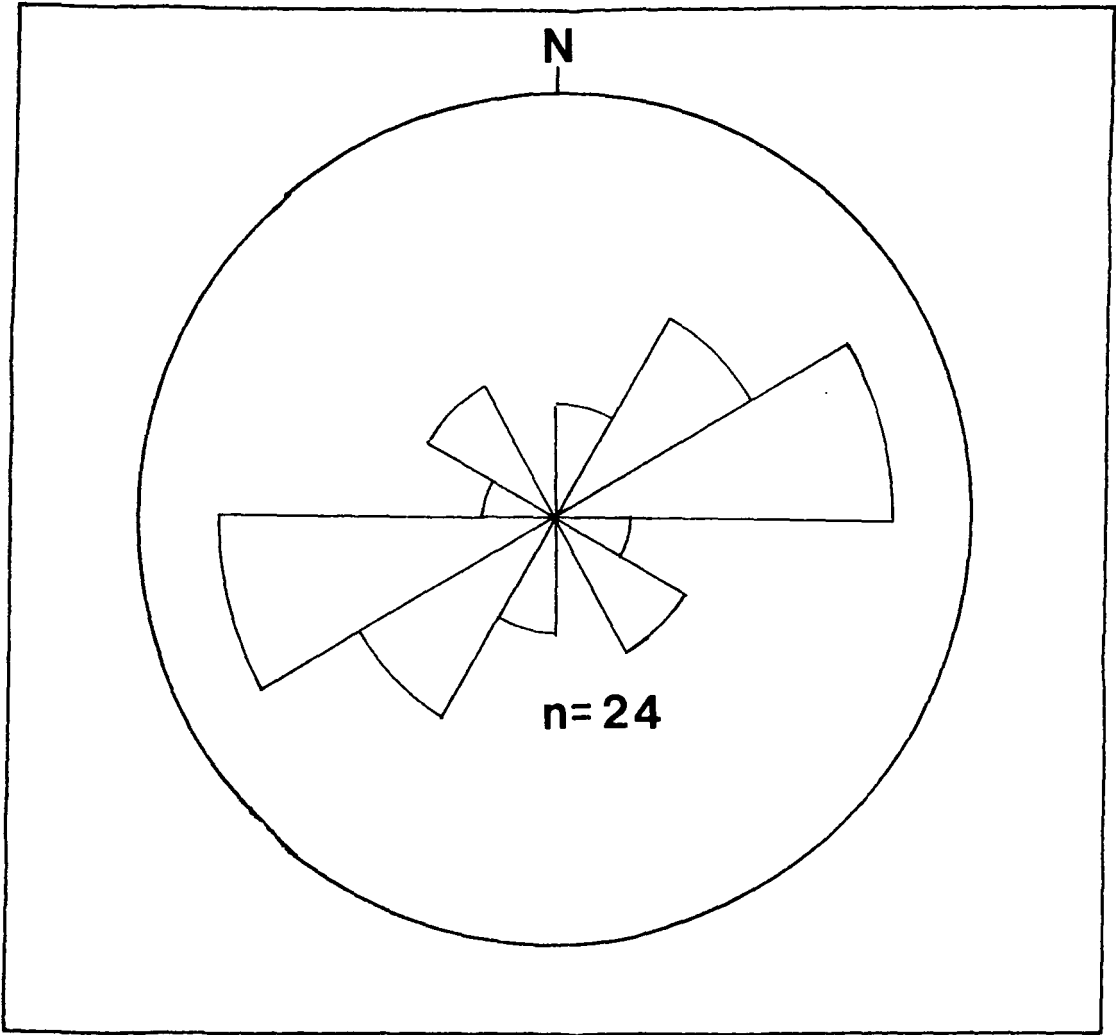


**Fig. 4.8** Rose diagram showing the orientation of the crests of symmetrical ripples from the upper limestones, Sully Bay and Sully Island.

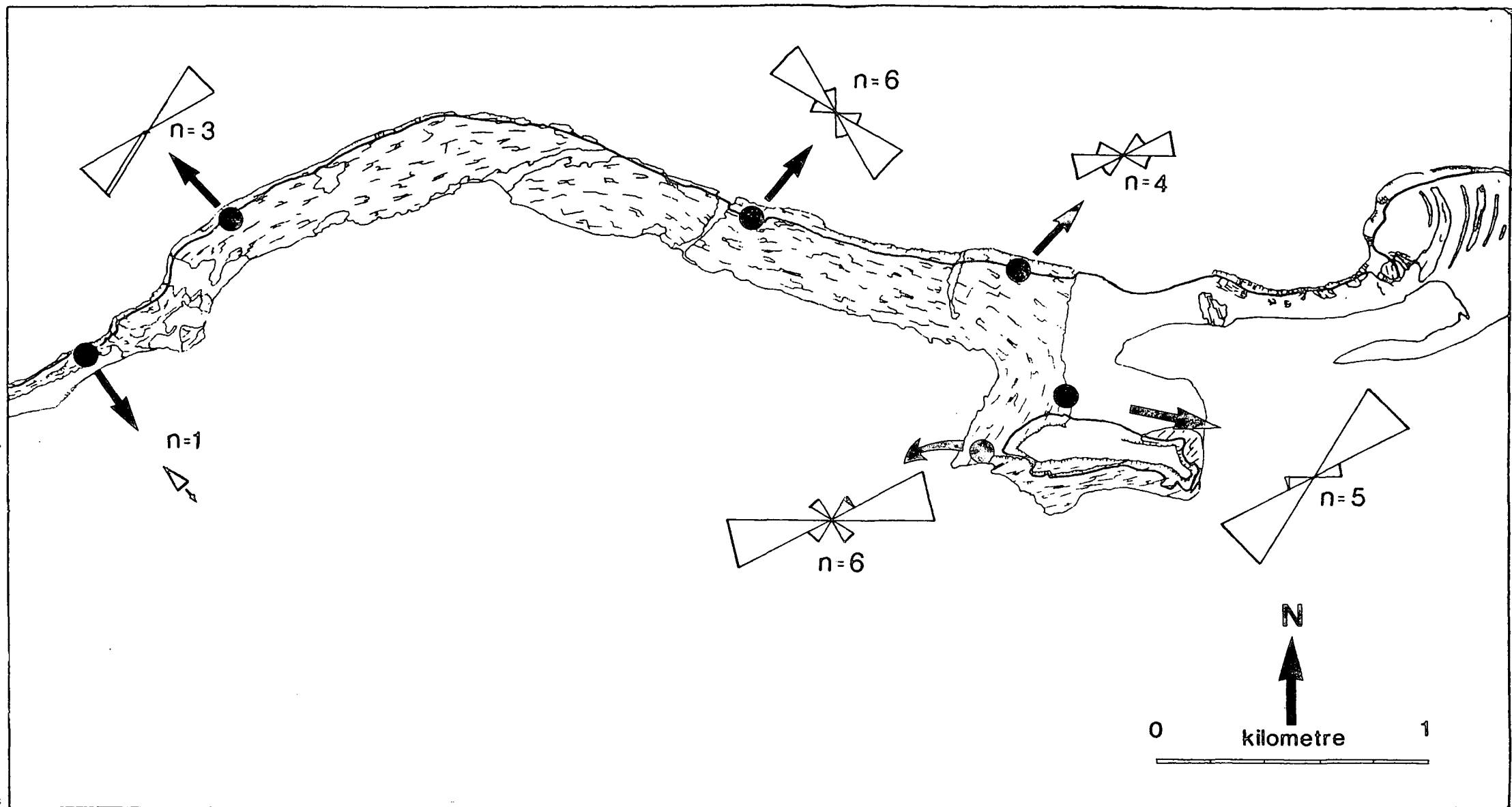


**Fig. 4.9** Individual rose diagrams showing the orientations of the crests of symmetrical ripples at each locality in the upper limestones. Sectors at 30° intervals.

One reading from asymmetrical ripples in a fluvial sandstone, Hayes Point, showing current direction.

they are associated with stromatolites and travertines. These beds consist of fine carbonate which is interlaminated on a millimetric scale. Coarser beds are graded and some have erosive bases. The coarser beds are noticeable in that they locally contain disarticulated ostracod valves ( Tucker, 1978 ), the only macrofauna as yet described in the Norian of South Wales. Within these beds laminoid fenestrae are abundant and are the result of desiccation and shrinkage of the beds, which causes buckling of the laminae. The beds are also cut by numerous desiccation cracks which are filled by crusts of fibrous calcite and sediment ( Fig. 4.11 ). The laminae tend to be white or yellow in colour, with some red layers. In thin section the red colour is present in specific beds and colour changes are sharp. Some laminae of red clay are present which are the result of dissolution of the limestones ( Fig. 4.12 ). This dissolution apparently took place during early burial of the limestones since laminar fenestrae can be lined by an iron rich sediment. Iron rich waters were apparently present during deposition of the limestones as well as early diagenesis. The changes in colour of the laminae may be the result of variations in the aridity of the environment in which the beds were laid down. The coarser graded beds are rarely red in colour, whilst the micritic horizons are commonly haematitic. Variations in the intensity of evaporative effects could be enough to change the Eh/pH conditions such that there was a change in the iron mineral formed. Evidence for more arid conditions during deposition of the red laminae is shown by the presence of rhombic crystals up to 300  $\mu\text{m}$  in length ( Fig. 4.13 ). These crystals are scattered throughout the laminae. Their rhombic nature suggests that they were originally dolomitic although they are now calcitic. Individual rhombs are at present composed of several smaller crystals, evidence for later dedolomitisation. Some laminae are composed of small peloids which in most beds have been partially coalesced to form a grumeleuse texture. The peloids are most clearly seen around the margins of cavities ( Fig. 4.14 ).

The laminated limestones in both Sully Island and Dinas Powys are associated with microbial beds. Some of the laminae themselves have a microbial form and there is a continuous transition between laminated beds and stromatolites. It is possible that <sup>cya-</sup> bacteria played a part in the formation of most of the laminated limestones, trapping fine sediment and stabilising the beds.

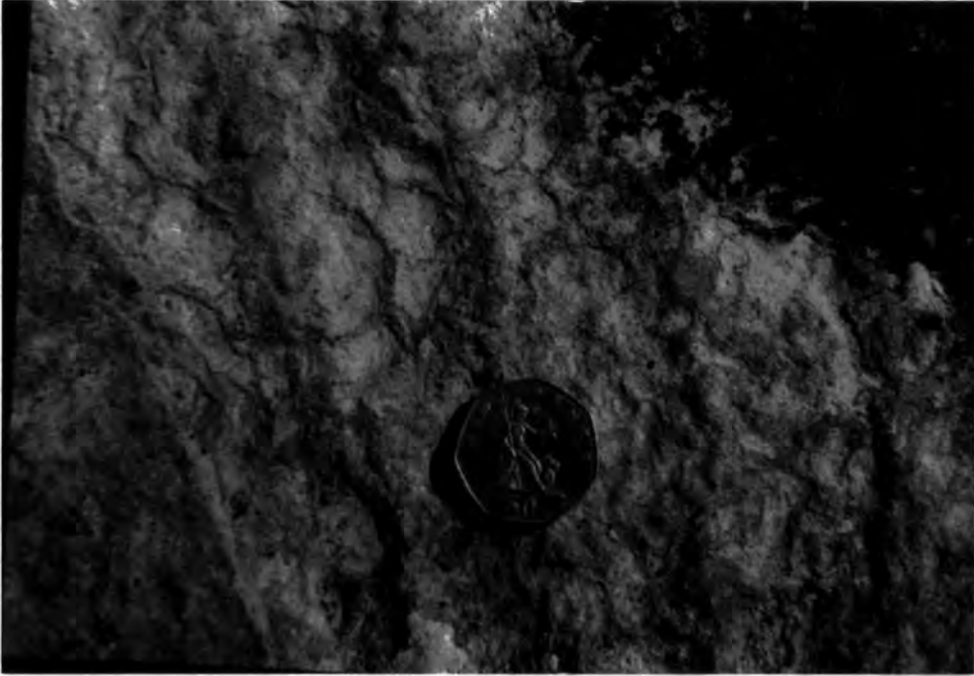


**Fig. 4.10** Symmetrical rippled surface of limestone which has been desiccated due to a change in the level of the water table. East Sully Bay.

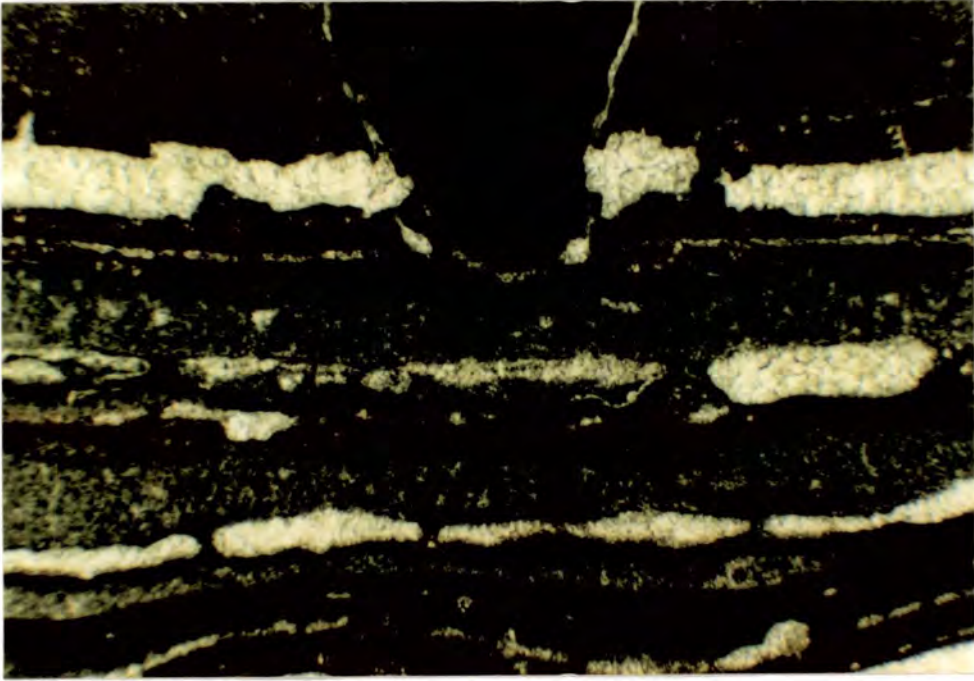


**Fig. 4.11** Photomicrograph of laminated limestone from the Dinas Powys exposure. Interlamination of micritic and coarser carbonate has been modified by formation of laminoid fenestrae. The degree of reddening of the laminae is the result of changes in the amount of iron in the sediment. The laminar fenestra in the centre of the photograph contains some internal sediment. A desiccation crack in the top of the photo is lined by spar and filled by micritic sediment. Plane polars.

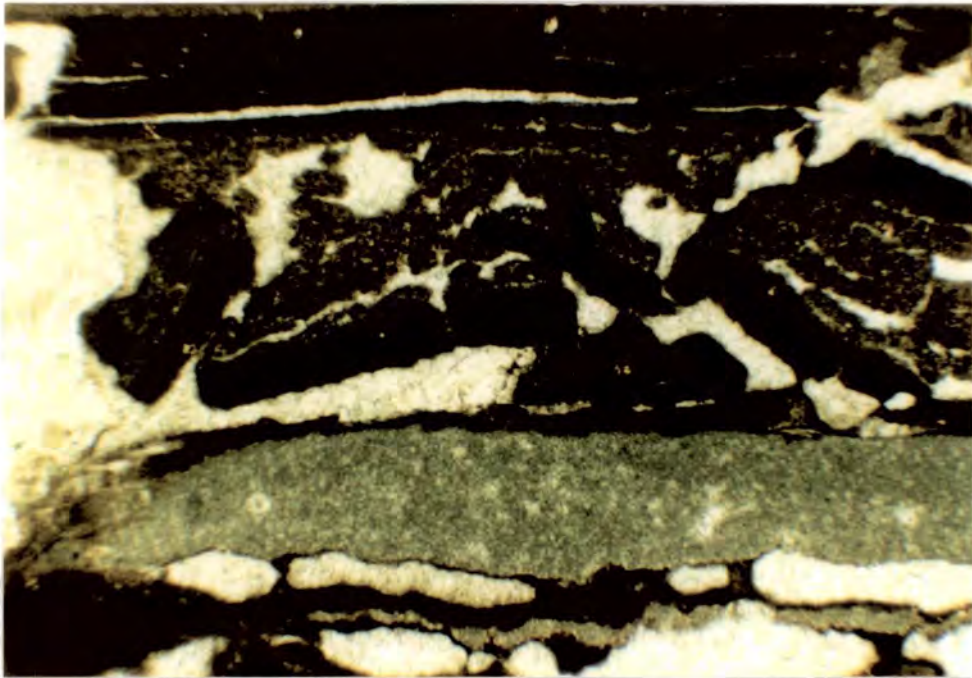


**Fig. 4.12** Photomicrograph showing a collapsed microbial lamination in Dinas Powys limestone formed by dissolution of the laminae. Plane polars.

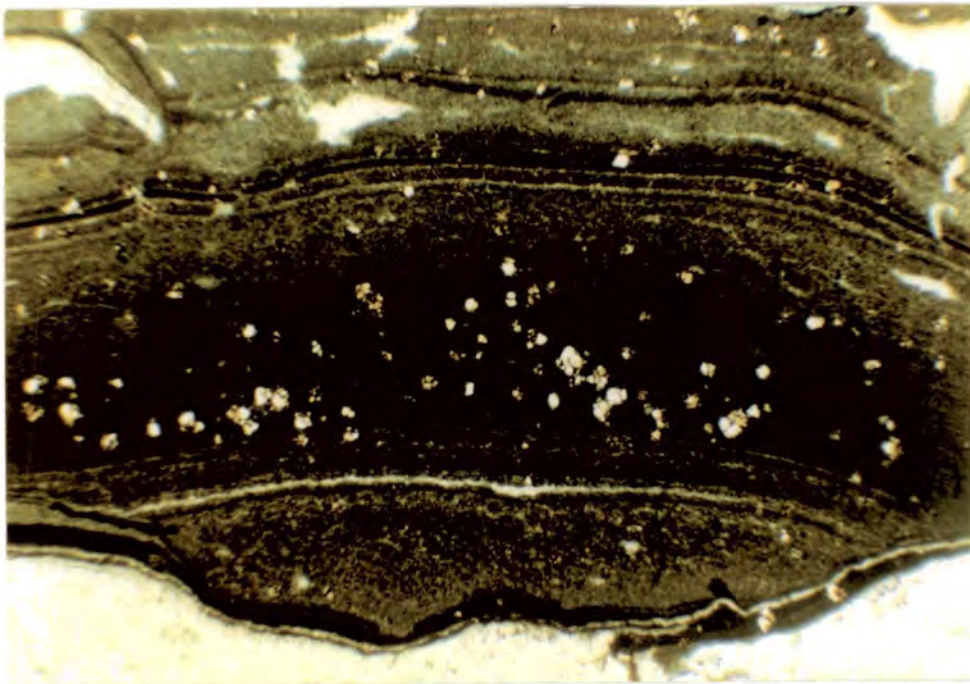


**Fig. 4.13** Photomicrograph of lamination containing rhombic crystals which were originally dolomitic but which were replaced by calcite during an influx of less evaporatively-enriched waters. Sample from Swanbridge. Plane polars.

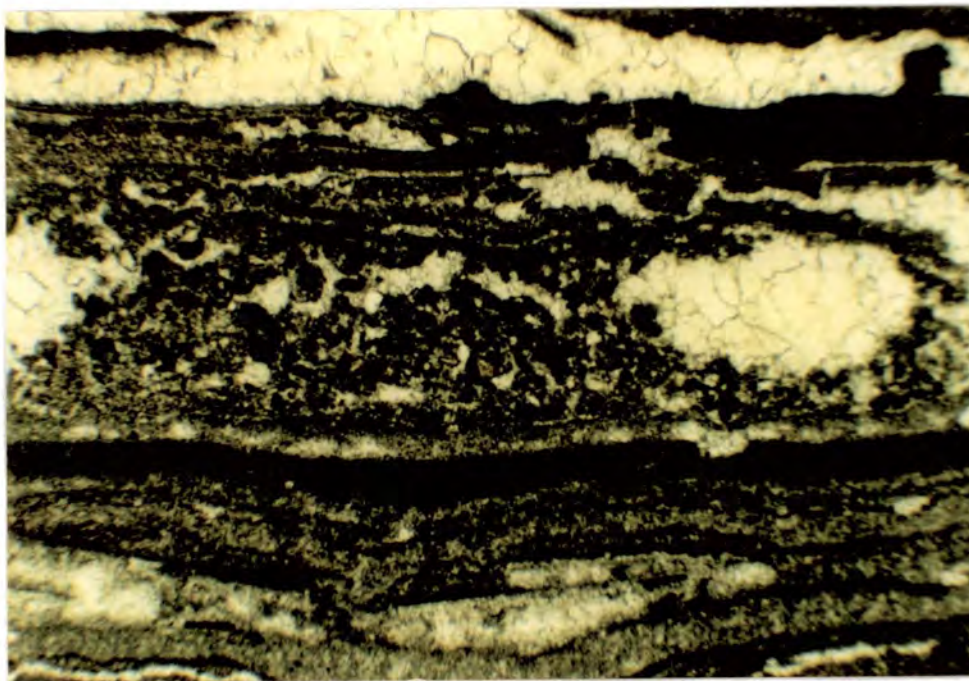


**Fig. 4.14** Photomicrograph of a peloidal / intraclastic lamination from Dinas Powys overlying sheets of flöe calcite and overlain by microbial laminae. The peloidal lamination contains fenestrae and the sediment forms a pillar in the centre of the photograph. Plane polars.

## 4.3 Calcretes

### 4.3.1 Introduction

There are several forms of calcrete in the Limestone Unit, which represent varying stages of maturity of calcretisation. Although the calcretes can be classed as pedogenic there is no direct evidence for biological activity within the calcrete horizons. The basal one metre of the limestones consists of a mature micritic calcrete containing several phases of karstification. In the upper part of the limestones immature calcrete horizons are abundant, taking the form of beds containing vertical nodules and in one case a number of larger amalgamated structures.

### 4.3.2 The Basal Calcrete

The basal part of the limestones is composed of a micritic calcrete between 1.0 and 1.5 metres in thickness which is rarely dolomitised and which contains a number of pedogenic structures ( Fig. 4.15 ). This calcrete is not related to the non-pedogenic groundwater calcrete in the underlying dolomites which has a different mode of origin.

The base of the micritic calcrete is irregular and has a relief of up to 0.5 metres ( Fig. 4.15 ). The irregularity of the base normally takes the form of a regular undulation which has been interpreted as a channeled surface ( Tucker, 1978 ). In places, however, the base is very irregular and cuts sharply into the underlying dolomites. The irregular surface is more likely the result of the pedogenesis rather than a relic erosional surface. Arakel ( 1982 ) has described the evolution of calcrete horizons in salinas in Western Australia and in mature profiles as massive structureless micritic calcrete forms. This massive calcrete is similar to that exposed at the base of the limestones on Sully Island and also has an irregular contact with the underlying host sediment.

The calcrete itself consists of a matrix of micrite and microspar which contains scattered clasts of quartz and Carboniferous Limestone. Circum-granular fractures surrounding nodules up to 3 centimetres in diameter, and scattered veins of

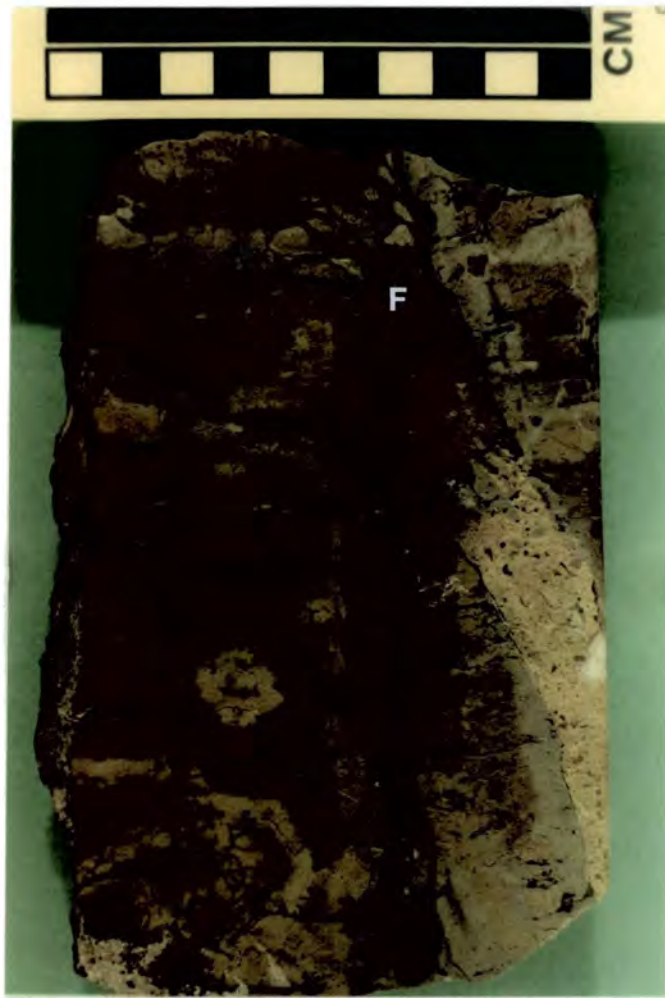


**Fig. 4.15** Polished and etched face of basal calcrete showing two phases of dissolution ( karstification ), the second of which has formed a karstic surface on the top of the calcrete which contains a fissure up to 2 centimetres in width extending 0.5 metres into the calcrete. The fissure contains breccia fragments of calcrete. To the left of the fissure at the top of the karstic surface is a laminated crust ( A ).

calcite are also present. There is no evidence of calcified tubules, microbial coatings or alveolar fabrics which are indicative of biologically induced precipitation of carbonate. As such the basal calcrete can be classified as an alpha-calcrete as defined by Wright ( 1988 ). This calcrete type forms from the evaporative precipitation of carbonate by  $H_2O$  and  $CO_2$  loss in more arid settings. This fits well with the Triassic palaeoclimate. The lack of biogenic input does not preclude the presence of vegetation in the soil itself. Tucker & Burchette ( 1977 ) described several forms of dinosaur footprint in the area of Hayes Point and so some vegetative cover can be assumed in order to feed the beasts.

The calcrete itself has been karstified and cut by several phases of early fracturing ( Fig. 4.16 ). The fractures are composed of micrite and are 2 to 6 millimetres in thickness, with diffuse boundaries. They extend vertically downwards up to 0.6 metres into the calcrete and may be preserved rootlet fractures. They do not appear to branch in any of the faces in which they are exposed and it is also possible that they are the result of physical processes acting during exposure of the calcrete. The fractures cut a series of dissolutional cavities in the calcrete which represent the first phase of karstification and thus they formed late in the evolution of the bed. These karstic cavities are generally oriented parallel to bedding and are filled by geopetal sediment and spar. There is a network of interconnected cavities throughout the calcrete, although they are more common in the upper 0.5 metres of the bed.

The topmost surface of the calcrete has undergone a second phase of karstification and is cut by fissures up to 5 centimetres in width and extending 50 cm into the bed ( Fig. 4.16 ). These fissures cut through the previous phases of dissolution and fracturing, and are filled by sediment and brecciated fragments of the calcrete. To the left of the fissure in Fig. 4.16 is a laminated crust 2 centimetres in thickness. This crust is similar in form to the surficial laminar calcrete of Wright et al. ( 1988b ) and may well be the result of microbial activity ( lichen stromatolites ). The karstified surface of the Pleistocene Key Largo Limestone in Florida, U.S.A. is coated by similar crusts ( Coniglio & Harrison, 1983 ), ( Fig. 4.17 ). Although the climate at present in the Florida area is somewhat less arid than that of the Upper Triassic in Southern Britain, the process of formation of the crust is similar.



**Fig. 4.16** Basal calcrete from south-east corner of Sully Island showing sub-horizontal solution cavities filled by sediment and brecciated calcrete.



**Fig. 4.17** Recent laminated crust 'lichen stromatolite', possibly of similar origin to the crust in Fig. 4.15, on Pleistocene limestone, Big Pine Key, Florida, U.S.A.

The karstification of the deepest part of a mature calcrete profile implies a substantial period of erosion after formation of the calcrete. The sequence of dissolution and fracturing is indicative that there were two periods of karstification between which there may have been a second period of pedogenesis which gave rise to the veining. Alpha-calcretes can take hundreds of thousands of years to form ( Wright, 1988 ). In this case the formation of a mature alpha-calcrete profile was followed by two periods of karstification, which involved the removal of a large part of the original profile. This process may have taken up to one hundred thousand years since the amount of material removed from the upper profile is not known and implies a substantial period of time between the deposition of the rippled dolomites and the formation of the overlying fenestral limestones.

In the clastic sequence to the west there is no evidence of calcretisation or the erosion and removal of the beds laterally equivalent to the upper dolomites. There is abundant evidence of periods of exposure which gave rise to the exfoliation of coarse clasts of Carboniferous Limestone within the sediment ( Tucker, 1974 ). Although karstification does not appear to have taken place it is likely that these exposed beds are equivalent to the calcrete exposed on Sully Island. The formation of the calcrete at Sully Island is related to the local palaeogeography of the area in which rapid changes in the form of deposition take place across the basin.

#### 4.3.3 Nodular Calcretes

Within the 3 to 6 metres of limestone overlying the basal calcrete, less mature pedogenic horizons are abundant. These take the form of beds containing vertically orientated nodules 5 to 10 centimetres in length and 1 to 2 centimetres thick. These horizons are common in the upper limestones exposed in Sully Bay and in the cliffs on the east side of Sully Island where the nodular appearance of the beds has been picked out by weathering ( Fig. 4.18 ). The nodular horizons can cover extensive areas up to 100 metres in diameter, although individual beds are no greater than 20 centimetres in thickness. Stacks of nodular beds are common in Sully Bay where cycles of exposure and deposition have taken place. At outcrop the nodular nature of the beds is accentuated by weathering. On bedding plane surfaces the spaced nature of the nodules in each horizon is shown ( Fig. 4.19 ).

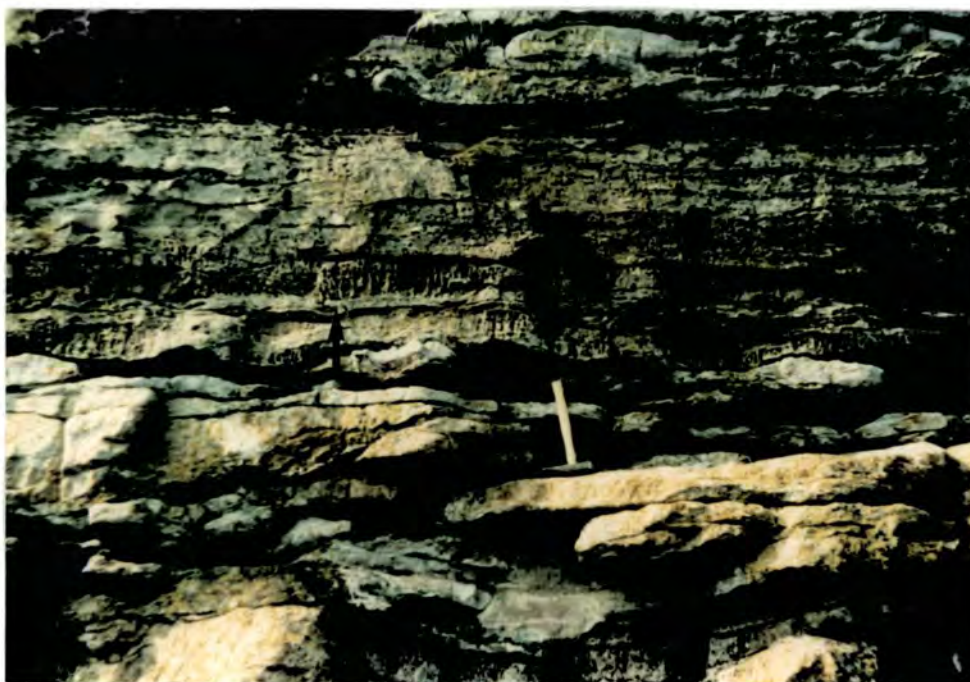


**Fig. 4.18** Cliff showing most of the Limestone Unit, east side of Sully Island. Several nodular calcrete horizons above the hammer have been picked out by weathering. Length of hammer 40 centimetres.  
(arrowed)



**Fig. 4.19** Top surface of nodular calcrete showing the spaced nature of the individual nodules. Desiccation of the nodules has been accentuated by weathering.

In cut faces the nodules are less easy to pick out. The nodules are composed of a fine microspar matrix which has cemented the sediment. The nodules are a finer red colour than the surrounding limestone and in cut faces are less regular in shape than is apparent in weathered surfaces ( Fig. 4.20 ). Individual nodules are composed of a number of coalescing smaller more spheroidal forms. Within nodules fenestrae tend to be better preserved than in the surrounding sediment. This has some implications for the timing of calcretisation relative to the cementation of the limestones. Regression of the lake shoreline and exposure of the limestones must have taken place relatively rapidly. Some fine sub-horizontal fractures in the nodules under 1 millimetres in thickness appear to be a result of the calcretisation rather than preservation of fenestrae. In the limestone not cemented by the nodules, some compaction or possibly sediment infill has taken place, resulting in the removal of much of the fenestral porosity ( Fig. 4.20 ). The nodular form of the calcretes is similar to structures described from red bed sequences in the Mercia Mudstone Group of Somerset ( Wright et al., 1988a ) and from the Devonian of South Wales ( Allen, 1986 ). The nodular calcretes represent an immature stage of the process of which the basal calcrete is the mature end-member. The nodules can again be classified as an alpha-calcrete type.

#### 4.3.4 Blocky Calcrete

In one area along Sully Bay a bed of red-yellow coloured blocky material is exposed interbedded with fenestral limestones 1.5 metres below the top of the Limestone Unit ( Fig. 4.21 ). The blocky bed is 0.3 to 0.6 metres in thickness and superficially resembles a conglomerate. It can be followed for 20 metres along the shoreline. This bed appears to have formed in a similar way to the nodular calcretes. The nodular structure is still apparent but individual nodules have coalesced to form larger structures up to 70 centimetres in diameter. The calcrete has not reached the mature stage in which nodules have fully coalesced to form a massive bed, and is an intermediate stage between the nodular and massive forms. The calcrete implies that a more extended period of exposure took place locally in the centre of Sully Bay, giving rise to a more mature calcrete. It is possible that this area had slightly higher relief during deposition of the limestones such that



**Fig. 4.20** Polished face of nodular calcrite showing the subtle colouration of the nodules which are cemented by microspar. Note the preservation of fenestrae within the nodules accentuated as joint-plane crystallaria.



**Fig. 4.21** Blocky calcrete underlying fenestral limestone, central Sully Bay. The 'nodules' have amalgamated and have a blocky texture similar in colour and form to the basal calcrete but not massive. This bed is 1.5 metres below the top of the Limestone Unit.

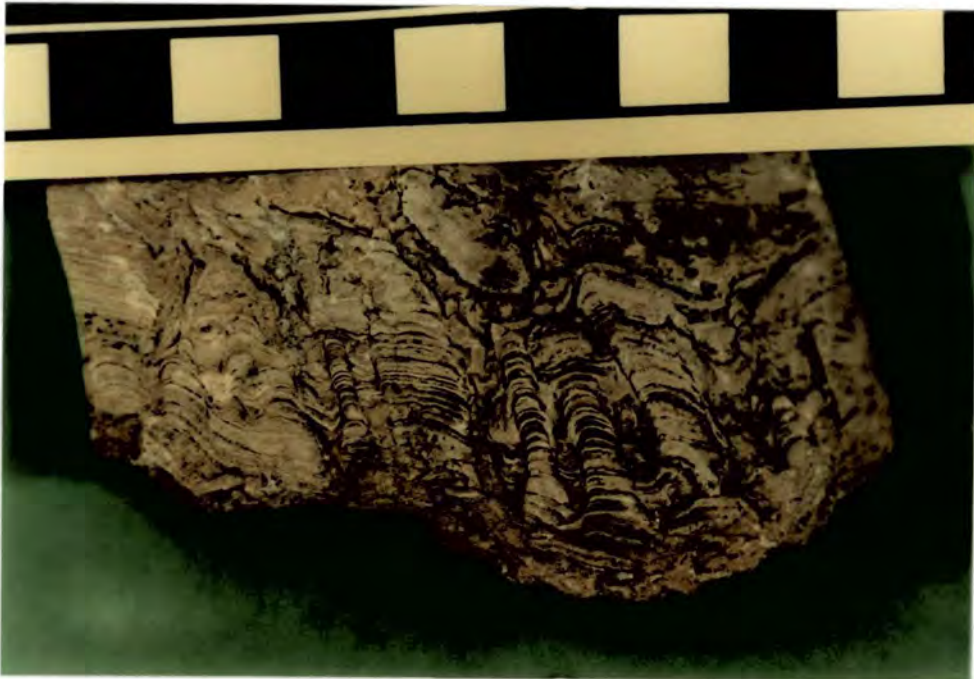


**Fig. 4.22** Weathered surface of columnar stromatolite, Dinas Powys. The columns are of constant basal radius and are overlain by planar-laminated beds.

exposure was prolonged. The deflection of ripple crest orientations immediately to the west of this area of calcretes may be an indication that the blocky calcrete was emergent and formed an irregularity in the lake shoreline when adjacent beds were in the sublittoral environment.

#### **4.4 Microbial Laminated Carbonates**

##### **4.4.1 Introduction**

There are several forms of microbially-laminated carbonate in the limestones at Sully Island and Dinas Powys. In this section laminar and domed stromatolitic forms and oncoids are described. There is evidence for the influence of microorganisms in many of the travertine deposits which will be discussed in Section 4.5. This section forms the main part of a paper in press describing the stromatolites ( Tucker & Leslie, in press ). Microbial beds are common in the Dinas Powys outcrop and in the cliffs east of Swanbridge, where they have been partially dolomitised. The microbial carbonates are subdivided on the basis of their morphology into laminar and columnar ministromatolites and oncoids. On a larger scale mound structures associated with polygonal fissures in eastern Sully Bay also appear to be of microbial origin.

##### **4.4.2 Columnar Stromatolites and Oncoids**

Columnar stromatolites are best exposed at Dinas Powys where they are interbedded with laminated limestones. The weathering of the rock has highlighted the morphology of the columns ( Fig. 4.22 ). Individual columns are up to one centimetre in width and 5 centimetres high, and are thus more correctly called ministromatolites. Most columns have a constant basal radius, although some change in width upwards. At Dinas Powys the ministromatolites form part of a larger mound structure 0.5 metres across and 0.3 metres in height. The microbial beds are intimately associated with the laminated limestones and travertines and columns can overgrow intraclasts ( Fig. 4.23 ) and flowstones.

In thin section the columns are composed of laminae of microspar or micrite and fibrous calcite ( Fig. 4.24 ), which are identical in form and preservation

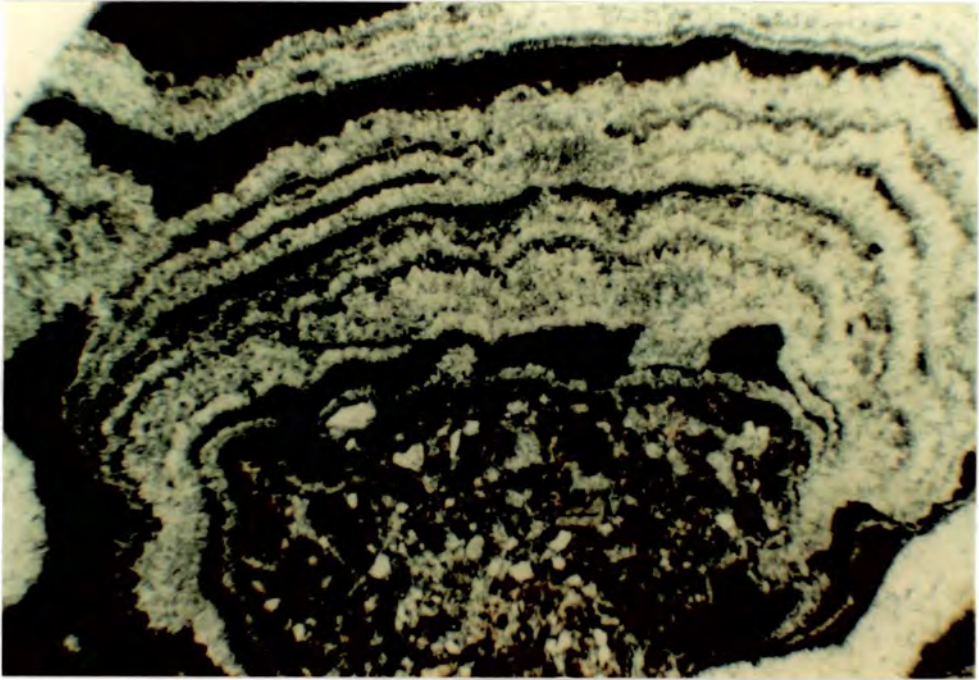


**Fig. 4.23** Photomicrograph showing a stromatolite overgrowing a clast of intrapelsparite. This specimen is not oncoidal - there is no growth on the base of the clast. Plane polars.

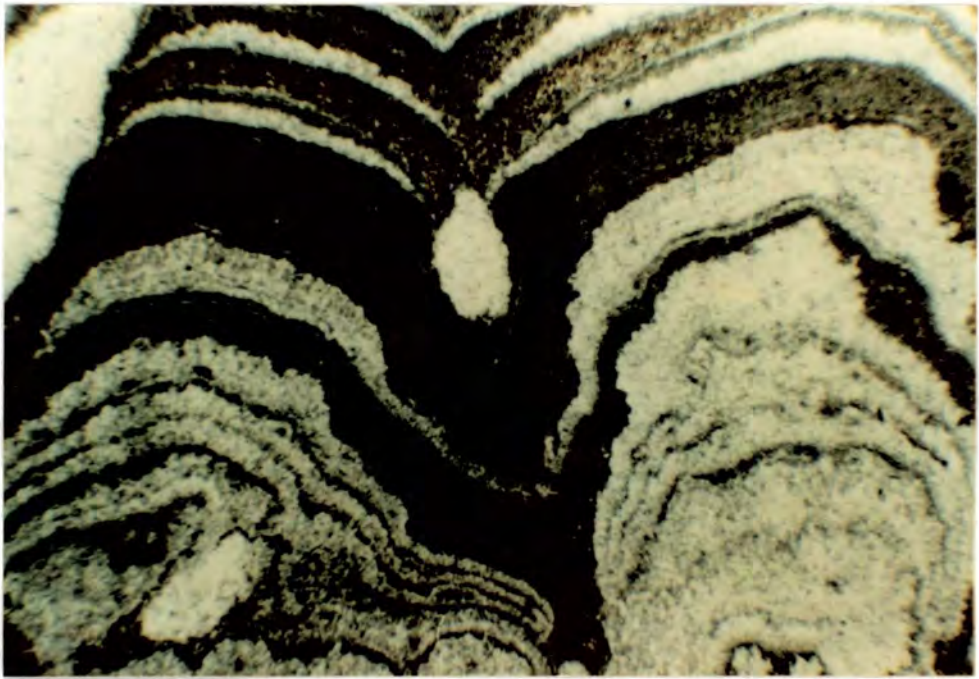


**Fig. 4.24** Photomicrograph of two columnar stromatolites which consist of laminae of sediment and fibrous calcite. The two columns are laterally-linked and merge upwards into one broad column. Plane polars.

to Proterozoic ministromatolites from the Canadian Shield ( Hofmann & Jackson, 1987 ). Individual laminae are thickest in the centre of columns. Many columns have amalgamated as they grew upwards, becoming laterally linked ( Fig. 4.24 ). These forms could be described as close-spaced laterally-linked stacked hemispheroids under the classification of Logan et al. ( 1964 ).

Oncoids up to 8 centimetres in diameter are present in the laminated limestones east of Swanbridge ( Fig. 4.25 ). The oncoids are similar in composition to the columnar forms. Individual laminae are asymmetric, in particular the outer laminae. Some oncoids consist of an inner concentrically laminated zone which has then been overgrown by a columnar form as the oncoid became fixed on the floor of the pool. Superficial oncoids <sup>can</sup><sub>also</sub> consist of several laminae overgrowing a nucleus of intraclastic limestone ( Fig. 4.26 ). Oncoids are not common in any of the microbial beds. They can occur individually within laminated beds ( Fig. 4.25 ). No oncoids have been found in the Dinas Powys exposures.

#### 4.4.3 Laminar Stromatolites

Laminar stromatolites occur within the finely laminated limestones east of Swanbridge and at Dinas Powys. East of Swanbridge weathering has picked out the dolomitised sparry laminae ( Fig. 4.27 ). The difference between the laminated and microbial beds is not great and individual laminae can contain microbial lamination within normally bedded sediment ( Fig. 4.28 ). Microbial beds commonly display most evidence of desiccation indicating their formation during periods of peri-supralittoral conditions. Locally within the planar laminated beds small columns are developed upon coarser clasts or upon the upturned edges of desiccation cracks ( Fig. 4.29 ). The microbial laminae are 0.1 to 2.0 millimetres in thickness and are laterally persistent. Fenestral limestones at the east end of Sully Bay contain some clasts with microbial lamination. In this case the mats of microbial material did not survive the perilittoral conditions and are present only as fragmented intraclasts.



**Fig. 4.25** Transported asymmetrical oncoïd in planar and locally domal ( to the left of the coin ) stromatolites, Swanbridge. Oncoïds occur scattered throughout the Swanbridge upper limestones but have not been found in beds.

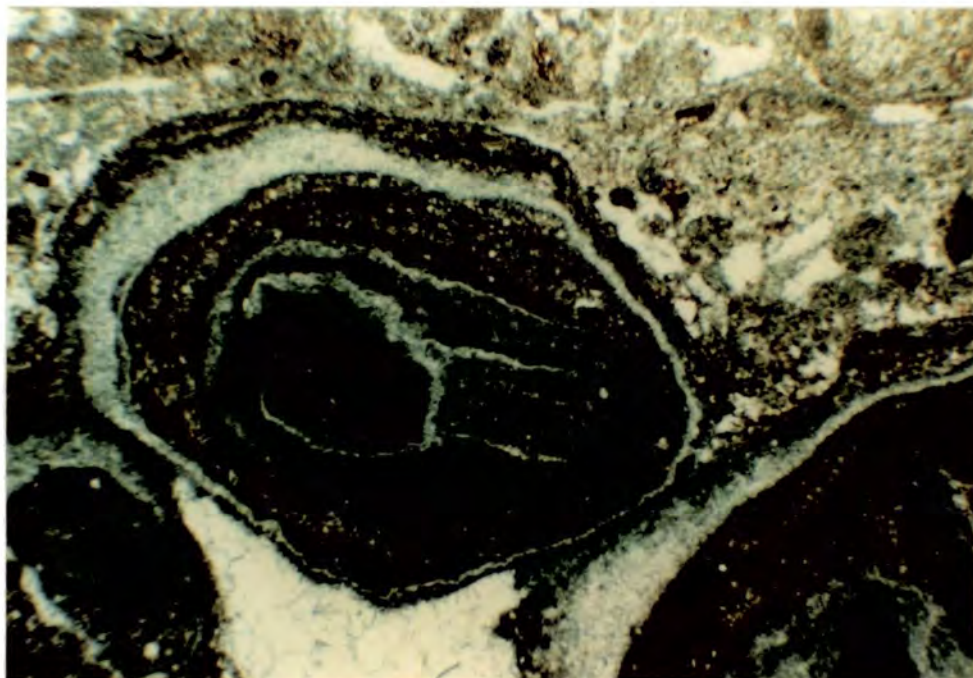


**Fig. 4.26** Photomicrograph of asymmetric pisoid within intraclastic limestone. The lamination in the pisoid is the result of microbial activity. This pseudo-oncoïd has overgrown two nuclei of limestone.

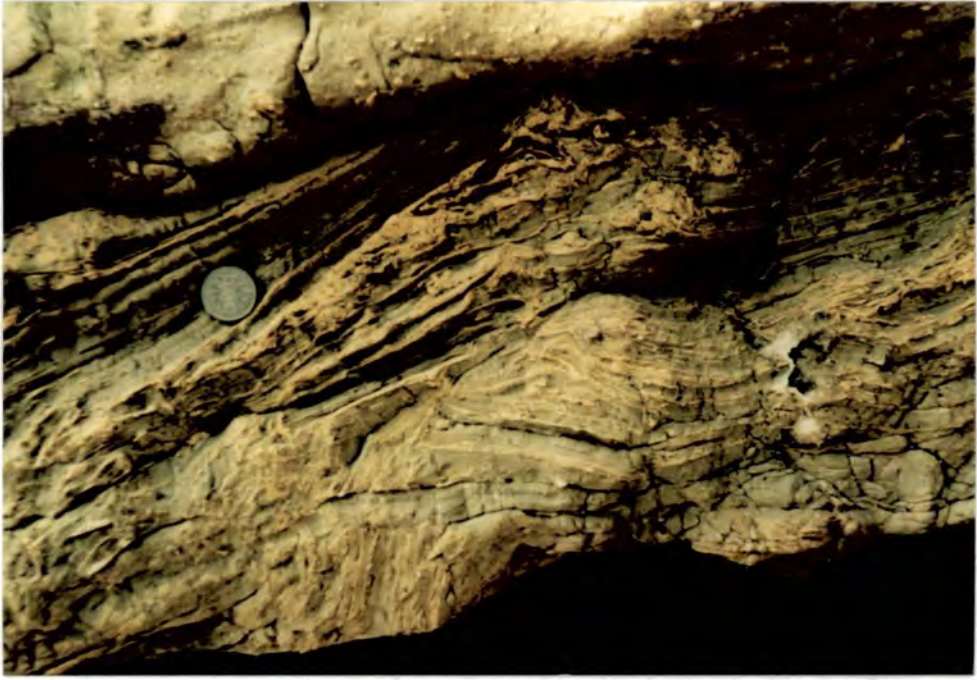


**Fig. 4.27** Dolomitised planar laminated stromatolites, Swanbridge. In this case the laminae of fibrous calcite are picked out by weathering, accentuating the lamination.

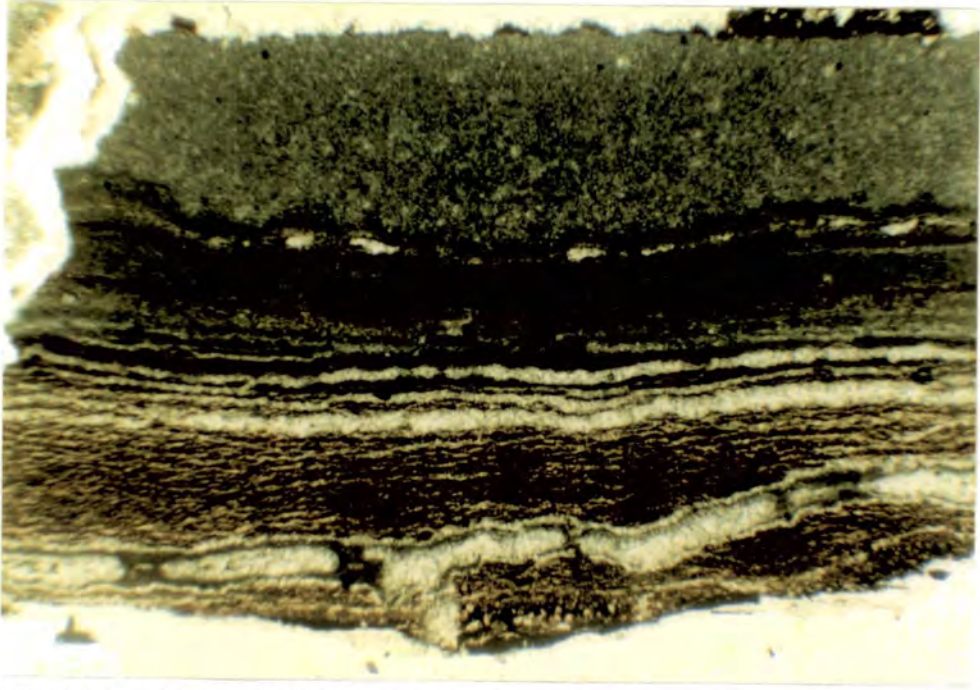


**Fig. 4.28** Photomicrograph of laminated limestones. The lowermost iron-rich lamination, which is cut by a later fracture, contains microfenestrae which are the result of the formation of individual microbial mats. Plane polars.

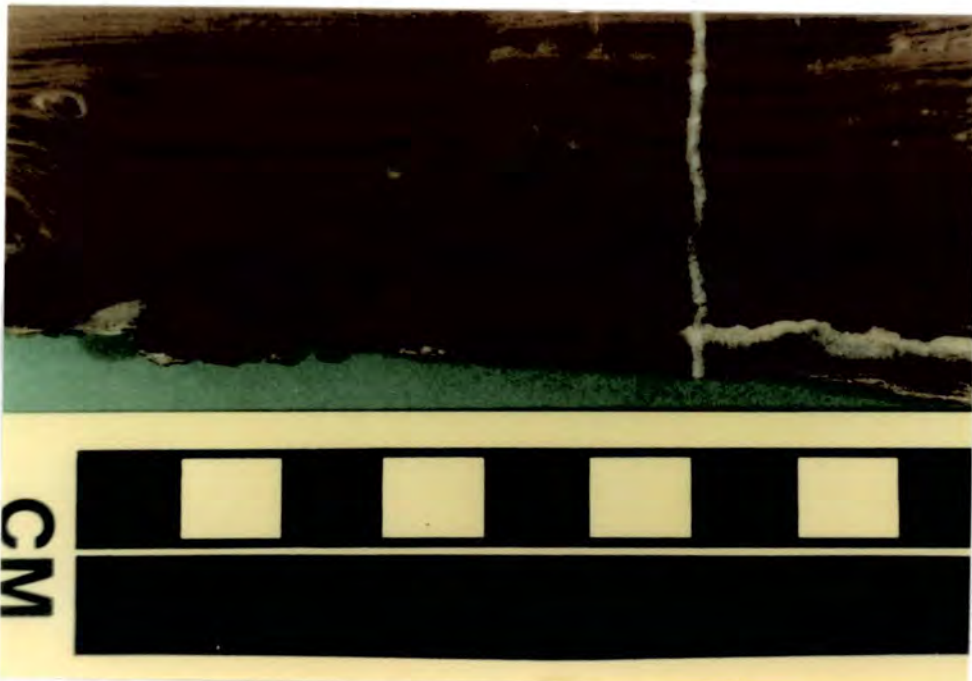


**Fig. 4.29** Polished surface of laminated limestone with locally developed domes in the centre of the photograph.

#### 4.4.4 Microbial Mounds

On the wave-cut platform at the eastern end of Sully Bay a series of mound-like structures up to one metre in width and 0.5 metres in height are exposed ( Fig. 4.30 ). These mounds are linear and can be up to 3 metres in length, and form a rough polygonal pattern. The surface of these mounds has been desiccated and small polygons 5 centimetres in diameter cover the surface. The crests of some of the mounds contain fissures which do not appear to be caused by desiccation ( Fig. 4.31 ). No internal structure can be seen in the mounds which have been dolomitised.

The shape of the mounds and their polygonal pattern suggests that they are related to polygonal fissures from which upwelling groundwaters issued ( Section 4.6 ). Preferential growth of microorganisms at these fissures has been described from several Recent salinas on the Australian coast ( Von der Borch et al., 1977; Ferguson et al., 1982; Handford et al., 1984 ). It is likely that the mounded structures in the limestones at Sully Bay represent the growth of stromatolites preferentially around points of groundwater emergence.

#### 4.5 Travertine Deposits

##### 4.5.1 Introduction

Travertine or spring deposits are locally common throughout the Limestone Unit at Sully Island and make up a large part of the Dinas Powys exposure, interbedded with laminated and stromatolitic limestones. In the limestones in the Sully Island area the travertines occur in localised areas related to the distribution of temporary spring outlets. Travertine accumulations can be up to one metre in thickness and 5 to 6 metres in diameter ( Fig. 4.32 ). These large travertine mounds are the result of long-lived springs which precipitated large amounts of carbonate. By contrast, individual sheets or crusts as thin as one millimetre formed during short periods of discharge. The travertine deposits are scattered throughout the Limestone Unit at Sully Island but are most common in the top-most 2 metres. The travertines themselves can be subdivided on the basis of the morphology of the carbonate precipitated. Sheets of calcite or flowstones are the



**Fig. 4.30** Diffuse mound structures up to 2 metres across which have a desiccated surface, east Sully Bay. These mounds are the result of the growth of microbial beds around areas of spring discharge. In this case the emergent waters did not precipitate carbonate.

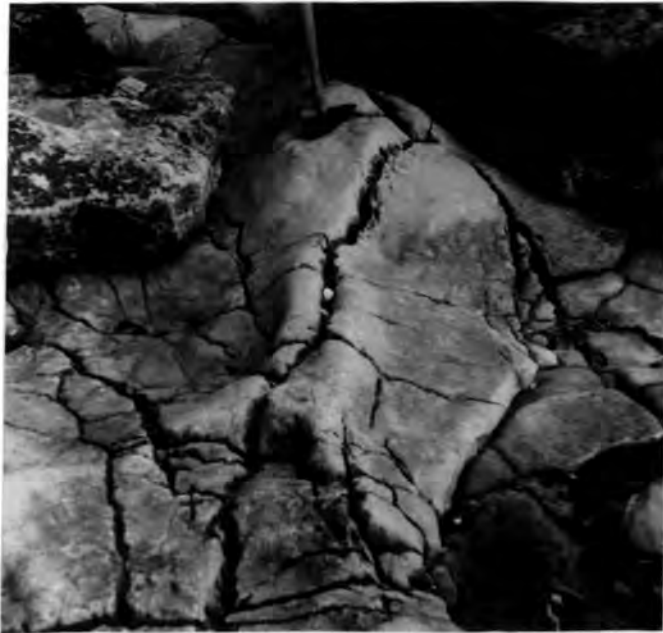


**Fig. 4.31** Elongate mound structure with some brecciation of the limestone ( below hammer ) at the mound crest Length of hammer 40 centimetres.



**Fig. 4.32** Large travertine accumulation 1 metre below the top of the limestones, south-west Sully Island, consisting of flowstone with minor pisoids and flöe calcite. This travertine is up to 0.7 metres in thickness and over 5 metres in diameter. Length of hammer 40 centimetres.



**Fig. 4.33** Plan view of a smaller travertine 2 metres in diameter, consisting of several sheets of flowstone under 1 centimetre in thickness. The weathered surface of the limestone cuts numerous domes which reflect the mammilated surface of the flowstone.

most common form of travertine. Also present in the travertines are flöe calcite and pisoids. The exposure of the travertines is not sufficient to relate individual travertine deposits to spring outlets.

#### 4.5.2 Flowstones

Flowstones or sheets of calcite are the most abundant of the forms precipitated by the spring waters. Flowstones formed as crusts on the surface of the limestones. Similar crusts also coat cavities which formed by fracturing and dissolution of the limestone. The formation of these cavities is discussed in Section 4.6. Individual flowstones can cover areas of up to 10 square metres. On average flowstones which occur independently of other travertine forms cover between 1 and 3 square metres. The surface of the flowstone both reflects the topography of the underlying limestone and also has a mammilated form which is the result of the presence of numerous small domes up to 3 centimetres in diameter ( Fig. 4.33 ). This irregular surface is a common feature of flowstones ( Folk et al., 1985 ) and is related to the fibrous crystal form of the calcite.

The majority of the flowstones are composed of sheets of fibrous or tabular calcite interbedded with sediment ( Fig. 4.34 ). Inclusions within the calcite crystals show up the successive positions of crystals during growth. The prismatic crystal terminations are well developed and are shown up against the overlying dark sediment ( Fig. 4.34 ). Individual crystals in successive sheets can be overgrown in optical continuity where the covering of sediment is not complete. The sheets of calcite are not laterally continuous and in some cases columns of locally developed fibrous calcite are developed ( Fig. 4.35 ). These are similar in form and scale to stromatolitic columns and there may have been a microbial influence in the localised precipitation of such material. Within the calcite sheets are small 'clots' of micritic material ( Fig. 4.34 ). These may be the result of bacterial activity during travertine formation. Similar forms of micrite have been described from Quaternary travertines in Italy ( Folk et al., 1985 ). The flowstone is interbedded with micritic sediment which is locally iron rich and when occurring between sheets of flowstone contains a number of small spar filled pores which have a net-like appearance ( Fig. 4.36 ). These structures may be the relics of stacks of <sup>cya</sup>no-<sub>bacterial</sub> mats which have been preserved from compaction



**Fig. 4.34** Photomicrograph of flowstone which is interbedded with micritic sediment. The flowstones show good crystal terminations against the overlying sediment. In the centre of the photograph, where the sediment cover is thin, several phases of calcite are in optical continuity. Some 'clots' of micrite ( arrowed ) within the flowstones may be the result of bacterial activity. Crossed polars.

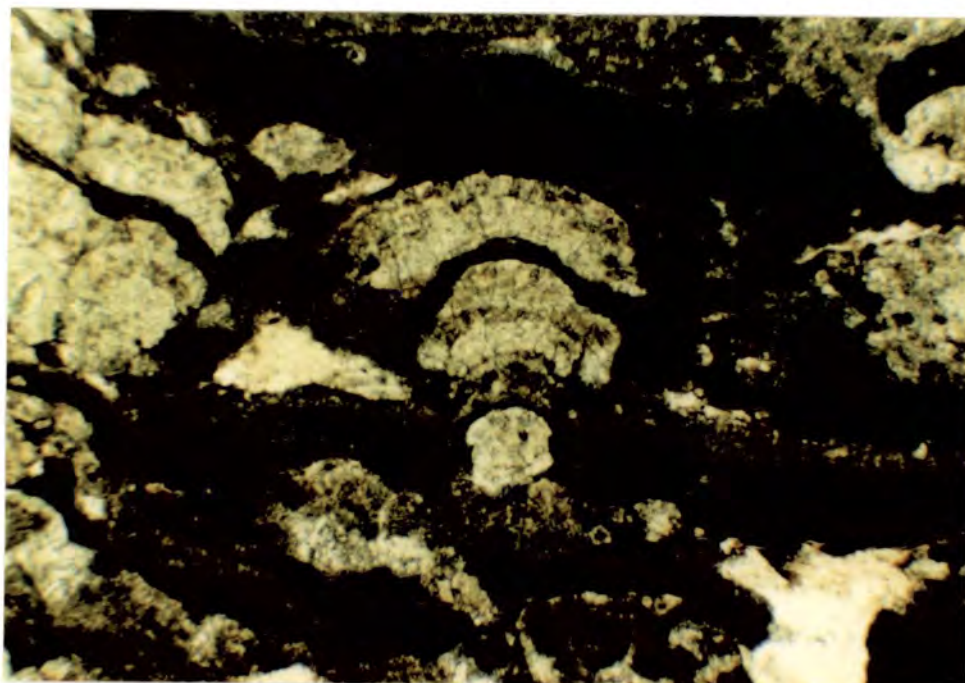


**Fig. 4.35** Photomicrograph of small column consisting of three phases of calcite growth within iron-rich micrite. The column increases in width upwards and is not linked to the adjacent flowstones. Plane polars.

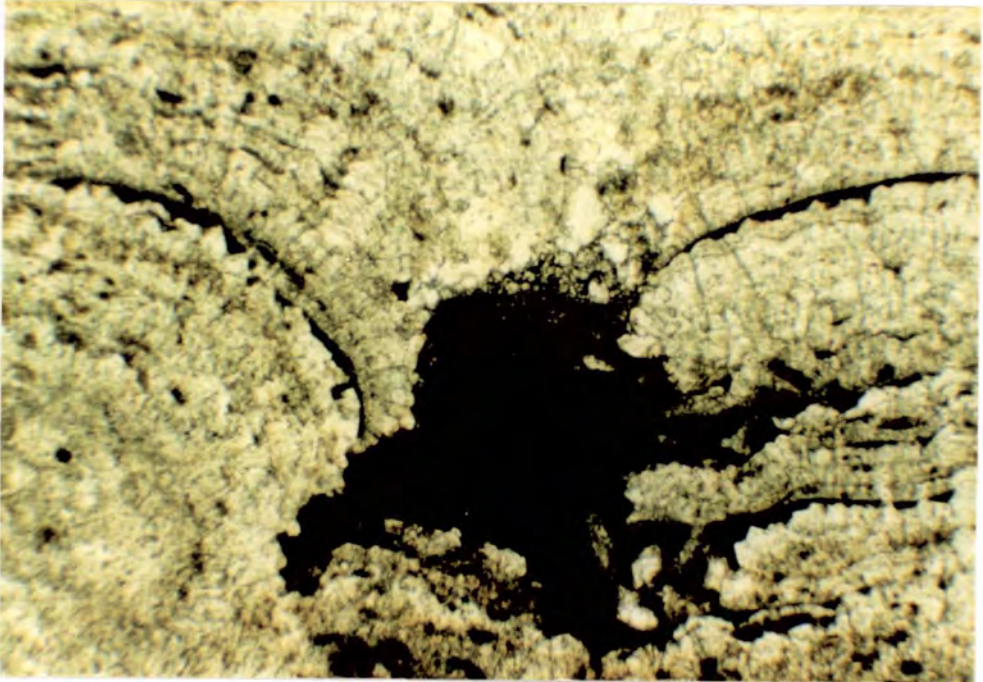


**Fig. 4.36** Photomicrograph of micritic sediment in between two domed flowstones. The sediment appears to have a microbial lamination and may have been preserved by the presence of the two flowstones. Numerous small clots of micrite in the flowstones. Field of view 1.2 millimetres. Plane polars.



**Fig. 4.37** Photomicrograph of a radial fan of columnar radiaxial calcite crystals in a flowstone. The columns can be up to 4 centimetres in length. Crossed polars.

by their proximity to the sheets of flowstone. During deposition the <sup>cyanobacterial</sup> mat probably covered the sediment surface and has been preferentially preserved by the more solid flowstone which has resisted compaction.

The second type of flowstone is composed of columnar calcite crystals which display a radiaxial fabric in crossed polars when studied in thin section. The columns are up to 5 millimetres in length and 0.2 to 0.5 metres thick. The columns contain very fine inclusions which in places are aligned along successive growth positions of the crystal. In most of the crystals the inclusions do not show any clear pattern. The radiaxial pattern of extinction indicates that on a microcrystalline scale the optic axes within any one crystal are convergent upwards. Radiaxial fabric has been described as both a primary and a replacement texture ( Kendall & Tucker, 1973; Kendall & Broughton, 1978; Kendall, 1985 ). It is now recognised that radiaxial fabric is not diagnostic of any one particular mode of formation. There are a number of lines of evidence to suggest that the radiaxial flowstones at Sully Island are a primary fabric. The radiating fan-type arrangement of successive crystals within one sheet is retained and this is similar to the crystal form of the travertines described by Folk et al. ( 1985 ). The flowstone sheets are interbedded with haematitic sediment ( Fig. 4.38 ). The terminations of each phase of crystal growth do not display prismatic crystal terminations, although such faces are implied by the inclusion pattern in some of the columnar crystals. Many of the terminations of the crystals appear to have been rounded ( Fig. 4.39 ). A similar feature has been described from Recent spring deposits in South Wales ( Braithwaite, 1979 ). In the Recent example the columnar calcite terminations have been rounded as a result of variations in the degree of saturation in the carbonate ion in the waters in which the travertines formed. The chemical composition of spring waters is known to be variable on an annual scale and also as a result of longer scale variations in climate. The action of soil-derived humic acids has been proposed as a further variable which can affect the solubility of carbonate. The columnar flowstones on Sully Island display a cyclical sequence of precipitation of columnar calcite followed by some dissolution of crystal terminations and deposition of sediment. During times when there was a reduced supply the sediment has filled in the depressions between individual crystals.

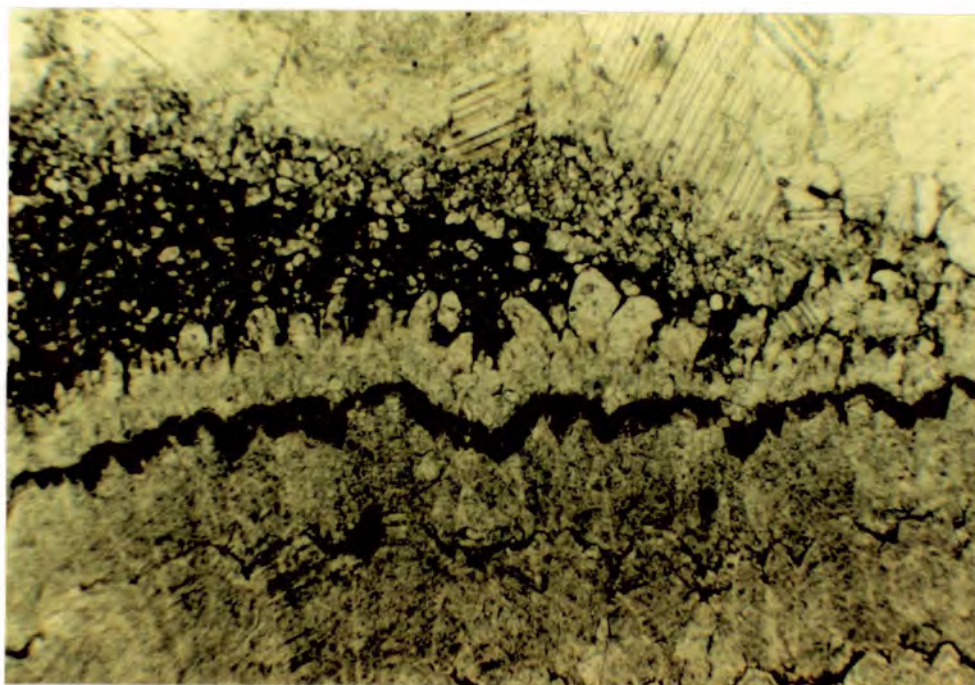


**Fig. 4.38** Photomicrograph of top of the flowstone columns in Fig. 4.37 . The tops of several phases of columns have been rounded by dissolution after formation.

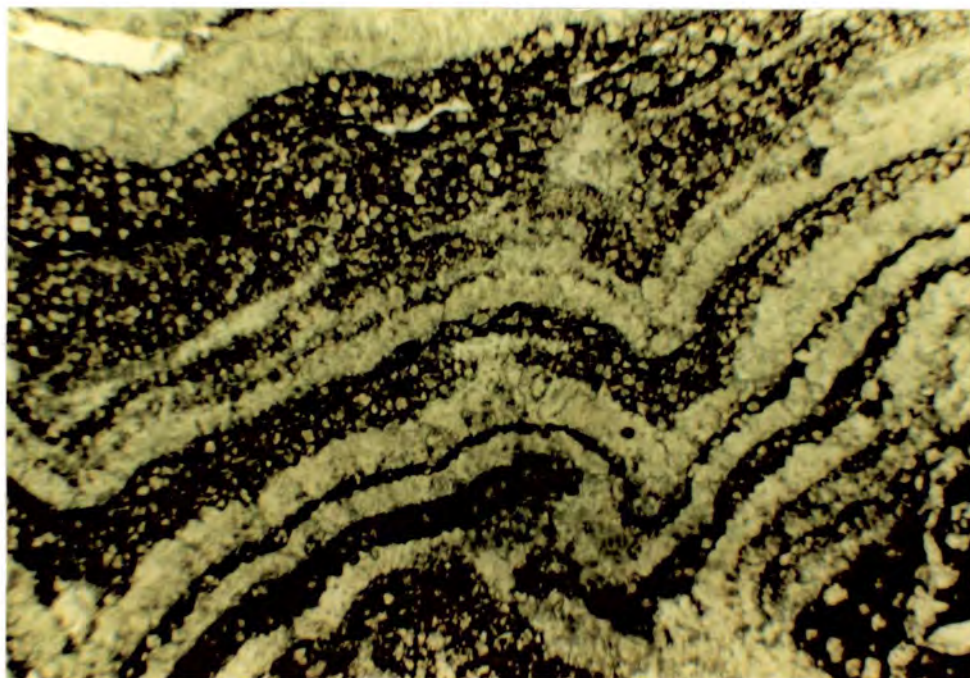


**Fig. 4.39** Photomicrograph of interlaminated columnar flowstone and iron-rich sediment containing rhombic dolomite. The very fine interlamination of calcite and dolomite is the result of decomposition of algal sheath material in the sediment laminae during diagenesis which releases  $Mg^{2+}$  into the microenvironment. Plane polars.

The sediment interlaminated with the columnar flowstones on a millimetric scale is a haematite-rich micrite in which dolomite rhombs up to 0.5 millimetres in length are developed ( Fig. 4.39 ). These dolomites are very iron rich themselves although the calcites contain little iron ( 100ppm ). The presence of well developed dolomite rhombs within millimetric laminations in a flowstone composed of primary calcite is a curious phenomenon. The formation of dolomite was extremely localised and there is no sign of alteration of the calcite adjacent to the micritic laminae. The laminae of haematitic micrite are constant in thickness across the appreciable surface topography of the flowstone ( Fig. 4.39 ). The sediment cover is only broken in areas where the fans of columnar calcite form overhangs. The morphology and fine interbanding of the sediment laminae is indicative of microbial lamination. Finely interlaminated calcite and dolomite have been described from a number of ancient carbonate sequences ( Gebelien & Hofmann, 1971 ). In these beds the concentration of  $Mg^{2+}$  into algal sheath material, which is observable in Recent algal mats, resulted in a microenvironment in which  $Mg^{2+}$  was released into the sediment during diagenesis. This  $Mg^{2+}$ , released upon the decomposition of the algal material, caused the precipitation of a magnesium rich carbonate phase which becomes a well ordered dolomite upon mineralogical and crystallographic stabilisation. The process of algal sheath decomposition can take place over hundreds of thousands of years ( Gebelein & Hofmann, 1971 ) and so the dolomite present in the flowstones is most probably a diagenetic mineral, albeit controlled by the distribution of primary organic rich layers. There is no evidence at present in the sediment for the original presence of organic material, although many microbial sediments have lost the evidence of their origins in the first few metres of burial.

Further evidence for the biogenic influence in the travertines is seen in flowstones interbedded with fenestral sediment in Sully Bay ( Fig. 4.40 ). In one of the finer sediment laminae a number of small, digitate structures 0.5 millimetres in height are present. These structures are composed of micritic sediment and are similar in form and size to those described by Folk et al. ( 1985 ). These have been interpreted as the products of photosynthetic bacteria which in the Italian examples formed daily laminae of shrub-like forms. In Fig. 4.40 six micritic laminae containing evidence of these bacterial clumps are present, interlaminated

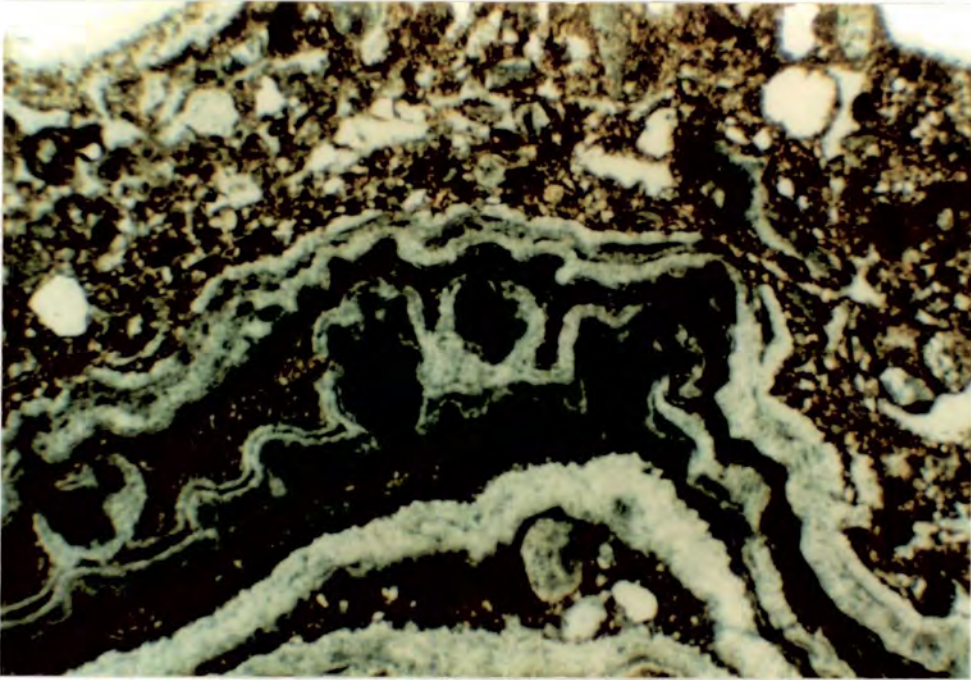


**Fig. 4.40** Photomicrograph of small digitate micritic structures within flowstones overlain and interbedded with intraclastic limestone. The micrite masses are similar in form to 'shrub-like' structures in Recent travertines in Italy which are the result of bacterial growth. Plane polars.

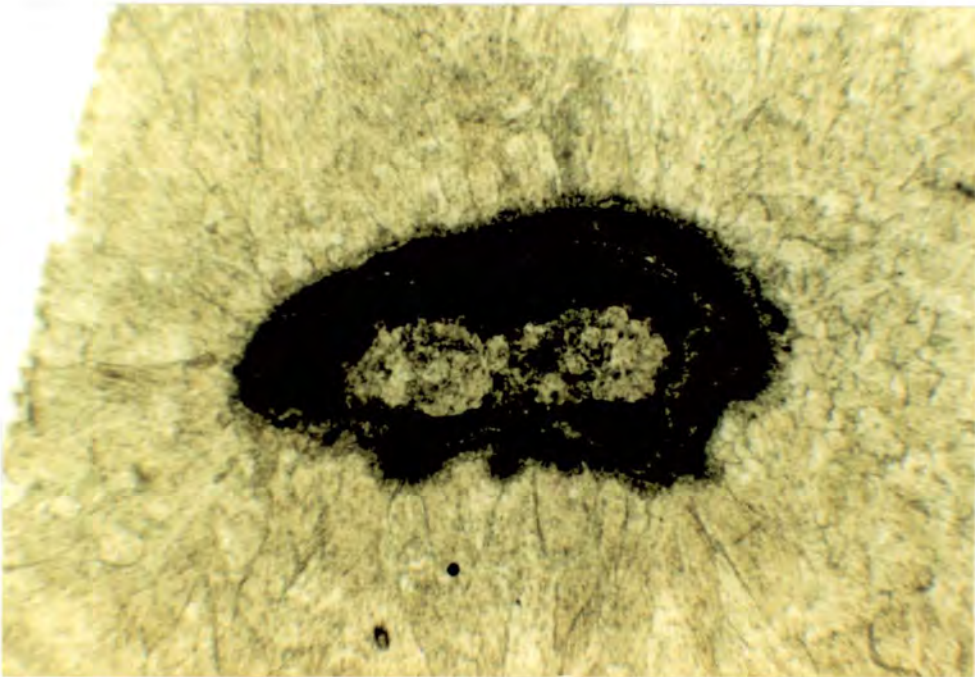


**Fig. 4.41** Photomicrograph of a pisoid with a nucleus of sediment. The pisoid itself is composed of irregular crystals of radiaxial calcite which have replaced a radial, probably calcitic precursor. Crossed polars.

with coarser sediment and flowstones. It is possible that in this instance the 'shrubs' were preserved by the relatively rapid precipitation of thin calcite sheets.

### 4.5.3 Minor Forms of Travertine

#### 4.5.3a Travertine Pisoids

Pisoids are commonly associated with flowstone in the travertines and also occur in cavities interbedded with sediment. There are two types of pisoid in the travertines.

Pisoids up to 2 centimetres in diameter and composed of irregular crystals of fibrous calcite are most commonly developed at Dinas Powys, although they also occur within larger travertine accumulations in the Sully Island area. These pisoids are nucleated around fragments of laminated limestone ( Fig. 4.41 ). The nuclei themselves in some cases have been overgrown by interlaminated sediment and microspar before growth of fibrous calcite commenced. The majority of the pisoids contain no sediment other than the nucleus, and are composed of an array of irregular calcite crystals which are roughly tabular in form. The extinction patterns within each crystal are variable but the majority show a radiaxial fabric. No crystal terminations are observed at the margins of these pisoids but in some a concentric pattern is present, and inclusion patterns give some indication of a radial fibrous precursor ( Fig. 4.42 ).

It is possible that the irregular crystal form in the pisoids is the result of the recrystallisation of an original fibrous or acicular precursor. Pisoids composed of concentrically banded radial acicular aragonite are forming at present in salinas in South Australia ( Ferguson et al., 1982 ). In the Dinas Powys area banded pisoids were cemented onto the sediment floor and overgrown by continuous sheets of flowstone. Small pockets of peloidal sediment are present between pisoids, showing a geopetal fabric and containing rare ostracod valves.

The second form of pisoid is composed of concentrically laminated sediment and fibrous calcite ( Fig. 4.43 ). As such these pisoids are similar to the nuclei of those composed mostly of calcite. The interlaminated pisoids are commonly associated with flowstones in the Sully bay area. The concentric laminae are

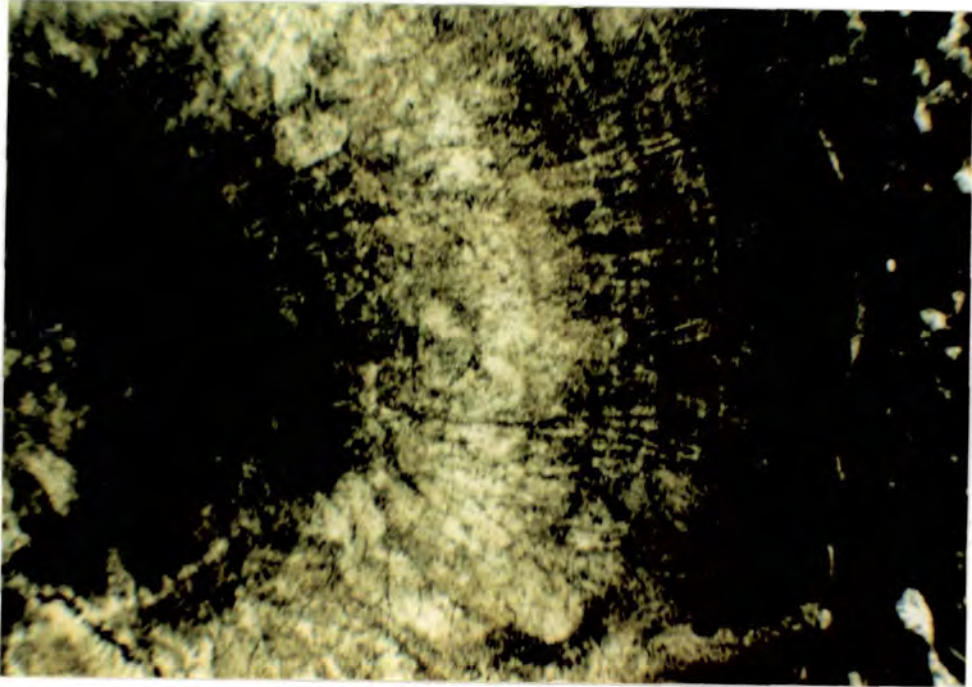


**Fig. 4.42** Photomicrograph of part of a pisoid showing both concentric and radial texture. The calcite is a replacement of a radial fibrous precursor. Plane polars.



**Fig. 4.43** Photomicrograph of a very asymmetrical pisoid consisting of laminae of sediment and calcite spar. These pisoids are associated with interlaminated flowstone and sediment and are composed of similar laminae. The pisoid in the photograph appears to have become attached to the sediment surface at an early stage during formation. Plane polars.

not constant in thickness and in individual pisoids can be markedly asymmetric ( Fig. 4.43 ). In some of the thicker laminae of spar crystal terminations can be seen. These pisoids contain a nucleus of sediment, commonly peloidal or consisting of fragmented travertine, of varying size ( Fig. 4.44 ). The pisoids form beds with abundant cavities which are filled with interlaminated sediment and fibrous calcite, which is similar in form to the structure of the pisoliths themselves. The pisoids tend to form lenticular beds several centimetres in height which overlie flowstones, and appear to have formed by the same process of alternating sedimentation and cementation. The pisoids became attached to the sediment floor during formation. None of the larger forms contain symmetrical outer laminae. Pisoids of alternating micritic laminae and aragonite cement from Australian salinas are identical in form to the pisoliths present in Sully Bay ( Handford et al., 1984 ). In the Triassic examples, the original carbonate appears to have been fibrous or acicular, now recrystallised to a more equant spar. There is no conclusive evidence for the presence of an aragonitic precursor for the sparry laminae.

#### **4.5.3b Flöe Calcite**

Flöe calcite is present in many of the larger travertine deposits in Sully Island and in the Dinas Powys outcrop, although it does not make up a large part of the travertines. Flöe calcite ( or aragonite ) has been described from a number of salinas and caves and requires a particular depositional and chemical environment in which to form ( Ferguson et al., 1982, 1988; Folk et al., 1985; Chafetz et al., 1989; Jagnow, 1989 ). Sheets of carbonate precipitate on the surface of pools of supersaturated waters. Loss of  $\text{CO}_2$  in spring waters can lead to extremely high levels of supersaturation ( up to 77 times saturation with respect to  $\text{CaCO}_3$  , Chafetz et al., 1989 ). Under these conditions, precipitation of carbonate takes place very rapidly and floating sheets form at the air-water interface, held by surface tension. These sheets are composed of needle-like crystals often with a botryoidal upper surface on a minute scale ( Ferguson et al., 1982; Chafetz et al., 1989 ). Formation of these sheets requires supersaturated waters and a relatively still water surface such as can occur in pools formed by rimstone dams ( Folk et

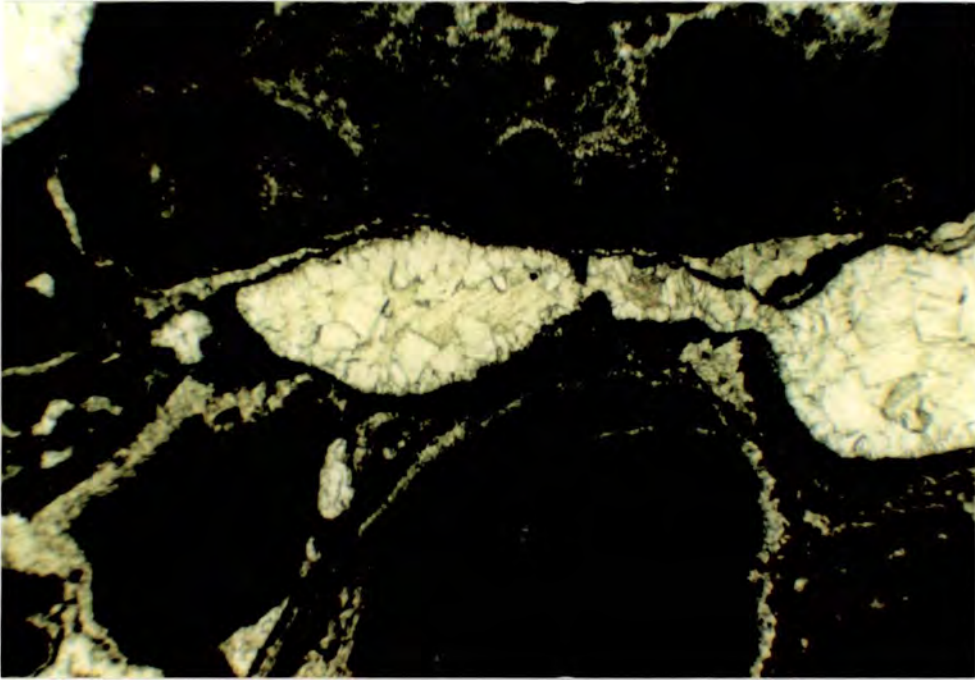


**Fig. 4.44** Photomicrograph of a large pisoid forming the base of a cavity showing vadose diagenetic textures. The cavity roof is composed of pelsparite sediment. Plane polars.

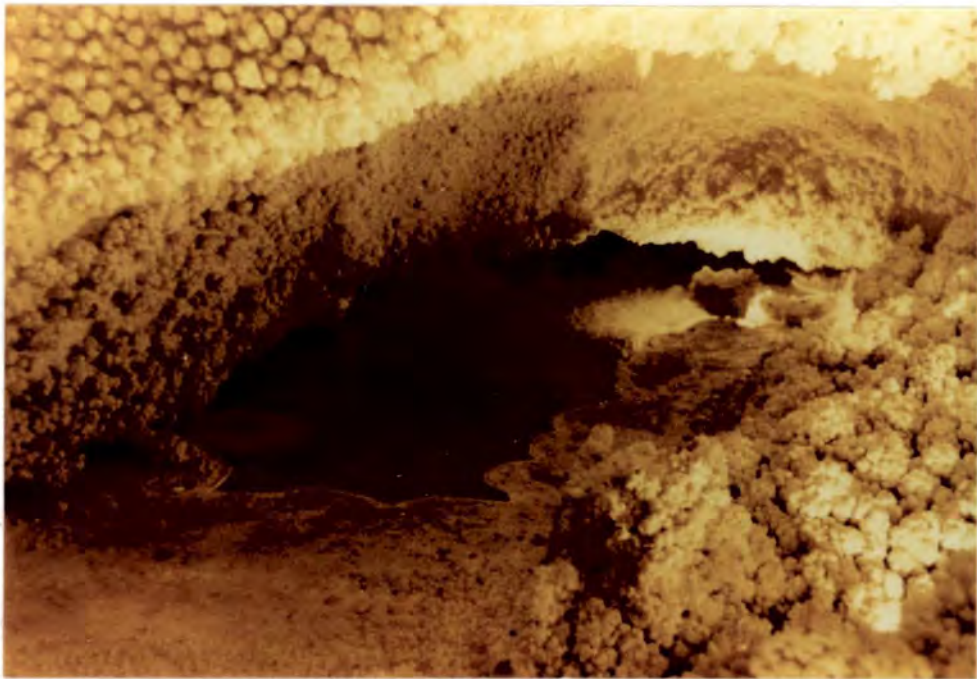


**Fig. 4.45** 'Cave-Ice' analogous to the flöe calcite which is present in the travertines in the limestones at Sully Island. In this pool the flöe calcite has grown out from the sides of pools and has become overgrown by further calcite which has strengthened the sheets. Width of pool approximately 2 metres. Caverns of Sonora, Texas, U.S.A.

al., 1985 ). When the surface of the pool is disturbed, the sheets will break up and settle to the bottom, forming fragmented stacks.

In the Triassic travertine deposits the morphology of individual sheets cannot be seen since they have been overgrown by later cements. The original form of the sheets does not appear to have been preserved and the stacks of flöe calcite are shown up only by the drapes of sediment which cover many of the sheets. The relic sheets in the travertines appear to have been very thin when they settled to the pool floor ( 50  $\mu\text{m}$  ). This is much less than the thickness of one millimetre given by Ferguson et al. ( 1982 ) for flöe aragonite from South Australia. The thickness of one millimetre may be the greatest thickness which can be supported by surface tension. More likely the sheets have been overgrown by further aragonite after settling. Flöe calcite also forms abundantly in caves where stacks of broken sheets up to 3 metres in height ( called raft mounds ) accumulate in pools underneath drip points from overlying stalactites ( Jagnow, 1989 ). The undisturbed conditions in caves are ideal for the formation of such forms of carbonate ( Fig. 4.45 ).

In Sully Island and Dinas Powys sheets of flöe calcite formed stacks at the base of pools, overlying flowstone and sediment. Individual stacks can be imbricated ( Fig. 4.46 ), indicating that current activity was at times present in the pools. The broken sheets usually form stacks of randomly arranged fragments up to 3 millimetres in length, overlain by fine sediment ( Fig. 4.47 ).

#### 4.5.3c Spherulitic Structures

In one sample taken from the Dinas Powys exposure a number of spheroidal masses between 0.1 and 1.5 millimetres in diameter are present ( Fig. 4.48 ). These spherules do not appear to contain a nucleus and form a bed several centimetres thick overlying and interbedded with laminated limestones typical of the Dinas Powys exposure. The spherules are composed of coarse calcite spar but the pattern of extinction in the crystals suggests a radial fibrous or acicular precursor ( Fig. 4.49 ). Inclusions within the calcite reflect the replacement pattern. The spherules do not appear to have formed *in situ* but have been transported and deposited in a pool downstream from the place of formation where there was a reduction in the current velocity. There appears to have been



**Fig. 4.46** Imbricated stack of flöe calcite in large travertine accumulation, southwest side of Sully Island. These sheets have been affected by current activity moving through the pool in which they formed.

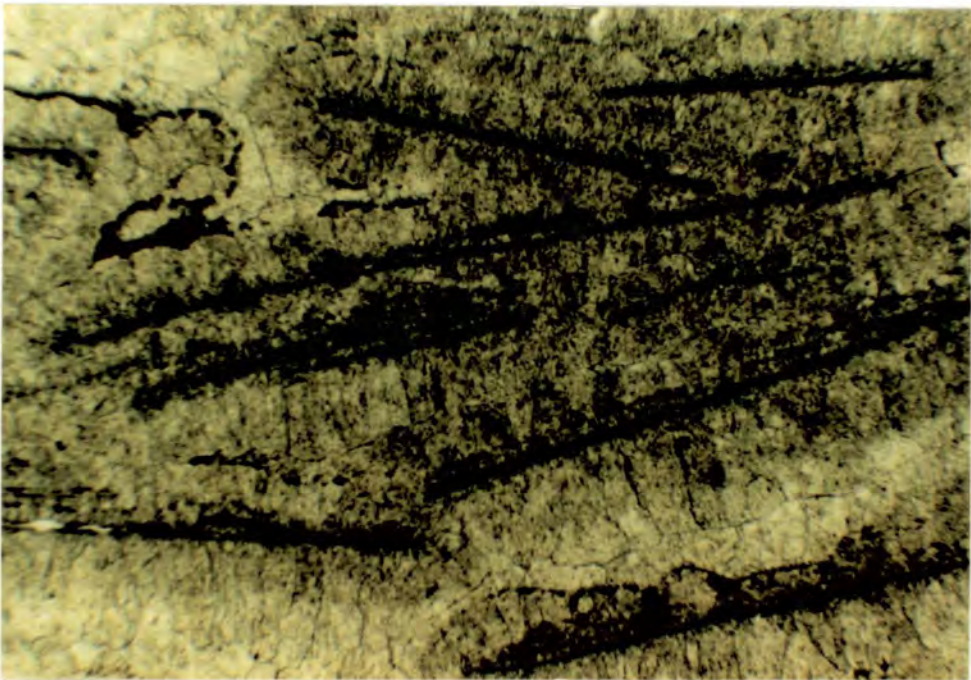


**Fig. 4.47** Photomicrograph of stack of broken sheets of flöe calcite overlain by a thin veneer of micrite sediment and overgrown by fibrous calcite. Late clear spar is present in the upper left-hand corner of the photograph. Plane polars.

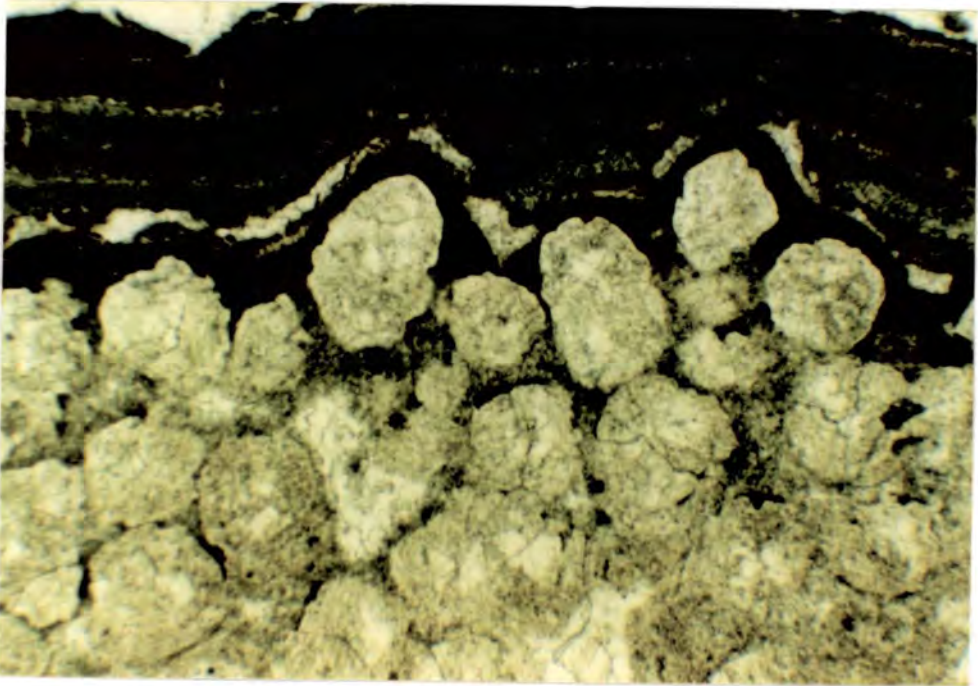


**Fig. 4.48** Photomicrograph of spherulites draped by laminated limestones at Dinas Powys. The spherulites were deposited in a pool after transportation. The environment in which they formed is not exposed. Plane polars.

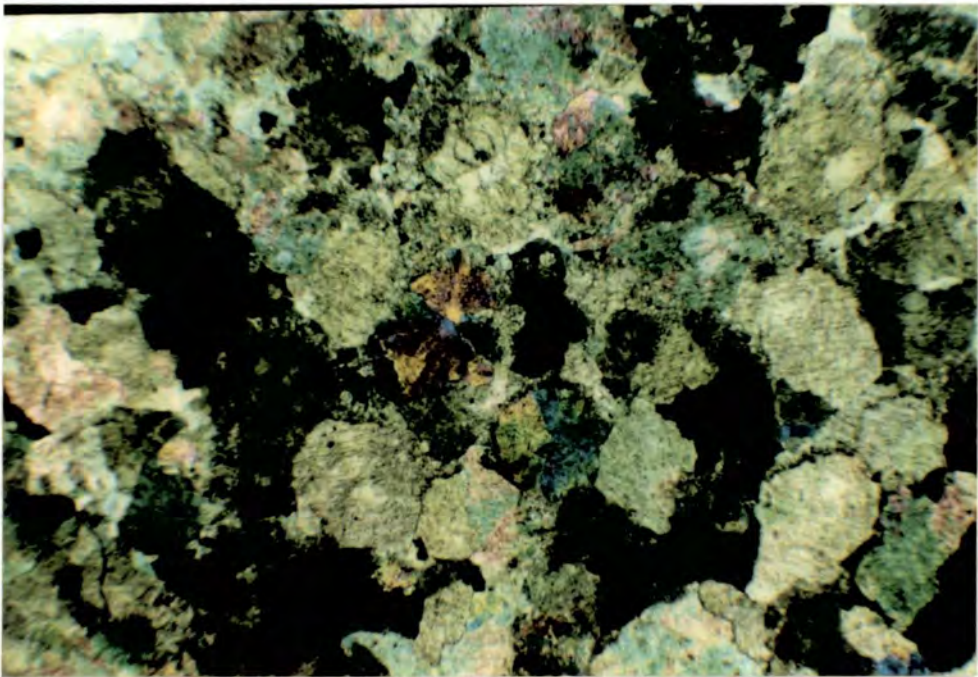


**Fig. 4.49** Photomicrograph of spherulites showing the radial extinction pattern ( seen in the two spherulites in the centre of the photograph ) which is an indication of an original radial circular texture. Crossed polars.

one phase of precipitation and deposition of the spherules in the pool, which have only been found in one sample.

There do not appear to be many analogous deposits to the spherules. The spherules of neomorphic spar described by Warren ( 1982 ) are displacive structures which have a very different origin from the Dinas Powys forms. The most similar structures are a collection of spherules rarely larger than 0.2 millimetres in diameter which are composed of radial acicular calcite with no nucleus ( Steinen et al., 1987 ). These spherules are associated with terraced travertines and saddle dolomite in a Jurassic sequence in Connecticut, U.S.A. and are interpreted as having formed in a hot spring environment where degassing of CO<sub>2</sub> at emergence gave rise to the very rapid precipitation of carbonate. Apart from the spherules and early saddle dolomite the Jurassic travertines are identical in form to those from the Triassic of South Wales. The presence of spherules in the Dinas Powys travertines is the only line of evidence which suggests the presence of hot spring waters in the Triassic. The other spring deposits do not show any evidence of hot water activity and although the spherules themselves were not sampled, there is no geochemical evidence for elevated temperatures during the precipitation of the travertines ( Section 5.2 ). There is some indication of hydrothermal activity in the Mendip Hills during the Triassic ( Green & Welsh, 1965 ) but in South Wales the evidence is not conclusive. The formation of the spherules, if not caused by the cooling of supersaturated waters, may have occurred as waters passed over a series of rapids in the palaeovalley below the spring outlet. The lack of exposure does not provide any information as to the palaeogeography of the area in which the travertines were laid down.

## **4.6 Tepee-like Structures**

### **4.6.1 Introduction**

Tepee structures in the Limestone Unit around Sully Island can be subdivided into two forms. Within the laminated limestones in particular small tepees with amplitudes of up to 20 centimetres are found. Larger tepee and saucer structures which form megapolygons up to 5 metres in diameter cover the topmost dolomitised surface of the Limestone Unit. These larger tepees can be related to



**Fig. 4.50** Small dome in dolomitised laminated limestones which has been modified by desiccation, forming a small tepee structure. Swanbridge.



**Fig. 4.51** Large saucer structure 5 metres in diameter in dolomitised topmost limestone. Ball Rock. Length of hammer 40 centimetres.

fissures in the underlying limestones which contain interlaminated cement and sediment.

#### **4.6.2 Tepees in the Laminated Limestones**

The laminated limestones are commonly desiccated and contain numerous polygonal cracks and laminoid fenestrae. On a larger scale the limestones have been deformed into small pseudoanticlines or tepees one metre across and up to 20 centimetres in height ( Fig. 4.50 ). Laminae within the tepees are not normally brecciated. These tepees are not associated with pisolites or large cemented cavities and can be described as immature peritidal ( perilittoral in this instance ) tepees ( Kendall & Warren, 1987 ). The tepees are found throughout the laminated limestones east of Swanbridge and tend to be spaced between 1 and 5 metres apart. They appear to have formed by the precipitation of cement in fractures caused by desiccation. There is little evidence for the expansion of the sediment itself other than the precipitation of dolomite rhombs within certain laminae ( Section 4.2 ). The period of desiccation during which the tepees formed was not great and there is no evidence of any pedogenesis in the laminated beds.

#### **4.6.3 Megapolygonal Structures**

##### **4.6.3a Tepee and Saucer Structures**

The topmost 1.0 to 1.5 metres of the Limestone Unit has been replaced by a coarse rhombic dolomite, obscuring almost all of the detailed sedimentary structure. The top surface of the limestones itself has been deformed into a series of megapolygonal tepee and saucer structures up to 5 metres in diameter ( Figs. 4.51, 4.52 ). The surface of the limestones has been severely buckled and can be tilted at an angle of 45 degrees to the horizontal with a relief of 0.5 metres ( Fig. 4.52 ). These more mature tepees appear to have formed both from expansion of the surface crust due to precipitation of carbonate and to the effects of groundwater resurgence. Similar structures formed in the back reef environment of the Permian Capitan Reef in New Mexico, U.S.A. where tepee structures up



**Fig. 4.52** Smaller saucer in dolomitised limestone showing a high degree of deformation of the surface of the limestones. Length of hammer 40 centimetres.

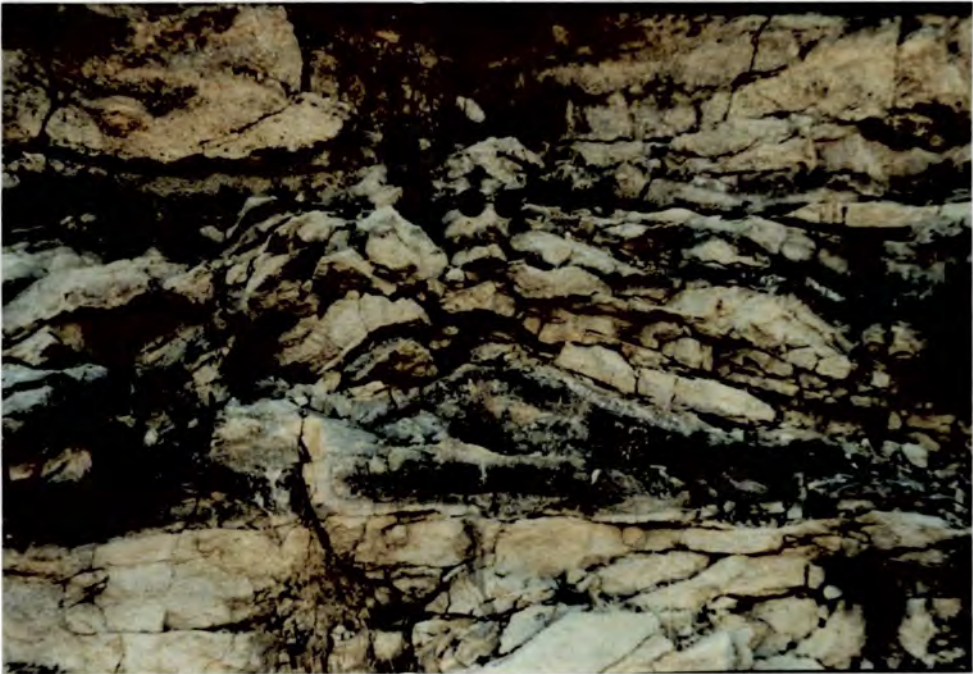


**Fig. 4.53** Small tepee in the Tansil Formation of the Capitan Reef Complex, New Mexico, U.S.A. The deformed limestone ( yellow ) contains an infill of botryoidal cements ( black and grey ). Tepee is 1 metre in height.

to 3 metres in height are preserved ( Fig. 4.53 ). These tepees are intensely fractured, contain large cavities filled by botryoidal cements and are associated with pisolites and oncolites. These tepees have been interpreted as the result of a resurgence of waters into the area as a result of a hydraulic gradient caused by evaporative pumping on the shelf behind the reef ( Handford et al., 1984 ), ( Fig. 4.54 ). Similar tepees are forming at present around the margins of a number of salinas on the Australian coast, in response to the movement of waters through semi-permeable barriers into the evaporative basins ( Muir et al., 1980; Ferguson et al., 1982; Warren, 1982 and Handford et al., 1984 ). Unfortunately in the case of the Sully Island tepees, dolomitisation has removed almost all evidence of other sedimentary structures associated with the tepees. On the basis of the size and amount of deformation these tepees can be described as mature ( Kendall & Warren, 1987 ). The dolomitisation has removed any evidence for the resurgence of groundwaters through the tepees but their size indicates that they were almost certainly groundwater conduits. The travertine deposits in the limestones provide abundant evidence for the resurgence of groundwaters and some flowstones can be seen in the upper dolomitised limestones. The maturity of the tepees suggests a relatively long period of exposure and desiccation during which deposition of limestone ceased. After formation of the tepees the limestones were overlapped by red dolomitic mudstones of the Mercia Mudstone Group. Within these mudstones are three white dolomitic beds which are similar in form to the topmost limestone. These dolomites are fenestral and contain microbial lamination and small tepees ( Fig. 4.55 ) and are the result of temporary ameliorations of the arid environment in which the red mudstones formed and a resumption of perilittoral lacustrine conditions. As such these beds are similar in form to those which formed in the upper red mudstones in Somerset ( Section 7.2 ).

#### **4.6.3b Polygonal Fissures as Groudwater Conduits**

Both the travertine deposits and the megapolygonal tepees are the result of upwelling groundwaters which must have risen through the already formed limestones. The primary porosity of the fenestral limestones will have been considerable and it is quite possible that waters could move upwards through the limestones without having to form specific pathways, which would permit the

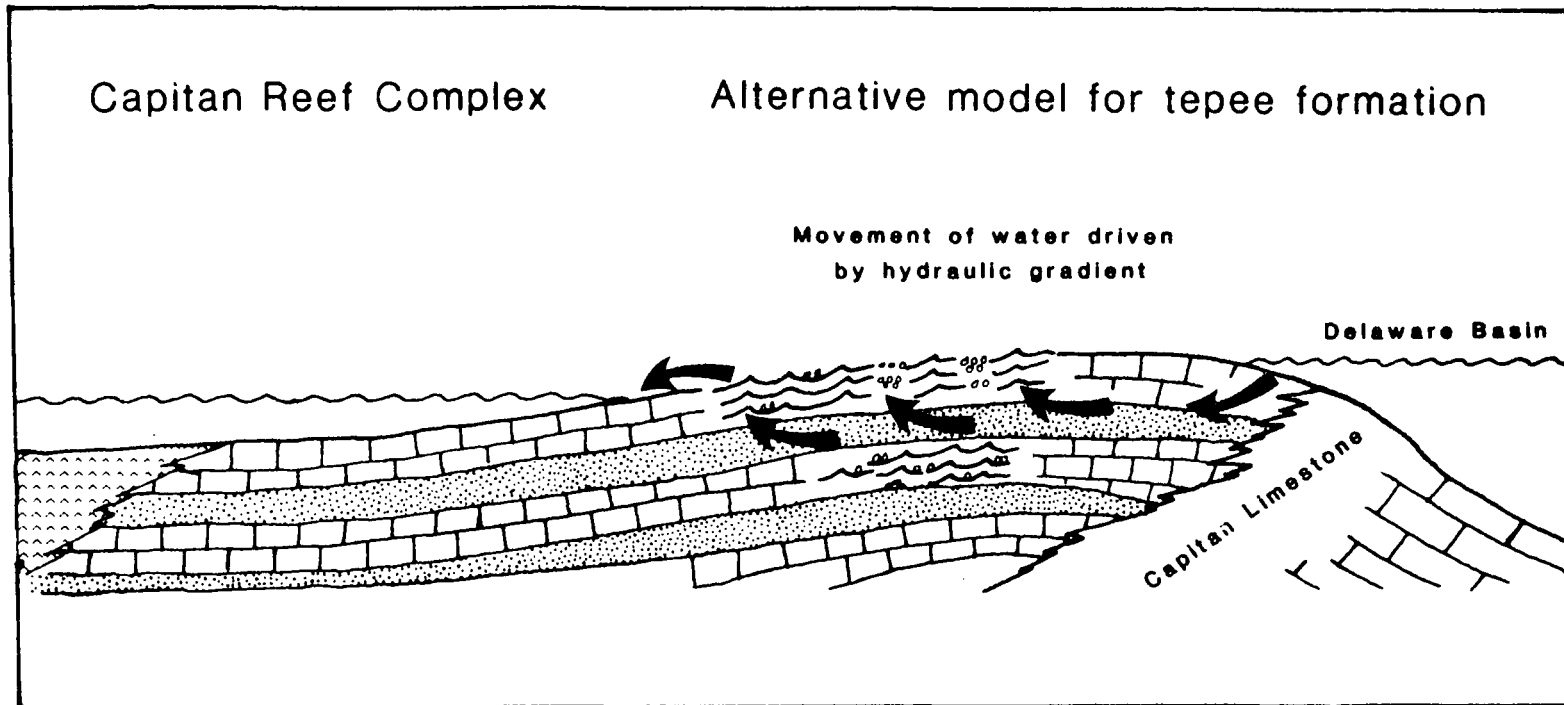


**Fig. 4.54** Model for movement of waters through the Permian Capitan Reef, New Mexico, U.S.A. driven by difference of water levels in the Delaware Basin and back-reef lagoon. This model has been used to account for the formation of tepees in the back-reef environment of the Capitan Reef. ( After Handford et al., 1984 ).



**Fig. 4.55** Microbially-laminated dolomite in the mudstones overlying the Limestone Unit, Ball Rock. There is some doming of the laminae but in this case there are no tepees developed.

water to emerge over a diffuse area rather than a specific point. In view of the fact that none of the travertines can be matched with a corresponding outlet it is likely that much of the groundwater appeared at the surface in this way.

Locally developed within the limestones and well exposed on the wave-cut platform in Sully Bay are a series of networks of fissures which form polygonal patterns between 0.7 and 5.0 metres in diameter. These fissures are up to 20 centimetres in thickness and are filled by interlaminated sediment and cement ( Fig. 4.56 ). In some fissures brecciated limestone is present, indicating that some degree of cementation had taken place before the fissures formed, leading to deformation and fracturing of the limestones. The polygonal pattern is well exposed on Sully Bay ( Fig. 4.57 ). Within the megapolygonal fissures small cement filled desiccation cracks are also present. The fissures tend to cover areas of between 20 to 100 metres in diameter along the shoreline ( Fig. 4.58 ). The areas are regularly spaced along the shoreline 200 to 400 metres apart. Unfortunately the exposure of the uppermost limestone is not sufficient to establish whether this spaced pattern is repeated by the tepees. The fissures are best developed in the centre of the areas. Polygons tend to become smaller towards the margins of the fissured zones, although the fissures themselves do not become thinner. At the margins of the areas fissures form in parallel east-west trending sets. These fissures can extend for 3 to 4 metres beyond the area of polygonal forms. Polygonal fissures form around localised springs which occur around the margins of Australian salinas. These mounds are 30 to 100 metres across and are capped by tepee and saucer structures. The fissures are filled by sediment and cement ( Ferguson et al., 1982; Handford et al., 1984 ). The fissures in Sully Bay lie less than one metre below the topmost surface of the limestones. The similarity in form and size suggests that the fissures are the non-dolomitised equivalent of the overlying tepees. The depth to which the fissures extends is not known but some appear to occur only in the topmost metre of limestone ( Fig. 4.59 ). It appears that groundwaters moved upwards through the permeable limestones forming a crust which was fractured and buckled due to prolonged exposure and precipitation. The fissures expanded as the surface fracturing extended down into the limestones and grew as successive phases of cementation filled the fractures ( Kendall & Warren, 1987 ).



**Fig. 4.56** Fissure containing interlaminated sediment and calcite cement in the upper limestones, east Sully Bay. The fissure is up to 10 centimetres in thickness and the infilling represents successive phases of opening of the fissure.

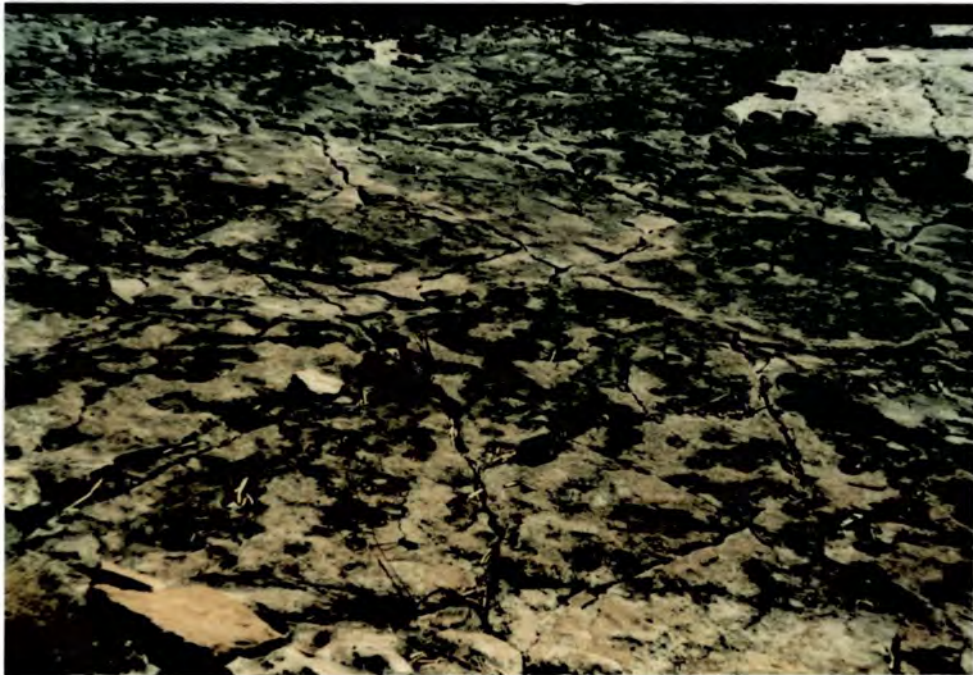


**Fig. 4.57** Megapolygonal pattern of fissures in upper limestones in central Sully Bay. The polygonal forms are up to 5 metres in diameter. Length of hammer 40 centimetres.

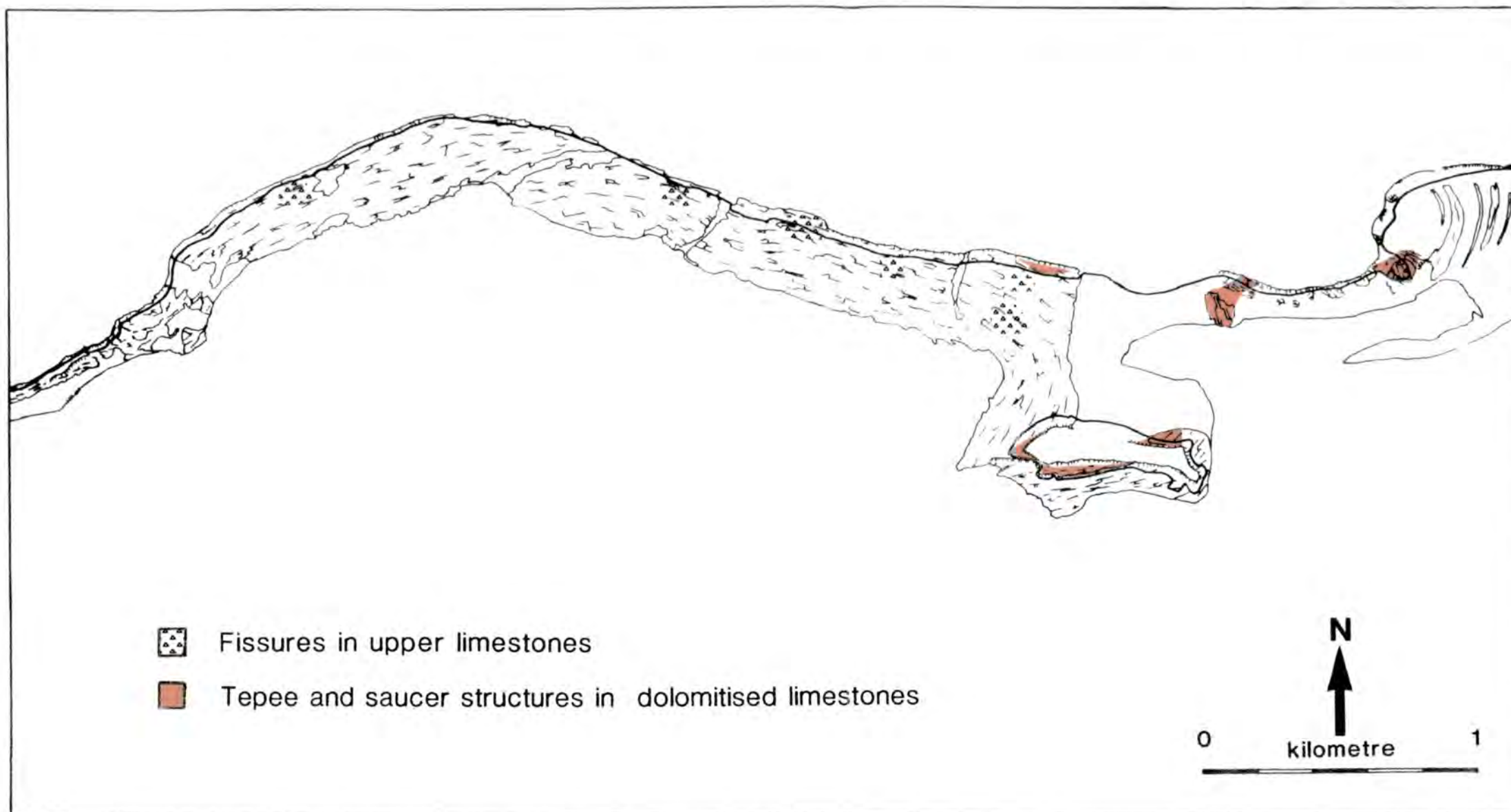


**Fig. 4.58** Distribution of polygonal fissures in the upper limestones and of tepee and saucer structures in the topmost dolomitised limestones.



**Fig. 4.59** Section through a fissure in east Sully Bay. The fissure connects with a horizontal cavity 0.5 metres below the limestone surface and contains brecciated limestone at the base of the fissure.

## 4.7 Vadose Diagenesis of the Limestones

### 4.7.1 Introduction

There is abundant evidence within the Limestone Unit for the fluctuation in level of the water table during deposition. Rippled and desiccated surfaces occur throughout the unit. This movement of the water table gave rise to a number of diagenetic features as well as being a major influence on the primary sedimentary structures. Both vadose and phreatic meteoric cements are present in the limestones although vadose structures are by far the most abundant. During times when the porosity of the limestones was filled, non-isopachous fringes of coarse fibrous cement formed. These are best seen in the coarse clastic limestones in the west of Sully Bay ( Fig. 4.60 ), and are similar in form to the non-isopachous spar described by Hird & Tucker, ( 1988 ) from the Carboniferous Limestone in South Wales.

### 4.7.2 Vadose Cavities in the Limestones

Cavities between 1 and 50 centimetres in diameter are exposed within the main limestone unit throughout the Sully Island area. The cavities are irregular in shape but tend to be sub-spherical in overall form and occur in groups ( Fig. 4.61 ). Larger cavities which are several metres in diameter occur along bedding planes. The spherical cavities do not appear to have formed preferentially along any sedimentary feature in the rock. The cavities contain an outer coating of fibrous calcite between 0.1 and 1.0 centimetres in thickness which is similar in form to the flowstones precipitated on the sediment surface. The remainder of the cavity is filled by sediment ( Figs. 4.61, 4.62 ). Cavities can be filled by successive phases of cement and sediment, although there is in all cases an outer lining of cement. The sediment can form geopetal surfaces if it does not entirely fill the cavity. Although the cavities are subspherical the walls often have a cusped form ( Fig. 4.62 ).

The formation of these cavities is probably the result of an influx of meteoric waters poor in carbonate or charged with humic acids derived from soil horizons. The extensive dissolution of the limestones was followed by a period of carbonate

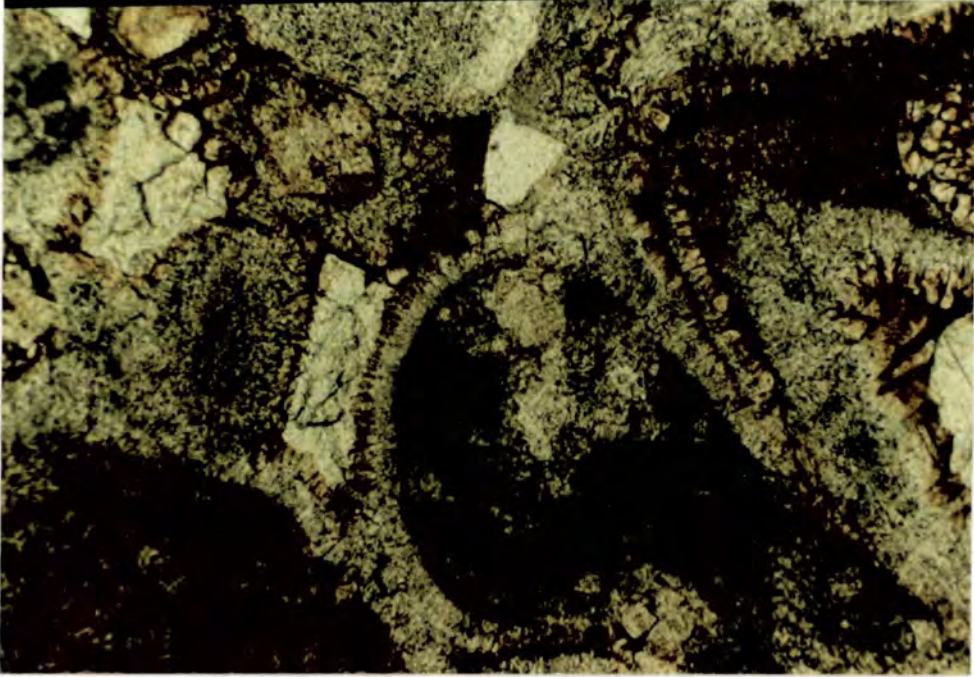


**Fig. 4.60** Photomicrograph of non-isopachous cements in a coarse clastic bed from Hayes Point. There are several phases of cementation but the non-isopachous fringe is probably the result of *freshwater* phreatic conditions. Plane polars.

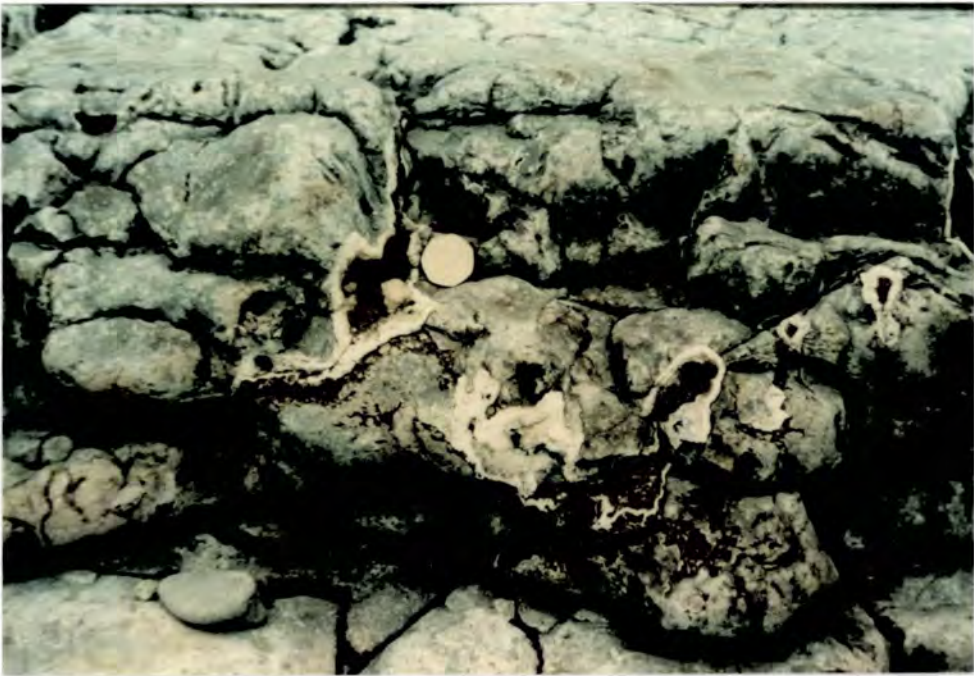


**Fig. 4.61** Vadose cavities in the upper limestones, central Sully Bay consisting of an outer band of calcite cement and an infilling of infiltrated sediment.

precipitation which filled the cavities. This variation in the carbonate saturation of the waters is also seen in the partial dissolution of flowstones. Larger, more laterally continuous cavities are less common in the limestones but are most abundant in the upper limestones. These cavities are the result of dissolution and not simply larger laminoid fenestrae, and contain fibrous calcite crusts which are identical in form to the flowstones and are developed on the roofs as well as the floors of cavities. Pisoliths and flöe calcite are also present in these cavities ( Fig. 4.63 ). The presence of large, intact sheets of flöe calcite is evidence that there was not great current activity at times in the cavities. If the flöe calcite formed within the cavity then this would require the water table to run through the cavity itself, and to be relatively stable for a period of time. That the water table was not very stable is indicated by the presence of the roof cements. These dissolutional cavities and cements are not the result of brecciation during tepee formation, although the cements are similar ( Ferguson et al., 1988 ).

Also present in the elongate cavities as well as in fenestrae are stacks of peloids which show a reverse graded texture which has been used as evidence for vadose diagenesis ( Fig. 4.64 ). The peloids are in many cases composed of clasts of quartz or limestone around which has accumulated a coating of micrite or microspar, thus forming superficial peloids. These peloids are between 0.1 and 2.0 millimetres in diameter and appear to have formed by the aggradation of fine sediment ( Macintyre, 1985 ), although calcification of algal filaments and chemical precipitation of micrite may have had some input into peloid formation. The peloids are composed of the same material which covers the floors of laminar fenestrae. The reverse grading of the peloids is well developed in larger cavities where stacks up to 4 millimetres in height have formed. Reverse grading is a common feature of vadose diagenetic environments ( Asserto & Kendall, 1977 ). It is likely that these peloids grew in an environment which was periodically agitated while being incorporated into the sediment floor while unattached peloids continue growing. There is no evidence of peloids continuing to grow after settling as described by Chafetz & Butler ( 1980 ).

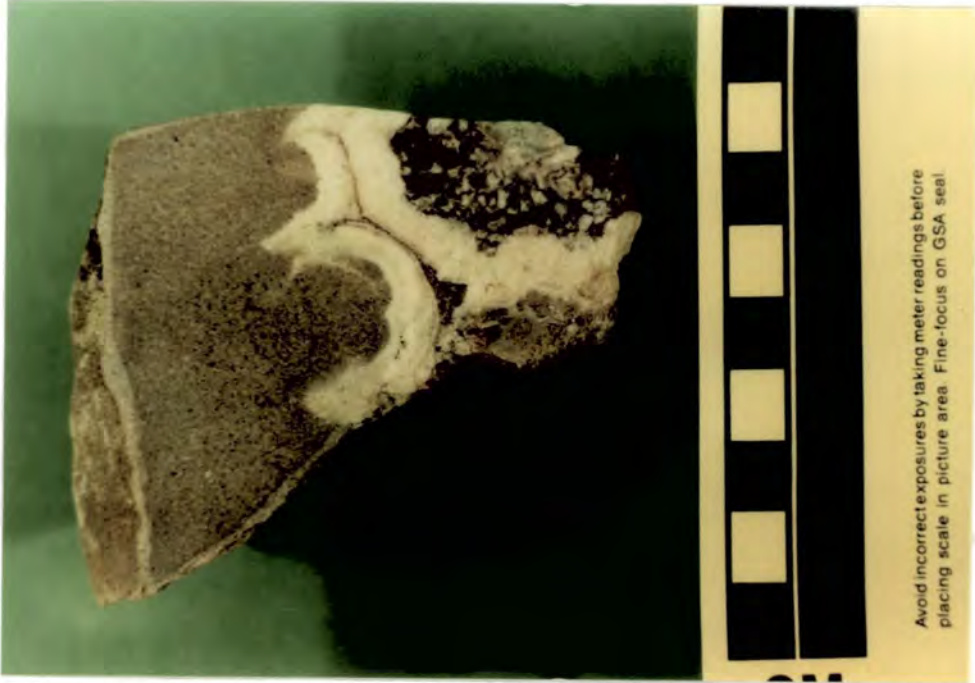


**Fig. 4.62** Polished surface of a vadose cavity from central Sully Bay in an intraclastic limestone showing the cuspate form of the cavity margins and the interlamination of cement and sediment within the cavity.

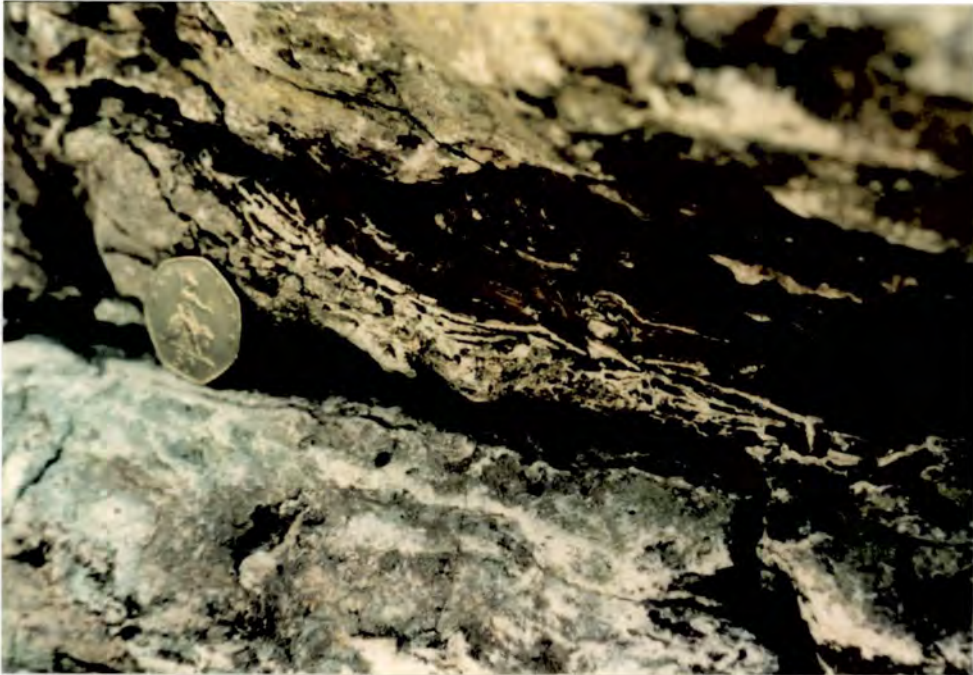


**Fig. 4.63** Bedding-parallel cavity in upper limestones, central Sully Bay containing sheets of flöe calcite which implies that the water table must have at times run through the cavity.

### 4.7.3 Vadose Diagenetic Sediments and Cements

Evidence for vadose diagenetic cementation is abundant within the limestones, in particular within the laminoid fenestrae in the laminated fenestrae ( Tucker, 1975 ).

In the intraclastic limestones as well as forming geopetal surfaces in the fenestral cavities fine sediment can also form pillars between the cavity floor and roof or with peloids in the cavity ( Fig. 4.65 ). These pillars form as waters withdraw from cavities and represent the concentration of sediment into menisci. There must have been some cementation within the menisci in order to preserve the sediment pillar ( Tucker, 1975 ). The pillars are best seen within the elongate cavities of the laminated limestones where they appear to occur at regular intervals ( Fig. 4.66 ). Within larger cavities several phases of sedimentation have taken place which can be correlated with thinner sediment laminae in pillars ( Fig. 4.67 ). These structures are pillars as opposed to ridges which have been observed in some laminar cavities ( G. Walkden, pers comm. ). Although composite pillars can be up to 0.5 millimetres in diameter, there are no cases where a 'ridge' has been cut parallel to the ridge orientation such that a greater thickness of sediment is cut through. The sediment formed as columns around point menisci rather than linear forms. The irregularity of the cavity surfaces makes it unlikely that ridges would form as waters withdrew. Peloidal beds are locally present in the laminated limestones and in places pillars can be made up of peloidal material.

Vadose cements are also best preserved in the laminated limestones. In larger cavities successive phases of cementation are overlain by sediment ( Fig. 4.68 ). In some cases cavities are filled with cements which are thickest on cavity roofs while later sediment has formed pillars in the reduced cavity as well as covering the cavity floor ( Fig. 4.69 ). The cements as preserved at present are fibrous or tabular and have had an acicular or possibly micritic precursor. Inclusion patterns within the crystals are aligned and indicate the position of the present crystal face terminations ( Tucker, 1975 ). Some cavities are coated in a thin cement layer under 0.1 millimetres in thickness which appears to be isopachous and which precedes the formation of pillars and sedimentation ( Fig. 4.70 ). This

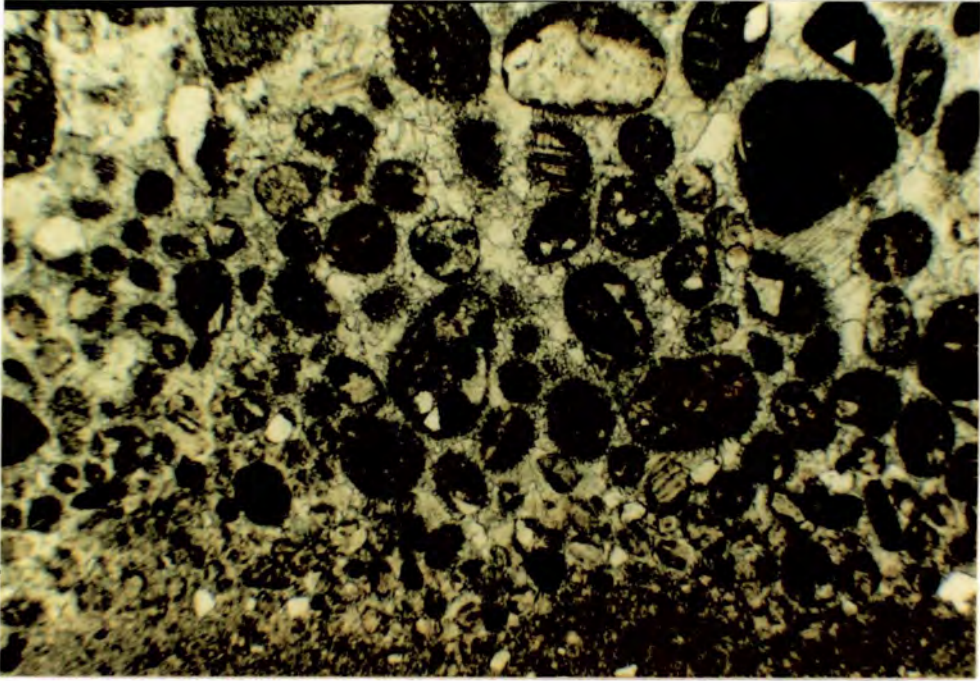


**Fig. 4.64** Photomicrograph of reverse-graded peloids in a vadose cavity. The accretion of micrite around angular clasts has formed the peloidal sediment. Plane polars.

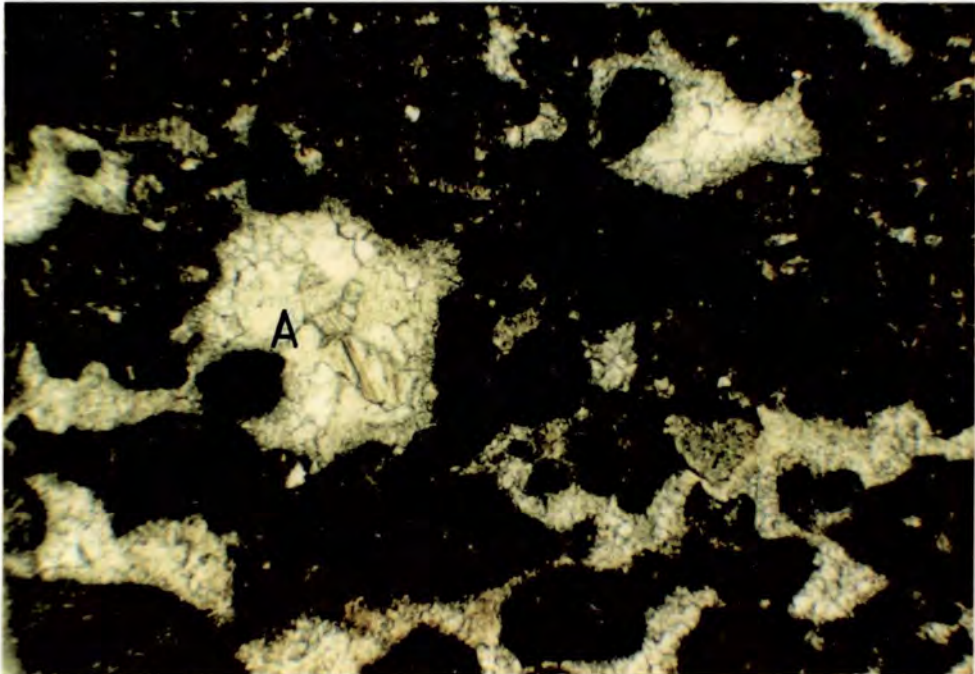


**Fig. 4.65** Fenestral limestone showing meniscus cementation of peloids within fenestral cavities ( A ). Plane polars. Peloids are composed of aggregated sediment.

Such pillars are also described in Wright ( 1983 ) from a Carboniferous calcrete in South Wales, although the association with vadose diagenesis is not made.

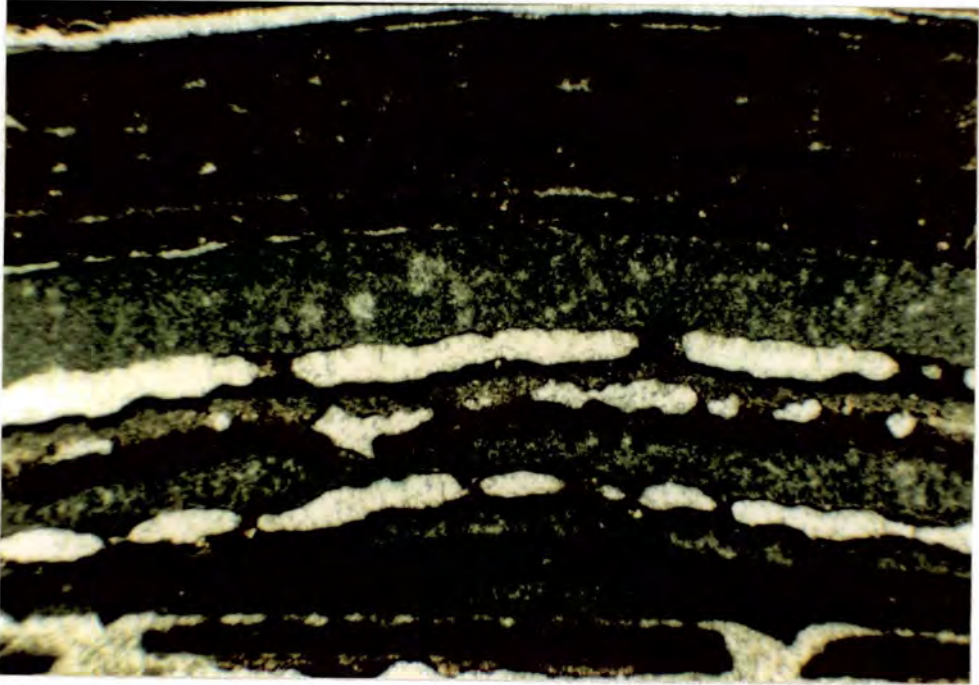


**Fig. 4.66** Photomicrograph of laminar fenestra in laminated limestones from Dinas Powys showing the relatively regular spacing of pillars within cavities. Note also the sediment on cavity floors. Plane polars.

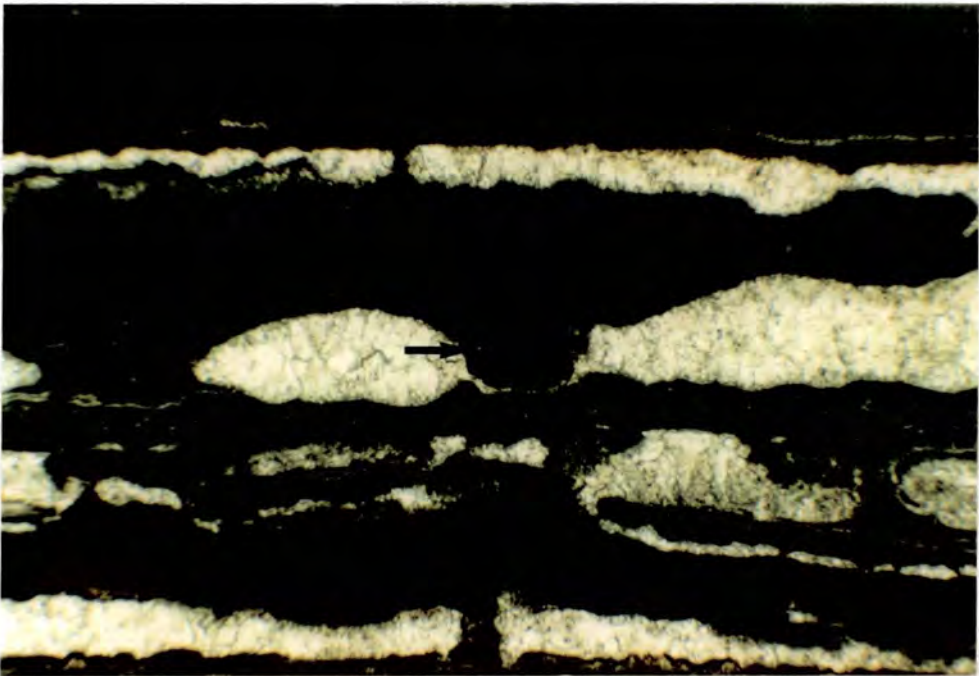


**Fig. 4.67** Photomicrograph of pillars in a laminar fenestra which is composed of several phases of accreted micrite. The latest phase of micrite also contains calcitic rhombs, originally dolomitic (arrowed). Plane polars.

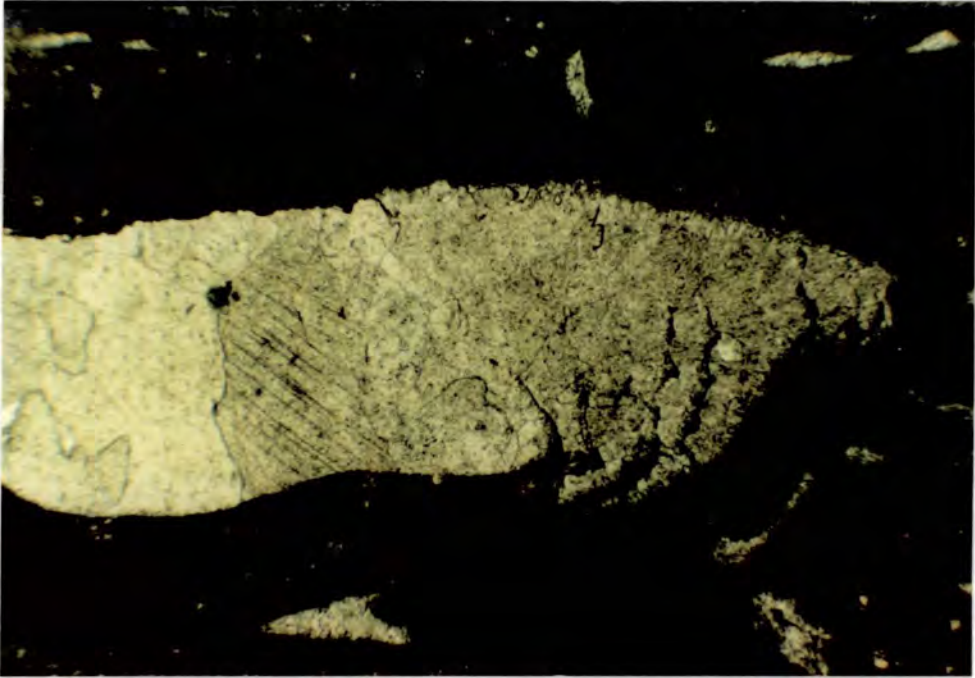


**Fig. 4.68** Photomicrograph of large fenestral cavity in which successive phases of cementation are overlain by sediment. Each phase of cement and sediment is the result of one cycle of water table fluctuation. Plane polars.

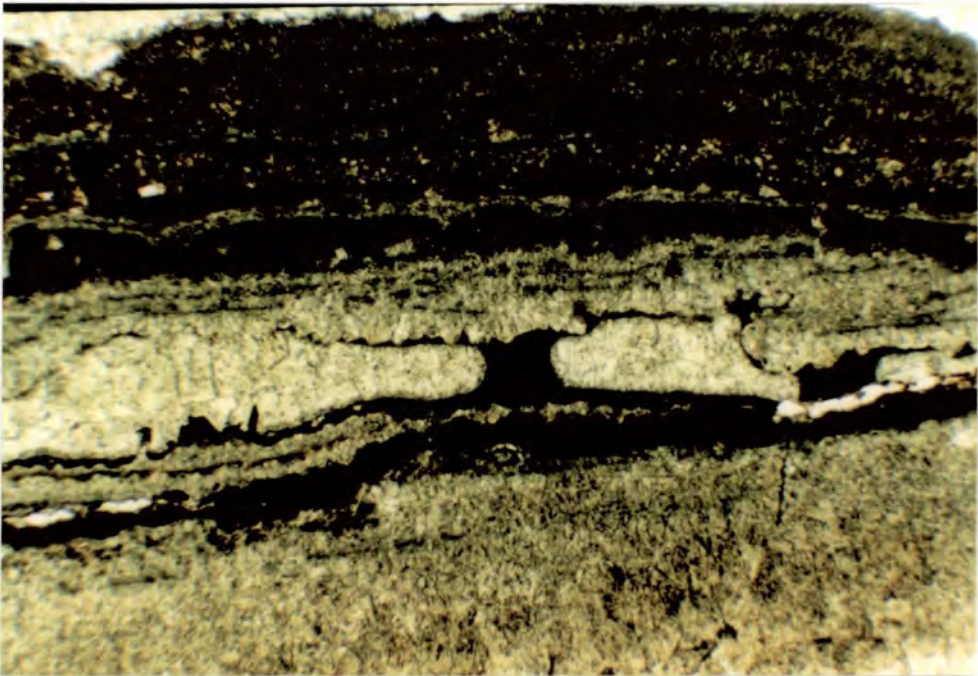


**Fig. 4.69** Photomicrograph of elongate cavity in which cementation has occurred on the roof of the cavity before a pillar of sediment has formed. Sediment is present on the floor of the cavity. Plane polars.

may represent a period of phreatic cementation before waters withdrew from the cavity. Movement of the water table was responsible for the periodic introduction of sediment into the cavity. In some cases there appears to have been a dissolutional phase in which cement phases have become unstable, indicating the fluctuation of water chemistry as well as water table fluctuations ( Fig. 4.71 ).

#### 4.7.4 Late Spar Cementation

The majority of the fenestral and laminar cavities within the limestones which are not filled by early vadose cements are occluded by clear inclusion-free equant spar, which represents the final phase of cementation in the Limestone Unit and is easily distinguished from the inclusion-rich earlier cements. Formation of drusy spar is normally the result of precipitation from magnesium-poor waters ( Folk, 1974 ). This filling by drusy spar appears to have taken place after dolomitisation of the limestones which is a result of alteration of the beds by hypersaline fluids from the overlying Mercia Mudstone Group. Within the dolomitised limestones the drusy spar fills remnant fenestral cavities and can be interstitial to the dolomites. Some dolomites have been partially calcitised ( Fig. 4.72 ). The drusy spars are post-Triassic but do not appear to be deep burial cements. The spar is patchily ferroan when stained and under cathodoluminescence contains an early non luminescent zone and a later finely banded zone of non luminescent and brightly luminescent cement ( Fig. 4.73 ). There are no dull luminescent zones in the late spar which are indicative of ferroan spars. This implies that the pore waters were sufficiently reducing to allow the incorporation of manganese into the calcite lattice but not iron ( Barnaby & Rimstidt, 1988 ). The latest spars do not then appear to be a deep burial event. Ferroan calcites can form at depths of as little as several hundred metres. ( Choquette & James, 1986 ). One hundred and ten metres of Jurassic rocks at present overlie the Mercia Mudstone Group in South Wales ( Waters & Lawrence, 1987 ). It is not known how great a thickness of sediment has been removed from the South Wales area but the thickness of the Jurassic in the Bristol Channel suggests that the cover may have been substantial ( Lloyd et al., 1973 ). Cope ( 1984 ) has argued for continuous deposition in the area in the Jurassic and Upper Cretaceous. The spar cements in the Sully Island limestones suggest a phase of cementation in waters which

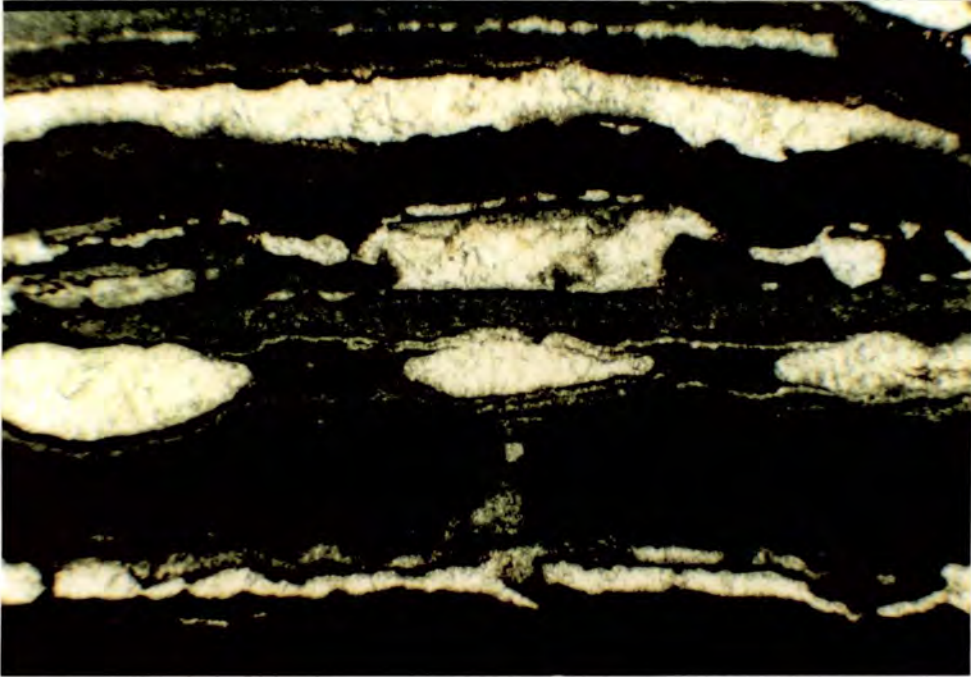


**Fig. 4.70** Photomicrograph in which the central cavity in the photograph contains an isopachous cement fringe which was precipitated before formation of the pillars. Plane polars.

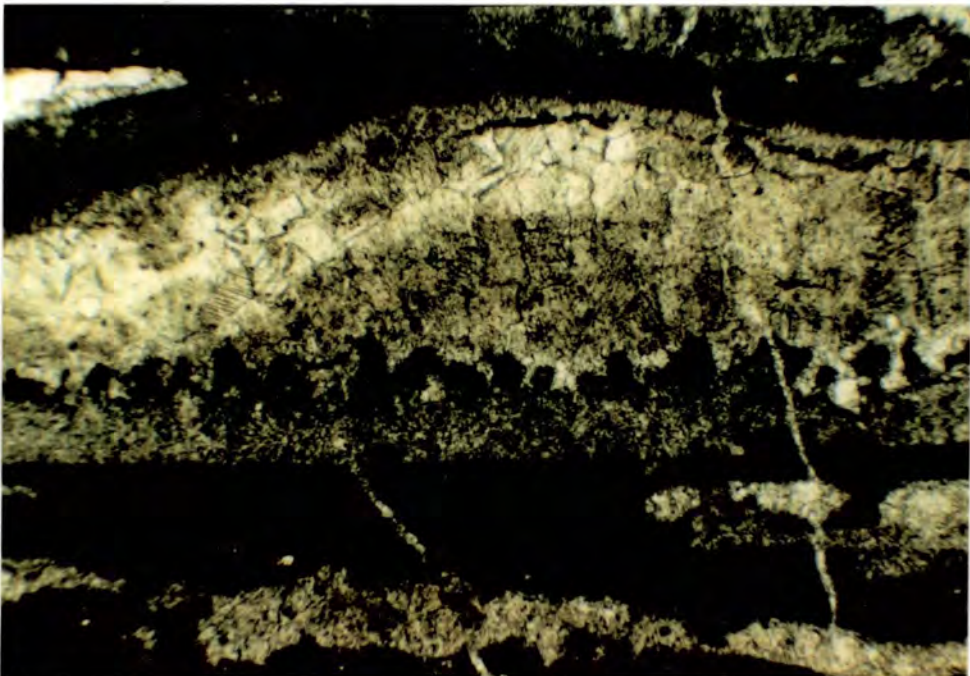


**Fig. 4.71** Photomicrograph of a dissolutional event which has caused the rounding of an early phase of cement which is overlain by sediment and further cement phases. Plane polars.

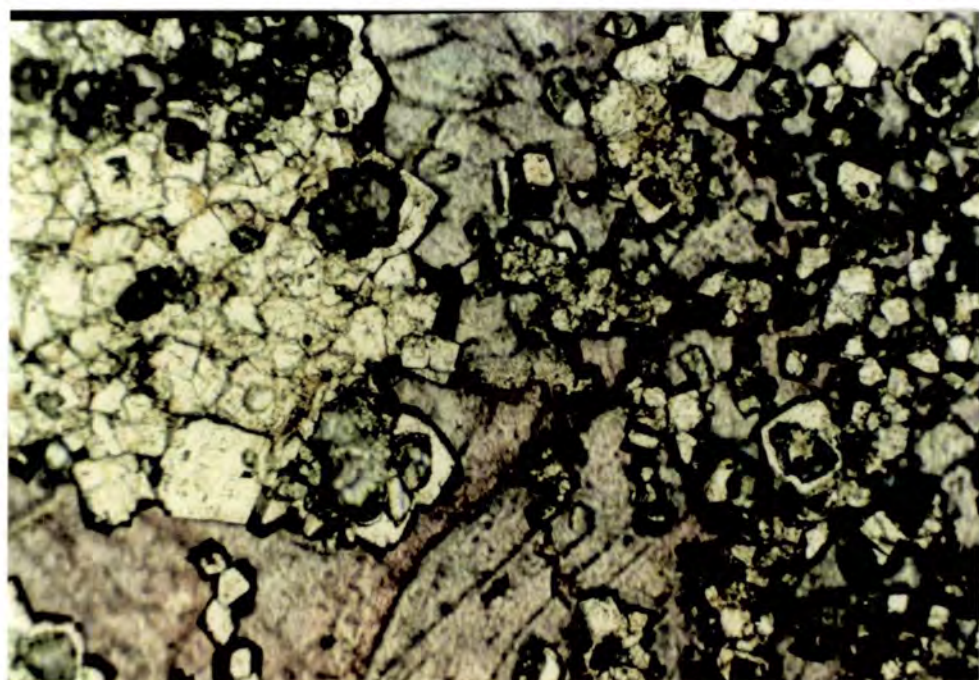


**Fig. 4.72** Photomicrograph of a dedolomite in the upper limestones showing the selective removal of the centres of dolomite crystals and replacement by poorly ferroan calcite. The slide has been etched ( hence the relief between the carbonate phases ) and stained. Plane polars.

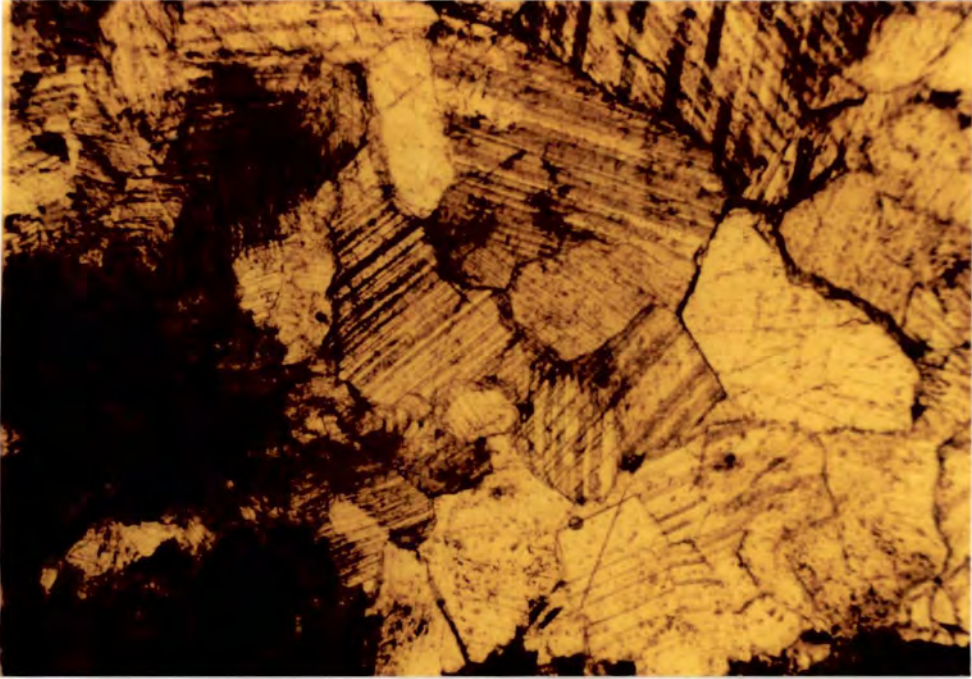


**Fig. 4.73A** Non-ferroan inclusion-free calcite spar which is the last phase of cementation in most of the limestone samples. Plane polars.

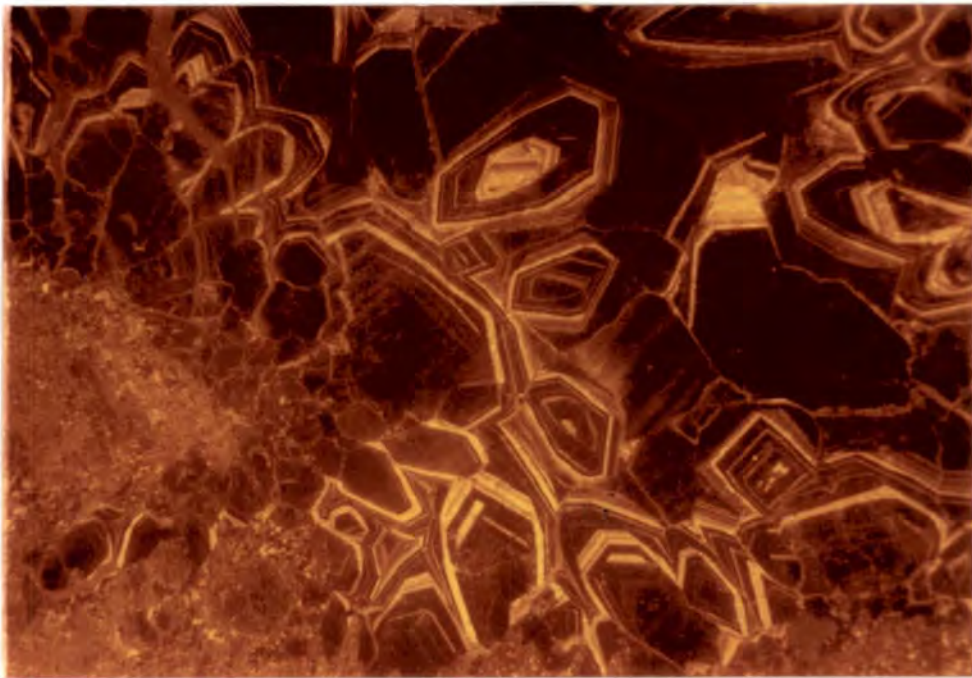


**Fig. 4.73B** Cathodoluminescence view of Fig. 4.73A showing non-luminescent and brightly luminescent zones in the spar. There are no dullly luminescent zones which are indicative of the incorporation of iron into the carbonate lattice. Note the dullly luminescent sediment in the bottom left of the photograph.

were insufficiently reducing for the incorporation of iron into the calcite lattice but which were nevertheless formed after at least several tens of metres of burial.

## **4.8 Analogous Depositional Environments to the Sully Island Succession**

### **4.8.1 Introduction**

The sedimentary structures within the limestones exposed at Sully Island and Dinas Powys represent a depositional environment which is relatively rare in the geological record. The association of tepee and saucer structures with travertine deposits and vadose diagenetic cements is, however, a relationship which has been described from other areas mostly from Recent sediments. Tepees themselves can form in a number of settings ( Kendall & Warren, 1987 ). The association of a number of the sedimentary structures within one area further constrains the environmental interpretations which can be made.

Tucker ( 1978 ) interpreted the Sully Island limestones as the deposits of a lacustrine perilittoral mudflat which underwent periodic exposure. In this model the limestones represent a depositional environment which is marginal to the hypersaline Mercia Mudstone Group. The limestones therefore formed on the shore of a hypersaline water body. There is a marked change in lithology between the limestones and the surrounding hypersaline dolomites. The reason for this change is given as a variation in lake water chemistry due to variations in climate in the South Wales area ( Tucker, 1978 ). The Sully Island sequence lies at most 50 metres below the base of the Blue Anchor Formation. Although only 30 metres of red mudstones are exposed in South Wales, boreholes have penetrated up to 110 metres of red mudstone. There is no evidence in these beds for a major change in the salinity of the waters in the South Wales area. It is more likely that the limestones at Sully Island are the result of a more localised change in the hydrological environment. Coastal salinas around the south and west coasts of Australia contain an analogous association of sedimentary structures to the limestones at Sully Island and the similarities will be briefly described.

#### 4.8.2 Australian Coastal Salinas

A number of salinas around the coastline of Australia have received attention in the recent literature as modern analogues to a number of problematic sedimentary sequences in the geological record. In particular, salinas in the Coorong Region of South Australia have been used as an example of an environment in which dolomite is precipitating directly from solution and compared with Proterozoic examples ( Muir et al., 1980 ). The majority of these salinas are evaporitic and contain an inner area of sulphate or halide salts. The marginal areas to these evaporitic beds are of interest in this study. They are commonly composed of carbonates which contain a similar assemblage of sedimentary structures to the limestones in Sully Island.

The majority of references to the Australian salinas have already been given in the preceding two chapters. The tepee/travertine/vadose cement association is found in many of the salinas including those in the Coorong Region. In all cases the sedimentary structures are the result of waters rising through the marginal sediments of the salinas, driven by a hydrologic flow from marine waters penetrating a semi-permeable barrier or from meteoric waters derived from inland areas.

Both aragonite and high and low magnesium calcite are precipitated in the marginal areas of the salinas. A range of carbonates from aragonite through to magnesite can form in the evaporative units. Aragonite is more common in the marginal zones, in particular in the salinas which derive their water from a marine source. Some of the flowstones in the salinas do appear to be composed of primary calcite. In Fisherman Bay, 180 kilometres north of Adelaide in South Australia the megapolygonal spring mounds are the result of upwelling meteoric waters derived from high land to the east ( Ferguson et al., 1982, 1988 ). This salina is the most similar in form to the Sully Island limestones both petrographically and geochemically.

The limestones at Sully Island contain a similar assemblage of sedimentary structures to the Australian salinas. The concentrically arranged zones of carbonate and evaporitic material however cannot be made out in Sully Island and for-

mation of evaporitic beds in the Sully Island subbasin at the same time as the limestones is unlikely. The limestones themselves are a distal intraclastic deposit which has been reworked by marginal lacustrine processes. The reasons for the formation of a limestone at Sully Island is most likely related to the local palaeogeography. The Limestone Unit and the underlying dolomites are as far as is known unique in the British Triassic. If the beds were simply in an environment marginal to the lacustrine conditions of the Mercia Mudstone Group then other occurrences of similar beds would have been encountered at outcrop or in boreholes. The fenestral intraclastic 'limestones' described by Waters & Lawrence ( 1987 ) are most likely examples of this marginal lacustrine facies.

The basement topography in the Sully Island area is complex and several exposures of Carboniferous Limestone surrounding the limestones can be assumed to have been high land during the Upper Triassic ( Fig. 4.5 ). The basement topography of the area suggests that the Sully Island area may have overlapped a ridge of basement to the north. The exposures of Carboniferous Limestone to the northwest of Ball Rock and north of Sully Bay may have been part of a continuous area of high ground. The progressive fining of clastic material from west to east is evidence that there was not a source of clastics from the north during deposition of the limestones ( Fig. 4.5 ).

To the south of the limestone outcrop Carboniferous Limestone is exposed on the south side of Sully Island itself and to the west of Hayes Point where basement is overlain by clastic stream and sheet flood deposits. At present the exposures of Carboniferous Limestone on Sully Island are level with the Evaporitic Dolomitic Unit. The Carboniferous Limestone to the west of Hayes Point is cut off to the east by a fault some hundred metres offshore ( Banner et al., 1971 ) and may have extended some distance offshore forming high ground in the Triassic. The extent of the southerly extension of the Carboniferous Limestone to the south of Sully Island is also uncertain. Banner et al. ( 1971 ) did not sample bedrock closer than 800 metres to the south of Sully Island where Triassic mudstones were found. In the British Geological Survey map of the offshore solid geology, a large area of Carboniferous Limestone roughly 700 metres to the southeast of Sully Island is present. Given the slight post-Triassic folding in the South Wales area

this Carboniferous Limestone would have been exposed in the Upper Triassic and may well have been linked to the exposures on Sully Island.

Taking into account the present day exposures of basement in the Sully Island area, a section can be drawn through the Sully Island area showing the movement and resurgence of waters ( Fig. 4.74 ). It is possible that during formation of the limestones the Sully Island area formed an embayment in the lake shoreline and that deposition took place in a basin which had limited circulation with the hypersaline waters in the main Bristol Channel basin to the south. The connection, if any, with the hypersaline waters will have been to the south of Sully Bay. This is the most likely place in view of the palaeogeography of the area. The Sully Island area thus formed a small embayment in the Upper Triassic shoreline at first forming an evaporative sabkha-like mudflat and then as meteoric waters became dominant in the subbasin depositing a sequence of limestones presumably at a time when there was a regression of the hypersaline waters.

The reason for the importance of upwelling groundwaters in the Sully Island area is not known, but may again be related to the local basement topography. The flow of groundwaters through the Carboniferous Limestone and clastic marginal deposits and into the basin will have taken place constantly in the Upper Triassic. There is no evidence at outcrop or in boreholes for the resurgence of groundwaters in other areas than in Sully Island and at Dinas Powys. There is evidence for the movement of waters through the marginal deposits at Hayes Point to the west of the limestones. Several beds appear to have been affected by the dissolution of evaporites and solution collapse structures are present ( Fig. 3.13 ). Lateral movement of groundwaters through the clastic sediments and into the limestones themselves appears to have taken place. The basal calcrete which forms the base of the Limestone Unit is likely to have formed a partial aquiclude. Similar calcrete aquicludes have been described by Arakel ( 1982 ) which are barriers to the vertical movement of groundwaters. It is likely that the replacement of the sulphates in the marginal clastics and Evaporitic Dolomites took place at this time. The upwelling of the groundwaters through the limestones appears to have been localised and ephemeral. The resurgence of the waters was related to the basinal topography of the Sully Island area and to the variations in the amount of water input into the basin. Changes in the groundwater level are shown by the various

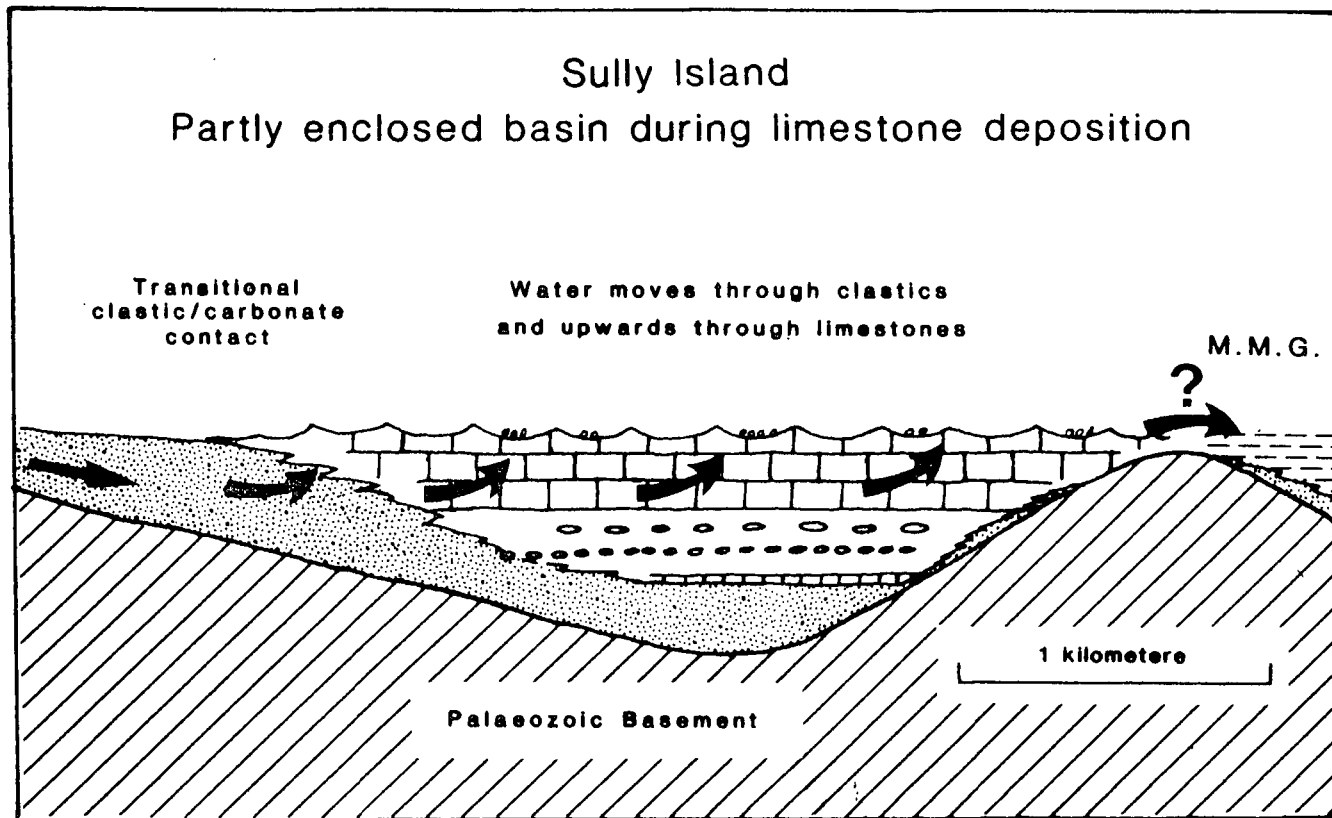


**Fig. 4.74** Sketch section, roughly west-east in orientation, showing the eastward movement of groundwaters through the marginal clastic beds and laterally and upwards through the limestones.

sedimentary structures in the limestones and by the variety of cements. The rippling of the limestones could be the result of increased discharge from spring outlets which gave rise to the formation of ephemeral lakes within the subbasin, rather than a transgression of the hypersaline waters which would have given rise to deposition of a more evaporitic sediment. Movement of the groundwaters through the limestones from the west into a thinner ( and narrower ) limestone bed would also lead to upward movement of the waters, similar to the resurgence of meteoric waters in Fisherman Bay ( Ferguson et al., 1988 ).

The localised nature of the travertine deposits is similar to that in the Recent salinas where discharge takes place over areas 100 metres in diameter and flowstones form in discrete areas associated with one particular water flow. The discharge through individual spring outlets appears to have been variable both in the volume and duration of flow, as well as showing variations in the chemistry of waters. The permeability of the limestones was such that vertical pathways through the sediment would be easily formed and blocked when flow of waters was reduced. The areas of polygonally arranged fissures in the limestones of Sully Bay represent the final movement of waters through more lithified beds associated with the formation of the tepee and saucer structures in the topmost metre of limestone. The presence of breccia in some of the fissures is evidence that the limestones had been partially lithified.

The depositional environment of the Dinas Powys limestones, although giving rise to a similar assemblage of sediments, was different from the Sully Island subbasin. The Dinas Powys limestones were laid down in a steep-sided palaeovalley with cliffs in places up to 50 metres in height. Travertine deposits in fluvial settings are common, particularly in arid environments ( Hunt et al., 1966; Casanova, 1984; Kostecka & Weclawick, 1987; Heimann & Sass, 1989 and others ). As opposed to the salina model where emergent waters precipitate carbonate, river waters lose  $\text{CO}_2$  in turbulent conditions. The environment in which the Dinas Powys travertines were laid down does not reflect high energy fluvial conditions. In particular the presence of flöe calcite indicates relatively still conditions, although with very highly supersaturated waters sheet calcite can form in more turbulent conditions ( Chafetz et al., 1989 ). The Dinas Powys limestones must have formed in a pool downstream from the point of emergence of the waters. The presence of

spherules indicate that at some point very rapid precipitation of carbonate took place. These spherules were then transported into the calmer environment in which the stromatolites and other travertine deposits were formed. Although not exposed at Dinas Powys, it is possible that the sediments were formed in a pool behind a travertine dam.

## **4.9 Conclusions**

### **4.9.1 Sully Island**

The Limestone Unit exposed on Sully Island and the surrounding shoreline represents a depositional environment which is unique in the British Triassic and rare in the geological record in general. The limestones are composed of a detrital component of Carboniferous Limestone clasts derived from the surrounding basement, mostly from the west of the area and a primary component which is the result of precipitation of various forms of carbonate within the unit. The formation of limestones containing no evaporite minerals despite the abundant evidence for extensive periods of desiccation is the result of several factors. There is no evidence for the presence of hypersaline waters in the Sully Island area during deposition of the limestones. The volume of resurgent spring waters would not be sufficient to completely dilute the hypersaline waters if the limestones were formed on the margins of the evaporative waters. It is more likely that the hypersaline waters underwent a regression such that the limestones were formed in a very different hydrological environment.

It is not likely that the flow of ground waters into the Sully Island basin was constant during the deposition of the dolomitic and limestone units. There is little evidence for the input of meteoric waters into the basin during deposition of the dolomites. The first indication of the presence of meteoric waters is the formation of the groundwater calcrete in the upper dolomite, which represents the farthest regression of the hypersaline waters in which the sulphates in the central part of the unit were formed. The groundwater calcretes may in fact have formed after deposition of the dolomite unit, before the formation of the pedogenic calcrete at the base of the limestones. The basal calcrete represents a long period of time, possibly hundreds of thousands of years, during which there was

a significant change in the hydrological environment. The influx of groundwaters may have taken place gradually over this period, possibly in response to a change in the climate in the South Wales area. The change in climate did not affect the deposition of red mudstones in the Mercia Mudstone Group and appear to have had a local effect due to the concentration of resurgent groundwaters in the Sully Island area. The limestones formed in an environment in which the level of the water table was very variable giving rise to both vadose and phreatic cements. Evidence for prolonged exposure of the limestones is abundant as are rippled bedding surfaces. Vadose conditions appear to have been prevalent, however, since most of the cavities contain meniscus cements.

The tepee/travertine/vadose diagenesis association is one which is commonly seen in Recent salinas which are affected by upwelling groundwaters around the margins of evaporite-filled basins. The concentric zonation of the salinas is not duplicated in the Sully Island area but the association of sedimentary structures is identical. The travertines in Sully Island in particular contain the same forms of precipitated carbonate as those in the Recent examples. The depositional environment of the limestones at Sully Island can thus be directly comparable with the modern examples from the south and west coasts of Australia.

#### **4.9.2 Dinas Powys**

The smaller outcrop of limestones exposed at Dinas Powys is the result of precipitation and deposition of carbonate within a fluvial valley, possibly associated with an emergent spring. Abundant travertine deposits are the result of precipitation from supersaturated waters which lost CO<sub>2</sub> on emergence or in turbulent flows. The limestones themselves formed in a pool of relatively quiet water possibly behind a travertine dam. As in the Sully Island limestones there is evidence for the desiccation and vadose diagenesis of the limestones, indicating a fluctuating water table in response to changes in the volume of spring discharge.

## **Chapter 5**

### **Geochemistry of the Sully Island and Dinas Powys Carbonates**

## Chapter 5

### Geochemistry of the Sully Island and Dinas Powys Carbonates

#### 5.1 Introduction

##### 5.1.1 Reasons for Geochemical sampling

The carbonates exposed in the Sully Island sequence and at Dinas Powys were laid down in a variety of depositional settings, under the influence of a number of different water types. The change in depositional style between the limestones and the surrounding dolomitic beds indicates a significant change in the hydrological and depositional environment. There is evidence within the limestones for the upwelling of carbonate rich groundwaters and the lack of evidence for evaporite minerals in the limestones indicates that the waters were not particularly rich in cations other than carbonate. In view of the evidence for different water types having had an influence in the deposition of the Sully Island sequence, a geochemical study was carried out in order to acquire further information on the chemistry of the depositional and diagenetic waters in which the carbonates formed. The stable isotopic and trace elemental geochemistries of travertine deposits and related deposits have been studied by several authors ( Manfra et al., 1976; Thompson et al., 1976; Handford et al., 1984 and Ferguson et al., 1988 ) and such studies have proved to be of use in the analysis of data from the limestones in South Wales.

##### 5.1.2 Sampling

In all cases the carbonate fraction of the rock was separated from the insoluble residue by digestion in acid and was then analysed as described in Appendix 2. No whole rock analyses were carried out. Care was taken to ensure that samples were monomineralic. Mixtures of calcite and dolomite were not analysed where this could be avoided, although some of the dolomites in the Evaporitic Dolomite Unit contain some interstitial calcite which could not be separated. Samples were collected using a hand-held rotary drill with a burr diameter of 0.9 millimetres.

Using this drill structures within the rock of a diameter of 1.2 millimetres could be sampled.

### **5.1.3 Methods of Preparation**

The methods of preparation of samples for stable isotopic and trace elemental analyses are different, although both involve the digestion of the carbonate fraction of the rock in an acid. For stable isotopic analyses the carbonate is dissolved in phosphoric acid and the CO<sub>2</sub> gas evolved is analysed as described in Appendix 2 .

Trace elemental analyses were carried out by dissolving the carbonate in weak hydrochloric acid as described in Appendix 1 . In this case the solution of cations derived from the carbonate is analysed. Since in most cases the insoluble residue is composed entirely of quartz there is no problem of contamination by leaching of cations from other sources.

## **5.2 Stable Isotope Analysis, Results**

### **5.2.1 Introduction**

In total, 55 stable isotopic analyses were carried out on the limestones and surrounding beds at Sully Island and Dinas Powys. Forty-five of these analyses were taken from the limestones in the Sully Island area and at Dinas Powys. The other 11 samples were taken from the dolomites surrounding the limestones in the Sully Island succession.

The travertine deposits in particular were sampled since they are composed of carbonate with few impurities and do not contain clastic carbonate derived from the Carboniferous Limestone. Also, the travertines should represent most closely the composition of the emergent groundwaters. Thirty samples were taken from the travertines and surrounding deposits. In addition, it was possible to sample successive bands of flowstone, of around 1 millimetre in thickness, to establish whether there were significant changes in the geochemical conditions in which the travertines were formed. Within the intraclastic beds the clast size was generally

too small to allow sampling of cements or precipitated carbonate. In these cases the sample is effectively a whole rock carbonate analysis. This inevitably involves the sampling of Carboniferous Limestone clasts within the sediment. For this reason fewer intraclastic limestones were sampled.

In the dolomitic units above and below the limestones, the dolomite rhombs are too small to be picked out and whole rock samples were again taken. Care was taken not to sample areas in which clastic material could be seen. In the case of nodules within the Evaporitic Dolomitic Unit, coarse calcite spar could be separated from the surrounding dolomites without contamination.

### 5.2.2 Evaporitic Dolomite Unit, Sully Island

The eight samples taken from the Evaporitic Dolomite Unit show a variety of stable isotopic compositions. The sequence of diagenetic replacements which have taken place in the dolomites has led to a complicated series of stable isotopic values. The dolomite which comprises the majority of the unit is itself variable in composition. The small sample size makes it difficult to make definite statements about the unit as a whole.

The eight samples taken from the Evaporitic Dolomite Unit have a  $\delta^{18}O$  composition of between  $+1.0$  and  $-6.4\text{‰}$ , and a variation in  $\delta^{13}C$  of  $+0.2$  to  $-3.5\text{‰}$ . Within this wide range of values five of the samples have a  $^{18}O$  of between  $-0.2$  and  $+1.0\text{‰}$  ( Fig. 5.1 ). These five values include samples taken from the groundwater calcretes, both within the nodules and from the matrix, a sample from the iron-rich pedogenetic horizon at the base of the unit and two samples taken from the sabkha-type replaced evaporite nodules. Of the remaining three samples one is taken from the marl interstitial to the sabkha nodules, one from the basal dolomite and one from the coarse rhombic dolomite from the top of the unit ( Fig.5.1 ). The presence of minor calcite in some of the samples does not appear to have significantly affected the stable isotopic results. No correlations between mineralogy and stable isotopic compositions could be seen in the data.

The sequence of replacements in the Evaporitic Dolomite Unit is complex and the timing of the recrystallisation of the basal dolomite and of dolomitisation of the groundwater calcrete nodules is not certain. None of the stable isotopic

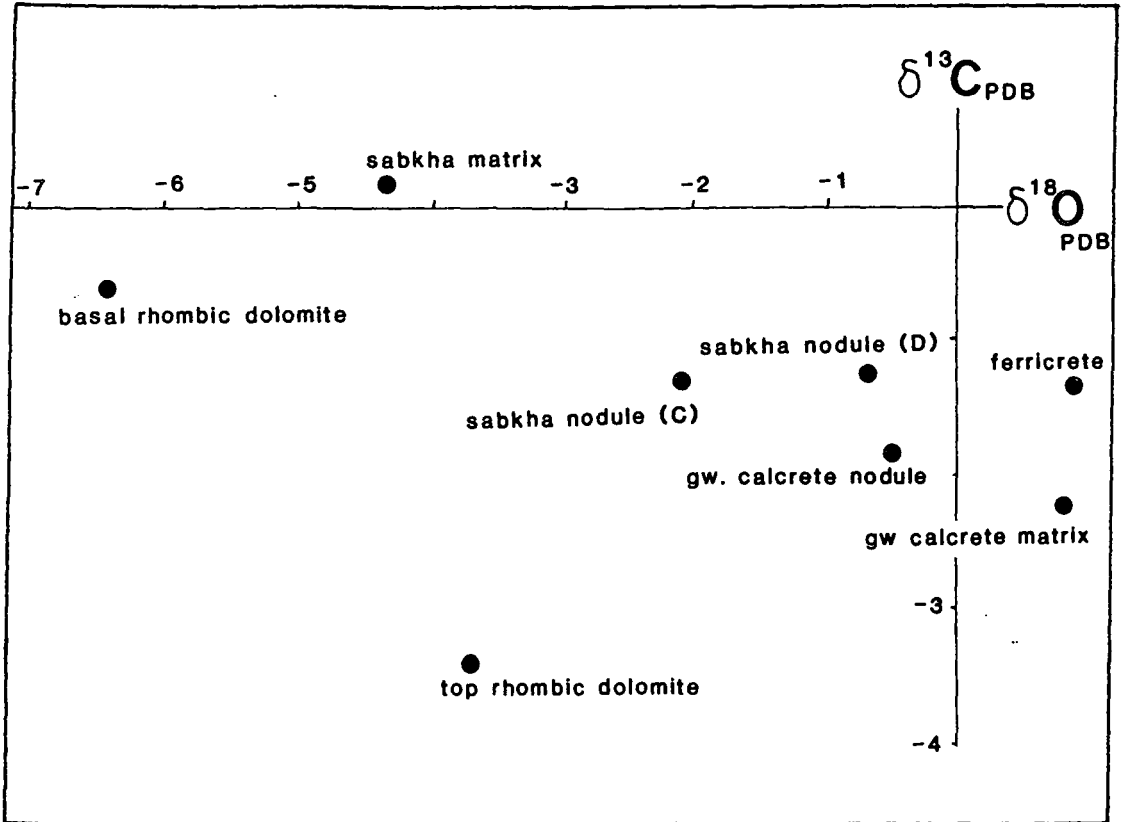


**Fig. 5.1** Stable isotopic analysis results from the Evaporitic Dolomitic Unit. Sample marked ( C ) is calcitic, all others are dolomitic.

values, however, indicates a marine origin for any of the waters involved in the diagenesis of the unit ( Taylor, 1983 ). The range given by Taylor for the stable isotopic composition of evaporitically-enriched marine waters has a  $^{18}\text{O}$  of between  $+4.0$  and  $+2.0\text{‰}$  . None of the samples of Mercia Mudstone Group or marginal deposits lie between these values. As has been discussed in Chapter 3, although the dolomite which comprises the majority of the unit is not a primary precipitate, it is likely to have formed during early diagenesis while still in contact with surficial waters. The five samples with  $^{18}\text{O}$  between  $+1.0$  and  $-2.0\text{‰}$  represent both sediments and nodules which have undergone a complex series of diagenetic steps. The similarity of their stable isotopic values suggests that the final composition is related to a diagenetic phase which affected much of the unit. This is most likely to be the replacement of an earlier carbonate phase by dolomite in a meteoric water-rich environment, during early burial. The sample most enriched in  $^{18}\text{O}$  is the iron rich bed which forms the base of the unit in the east of the Sully Island area. This bed represents a period of exposure and pedogenesis during which the original fenestral sediment was replaced. By contrast the fenestral dolomite is most depleted in  $^{18}\text{O}$  (  $-6.4\text{‰}$  ), a very depleted value for a dolomitic sample. The  $^{13}\text{C}$  value between the two samples is essentially unaffected. The difference between the two parts of the same horizon suggests that the iron-rich dolomite was replaced by evaporatively enriched waters. This may represent the earliest replacement in the sequence, which took place before much of the unit was laid down. The sequence of replacements seen in the replaced evaporitic nodules suggests a more complex diagenetic history. Taking the 5 samples which have  $^{18}\text{O}$  between between  $+1.0$  and  $-2.0\text{‰}$  , then the differences in  $^{18}\text{O}$  can be related to the mineralogy of the samples and to the different fractionation factors for calcite and dolomite. The sabkha nodule composed of calcite is the most depleted in  $^{18}\text{O}$  , while the iron rich basal dolomite is  $^{18}\text{O}$  enriched. The stable isotopic composition of coexisting dolomite and calcite has been the subject of some discussion ( Land, 1980 and see Section 10.2.2 ). In this case if coprecipitation is assumed then a fractionation factor of  $+2.1\text{‰}$  for  $^{18}\text{O}$  can be assumed for dolomite relative to calcite. This lies within the limits set by Land ( 1980 ) and it is thus possible that the calcite and dolomite formed in waters of essentially the same composition. It is more likely, given the apparent replacement of calcite by dolomite, that the replacement of the sulphate nodules

by calcite was an early phase of diagenesis. The formation of the main dolomite which now comprises the majority of the unit along with partial replacement of the calcite will have taken place later, although still in a meteoric-water dominated environment. Measurement of the  $^{18}\text{O}$  value of the quartz nodules was not made but it is likely that the selective replacement of the sulphate by silica also took place during this time. The replacement of most of the Evaporitic Dolomite Unit took place in waters of essentially similar composition and the series of diagenetic events which took place at this time cannot be separated on the basis of geochemistry.

In this model of diagenetic replacements the sample taken from the marl in the centre of the most prominent sabkha band does not fit well with the other data points ( Fig. 5.1 ). The depleted  $^{18}\text{O}$  of the sample and slightly enriched  $^{13}\text{C}$  value are anomalous. It is not likely that this bed has been affected by a further diagenetic event nor could the bed have been impermeable to waters moving through the rock during early burial. The sample cannot be explained by the model used and may be the result of an error in preparation of the sample. Unfortunately the small sample size did not allow the duplication of analyses.

The two samples which are composed of an array of coarse rhombic crystals are in general depleted in  $^{18}\text{O}$  relative to the other samples in the unit. Their  $^{13}\text{C}$  values are also more varied than those in the 5 grouped samples ( Fig. 5.1 ). The dolomite at the top of the unit is depleted in  $^{18}\text{O}$  and in  $^{13}\text{C}$ . This stable isotopic signature represents a replacement of the dolomitic sediment in waters of meteoric origin. This replacement may have taken place during the formation of the overlying limestones. There is little evidence for the recrystallisation of the whole Evaporitic Dolomite Unit sequence and the position of the coarse dolomite underlying the calcrete suggests that it is related to the formation of the overlying beds. The recrystallisation of the dolomite may have taken place before the formation of the micritic calcrete which will have formed an aquiclude to the downwards movement of waters. The  $^{18}\text{O}$  value of the dolomite (  $-3.4\text{‰}$  ) suggests formation in waters of similar composition to those in which the replacement of the main part of the Evaporitic Dolomite Unit took place. The coarse nature of the topmost dolomite is the result of proximity to the upper limestones. The presence of scattered rhombs within the dolomite unit suggests

that this recrystallisation took place progressively from above. The depleted  $^{13}\text{C}$  value of this upper dolomite is indicative of the input of some soil  $\text{CO}_2$  during the formation of the coarse dolomite. The most depleted bed in the unit, the basal dolomite, is also composed of a coarse rhombic array. This bed is also slightly enriched in  $^{13}\text{C}$ . The recrystallisation of the bed to a coarse dolomite took place after the calcretisation of the eastern part of the bed. The similarity between the rhombic array in the upper dolomite and that in the basal bed is suggestive of a similar diagenetic sequence. The selective recrystallisation of this bed may be the result of the fenestral nature of the bed as opposed to the more clay-rich, less permeable dolomite which comprises the majority of the unit. Lithological control is the most likely explanation for the coarse rhombic dolomite being restricted to one bed. The very depleted nature of the  $^{18}\text{O}$  values may be the result of replacement by meteoric waters which moved laterally through the marginal clastics with no exposure to evaporative conditions at the surface.

The stable isotopic values of the Evaporitic Dolomite Unit are at first sight complex. If one sample is discarded, a pattern in the stable isotopic variations can be seen and related to the petrographic evidence in the unit. The unit appears to have been primarily influenced by the influx of meteoric waters into the area during the deposition of the Limestone Unit. Replacement of the carbonate precursor in this water type gave rise to relatively depleted  $^{18}\text{O}$  values ( between  $+1.0$  and  $-2.0\text{‰}$  ) and  $^{13}\text{C}$  values of between  $-1.0$  and  $-2.2\text{‰}$ . The replacement of the sulphate nodules by calcite ( and the formation of the calcitic groundwater calcrete ) and the subsequent phase of dolomitisation cannot be distinguished geochemically. Most of the replacements in the unit appear to have taken place in waters of essentially the same chemical composition. Some localised replacement of the anhydrous dolomite in the unit has taken place giving rise to a coarse rhombic dolomite. This has occurred in the topmost dolomite, related to the overlying calcretisation and in the basal dolomite bed presumably as a result of the movement of meteoric waters through the laterally equivalent marginal clastics.

### 5.2.3 Limestone Unit, Sully Island and Dinas Powys

#### 5.2.3.a Introduction

The Limestone Unit is composed of a wide variety of carbonate types which are a result of a number of sedimentological processes which were active during deposition and early burial. As such, the limestones are of greater value than the underlying dolomites, in that they are a direct record of the composition of the waters in which they formed. For this reason the majority of stable isotopic samples were taken from the Limestone Unit, in particular from the travertines which contain little clastic material. Travertines from Sully Island and Dinas Powys were sampled. In this section the travertine deposits will be considered separately from the other limestones sampled.

#### 5.2.3.b Intraclastic Limestones, Sully Island

In total 17 samples of limestones from Sully Island were analysed including intrapelsparites, calcretes, microbial beds and where possible the pore-filling late spars in cavities. The results from these analyses are plotted in Fig. 5.2 . The limestones show relatively little variation in  $\delta^{18}O$  ( -3.0 to -5.5‰ ) compared with the range in  $\delta^{13}C$  ( -0.5 to -8.0‰ ). Within the spread of values certain groups can be made out ( Fig. 5.2 ). The values show a slight but significant positive covariance of  $^{18}O$  and  $^{13}C$  . Such trends can be interpreted as being the result of mixing of two water types of different chemical composition ( Hudson, 1977 ). This trend in stable isotopic composition is most clearly seen in the travertine deposits and will be discussed more fully in the next section.

The intrapelsparite limestones which were sampled display a range of  $\delta^{13}C$  compositions with relatively constant  $\delta^{18}O$  ( Fig. 5.2 ). These limestones contain between 20 and 50% of intraclasts of Carboniferous Limestone which itself represents an unknown factor in the total composition of the sample. Hird ( 1985 ) has described the stable isotopic geochemistry of dolomitic Carboniferous Limestone from South Wales. These dolomites have a variable stable isotopic composition, with  $\delta^{18}O$  between 0.0 and -9.0‰ and  $\delta^{13}C$  between +4.0 and -2.5‰ . Use of the data from samples containing Carboniferous Limestone clasts must therefore

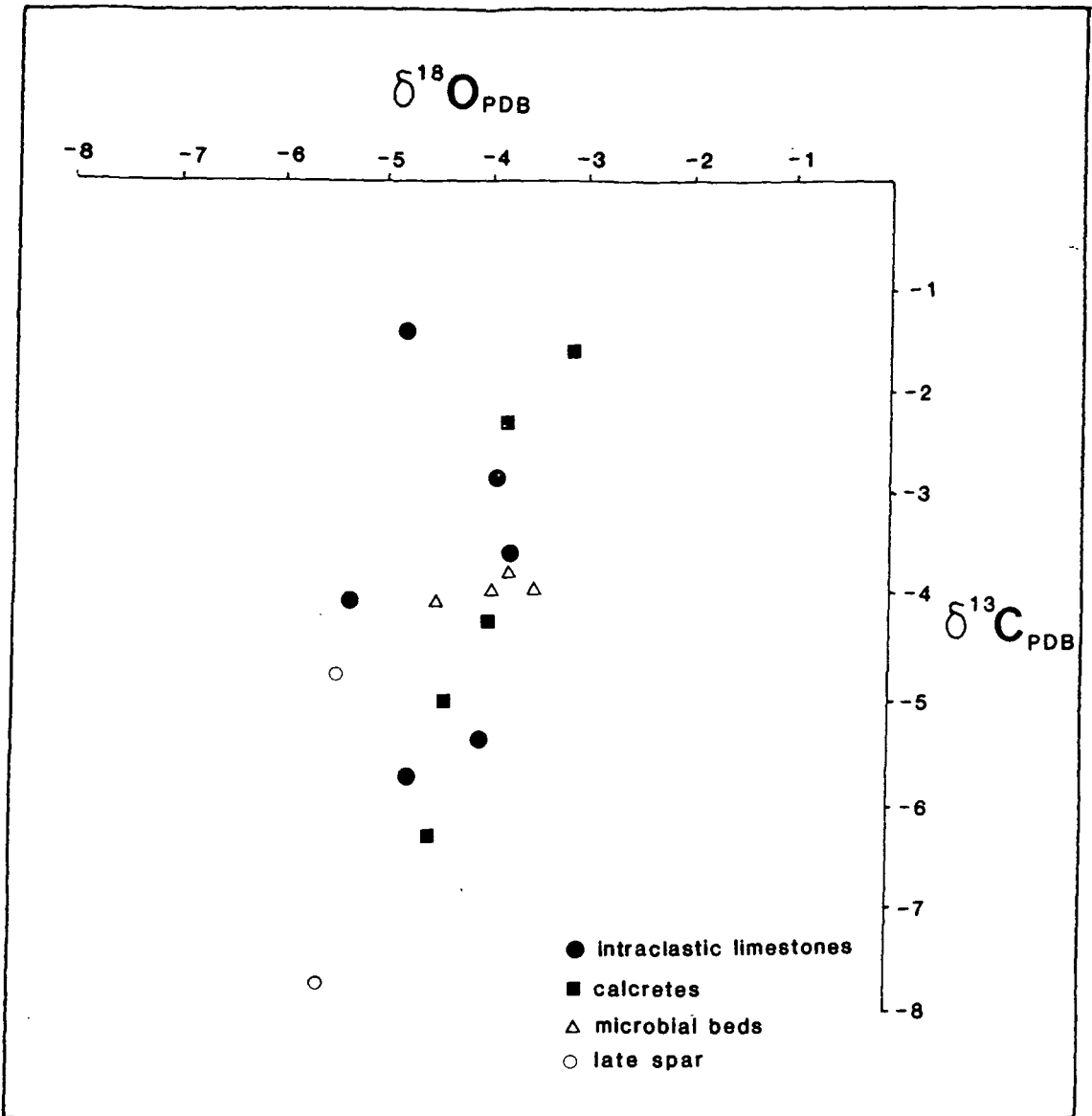


**Fig. 5.2** Stable isotopic analysis results from the Limestone Unit, Sully Island, not including travertine deposits.

be treated with caution. Despite the uncertainty of the detrital carbonate input none of the intraclastic limestones shows any marked variation from the pattern shown by the limestones in general.

Five calcrete samples were analysed in this study, three from the basal unit and two from the less mature nodular horizons in the upper limestones. The two calcrete types can be seen to be distinct geochemically as well as petrographically ( Fig. 5.2 ). The two samples taken from a nodular calcrete horizon in the east of Sully Bay have  $\delta^{13}\text{C}$  compositions of  $-1.7$  and  $-2.3\text{‰}$ . These samples are among the least depleted of the limestone samples and do not appear to have been greatly influenced by soil  $\text{CO}_2$  during their formation. In this respect they are a result of very early pedogenesis and do not represent the formation of a soil horizon. The  $^{18}\text{O}$  values do not show any evidence of strong evaporative enrichment. Three samples were taken from the more mature basal calcrete. This bed is similar in  $\delta^{18}\text{O}$  composition to the nodular calcretes but is depleted in  $^{13}\text{C}$  by on average  $3.2\text{‰}$ . This suggests that in the more mature calcrete, soil-derived  $\text{CO}_2$  has had an effect during precipitation of carbonate. The mature calcrete does not show any evidence of evaporative enrichment of  $^{18}\text{O}$ . This appears to be common in some calcrete horizons ( P. Wright, pers comm. ). Although there is no evidence at present for vegetative cover ( Section 4.2.2 ) it is possible that oxidation of organic matter within the soil may have had an influence in the depleted  $^{13}\text{C}$  values. Similar stable isotopic values have been reported from palaeosols in the geological record ( Platt, 1989 ). The range in  $^{13}\text{C}$  values in the Sully Island calcretes is consistent with stable isotopic values recorded from recent carbonates influenced by soil-derived  $\text{CO}_2$  ( Cerling, 1984; Cerling et al., 1989).

Four samples were taken from the microbially laminated limestones ( Fig. 5.2 ). All of these samples are similar in composition and are clustered around  $-3.9\text{‰}$   $\delta^{18}\text{O}$  and  $-4.0\text{‰}$   $\delta^{13}\text{C}$ . The stromatolitic beds are slightly depleted in  $^{13}\text{C}$  and carbonate taken from columnar stromatolites is geochemically indistinct from that in laminated limestones. The carbonate in the microbial beds does not appear to have been affected by the oxidation of organic material during precipitation. The depletion observed is most likely due to the fact that the microbial laminae are composed of detritally-derived carbonate which is not being

recrystallised or replaced during organic breakdown but which is being passively trapped by the microbial structures.

Two samples of cavity-filling drusy spar were analysed. These two samples are the most depleted in  $^{18}\text{O}$  of the limestones (  $-5.5$  and  $-5.7\text{‰}$  ). The  $\delta^{13}\text{C}$  values are  $-4.8$  and  $-7.8\text{‰}$  respectively. This last  $^{13}\text{C}$  value is the most depleted of the limestones. Relative to the sediments in which the spars formed, the cavity fills are depleted in both  $^{18}\text{O}$  and  $^{13}\text{C}$  by between  $1.0$  and  $2.0\text{‰}$  .

Taking into account the abundant evidence for exposure of the limestones as well as the fluctuations of the groundwater table in the area, the consistency of the  $\delta^{18}\text{O}$  values is surprising. The lack of evaporative enrichment in the calcretes in particular is not what would be expected. The stable isotopic composition of the intraclastic limestones suggests that the Carboniferous Limestone which forms the majority of the clasts is of an overall similar composition to the primary carbonate in the Limestone Unit. One sample of Carboniferous Limestone taken from a clastic limestone at Hayes Point has a  $\delta^{18}\text{O}$  of  $-3.7\text{‰}$  and a  $\delta^{13}\text{C}$  of  $-0.9\text{‰}$  . The variety of lithologies in the partially dolomitised Carboniferous Limestone in the South Wales area is such that this cannot be taken as an average composition of the carbonate detritus entering the Sully Island basin. The stable isotopic variations seen in the limestones, however, indicate that changes in the composition of the primary carbonate phase were of more importance than variations in the composition of the detrital carbonate input. The  $\delta^{18}\text{O}$  values of between  $-3.5$  and  $-5.5\text{‰}$  are indicative of precipitation from waters of a non-marine origin. In view of the palaeoclimatology it is likely that the waters from which the carbonate precipitated had undergone some evaporative enrichment. The  $^{18}\text{O}$  composition of the precipitation in the South Wales area during the Upper Triassic is likely to have been between  $-6\pm 2\text{‰}$  , by comparison with the composition of precipitation at the present day ( Yurtzever, 1975 ), which is consistent with the composition of the emergent groundwaters at Sully Island. There do not appear to have been any periods of extreme evaporation giving rise to high enrichments in  $^{18}\text{O}$  . This may be due to a relatively constant inflow of meteoric waters into the Sully Island area during formation of the limestones. Although individual spring outlets were ephemeral the total volume of waters en-

tering the basin may have remained constant providing an input of isotopically depleted waters which counteracted the evaporative effects.

The more varied  $\delta^{13}C$  values reflect the number of influences which will have had an effect on the carbonate during precipitation of the Limestone Unit. The influence of soil-derived  $CO_2$  appears to have had more effect than the oxidation of organic material although there is abundant evidence for the original presence of biogenic material. Some of the non calcretised intraclastic limestones are depleted in  $^{13}C$  ( around  $-5.5\text{‰}$  ) which may reflect the oxidation of organic material within the limestones.

### 5.2.3c Travertine Deposits, Sully Island and Dinas Powys

Twenty-three samples from the travertines and related deposits at Sully Island and Dinas Powys were analysed. A further three samples were taken from the fillings of polygonal fissures in the upper limestones. A number of carbonate types within the travertine deposits were sampled. Flowstones and pisoids were relatively easy to sample whereas flöe calcite could only be analysed as a whole rock sample along with surrounding cements. Some micrite sediment associated with the travertines was also sampled. Certain flowstones were of sufficient thickness to allow the sampling of successive bands of fibrous calcite within one flowstone sheet. The results of the stable isotopic analyses of the travertine deposits is presented in Fig. 5.3 .

The spread of  $\delta^{18}O$  values within the travertines is greater than that in the clastic limestones ( between  $-2.0$  and  $-8.0\text{‰}$  ). There is also a more obvious positive covariance between  $^{18}O$  and  $^{13}C$  . Three flowstone layers were sampled in successive bands of slightly greater than 1 millimetre in thickness. These analyses are represented by the points connected by arrows in Fig. 5.3 . Although the three flowstones vary in absolute stable isotopic composition, the trend of the data in each flowstone is the same and indicates covariance of  $^{18}O$  and  $^{13}C$  in the waters during precipitation. Successive bands in the flowstones can vary by as much as  $\pm 1.5\text{‰}$  . The travertine data plotted as a whole also shows a covariant trend. In general the travertines from Dinas Powys are less depleted in stable isotopic composition than those from Sully Island ( Fig 5.4 ).

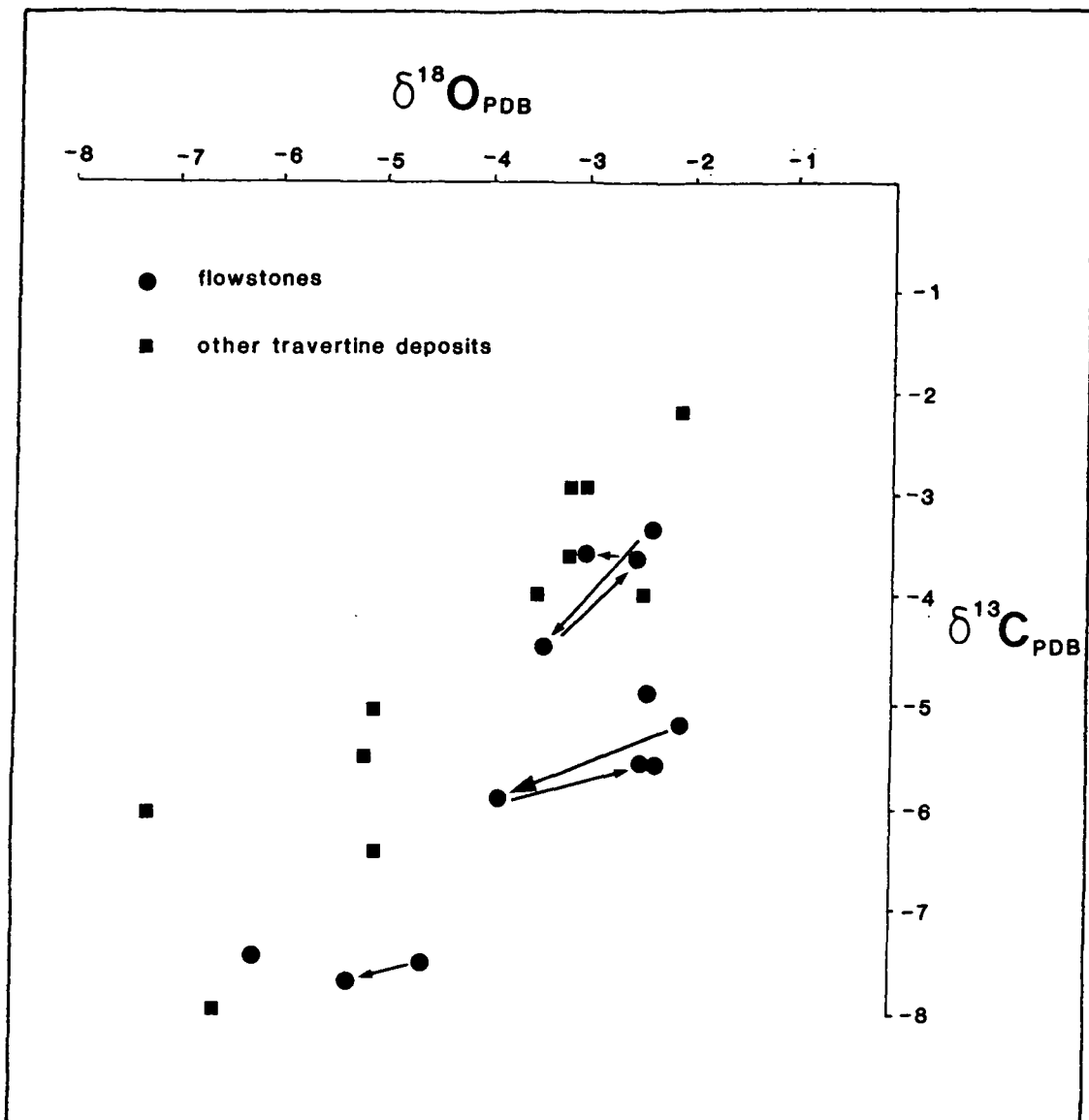


**Fig. 5.3** Stable isotopic analysis results from the travertine deposits, Sully Island and Dinas Powys. The arrows indicate the stable isotopic variations between successive bands ( 1.5 millimetres in thickness ) within single flowstones

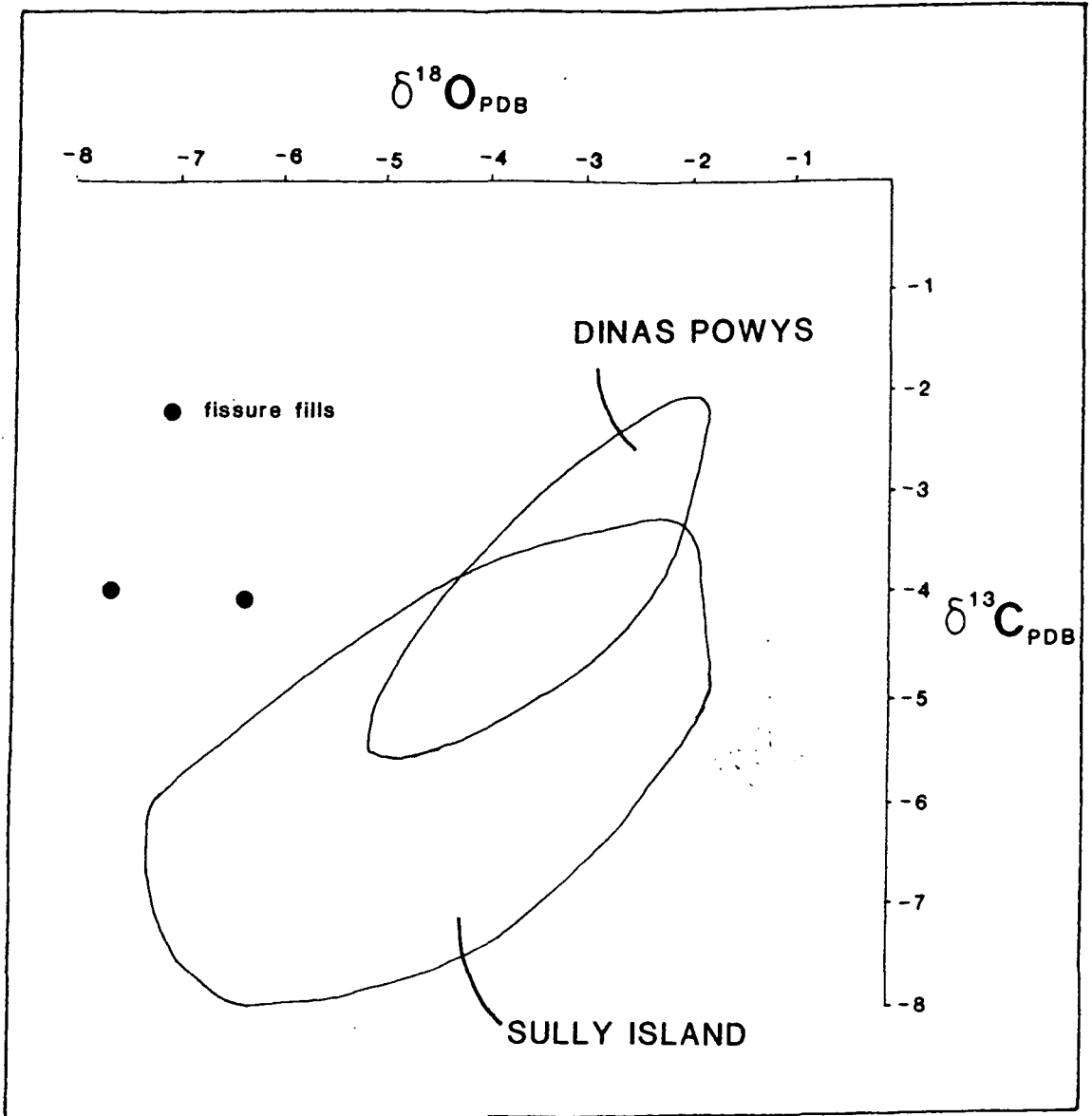


**Fig. 5.4** Stable isotopic analysis results from two fissure-fills from the megapolygonal fissures, Sully Island and the difference in composition of the travertines from Sully Island and Dinas Powys.

The three samples taken from the fissure-fills form a separate group to the travertine deposits. These samples are very depleted in  $^{18}\text{O}$  ( between  $-6.4$  and  $-7.8\text{‰}$  ) but are not depleted in  $^{13}\text{C}$  relative to the travertines of equivalent  $\delta^{18}\text{O}$  composition ( Fig. 5.4 ). These fissures are interpreted as having been the conduits for the upward moving groundwaters during the formation of the tepee and saucer structures in the upper limestones. As such the calcite precipitated within these fractures should represent the composition of the groundwaters before contamination by surface effects. The  $^{18}\text{O}$  values of the calcite are among the most depleted of those seen in the limestones and can be said to represent the  $\delta^{18}\text{O}$  value of the waters before evaporative effects took place. These values presumably represent the composition of the meteoric waters derived from precipitation in the South Wales area. It is also possible, however, that the emergent waters were warm ( see Section 4.5.3c ). This might account in part for the depletion of the  $^{18}\text{O}$  values of the emergent groundwaters. The enrichment in  $^{13}\text{C}$  relative to the travertines is most likely due to a lack of input of soil or biogenic-derived  $\text{CO}_2$  into the waters before emergence. If the stable isotopic composition of the fissure-fills is taken as representing the precipitation of carbonate from unaltered groundwaters, then the most  $^{18}\text{O}$  depleted travertines must have been affected by changes in  $^{13}\text{C}$  before evaporative effects took place. This would involve a depletion of up to  $4.0\text{‰}$  which implies a high input of depleted  $\text{CO}_2$  in the emergent waters. The association of organic material around spring mounds is common in travertines in the geological record ( A. Kendall, pers comm. ) and it seems likely that the areas of greatest microbial activity would be around areas of resurgence. The amount of organic material within the travertines is not great at present but there is evidence for a large amount of organic influence in the precipitation of some of the flowstones ( Fig. 4.34 ). Flowstones which are less depleted in  $^{18}\text{O}$  and  $^{13}\text{C}$  imply that after the initial emergence the two isotopes were similarly affected. This is most likely the result of the evolution of the emergent spring waters at the surface forming a more enriched water type which was affected by surface processes. The spring water itself will have evolved by evaporation during flow across the surface of the limestones. There may also have been pools of evaporatively enriched waters during periods of high water table with which the emergent waters will have mixed. Both processes will have operated at different times during the formation of the limestones. The strong variation in the

stable isotopic composition of the flowstones may also be partly due to changes in the chemistry of the emergent waters. The composition of spring waters is not constant through time and any variations in the water chemistry would be reflected in the stable isotopic values of the travertines. Both the composition and the volume of discharge of the waters could have varied during precipitation of the flowstones, giving rise to changes in flowstone chemistry.

The dolomite interbedded with the columnar calcite flowstone was also sampled. This dolomite is interlaminated on a millimetric scale with primary flowstone and appears to have formed in a magnesium-rich microenvironment related to the decomposition of organic material. The dolomite has a stable isotopic composition of  $-3.0\text{‰}$   $^{18}\text{O}$  and  $-2.9\text{‰}$   $^{13}\text{C}$ . This is equivalent in  $\delta^{18}\text{O}$  to the interlaminated flowstones ( Fig. 5.3 ) but is among the least depleted in  $^{13}\text{C}$  of the travertines. The enrichment of  $^{13}\text{C}$  and slight depletion of  $^{18}\text{O}$  is not what would be expected from a dolomite formed due to the breakdown of organic matter. However if the dolomite was formed in a closed system, then the anomalous stable isotopic values may be the result of formation in a water which is initially of the same composition as that of the surrounding travertines which has subsequently been modified by a reduction of organic material leading to the enriched  $^{13}\text{C}$  values.

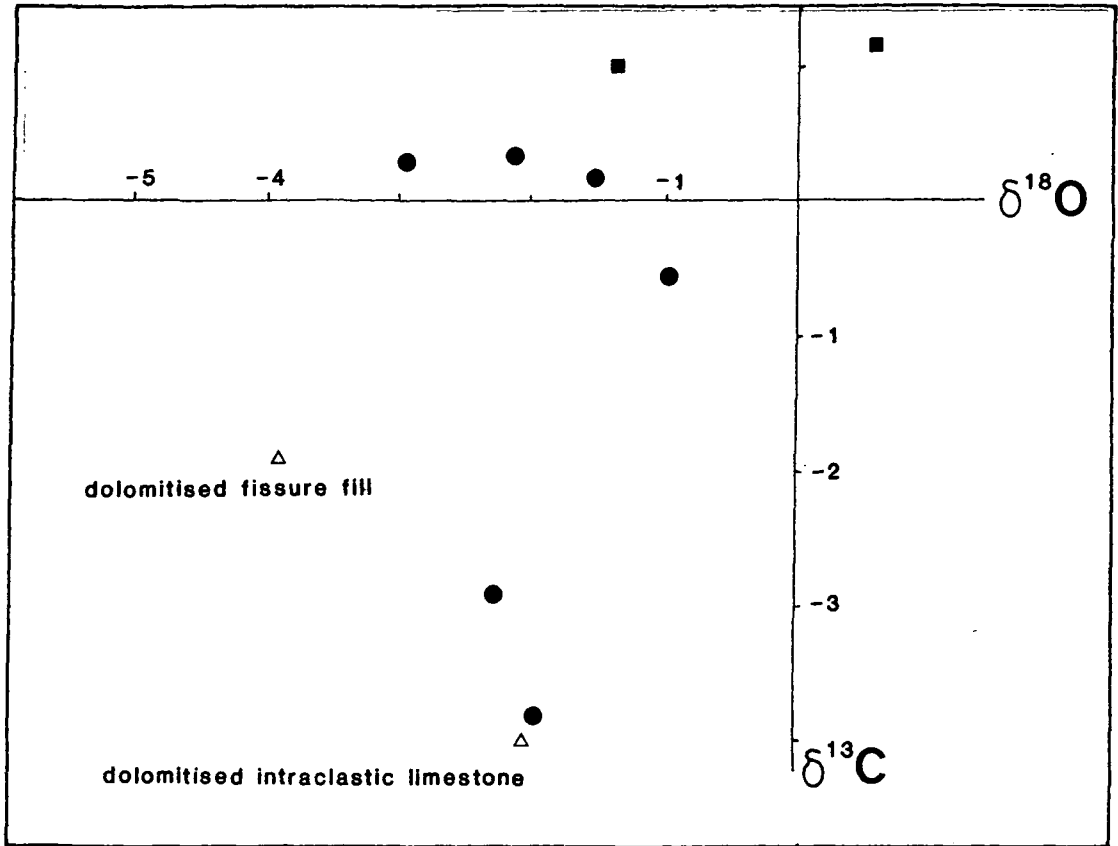
The travertine deposits at Dinas Powys appear to have been less affected by biogenic input and are on average more enriched in  $^{18}\text{O}$  than those from Sully Island. These travertines were formed in a fluvial palaeovalley and do not appear to have formed downstream from the actual spring outlet as evidenced by the spherulites ( Section 4.5.3c ). If the emergent waters in the Dinas Powys area are assumed to have had the same chemical composition as those in Sully Island then the waters from which the Dinas Powys travertines formed had undergone some evaporation prior to precipitation of the calcite. In view of the fact that the travertines in Dinas Powys are associated with stromatolitic beds, the flowstones do not show any evidence of depletion of  $^{13}\text{C}$ . It does not appear that the presence of stromatolitic beds implies that there was an input of biogenic  $\text{CO}_2$  into the carbonate as noted in the previous section. The mixing of water types or the evolution of the spring water at the surface is again suggested by the covariant trend of the Dinas Powys data as a whole. The stable isotopic data from the travertines on Sully Island are comparable with those from salinas in

Australia where the emergent waters are originally of meteoric origin ( Ferguson et al., 1988 ). The variations within individual sheets of flowstone can also be compared with changes in stable isotopic composition from some marginal salinas ( Handford et al., 1984 ). In the Australian examples the variation in stable isotopic value is the result of changes in the relative input of marine and continental waters into the basin.

#### 5.2.4 Transitional Mercia Mudstone Group, Sully Island

As well as two dolomitised limestones, three samples from the interbedded evaporitic mudstones and dolomites overlying the Sully Island succession were analysed ( Fig. 5.5 ). The two dolomitised limestones are taken from different original lithologies, one from a fissure-fill and one a replaced fenestral limestone. Both samples are enriched in  $^{18}O$  relative to the original rock type. Both, however, are depleted relative to the dolomite in the overlying mudstones. In particular the dolomitised fissure-fill has a  $^{18}O$  of  $-4.8\text{‰}$  which is depleted by more than  $3.0\text{‰}$  relative to the overlying beds. In many cases dolomitisation of the upper limestones is only partial and fibrous calcite cements are selectively preserved. In the case of the fissure fill some of the cements, which contain the most depleted  $^{18}O$  values in the limestones, are unaltered. Furthermore there are some dedolomites within the upper limestones. The  $^{18}O$  value of  $-4.8\text{‰}$  represents a number of carbonate types within the bed and is not related simply to the dolomitisation. The fenestral limestone which is completely dolomitised ( as proved using XRD ) has a  $^{18}O$  of  $-1.8\text{‰}$  which is very close to the value of the overlying dolomitic mudstones. ( Fig. 5.5 ). In view of the fact that dolomitisation forms a 'front' through the Limestone Unit it is probable that it is a Triassic event related to the immediately overlying beds rather than a burial event. The dolomitic, hypersaline nature of the overlying beds supports this theory.

The transitional beds of the Mercia Mudstone Group immediately overlying the limestones are more enriched in  $^{18}O$  and  $^{13}C$  than the underlying dolomitised limestone by  $0.4\text{‰}$  and  $0.8\text{‰}$  respectively. The higher transitional Mercia Mudstones are progressively more enriched in both stable isotopes, and trend towards the composition of the Mercia Mudstone Group in the Penarth Cliffs ( Fig. 5.5 ). The transitional nature of the reduction in meteoric influence in the mudstones is



- transitional Mercia Mudstone Group above Limestone Unit
- Mercia Mudstones, Penarth and Barry Cliffs

**Fig. 5.5** Stable isotopic analysis results from the dolomitised limestones, transitional Mercia Mudstone Group beds overlying the Limestone Unit on Sully Island and from two Mercia Mudstone Group samples 15 metres below the Blue Anchor Formation in Penarth and Barry Cliffs.

also shown by the three dolomitic beds interbedded with the mudstones. These three beds represent a temporary return to more marginal conditions before the transgression of the Sully Island area was complete and the meteoric water input was fully diluted by the hypersaline lake waters. Although the change from limestone to dolomitic mudstones is abrupt the input of meteoric waters into the area was not stopped by the transgression of the hypersaline waters immediately but gradually diluted. The deformed upper surface of the limestones is evidence that the flow of groundwaters was not diminished during formation of the uppermost limestones, although there may have been a reduction in the input of clastic material into the basin. The stable isotopic values in the dolomitic mudstones overlying the limestones thus represent a gradual change in the hydrological conditions in the Sully Island area, which correspond to the sudden lithological change at the top of the Limestone Unit.

### **5.3 Trace Elemental Analyses, Results**

#### **5.3.1 Introduction**

In total, 60 samples from the Sully Island sequence and the limestones at Dinas Powys were analysed using Atomic Absorption Spectrophotometry ( AAS ) and a further 53 using Inductively Coupled Plasma Atomic Emission Spectrometry ( ICP-AES ). Both analytical techniques are described in Appendix 1 . Problems arose during the analysis of samples using AAS and the results obtained by this technique were not considered to be reliable. The dataset of samples analysed by AAS will not be considered with the exception of the sodium analyses which were not available using the ICP-AES. The ICP-AES provided information on the abundances of a number of major and minor elements. In this study the data for elements Ca, Mg, Fe, Mn, Zn and Sr were utilised.

#### **5.3.2 Evaporitic Dolomite Unit**

Eight samples from the Evaporitic Dolomite Unit were analysed by ICP-AES. Of these samples, four are taken from samples which are within the replaced nodular sulphate beds; one is from a nodule in the groundwater calcrete and three are

from the upper and lower perilittoral dolomites. Three of the samples are entirely dolomitic, and five contain up to 35% calcite. The dolomitic samples are from the perilittoral sections whereas those which contain calcite are replacements of sulphate nodules or adjacent sediment. In the four samples taken from nodular structures there is petrographic evidence for a calcitic precursor.

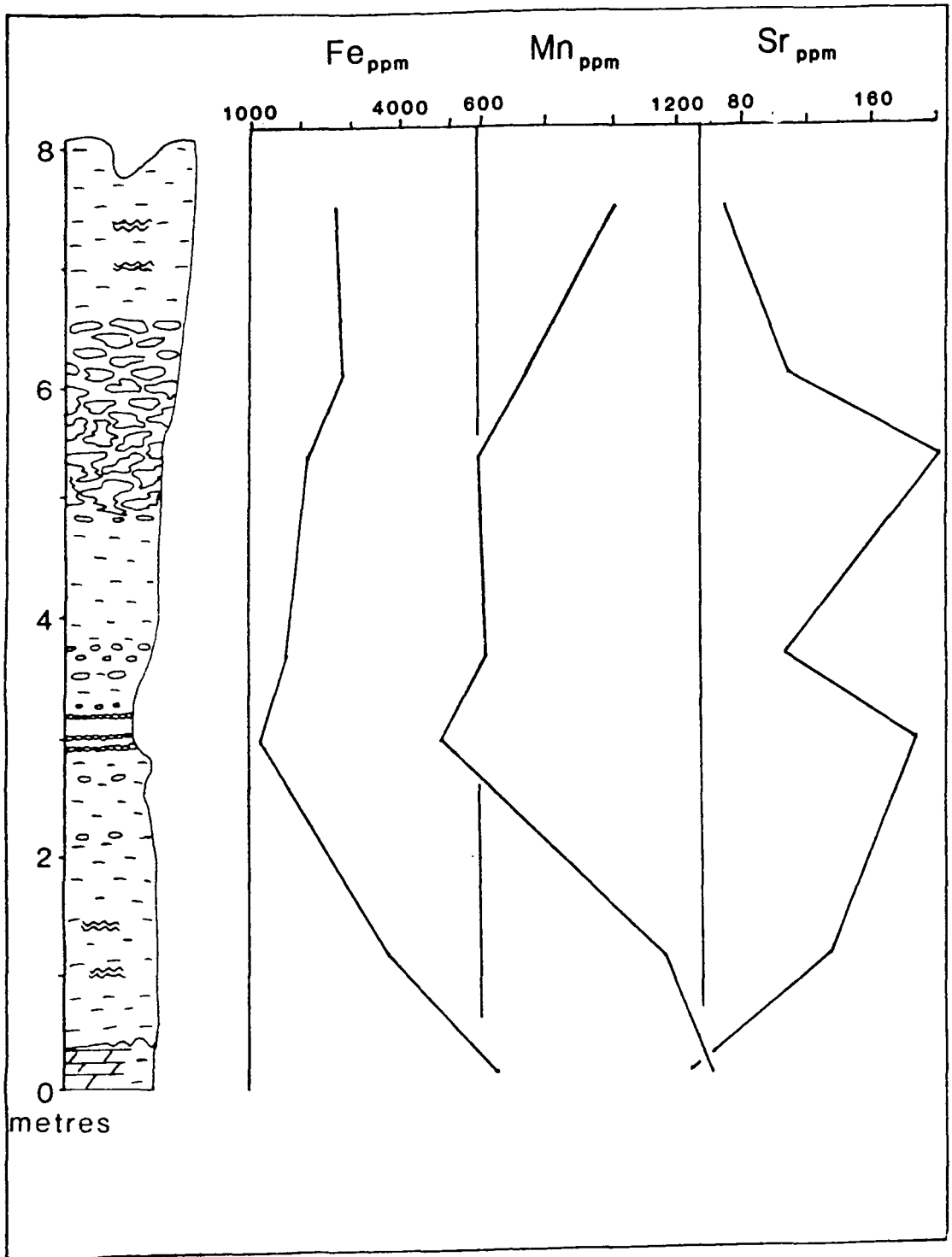
There is some correlation between the presence of calcite in the samples and the trace element distribution ( Fig. 5.6 ). Zinc is consistently low throughout the unit but the variations in Fe, Mn and Sr appear to be related to the mineralogy of the sample. Both Fe and Mn are on average more abundant in the fully dolomitic sections of the unit ( Table 5.1 ) whereas the proportion of Sr is greatest in the evaporitic central sections of the unit.

Table 5.1 The average distribution of Fe, Mn and Sr within the subfacies of the Evaporitic Dolomitic Unit.

subfacies	Fe <sub>ppm</sub>	Mn <sub>ppm</sub>	Sr <sub>ppm</sub>
perilittoral	4000	1100	100
evaporitic	2500	600	300

The only exception to this pattern is the anomalously high value of Fe in the sediment within the 'evaporitic' sabkha band ( Fig. 5.6 ). At outcrop this bed appears to be more heavily iron stained than the surrounding sediments and in thin section there is evidence for pedogenesis ( Section 3.2.2 ). The concentration of iron in this bed ( over 8000<sub>ppm</sub> ) is further evidence for pedogenetic action.

The relationship of the trace elemental distributions with mineralogy can be related to the diagenetic history of the unit. A decrease in the amount of Fe and Mn and an increase in Sr could be the result of an input of more saline waters during deposition ( Robinson, 1980 ). This would relate trace element distribution to the original depositional environment of the beds, which has been described by Veizer & Demovic ( 1974 ) from replaced marine sequences. Several diagenetic replacements have taken place in the unit after deposition. Furthermore the beds which would be expected to contain most Sr are the ones which



**Fig. 5.6** Vertical variations in the abundances of Fe, Mn and Zn in the Evaporitic Dolomitic Unit.

contain the least. In this case the original depositional environment does not appear to have influenced the final composition of the beds. The replacement of the sulphate nodules appears to have taken place in Sr-rich waters of meteoric origin. The relic calcite in the groundwater calcrete nodules appears to be of similar composition. The replacement of the sulphate nodules by calcite is most likely to have taken place in the waters in which the overlying calcrete formed. Subsequent dolomitisation took place in waters relatively enriched in Fe and Mn. The differences in trace elemental composition are of too great a magnitude to be the result of differences in partition coefficients ( Veizer, 1983 ).

The changes in both mineralogy and geochemistry of the diagenetic phases is a result of changes in the hydrological regime of the Sully Island area. The gradual incursion of groundwaters into the Sully Island area is assumed to have taken place over a long period of time during which the basal calcrete was formed. In this period it is possible that the groundwaters were evolving chemically as well as from mixing with the original hypersaline lacustrine waters. There does not appear to be any correlation between the stable isotopic composition of the waters and the trace elemental distributions. A more detailed study would be required to fully establish the geochemical relationships between the different diagenetic phases in the Evaporitic Dolomitic Unit. The relatively Fe and Mn poor and Sr rich compositions of the calcite in the nodular sections of the Evaporitic Dolomite Unit may reflect the mixing of the two waters before meteoric waters were predominant in the hydrology of the area.

The sodium values in the Evaporitic Dolomite Unit do not show any significant variations within the unit but are relatively enriched in Na relative to the overlying limestones (  $600_{ppm}$  as opposed to  $250_{ppm}$  ). If Na is a dependable indicator of palaeosalinity then the values obtained from the Sully Island succession indicate the change in hydrological setting between the dolomites and limestones ( Veizer et al., 1977 ).

### 5.3.3 Limestone Unit, Sully Island and Dinas Powys

Thirty nine samples were taken from the Limestone Unit in Sully Island and from the exposure in Dinas Powys. As in the stable isotopic analyses of the limestones particular attention was paid to the travertine deposits which do not contain intraclastic material. A number of intraclastic fenestral limestones sampled from the wave-cut platform in Sully Bay were analysed in order to see if the trace elemental composition of the limestones varied laterally in the Sully Island area within one horizon.

All of the limestones in the Sully Island and Dinas Powys areas are composed of low-magnesium calcite. None of the calcites in the travertine deposits contain over 3%  $\text{MgCO}_3$ . The intraclastic limestones, however, contain detrital dolomite and therefore have a greater proportion of  $\text{MgCO}_3$ . The most clastic beds in the sequence at Hayes Point contain 10% dolomite. Taking into account the proportion of clasts in the rock then less than 20% of the carbonate clastic input into Sully Island was dolomitic. In most cases in the clastic limestones the amount of  $\text{MgCO}_3$  in the rock is not significantly greater than in the travertines. It would appear that the input of dolomitic detritus was not great, despite the fact that the sample of Carboniferous Limestone analysed in this study was a dolomite.

The travertine deposits are relatively low in the four trace elements analysed in this study ( Fe  $200_{ppm}$ , Mn  $300_{ppm}$ , Sr  $78_{ppm}$  ). The exception to this is Zn which is on average twice as abundant in the travertines (  $150_{ppm}$  ) relative to the other limestones. The distribution of Fe and Mn appears to be mostly dependent on the proportion of clastic material in the limestones. The depositional environment of the limestones was most likely an oxidising one in which the incorporation of Fe and Mn into the carbonate lattice was not favoured. The meteoric waters would also be initially poor in Sr and so the low trace elemental abundances in the limestones is not surprising. The variations which are seen in the trace elemental compositions is most likely to be the result of the influence of Carboniferous Limestone clasts within the limestones which appear to have contained a greater proportion of Fe and Mn than the primary carbonate.

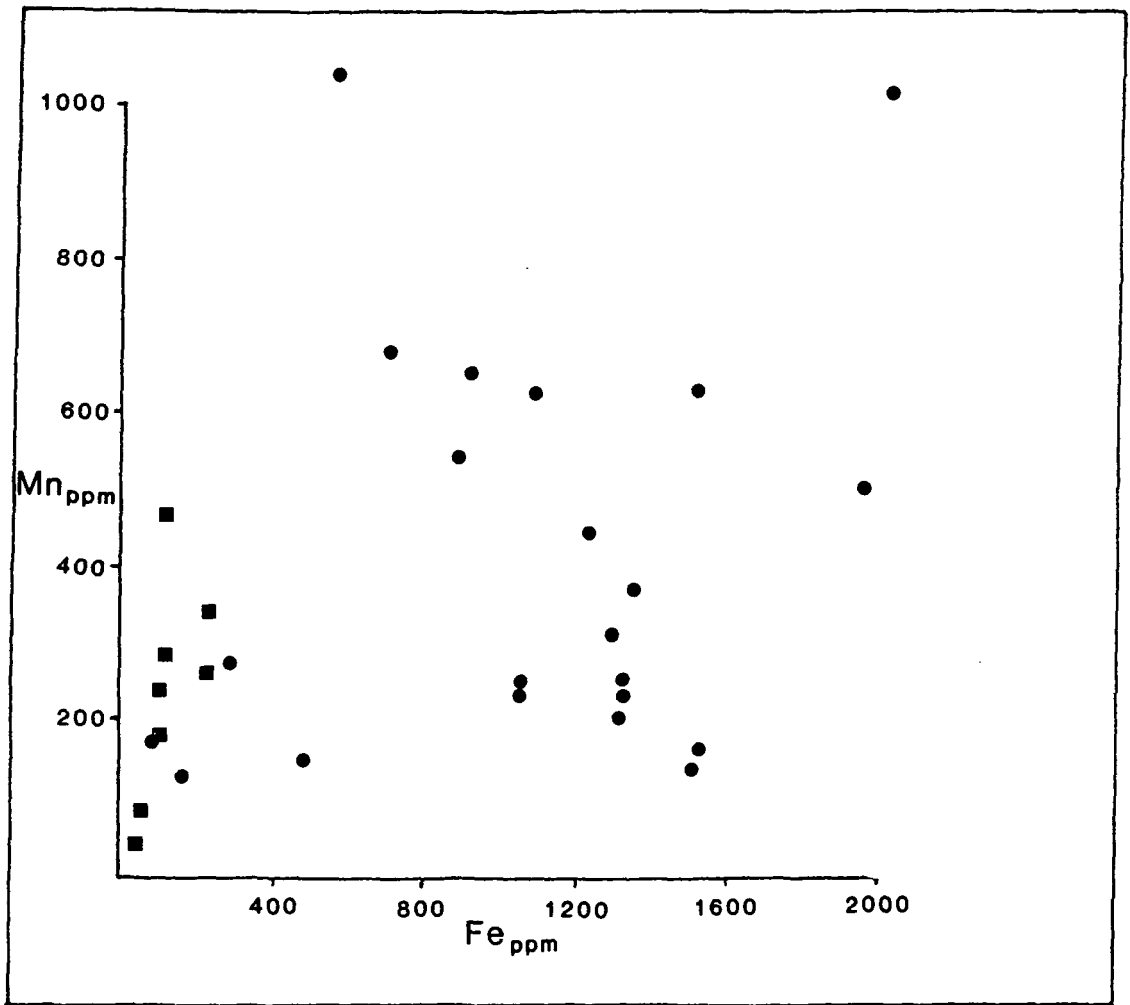


Fig. 5.7 Cross-plot of Fe against Mn in the Limestone Unit, Sully Island. Squares are travertine deposits, circles intraclastic and calcretised limestones.

If the values of Fe and Mn in the limestone unit are plotted together then some further relationships can be seen. The limestone unit as a whole shows no trend, probably due to the clastic input. The travertines, however, display a positive covariance of Fe and Mn ( Fig. 5.7 ). This trend in the travertines, in particular in the flowstones, is most likely to be a mixing or evolutionary trend similar to that shown by the stable isotopic values and indicates the mixing of emergent spring waters with ( or evolution into ) a more evolved water type which is enriched in trace elements and presumably affected by evaporation. Sr does not show this relationship with the other trace elements. It is uniformly low in the limestones and rarely exceeds  $100_{ppm}$  in the Sully Island sequence. This is evidence to suggest that aragonite was not a primary mineral in the Sully Island sequence. The low Sr values may be related to the fact that the non-evaporitic depositional environment in which the limestones were laid down was one in which the uptake of Sr into the carbonate lattice was not favoured ( Veizer & Demovic, 1974 ).

Interestingly the amounts of Zn within the travertine are significantly greater than in the other limestones ( over  $150_{ppm}$  as opposed to under  $100_{ppm}$  ). The amount of Zn in the travertines is greater than that in the dolomitic units in the Sully Island sequence. The reasons for the increase in Zn in the travertines may be related to the uptake of metals by the circulating groundwaters during passage through the Carboniferous Limestone. There is little direct evidence for the presence of mineralised waters in the South Wales area other than the presence of spherulites ( and, possibly, the depleted  $^{18}O$  values of the travertines ) which may be the result of hydrothermal activity. Triassic hydrothermal activity has been described by Green & Welsh ( 1965 ) and so it is possible that the slight increase in Zn in the flowstones is a reflection of slight mineralisation of the waters in the South Wales area.

The trace elemental composition of the limestones appears to be related to the hydrological environment in which the limestones formed. The limestones contain less Fe and Mn relative to the underlying and overlying dolomitic beds, roughly equal amounts of Sr and, in the travertines, more Zn. The trace elemental variations can be attributed to the hydrological change which took place during deposition of the limestones.

## 5.4 Conclusions

The sequence of rocks exposed around Sully Island and in Dinas Powys represents a series of lithologies which are unique in the British Triassic. The geochemistry of the beds gives some indication of the depositional and diagenetic history of the Sully Island sequence.

The Evaporitic Dolomite Unit appears to have been mostly replaced in a meteoric water type, firstly associated with the formation of the groundwater calcrete and then in a later phase of dolomitisation. There is some evidence for the diagenesis of the Evaporitic Dolomite Unit in a mixed meteoric-hypersaline environment before fully meteoric conditions were established. The Evaporitic Dolomite Unit is enriched in  $^{18}\text{O}$  by on average  $3\text{‰}$  ( Fig. 5.8 ). This could be the result of differences in fractionation factor between calcite and dolomite rather than variations in depositional environment ( Land, 1980 ). The limestone unit is more varied in stable isotopic composition. The clastic limestones have a relatively constant  $\delta^{18}\text{O}$  while the  $\delta^{13}\text{C}$  is more variable, reflecting the actions of soil and organically-derived  $\text{CO}_2$  . There is a poorly developed covariant trend in the data which is better shown in the results from the travertine deposits. This trend is also shown by variations within individual flowstones. On a millimetric scale flowstones can vary in stable isotopic composition by up to  $\pm 2.0\text{‰}$  . The covariance of  $^{18}\text{O}$  and  $^{13}\text{C}$  in the travertines is the result of evolution of the emergent groundwaters and mixing with surficial waters which had been affected by evaporation and were geochemically altered. The variations in the stable isotopic values may also have been affected by changes in the chemistry of the spring waters themselves, or by the volume of discharge of water at the spring outlet. This evaporatively enriched water is not analogous to the hypersaline water in which the Mercia Mudstone Group was laid down but formed in a local pool in the Sully Island subbasin as the result of increased water discharge. The Dinas Powys travertines tend to be more enriched in  $^{18}\text{O}$  and  $^{13}\text{C}$  than those in Sully Island. The limestones exposed at Dinas Powys were deposited in a fluvial environment in which the river water may have been enriched in  $^{18}\text{O}$  by evaporation during flow before formation of the travertines.

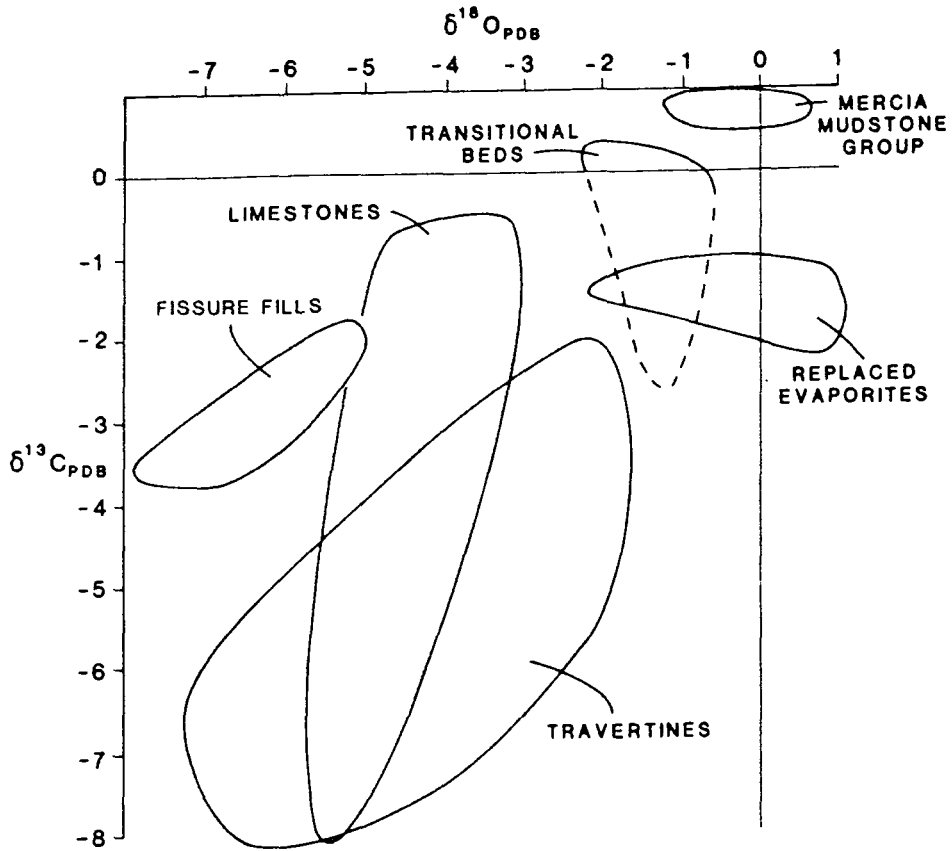


**Fig. 5.8** Summary diagram of the stable isotopic variations in the lacustrine marginal beds in the Sully Island and Dinas Powys areas, South Wales. The 'replaced evaporite' group does not include the rhombic dolomites from the base and top of the Evaporitic Dolomite Unit or the matrix to the sabkha nodules.

The mudstones overlying the limestones in the Sully Island succession show an upward trend of progressive enrichment in  $^{18}O$  and  $^{13}C$  which indicates the gradual reduction in the influence of meteoric waters in the rocks overlying the limestones as the hypersaline lacustrine conditions of the Mercia Mudstone Group became fully established.

In terms of trace elemental composition the Evaporitic Dolomite Unit, other than the iron-rich sediment of the sabkha band which may be related to pedogenesis, is related to the mineralogy of the diagenetic phases. The replaced nodular sulphates contain calcite which is enriched in Sr and depleted in Fe and Mn relative to the surrounding fully dolomitic perilittoral sections. This calcite, which is probably related to the formation of the originally calcitic groundwater calcrete, forms an earlier transitional diagenetic phase before replacement by a dolomite which appears to have formed in a fully meteoric water type.

The overlying limestones are relatively poor in most trace elements. Their composition is complicated by the presence of clasts of Carboniferous Limestone which obscure the chemical composition of the primary carbonate in the beds. In the travertines, however, Fe and Mn show a covariant trend which can again be related to the mixing of two water types. Sr is uniformly low but Zn is anomalously high in the travertines, which is slight evidence for the mineralisation of waters in the Triassic of South Wales.

## **Chapter 6**

### **Marginal Lacustrine Deposits in South Wales: Conclusions**

## Chapter 6

### Marginal Lacustrine Deposits in South Wales: Conclusions

#### 6.1 Introduction

The marginal carbonates exposed in South Wales are of particular interest since they represent a depositional environment which is unusual in the geological record and unique in the British Triassic. The preservation potential of travertines in particular is low and few pre-Quaternary examples are known. The transition between proximal clastic deposits and the overlying and laterally equivalent mudstones is exposed in many areas in Southwest Britain but the sequence seen in the Sully Island area is the result of a particular combination of basement topography, groundwater hydrology and regression of the hypersaline lake margin.

#### 6.2 The Evaporitic Dolomite Unit

The Evaporitic Dolomite Unit consists of up to 8 metres of generally structureless dolomites containing some clastic material and abundant ferroan cements. On the basis of the sedimentary structures the unit can be subdivided into four sections with the base being placed at a distinctive dolomitic bed which indicates the removal of topographic relief at the lake shoreline and a period of exposure before deposition of the dolomites. The upper and lowermost sections are composed of a rippled and laminated dolomite which was laid down in a perilittoral mudflat environment at the edge of the hypersaline lake. The central two sections record a regression of the lake shoreline and the establishment of supratidal evaporitic conditions. There are 8 bands of nodules, originally composed of sulphate, which are the result of precipitation of gypsum and/or anhydrite within the sediment. There is some evidence of pedogenesis of the sediment during precipitation of the sulphates. Of particular interest is the presence of two 'sabkha' type sulphate bands in the replaced evaporite section. These two sabkha bands are laterally continuous over several kilometres in contrast to the other less well

developed sulphate bands. The two sabkha bands may represent a regression / transgression pair such as that seen in the Trucial Coast. The poorly developed sulphate bands represent a transitional period between the perilittoral beds and the sabkha bands which also show evidence of calcretisation.

After deposition of the dolomites containing the sulphates of the sulphate bands there was a change in the hydrological environment in the Sully Island area and a groundwater calcrete was precipitated. The calcrete has formed in several metres of sediment which may originally have been a perilittoral dolomite although there is no evidence preserved in the bed at present. The calcrete represents a further regression coupled with the influx of meteoric derived waters into the Sully Island area. Precipitation took place several metres below the sediment surface, and continued formation of calcrete deformed the first-formed nodules. Later precipitation of calcrete nodules took place when the water table was rising and the upper part of the calcrete horizon is undeformed. The groundwaters in time dissolved the sulphate in the underlying sections and precipitated calcite containing relic laths of anhydrite in the nodules.

Overlying the groundwater calcrete are 2 metres of perilittoral dolomites formed in a marginal lacustrine setting. The position of these beds in the sequence of hydrologic changes is uncertain. The calcrete represents a time of groundwater influx during regression of the lake shoreline. The overlying dolomites could have formed before the influx of meteoric waters in which the calcrete formed, or could represent the temporary return of the hypersaline lake shoreline. The formation of a groundwater calcrete occurs several metres below the surface but will not take place at greater depth. The amount of sediment which will have been present above the calcrete during its formation is therefore limited. At present there is 4 metres of dolomite above the calcrete base. This is the maximum that would be possible to allow the calcrete to form. It would seem more probable that the calcrete formed during a temporary incursion of meteoric groundwaters after which there was a return to hypersaline conditions before the fully meteoric conditions in which the limestones formed. The dolomitisation of the calcitised nodules and the calcrete nodules is evidence for a return to more hypersaline conditions.

The Evaporitic Dolomite Unit represents a regression / transgression event in which perilittoral dolomites are separated by a period of regression in which sulphates were precipitated and calcretisation took place. The reason for the formation of sabkha type sulphates in the Sully Island area is the result of the embayed shoreline in which a mudflat type environment formed in contrast to the clastic stream and sheet flood deposits in other parts of South Wales.

Geochemically, the dolomite unit represents the several phases of replacements which have taken place in the beds during the changes in hydrological environment. None of the stable isotopic compositions of the dolomites record a hypersaline water type. The samples are depleted in  $^{18}O$  and were replaced by a water type which is related to the dolomitisation of the calcitic nodules during deposition of the upper perilittoral dolomites. These beds probably formed in a mixed meteoric-hypersaline water type.

Trace elemental compositions in the unit are controlled by the mineralogy of the beds. The relic calcite in the nodules in the central sections of the unit are depleted in Fe and Mn and enriched in Sr relative to the dolomite which forms the majority of the unit. The reason for the enrichment of the more meteoric water in Sr is not known, although the Mercia Mudstone Group in South Wales which appears to have formed in meteoric-derived waters is also rich in Sr ( celestite beds are common ).

### **6.3 The Limestone Unit, Sully Island and Dinas Powys**

#### **6.3.1 Sully Island**

The 8 metres of limestone or dolomitised limestone exposed in the Sully Island area represents a substantial period of time during which the hypersaline waters of the lacustrine facies of the South Wales area were not present and the deposition was dominated by meteoric waters. The basal calcrete is an indication of a substantial period during which the calcrete was formed and then karstified. The maturity of the calcrete suggests that the majority of the profile has been removed. This may have taken in total hundreds of thousands of years from the deposition of the underlying dolomites to the formation of the intraclastic

limestones above the karstic surface. During this period there was a significant change in the palaeohydrology of the Sully Island area. The marginal lacustrine conditions of the underlying dolomites were replaced by an intraclastic limestone formed in a depositional environment controlled by fluctuations in the input of resurgent meteoric groundwaters into the subbasin. This implies both a regression of the lake margin and the concentration of flow of groundwaters into the Sully Island area. The flow of groundwaters into the area is the result of the particular basement topography in around Sully Island which forms a natural basin in which waters will be channeled upwards. The limestones themselves are fenestral intrasparites, mostly composed of clasts of Carboniferous Limestone derived from the west and southwest. The superposition of calcretised and rippled horizons in the limestones indicates that the water table fluctuated rapidly and often during deposition. Microbial influence is most clearly seen in the laminated fine limestones in which columnar stromatolites and oncoids are developed. The intraclastic limestones also contain locally developed stromatolites, some of which show evidence of bacterial shrubs which are preserved by precipitation of calcite crusts. The preservation potential of these microbial beds is low, as shown by the number of fragments of microbial mat seen in the clastic limestones. Other than the microbial laminae, there is little evidence of fauna within the Sully Island area. Disarticulated ostracod valves, seen in thin section only, are the only fauna preserved in the limestones. Although there is evidence for the presence of dinosaurs in the area, this is restricted to the preservation of footprints within several beds in the marginal deposits.

The input of meteoric waters into the limestones was volumetrically fairly constant. The meteoric waters appear to have been transported laterally through the marginal clastic beds and upwards through the limestones. Movement of meteoric waters through the clastic beds to the west of Sully Island is shown by the dissolution of evaporites seen in the beds and the resulting collapse structures. The dissolution of sulphates in the marginal beds will have enriched the waters in  $\text{Ca}^{2+}$  which will have encouraged precipitation of carbonate as the waters emerged through the spring outlets. Local spring deposits ( travertines ) are abundant throughout the limestones and contain a variety of calcite forms which indicate precipitation from carbonate-rich waters. The travertines were intimately associated with microbial activity. Bacterial 'clots' of micrite and

millimetric laminae of dolomite in primary calcite flowstone are evidence of organic activity during travertine precipitation. Some of the flowstones are primary, some appear to have been recrystallised from a fibrous precursor. The rounding of terminations of some flowstones indicates the fluctuation of water chemistry leading to dissolutional events. Within the travertines, specific spring outlets are not seen. The groundwaters rose through local but diffuse zones in the permeable limestones so that there were no point sources in the travertines. In the uppermost limestones dolomitisation has obscured all but the most coarse of sedimentary structures, but the deformation of the beds into tepee and saucer structures can still be seen. The intense deformation is the result of both precipitation of carbonate in the surficial sediment and the buckling of the surface crust by the upwards movement of groundwaters. The conduits for the passage of waters to the upper limestones are more specific, taking the form of zones of polygonal fissures through which groundwaters were channeled upwards. The reason for the more discrete zones of water movement is probably the rapid lithification of the limestones by vadose cementation.

Evidence for vadose diagenesis in the limestones is abundant and the fluctuations of the water table appear to have been common enough to form several phases of vadose cements in some cavities. There is some evidence for cementation in phreatic conditions but the majority of cavities contain evidence for vadose conditions. Vadose diagenesis is most clearly seen in the laminated limestones where elongate cavities contain pillars of sediment drawn into menisci as waters withdrew from the cavities.

The limestones are depleted in both  $^{18}\text{O}$  and  $^{13}\text{C}$  which is an indication of the meteoric water type.  $^{18}\text{O}$  and  $^{13}\text{C}$  display a covariant trend which is best shown in the travertines which do not contain clastic carbonate. The covariance is the result of the evolution of the emergent meteoric waters and mixing with more evolved surficial waters which had been affected by evaporation. Changes in the chemistry of the spring waters may also have contributed to the stable isotopic composition variations. The organic influence within the travertines appears to have been greatest in the travertines closest to areas of discharge. The basal calcrete shows some evidence of the depletion of  $^{13}\text{C}$  resulting from the input of soil-derived  $\text{CO}_2$ . The nodular calcretes do not show as much depletion and

were not mature enough to develop a soil zone. There is no evidence in the stromatolitic beds of greater depletion of  $^{13}\text{C}$  resulting from the input of organic  $\text{CO}_2$ , relative to the other limestones.

In terms of trace elements, the limestones are depleted in Fe and Mn relative to the dolomites. In the travertines the two trace elements show a covariance which can again be related to the mixing of two water types. The distribution of Sr in the limestones does not show any pattern and is uniformly low. The travertines are enriched in Zn relative to the other beds in the Sully Island succession which may be evidence for slight mineralisation of the circulating groundwaters.

### 6.3.2 Dinas Powys

The smaller exposure at Dinas Powys is lithologically and geochemically similar to the limestones in Sully Island, indicating that they were formed in a generally similar depositional environment. The limestones overlie a fluvial conglomerate and were deposited in a steep-sided palaeovalley which was controlled by the topography of the Carboniferous Limestone. The fluvial conglomerate represents a high energy environment, possibly a flash-flood event. The overlying finely laminated limestones, however, represent a change in the depositional environment to a lower energy fluvial system containing carbonate-rich waters, which was periodically exposed and in which stromatolites and ostracods were able to survive. The Dinas Powys limestones appear to have formed in a pool, possibly behind a barrage of travertine, in which laminated and stromatolitic limestones could form and where travertines were being precipitated from carbonate-rich waters.

Geochemically the limestones at Dinas Powys are almost identical to those in the Sully Island area, indicating precipitation from waters of a similar chemical composition. The Dinas Powys travertines are less depleted in  $^{13}\text{C}$  than those at Sully Island, due to less microbial influence during precipitation, or possibly less influence from soil  $\text{CO}_2$ . Other than the depletion in  $^{13}\text{C}$ , the limestones at Dinas Powys are geochemically indistinguishable from those at Sully Island.

#### 6.4 The Sully Island Sequence

The sequence of sedimentary rocks exposed on Sully Island is indicative of a depositional environment which is atypical of the British Triassic. The Sully Island succession is the result of the coincidence of a high input of meteoric waters along with a basement topography which encouraged the upwelling of the meteoric waters in one localised area. As such the Sully Island area is analogous to the depositional environment of several Recent salinas on the southern and western coasts of Australia. In these settings, carbonate is precipitated around local spring outlets in areas of groundwater resurgence. The assemblage of sedimentary structures in these Recent salinas is very similar to those seen in the limestones at Sully Island. In particular the association of tepees, travertines and vadose diagenesis is identical. The only major differences in the Sully Island limestones are the lack of a large faunal input into the limestones and the absence of evidence for an aragonitic precursor. The Sully Island limestones can thus be directly compared to the Australian salinas in terms of hydrological environment and depositional setting.

On a larger scale the Australian salinas show a concentric pattern of marginal carbonates surrounding a central zone of evaporites. In Sully Island the limestones overlie the evaporitic beds and there is no indication of a concentric arrangement of lithologies. The limestones were formed in a completely different hydrologic environment and there is no evidence for the precipitation of evaporitic minerals despite the periodic extreme desiccation. The two environments appear to be more dependent on the hydrology during deposition and form distinct beds with a vertical rather than lateral zonation. The base and top surfaces of the limestones represent abrupt changes in lithology which both signify a period of time in which deposition was slow or absent and during which there was a marked change in the hydrological environment. This change may have occurred over a long period of time but at the top of the limestones there is little evidence for this. The gradual change in chemical composition of the mudstones overlying the limestones indicates the progressive dilution of the meteoric input in the hypersaline lake waters.

## 6.5 Summary

The Sully Island sequence formed in an embayment of the lake shoreline in which a marginal mudflat containing sabkha evaporites developed in response to a regression of the lake waters. The sabkha sulphates represent the furthest regression of the shoreline which was followed by a transgression after which deposition of perilittoral carbonates took place. This regression / transgression sequence is interrupted by an incursion of meteoric waters into the basin during which time the sulphates were replaced and a non-pedogenic calcrete was precipitated in the dolomite unit. A second more permanent influx of meteoric waters during time of regression of the lake waters gave rise to the formation of a mature calcrete followed by the deposition of a limestone sequence which formed in a basin in which there was no input from the hypersaline lake waters. The limestones contain a number of sedimentary structures related to the effects of a fluctuating water table, which was controlled by the input of meteoric waters through numerous spring outlets. The topmost surface of the limestone has been deformed into a number of tepee and saucer structures which indicate a substantial period of exposure during which groundwaters were still rising through the limestones. This top surface was finally transgressed by the hypersaline lake waters, and dolomitic mudstones of the Mercia Mudstone Group were laid down. The geochemistry of the Evaporitic Dolomite Unit is controlled by the phases of diagenetic replacements which have taken place. The composition of the limestones is indicative of the meteoric water origin. The overlying mudstones also show the gradual dilution of the meteoric input into the hypersaline lake waters.

## **Chapter 7**

### **Mercia Mudstone Group: Introduction and Petrography**

## Chapter 7

### Mercia Mudstone Group: Introduction and Petrography

#### 7.1 Introduction

##### 7.1.1 The Mercia Mudstone Group in Southwest Britain

Triassic rocks in the southern part of Britain crop out over an area extending from Yorkshire in the northeast and Lancashire in the northwest through Cheshire, Nottinghamshire and Worcestershire into Glamorgan, Somerset and Devon. The Triassic subcrop extends over much of Southeast England and offshore in the North Sea to the east and the Bristol Channel and Irish and Celtic Seas to the west. The Triassic rocks have been subdivided into a lower Sherwood Sandstone Group consisting of red and yellow conglomerates and sandstones and an upper Mercia Mudstone Group which is composed of mudstones and siltstones. The boundary between the two Groups is transitional over 10 and 20 metres and is diachronous, being between Scythian and Anisian in age in different areas ( Warrington et al., 1980 ). The Upper Triassic Mercia Mudstone Group was laid down in rift-related basins ( Whittaker, 1975 ) during a period of little fault activity and negligible extension ( Holloway, 1985 ). There was appreciable subsidence still taking place however, and up to 800 metres of Mercia Mudstone Group sediments accumulated in the Worcester and Somerset Grabens. In the offshore Celtic Sea Basin, 1200 metres of mudstones were deposited.

In this study coastal exposures in South Wales, Somerset and Devon were examined. The topmost 170 metres of Mercia Mudstone Group were examined, taking in the Norian and Lower Rhaetian Stages. Further sampling of the succession was not possible due to lack of outcrop. The areas studied are marginal to the deeper basinal deposits of the Inner Bristol Channel, Somerset and West Wessex basins ( Fig. 7.1 ). The Upper Mercia Mudstone Group can be subdivided at outcrop into the Blue Anchor Formation composed of green and grey mudstones and dolomites and the underlying undifferentiated red mudstones ( Warrington et al., 1980 ). The red mudstones themselves which are the object of this study, are

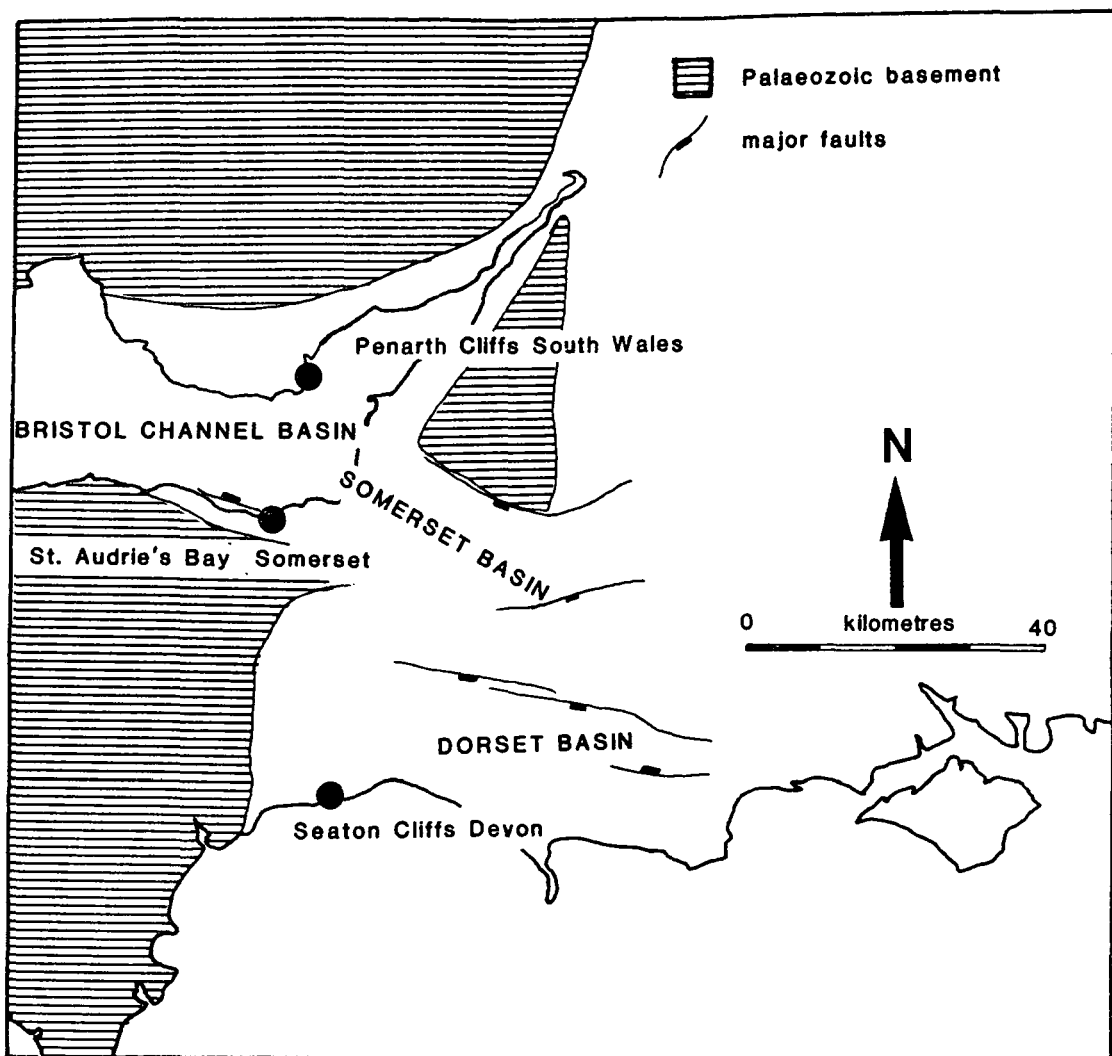


**Fig. 7.1** Location map showing the position of the three cliff sections in the Upper Mercia Mudstone Group sampled in this study.

homogeneous and rarely contain any sedimentary structures, although sulphate and halide salts are locally common.

### 7.1.2 Problems of Correlation of the Mercia Mudstone Group

The Mercia Mudstone Group consists mostly of unfossiliferous, poorly bedded red mudstone with few sedimentary structures and very few recognisable laterally continuous units. The lack of such features has posed a problem in the correlation of the mudstones for much of the last century ( Audley-Charles, 1970a ). Neither chrono nor lithostratigraphic correlation has been possible in the mudstones except on a local scale. For this reason the Triassic Working Group Report in 1980 did not subdivide the Mercia Mudstone Group formally but recognised local names for sandstone and halite beds within the mudstones ( Fig. 7.2 ). The terms Bunter, Keuper and Rhaetic were abandoned since they both have chrono and lithostratigraphic connotations. The terms Sherwood Sandstone Group, Mercia Mudstone Group and Penarth Group were proposed and these are used in this report. The term Keuper Marl has some value as a lithological term describing the red mudstones underlying the Blue Anchor Formation. It is hoped that in the future it may be retained as an informal descriptive term although at present it is still being used incorrectly and should not be returned into more widespread usage until confusion arising from its earlier meaning has been removed.

At present the study of the Mercia Mudstone Group has reached the stage that within local basins the beds have been subdivided but no regional correlations have been attempted ( Elliott, 1961; Jeans, 1978; Arthurton, 1980 and Taylor, 1982 ). The problems in attempting a regional correlation are numerous. The fossil record is almost completely absent in the Upper Mercia Mudstone Group ( Warrington, 1974; Warrington et al., 1980 ). Palynology has enabled the dating of parts of the Mercia Mudstone Group. The sandstone unit in Devon ( the Weston Mouth Sandstone Member ) has been dated as Carnian ( Warrington et al., 1980 ). The Blue Anchor Formation in all three areas covered by this study has yielded palynomorph assemblages of Rhaetian age. The red mudstones however have yielded no datable fossils of any type. They can on the basis of the surrounding beds be at least partly assigned to the Norian.

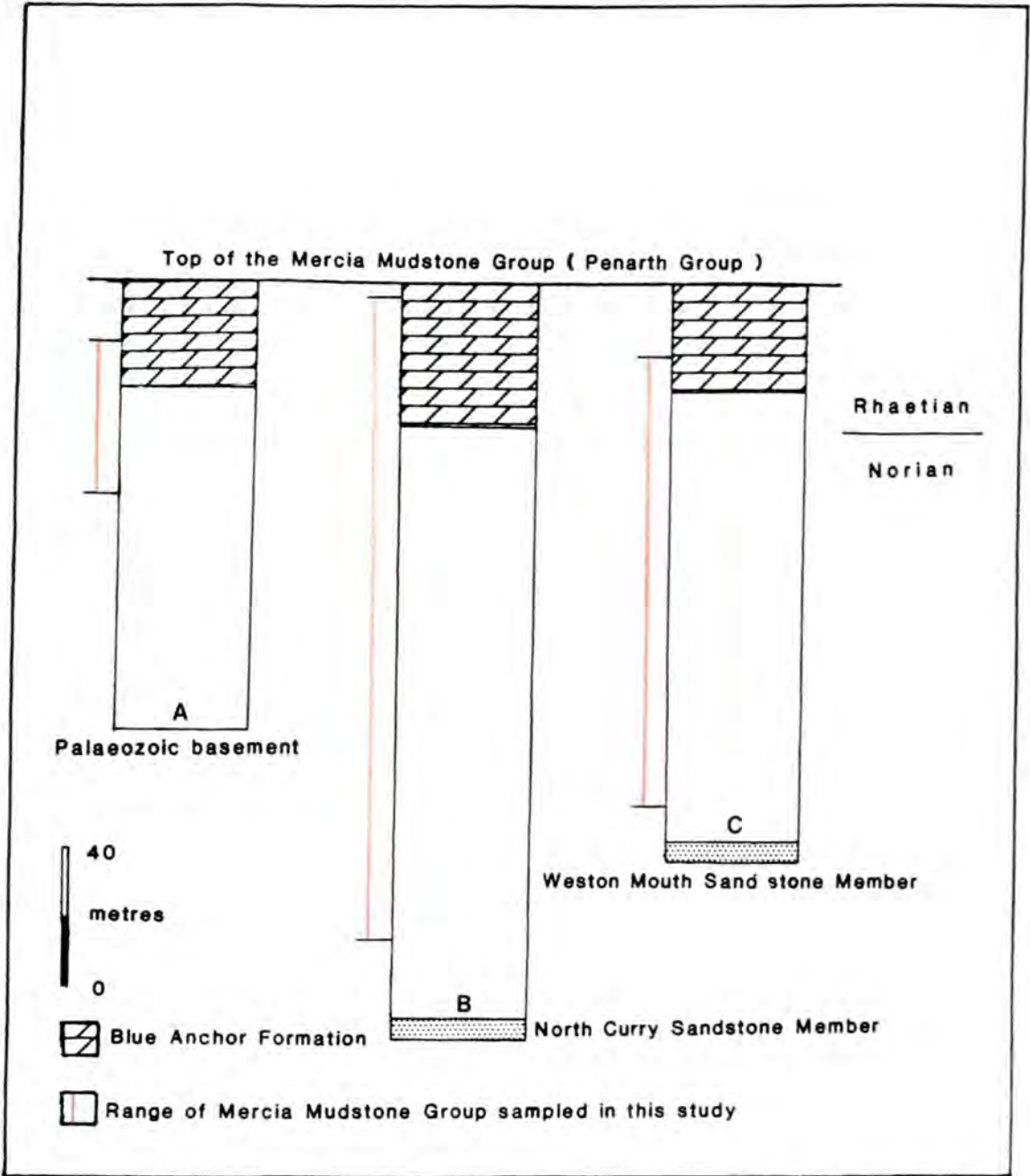


**Fig. 7.2** Summary logs of the Mercia Mudstone Group showing the range of mudstones sampled in this study. A - South Wales. B - Somerset. C - Devon.

The prominent sandstone units which occur throughout Devon and Somerset have been placed at the top of the Carnian ( Fig. 7.2 ). They are considered to be correlatives of the Arden Sandstone Member in the Worcester Graben ( Warrington et al., 1980 ). The Weston Mouth Sandstone Member in Devon is exposed in the cliffs on the coast at Weston. Most of the sandstone units are only recognised in boreholes. The continuous sections sampled in this study do not include any of the Carnian Mercia Mudstone Group. The sandstone units have been used to correlate geophysical data in boreholes ( Fig. 9.3 ).

Before this study the mudstones sampled had not been subdivided on any basis since they do not contain any distinctive correlatable beds ( Fig. 7.2 ). The datum which was used in this study is the base of the Blue Anchor Formation which has been assumed to be a chronostratigraphic boundary at or just overlying the Norian/Rhaetian contact. Since this boundary is easily recognisable at outcrop and in boreholes, it proved ideal as a marker horizon throughout the area of study.

The subdivision of the Mercia Mudstone Group in boreholes on the basis of gamma-ray and sonic log response is the only regional correlation which has so far been carried out ( Lott et al., 1983; Penn, 1987 ). In the logs, both sandstones and halite units can be recognised. Furthermore boundaries have been drawn within the mudstones units themselves on the basis of changes in log response which are independent of other lithologies. It is these boundaries, occurring within the mudstones, which are of greatest interest since they should be present in the exposures of Mercia Mudstone Group in Devon and Somerset ( Fig. 7.2 ).

### 7.1.3 Previous Work

Numerous authors have studied the Mercia Mudstone Group ( or Keuper Marl ) in the past century. Almost all studies have included work on the petrography of the rocks and some have specifically looked at clay mineralogy. Geochemical and gamma-ray studies have only begun in the last ten years. A more or less complete list of early references is given in the *Proceedings of the Symposium on the Triassic Rocks of Britain* published in the *Quarterly Journal of the Geological*

*Society of London*, Volume 126 pages 1-291 in 1970. This collection of papers represents the stage of research reached in the late 1960's.

The Mercia Mudstone Group of the Cheshire Graben has been subdivided on the basis of two prominent halite units, the Upper and Lower 'Keuper' Saliferous Beds ( Evans et al., 1968 ). Arthurton (1980 ) defined areas of laminated and blocky mudstone in the Lower Mercia Mudstone Group but on a small scale, attributing the different types to periods of flooding and desiccation respectively. The first subdivision of the Mercia Mudstone Group was carried out by Elliott ( 1961 ) who described six units on the basis of sedimentary structures in the Nottinghamshire basin east of the Cheshire Graben. The topmost unit included the Blue Anchor Formation and the underlying five were red mudstones where unit boundaries were often defined by locally-derived sandstone beds ( skerries ). These subdivisions are by their nature confined to the one basin and cannot be used in this study area. Elliott's topmost unit, the Parva Formation, was divided into the Blue Anchor Formation and the Glen Parva Formation which comprised the red mudstones in the original unit. One of Elliott's subdivisions was redefined by Taylor ( 1982, 1983 ) who divided the Norian Trent Formation into two members on the basis of clay mineralogy and stable isotopic composition. The boundary between Taylor's two Members is a transitional one and as such the subdivision of the Trent Formation is an arbitrary one, based on a continuous change of two geochemical variables. The Mercia Mudstone Group in Worcester has been discussed by Green & Melville ( 1956 ) and Wills ( 1976 ) who described 500 metres of mudstone with locally derived sandstones.

In the area covered by this study, Tucker ( 1977, 1978 ) described the marginal deposits laterally equivalent to the South Wales Mercia Mudstone Group but did not look at the mudstones themselves. In Somerset Thomas ( 1940 ) described the Mercia Mudstone Group and marginal deposits in detail but did not subdivide the mudstones. Mayall ( 1979, 1981 ) studied the Blue Anchor Formation primarily in Somerset but also in Devon and South Wales and was able to define two Members on the basis of clay mineralogy and faunal assemblage. In Devon, Jeans ( 1978 ) proposed three large-scale cycles of carbonate-sandstone-mudstone within the Mercia Mudstone Group. The section covered in this study comes from Jeans' upper mudstone cycle. However his interpretation has been questioned and it

is likely that one of the cycles is the result of repetition of the sequence due to landslipping.

The study of Taylor ( 1982, 1983 ) in particular was of use in approaching the problems of correlation in the Mercia Mudstone Group of Southwest Britain.

#### **7.1.4 Depositional Environment of the Mercia Mudstone Group**

The environment of deposition of the Mercia Mudstone Group has also been the subject of debate throughout this century. Several interpretations have been put forward to account for the deposition of a sequence of homogeneous red mudstones:-

1) Hypersaline marine sea. Deposition of the mudstones in a hypersaline sea with restricted circulation with normal marine waters was proposed by Sherlock ( 1928 ), Klein ( 1962 ) and Evans et al. ( 1968 ). Warrington ( 1970 ) and Jeans ( 1978 ) also favoured this model which is similar to that proposed for the Upper Keuper in the Jura, France ( Lucas & Ataman, 1968 ). This model assumes a relatively permanent body of water in the basins during deposition of the Mercia Mudstone Group .

2) Playa-alluvial basin. This model proposes the precipitation of evaporites in ephemeral lakes in a distal peneplain. This model was put forward by Bosworth ( 1913 ) and later by Audley-Charles ( 1970b ) and Tucker ( 1977, 1978 ). In this model the playas are generated during periods of increased continental runoff and sulphates precipitated in marginal sabkhas as the waters evaporate. In this model the depositional environment is similar to, but on a much larger scale than, the playas described from Saline and Death Valleys in California, U.S.A. ( Hunt et al., 1966; Laeger & Kerr, 1966 and Hardie, 1968 ). The halite precipitated in the modern examples has a very low preservation potential, suggesting that much of the salts originally present in the Mercia Mudstone Group were not preserved.

The playa-alluvial model has been modified by the suggestion that periods of extensive halite precipitation were the result of marine incursions into the basins ( Wills, 1970; Arthurton, 1980; Taylor, 1982 and Holloway, 1985 ). This model

is similar to that of the Ranns of Kutch, a siliciclastic sabkha in Southwest India in which a large area of supratidal flat is flooded annually ( Glennie & Evans, 1976 ). At present the periodic influx of marine waters into the Triassic basins is the most widely accepted theory ( Holloway, 1985 ).

The method of transport of large amounts of fine material into the Upper Triassic basins has also been discussed ( Audley-Charles, 1970b; and others ). Marine, lacustrine, fluvial and aeolian processes have all been cited as possible mechanisms for the transportation and deposition of clays.

One process which has been proposed to account for the presence of extensive red mudstone formations involves the transport of clays as pedogenetic aggregates ( Nanson et al., 1988; Rust & Nanson, 1989 ). In this model, sand-sized aggregates of clay minerals are produced by pedogenetic processes ( pedoturbation ) within vertisol profiles based on observations in Recent arid fluvial systems in Central Australia. These aggregates are durable enough to withstand fluvial action and can therefore be transported and deposited as part of the sand fraction of a river ( Rust & Nanson, 1989 ). Once deposited, however, the individual aggregates are rapidly compacted and lose their pelleted nature, forming a homogenous mudstone. Vertisols are present in the Mercia Mudstone Group ( Wright et al., 1988a , and see Section 7.2.4 ) and the process of transportation of clays as coarse aggregates is therefore a possible means of moving large amounts of clays into the basins. The pedogenic aggregates of Rust & Nanson ( 1989 ) were formed as part of a fluvial dominated depositional system. In the study area there are very few coarse units within the Mercia Mudstone Group and positive evidence for fluvial processes is not abundant. Furthermore, although vertisols are locally present there is little evidence for widespread pedogenesis of the mudstones. Although it is quite possible that the formation and movement of pedogenetic aggregates of clay occurred in the Upper Triassic, the extent to which this process took place cannot, as yet, be estimated. The lack of any evidence for fluvial transportation of material into the basins and the scarcity of coarse beds indicative of fluvial action indicates that the process was not a major source of clay input into the Mercia Mudstone Group.

In the following chapters evidence will be presented to show that the most likely

depositional environment for the Upper Mercia Mudstone Group is that of a playa-alluvial system in which periodic small-scale pluvial events give rise to ephemeral lacustrine conditions in which the evaporites form, alternating with more arid conditions during which local pedogenesis took place.

#### **7.1.5 Aims of the Present Study**

This part of the research project is concerned with the resolution of several of the problems associated with the Mercia Mudstone Group in Southwest Britain.

In this study the Upper Mercia Mudstone Group at outcrop was analysed in detail in order to define, if possible, the precise depositional environment in which the red mudstones were formed. The depositional environment of the Blue Anchor Formation and its transition into the Penarth Group have been described by Mayall ( 1981 ). The depositional environment of the red mudstones in particular was studied because they contain the least obvious indications of their origin.

In South Wales there is good evidence to suggest the presence of a permanent lake at some stage in the Norian ( Tucker, 1977, 1978 ). The Mercia Mudstone Group itself is not different in appearance from the laterally equivalent outcrops in Somerset where there is no evidence for a standing body of water. The sedimentology and geochemistry of the South Wales Mercia Mudstone Group were studied to see if there were any subtle differences in the mudstones.

Since the published record of geophysical logs in the Mercia Mudstone Group is now reasonable ( Lott et al., 1983; Penn, 1987 ), a portable gamma-ray spectrometer was used to try to identify the geophysical subdivisions within the Mercia Mudstone Group at outcrop. The gamma-ray spectrometer also provides information on the distribution of potassium, uranium and thorium within the rock, which has been proven useful in previous studies of mudrocks ( Pliler & Adams, 1962 ).

Clay mineralogy and stable isotopic and trace element geochemical analyses were carried out in order to find the reasons for the gamma-ray variations. The correlation of geochemical and geophysical techniques was thought to be particularly beneficial since the majority of data available on the Mercia Mudstone Group

is in the form of geophysical logs. In the Nottinghamshire Basin changes in clay mineralogy and stable isotopic composition take place between 25 and 70 metres below the base of the Blue Anchor Formation ( Taylor, 1982 ). The exposures in Devon and Somerset provide up to 150 metres of continuous section below the Blue Anchor Formation. It was hoped that similar changes to those in Nottinghamshire would be observed in Southwest Britain.

This study is primarily concerned with the detection of variations in the Mercia Mudstone Group which cannot be observed at outcrop. Work in the field was carried out in order to collect samples for later analysis. A rough log of the Lower Blue Anchor Formation and upper red mudstones was made but in the majority of the section sampled there were no sedimentary features of interest in the mudstones at all. The petrography of the upper parts of the section is described in Section 7.2 .

## **7.2 Petrography of the Upper Mercia Mudstone Group**

### **7.2.1 General Petrography and Mineralogy**

The Mercia Mudstone Group is composed of five main mineral types: clay minerals, carbonates, quartz, sulphates and iron oxides/sulphides. The average abundances of each of the mineral species are given in Table 7.1 . Minor amounts of heavy minerals which were extracted from mudstones in Penarth Cliffs, South Wales have been described ( Al-Kattan, 1976 ). Of the seventeen minerals described by Al-Kattan, only celestite, strontianite and iron oxides were detected in a preliminary heavy mineral extraction in this study. The mudstones contain very few heavy minerals and since those identified were of no use in the description of the depositional environment, further analyses were not carried out.

The two mineral types of most importance in the mudstones are the clay and carbonate fractions, which are discussed in Chapters 8 and 10 respectively. The stoichiometry and ordering of the dolomite phase was analysed using the XRD techniques described in Hardy & Tucker ( 1988 ). This proved to be partially successful since the presence of clay minerals obscured some of the relevant peaks.

Table 7.1 Average abundances of the main mineral types in the Mercia Mudstone Group.

Mineral species	Abundance %
quartz	26
carbonate	25
sulphates	10
clay minerals ( total )	38
illite	32
chlorite	4
mixed-layer clays	2

Twelve dolomitic mudstone samples from the three study areas were analysed. All of the samples were calcian, containing between 52 and 56% Ca in their structure. This may be an indication that the dolomite is early diagenetic in origin. Trace element analyses of the dolomites indicates that there is between 0.5 and 2.0% Fe in the structure. This also affects the position of the XRD peaks from which the stoichiometry is calculated, but the presence of 2 % Fe will not affect the calculation of the Ca/Mg ratio. It was not possible to analyse the ordering of the dolomites because the ( 015 ) dolomite XRD peak which is an indicator of the amount of ordering in the crystal was obscured by a minor illite peak (  $2\bar{0}2$  ), see Appendix 5 . The clay fraction, which is mostly composed of illite, could not be removed from the sample since it is present as flocculated pellets and as coatings on detrital grains. For this reason, no ordering data were acquired and the preliminary study of twelve samples was not followed up.

Of the other mineral types in the mudstones, quartz is present throughout the sequence as a detrital component occurring as sub-rounded grains of silt size (  $60 \mu m$  ) or less. The iron minerals present occur as coatings of hydrated iron oxides and sulphides which are responsible for the red and green colour of the mudstones. Despite the strong colour the presence of hematite was on the limits of detection of x-ray diffraction probably due to the hydrated nature of the iron oxide.

The sulphate in the Mercia Mudstone Group at outcrop is composed almost entirely of gypsum which exists as horizons of nodules ( or their solution residues, Fig. 7.3 ), veins of various forms, and is occasionally disseminated within the mudstone. Celestite occurs locally in the mudstones either disseminated throughout the bed or as massive beds up to 10 centimetres in thickness.

The original presence of halite is indicated by the occurrence of casts of individual simple cubic crystals 1 to 5 millimetres in diameter on bedding planes. These occur rarely in the red mudstones in the Devon and Somerset sections. There is no evidence for the original presence of massive beds of halite which are preserved in the deepest parts of the basins ( Warrington, 1974 ). The halite precipitated in the marginal parts of the basins such as those exposed in Devon and Somerset would have taken the form of crusts on the surface of the desiccated playa which



**Fig. 7.3** Laterally impersistent beds of nodular gypsum in the Mercia Mudstone Group in Penarth Cliffs, South Wales.

would be dissolved during the next input of water into the basin. Large hopper-type halite crystal casts such as those described from Nottinghamshire ( Elliott, 1961 ) were not found in this study.

The nodular morphology of the sulphate in the Mercia Mudstone Group is not related to the original depositional environment. No such structures have been described from similar environments in Recent times and it is unlikely that such large nodules are a primary precipitate. The large, oblate nodules have an average diameter of 40 centimetres and have recrystallised from an earlier morphology, either surficial sulphate crusts or disseminated crystals which formed within the sediment, similar to modern sabkha environments. In the outcrops of Mercia Mudstone Group exposed in the study area the original mode of formation of the sulphate cannot be distinguished.

There is evidence, however, in exposures of Norian Mercia Mudstone Group to the east of the study area that the sulphate formed within the sediment. A sequence of red mudstones containing sulphate interbedded with laminated siltstones are exposed in cliffs east of Bristol ( Curtis, 1982 ). These sulphates are interpreted as having formed within the sediment in the first few metres of burial. Within the study area it seems probable that the sulphate formed in a similar sabkha-like environment. Nodular gypsum makes up the majority of the sulphate within the Mercia Mudstone Group. The only sulphate which shows a different morphology is associated with vertisol horizons ( Wright et al., 1988a ). These will be discussed separately in Section 7.2.4 .

Sedimentary structures within the red mudstones themselves are almost completely absent. The most common difference is that of an increase of shaliness at some horizons. The majority of the mudstones are blocky in texture. Shaly horizons are noticeable in that they are commonly a darker red than the surrounding mudstones. These beds are the result of increased continental runoff during which there was surface water moving into the basin centre. This would have taken the form of sheet floods of low intensity. Larger scale events are marked by horizons of cross-laminated red siltstones no more than 5 centimetres in thickness. These laminated beds occur most commonly in Somerset, where evidence for continental runoff is more pronounced. Some laminated beds occur in South Wales, with none at all in Devon.

The cause of the colour change in the mudstones between red and green/grey has been discussed by several authors. Aljubouri ( 1972 ) attributed the change to the presence of haematite in the red and pyrite in the green mudstones. The total amount of iron does not vary between the two mudstone types. Pyrite has not been identified in either XRD or heavy mineral studies. However, the more common haematite is present but on the lower detection limits on the XRD and so the failure to detect pyrite does not preclude its presence. It is more likely that the green colouration in the mudstones is the result of  $Fe^{2+}$  adhering to the charged surfaces of the clay minerals ( De Lange et al., 1989 ). The Mercia Mudstone Group contains green coloured beds of two types; massive dolomitic beds such as those of the Blue Anchor Formation and green mudstones mineralogically similar to the red beds. The green mudstones occur in three forms:-

- 1) clearly defined beds between 5 and 30 centimetres in thickness.
- 2) randomly orientated irregular patches commonly occurring in poorly defined bedding parallel zones.

3) individual spherical or sub-spherical patches ( fish-eyes ) commonly containing a nucleus of black organic matter ( Aljubouri, 1972 ).

The majority of the green colour in the mudstones is present in clearly defined beds. This suggests that the colouration has a cause that is related to depositional processes since there is no other lithological difference between the green and red beds. The colour change between red and green in arid sediments has been related to iron oxidation state by Walker ( 1975 ). Variations in the Eh and pH of the waters from which iron minerals are precipitating can lead to the formation of haematite or pyrite ( Fig. 7.4 ). The influx of meteoric derived continental waters into a more evaporated, alkaline brine would lead to a reduction in both Eh and pH which could cause pyrite to be precipitated in preference to haematite. It is unlikely that the Eh of the waters was highly variable since the clay mineral palygorskite is present as a minor phase in both red and green beds. This authigenic clay is stable in alkaline conditions over pH 7 . The pH cannot have exceeded 8.5 during formation of the pyrite or magnetite would have become the stable iron phase ( Fig. 7.4 ). A fluctuation of Eh between values of 0.0 and -0.2 would have been sufficient to cause the colour change. There may well have been other influences on the iron phases precipitated but as yet there is no published information. The green mudstones do not seem to be related in any way to the precipitation of sulphates, nor do they contain any particular sedimentary structures. The rapid colour change seen in the mudstones ( Fig. 7.5 ) indicates that the chemistry of the waters changed relatively rapidly. The water composition must have been close to the boundary between haematite and pyrite formation since the change is only shown by a difference in iron mineral. The green mudstone beds are most common in the 20 metres below the Blue Anchor Formation ( Fig. 7.6 ). In Somerset this part of the mudstone succession also contains prominent green dolomitic beds ( Fig. 7.7 ) which are similar in form to the dolomites of the Blue Anchor Formation. This could indicate an amelioration of the arid conditions of the Norian.

### 7.2.2 Dolomitic Beds

The petrography of the Blue Anchor Formation in Southwest Britain has been

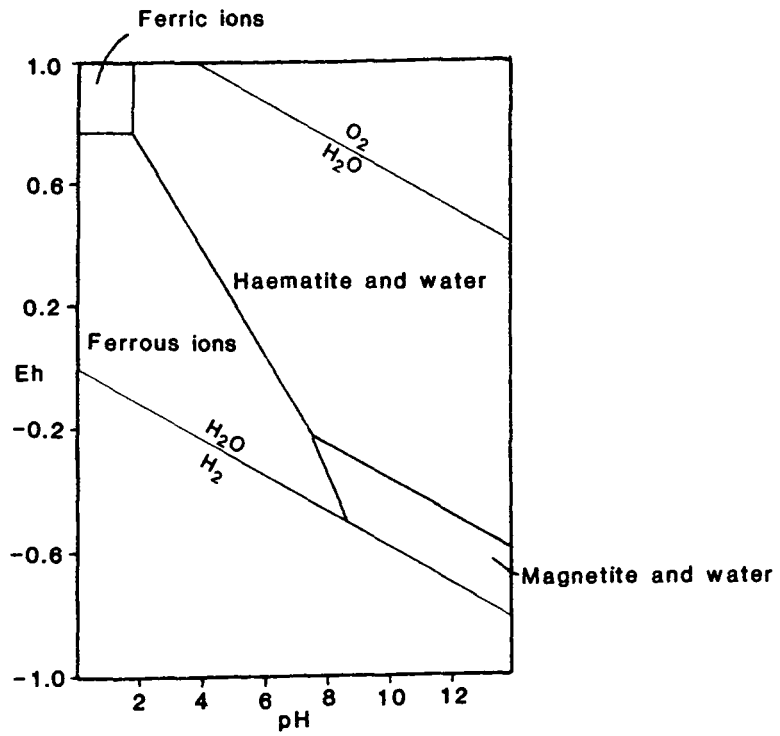
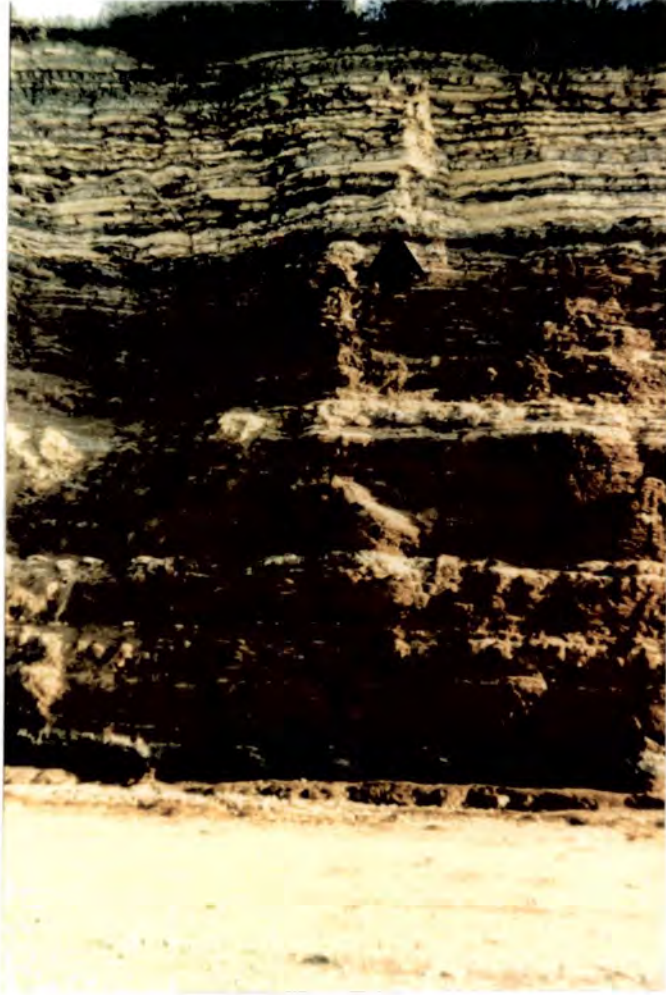
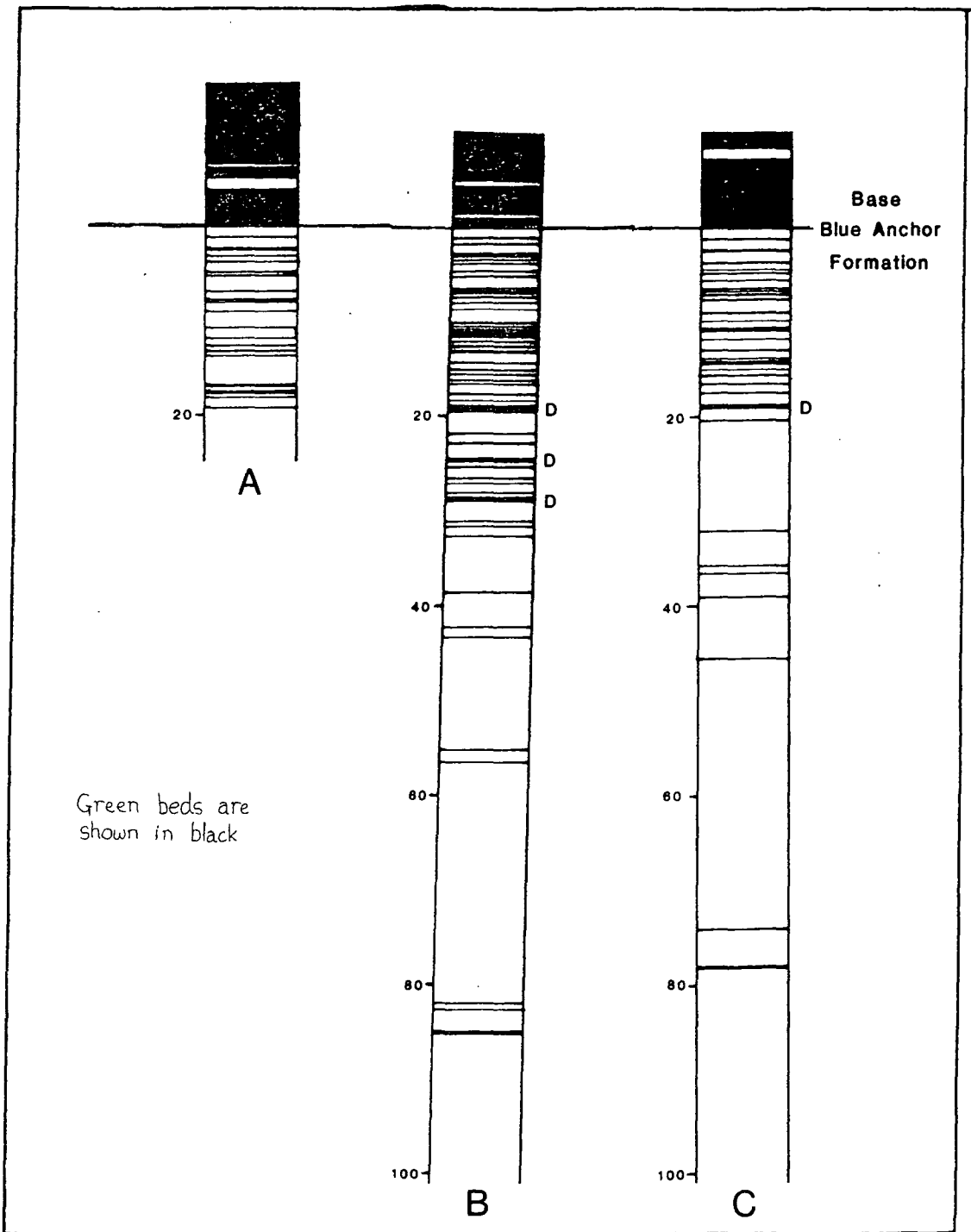


Fig. 7.4 Stability fields of haematite and magnetite in water. From Walker ( 1975 ).



**Fig. 7.5** The transition between the Blue Anchor Formation and the underlying red mudstones in the cliffs at Penarth, South Wales. The base of the Blue Anchor Formation, taken at the topmost prominent red band, is arrowed.



**Fig. 7.6** Distribution of green beds in the Mercia Mudstone Group underlying the Blue Anchor Formation. D - massive dolomitic beds. Heights are given in metres below the base of the Blue Anchor Formation. 100 metres below the Blue Anchor Formation in Devon and Somerset there are few green beds. In Somerset the top 20 metres of the Blue Anchor Formation is not shown. A - Penarth Cliffs, South Wales. B - St. Audrie's Bay, Somerset. C - Seaton and Branscombe Cliffs, Devon.

described by Mayall ( 1979, 1981 ) who covered petrography and clay mineralogy in detail. Mayall interpreted the Blue Anchor Formation as an evaporative marginal lacustrine deposit. Fully marine conditions were established in the top-most few metres of the Blue Anchor Formation ( the Williton Member ) which unconformably overlies the lower Blue Anchor Formation.

Several dolomitic beds occur within the upper red mudstones between 20 and 30 metres below the Blue Anchor Formation ( Fig. 7.7 ). These beds can be clearly distinguished from the green mudstones by their resistance to erosion on the shore at St. Audrie's Bay where they form prominent tilted platforms. Four dolomitic beds, between 0.2 and 0.9 metres in thickness, are exposed. These beds contain 60 to 80% carbonate as opposed to the mudstones which contain under 60% dolomite and calcite. The difference in the amount of carbonate is reduced by the increase in the coarse detrital fraction in the dolomites. Sub-rounded quartz clasts up to 200  $\mu\text{m}$  are common. There are also some clasts of a ferromagnesian mineral and rare plagioclase feldspar. These make up a very small part of the whole rock and their identification is difficult. They do not show up in XRD analyses.

The dolomitic beds show a poor internal lamination which is locally disturbed. This lamination is similar to that derived from algal mats. The top surfaces of the dolomites are arranged into polygons up to 20 centimetres in diameter with an average of 15 centimetres. The centre of each polygon is raised into a mound with some 5 centimetres of relief ( Fig. 7.8 ). Some microfossils have been recovered from these beds ( M. Talbot, pers comm. ) but no larger faunas have been described. As well as microbial lamination the dolomitic beds also contain well developed asymmetric ripples ( Fig. 7.9 ). The cross bedding has a wavelength of 3 to 5 centimetres. The rippling indicates a current direction of 22 degrees east of north in St. Audrie's Bay ( seven readings ). The current direction indicates transport from the Brendon Hills, 7 kilometres to the southeast rather than the closer Quantock Hills which lie 3 kilometres southwest of St. Audrie's Bay. The lack of any coarse clastic material in the St. Audrie's Bay section indicates that in Upper Norian times the Quantock Hills were not a major source of detritus into the basin and may well have had little relief relative to the peneplain on which deposition was taking place. Both the Brendon and Quantock



**Fig. 7.7** Microbially and cross-laminated dolomite in the upper red mudstones in St. Audrie's Bay, Somerset. The bed is 0.6 metres in thickness and has a transitional base and sharp upper contact.



**Fig. 7.8** Desiccated upper surface of the dolomite bed shown in Fig. 7.7. The raised polygonal forms are suggestive of a microbial influence in the formation of the beds.

Hills are composed of Devonian quartzose sandstones and shales ( Thomas, 1940; Whittaker & Green, 1983 ).

In the mudstones of the Mercia Mudstone Group the only visible clastic components are quartz and very ferromagnesian minerals. The coarser dolomitic units also contain rare feldspathic clasts, indicative of an increase of runoff into the basin which transported the mineralogically less stable clasts derived from the Devonian rocks into more distal parts of the basin. The abundant rippling and microbial lamination suggest the presence of at least a temporary water body during deposition of the dolomites. It is likely that the dolomites exposed in the Somerset succession were deposited in a perilittoral environment marginal to an ephemeral water body during a period of increased continental runoff. They are more similar in origin to the dolomites of the Blue Anchor Formation and represent a period of less arid conditions. The top surface of the dolomites is desiccated and overlain by red mudstones with no transition. This indicates the rapid return to the more arid conditions of the red mudstones.

In Devon one similar dolomitic unit is exposed, occurring 17.5 metres below the base of the Blue Anchor Formation. This bed is 0.65 metres in thickness and contains some cross lamination which is poorly preserved and does provide information on current directions. The top surface is desiccated although there is no evidence for any microbial influence. This bed also contains a greater coarse clastic fraction, in this case composed entirely of quartz. This dolomitic unit is likely to have formed in a similar environment to those in Somerset but in a more distal setting. The lack of microbial input is possibly the result of the dolomite being precipitated sublittorally in a more basinal environment. The desiccated top surface of the dolomite indicates that the lacustrine conditions were temporary and that more typical arid conditions were rapidly re-established.

In the North Somerset Graben a similar series of green dolomites can be followed from the Somerset coast into the Burton Row Borehole ( Whittaker & Green, 1983 ). These can be related to an increase in runoff within the Somerset Basin. Individual dolomitic beds cannot be correlated over more than a few kilometres however. It is possible that individual lakes were not extensive and were scattered across the peneplain rather than forming one very large water body. The



**Fig. 7.9** Asymmetrical ripples on the top surface of a dolomite bed in folded Mercia Mudstone Group, Watchet. In unfolded beds in St. Audrie's Bay the rippled horizons indicate a current direction from the south-west.

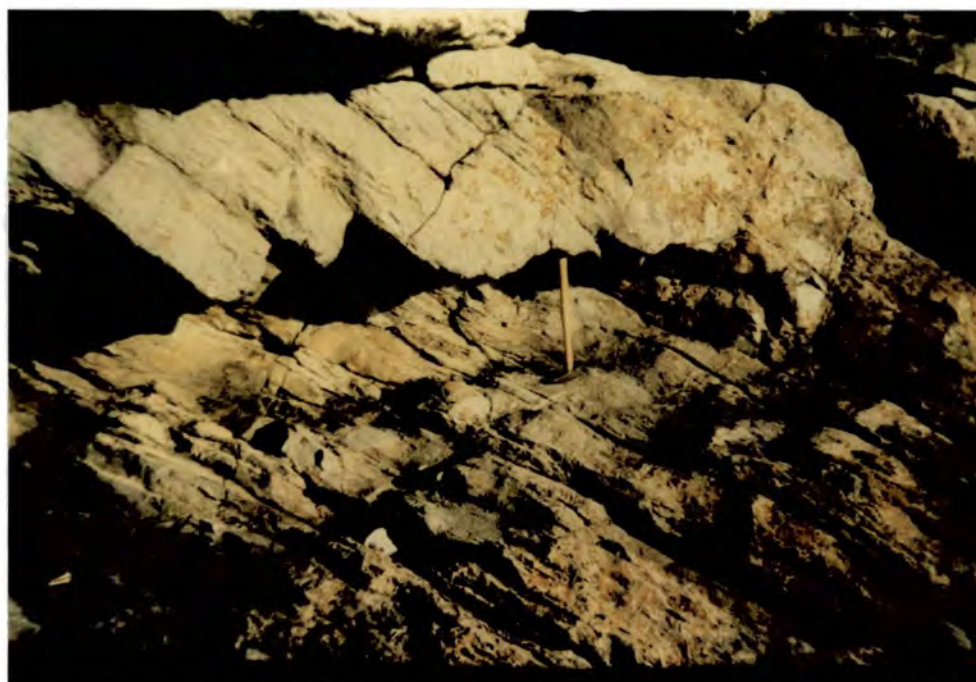


**Fig. 7.10** Wave-cut notch and platform in Carboniferous Limestone at Barry Island, South Wales. The Carboniferous Limestone is overlain by Upper Triassic marginal clastic deposits and by mudstones of the Mercia Mudstone Group. These structures are indicative of a relatively permanent lake shoreline for up to thousands of years in the Upper Triassic.

dolomitic beds within Devon and Somerset cannot be correlated. In Devon the single dolomitic bed does not represent increased runoff on the same scale as that in Somerset, although it is probable that the bed formed during the same less arid period in the Upper Norian.

### 7.2.3 Shoreline Deposits

In Devon and Somerset the exposures of Mercia Mudstone Group studied do not contain any evidence of the relationship with the pre-Triassic basement. Thomas ( 1940 ) described the Triassic rocks in North Somerset and found coarse clastic deposits underlying the Mercia Mudstone Group. These were described as fluvial and alluvial beds. There is no evidence of any coarse clastic material of Norian age in the South Devon area where the most proximal basement exposed at that time was 40 kilometres to the west.

In South Wales there are several coastal outcrops in which the relationship between the Mercia Mudstone Group with the underlying basement is exposed ( Tucker, 1977, 1978 ). At Sully Island a wedge of clastic material overlies a planar surface of Carboniferous Limestone basement ( Fig. 2.6 ). This wedge consists of well sorted gravels at the thin end which pass laterally into rippled sandstones and siltstones as the wedge thickens. The clasts in the wedge are all composed of Carboniferous Limestone. Tucker ( 1978 ) interpreted these gravels as being a marginal lacustrine beach deposit which passes laterally into the mudstones of the Mercia Mudstone Group.

Four kilometres to the west of Sully Island, 20 metres of red mudstones below the Blue Anchor Formation are exposed at Barry Island, overlying a steeply dipping surface of Carboniferous Limestone. The limestone basement in this area has been cut into several terraces ( Tucker, 1978 ) up to 15 metres wide which are overlain by coarse breccias which grade into better sorted sandstones ( Fig. 7.10 ). These terraces are the result of erosion of the basement on the shoreline of a relatively permanent water body ( Tucker, 1978 ). The formation of such terraces in the basement requires a time period of several thousands of years. The water body was therefore present for a much longer time than those which formed the dolomites in Somerset and Devon. Thus in South Wales there



was a permanent lake for much of the Upper Norian. Interestingly the mudstones which are laterally equivalent to the terraces are not noticeably different from those in Devon and Somerset.

The South Wales Mercia Mudstone Group was therefore laid down in a different depositional environment from that in Devon and Somerset. The extent of the lake in South Wales cannot be estimated due to a lack of appropriate outcrop but it is probable that it covered the area of Penarth Cliffs where the majority of sampling in this study took place ( Section 8.1.1 ). In the Penarth section there are sulphate beds which are laterally equivalent to the terraces exposed on Barry Island ( Fig. 7.11 ). There is within the terraces evidence that the lake level fluctuated causing regression and transgression of the lake margin. In this case sulphates would be precipitated in marginal areas of the lake as the water level dropped. On a playa-alluvial peneplain such as that present in the Upper Triassic, a slight lowering of water level would lead to a massive reduction in the area covered by water. This regression could cause a ponding of water in small depressions in the peneplain forming laterally impersistent evaporite beds such as those seen at Penarth ( Fig. 7.3 ). The sulphate beds are at present composed of nodular gypsum. The gypsum was probably originally precipitated as small crystals in the first few metres of the sediment column. The horizons of large nodules are still laterally impersistent, reflecting the original pattern of formation in small ponds scattered across the peneplain.

The evidence for the existence of a permanent water body in South Wales is restricted to the marginal areas where the basement contact is exposed. The mudstones themselves are indistinguishable at outcrop from those in Devon and Somerset. This in itself might be considered as evidence that the Mercia Mudstone Group in all three areas formed in similar conditions. The sedimentary structures which are present in Devon and Somerset do not suggest the presence of a permanent water body, however, and the mudstones in South Wales are geochemically different from those in the other areas, as will be discussed in the following chapters. There is some seismic evidence for the presence of a Permo-Triassic graben in the Inner Bristol Channel ( Brooks & Al-Saadi, 1977; Brooks, 1987 ). This structure, although not active in the Upper Triassic, might have formed an area of higher land due to the rotation of the fault blocks, separating

the South Wales and Somerset areas into subbasins. The presence of islands in the Bristol Channel which are composed of Carboniferous Limestone is further evidence for a barrier between the two areas.

The reasons for the presence of a relatively permanent lake are not certain. The climatic conditions in South Wales can be assumed to have been similar to those in Somerset 25 kilometres to the south. It is possible that the areas of highland in central Wales provided a particularly high amount of runoff to the south which was then channeled through canyons to the South Wales area. A large system of streams draining the area of the South Wales Coalfield has been described by Tucker ( 1977 ). Harrison ( 1971 ) described a series of Upper Triassic cyclically interbedded carbonates and clastics from the Mochras Farm Borehole in the onshore part of Cardigan Bay. These were interpreted as being interbedded playa-alluvial and hypersaline lacustrine beds which were progressively inundated by marine waters in the Rhaetian. Conglomeratic beds indicate the periodic deposition of high energy sediments. The presence of oolites suggests that there may have been a Carboniferous source for some of the detritus, possibly from the northwest. The Mochras Farm section indicates that continental runoff from the Welsh highlands to the west was high during the Upper Triassic. It is possible that the Welsh highlands were particularly prone to high rainfall in the Upper Triassic. In this case the high input of continental runoff into the South Wales area would not necessarily be seen in the Somerset Basin.

#### 7.2.4 'Calcretes'

The majority of mudstones examined in this study contain no structures save a crude bedding shown by rare green units. Distinctive calcrete-type structures are exposed in the mudstones in the cliffs west of Watchet Harbour in Somerset ( ST066436 ) and at Branscombe Cliffs in Devon ( SY192879 ). The exposures in Somerset are the best developed ( Fig. 7.12 ) where several cycles of *vertisol* are present ( Wright et al., 1988a ). The cliff section at Watchet is part of a fault block and as such is not of use in the study of the Upper Mercia Mudstone Group which requires continuous section below the Blue Anchor Formation. Six cycles of nodular *vertisol* are present at Watchet. Vertical nodular structures up to 0.5 metres in height form the top of each cycle. The nodules themselves

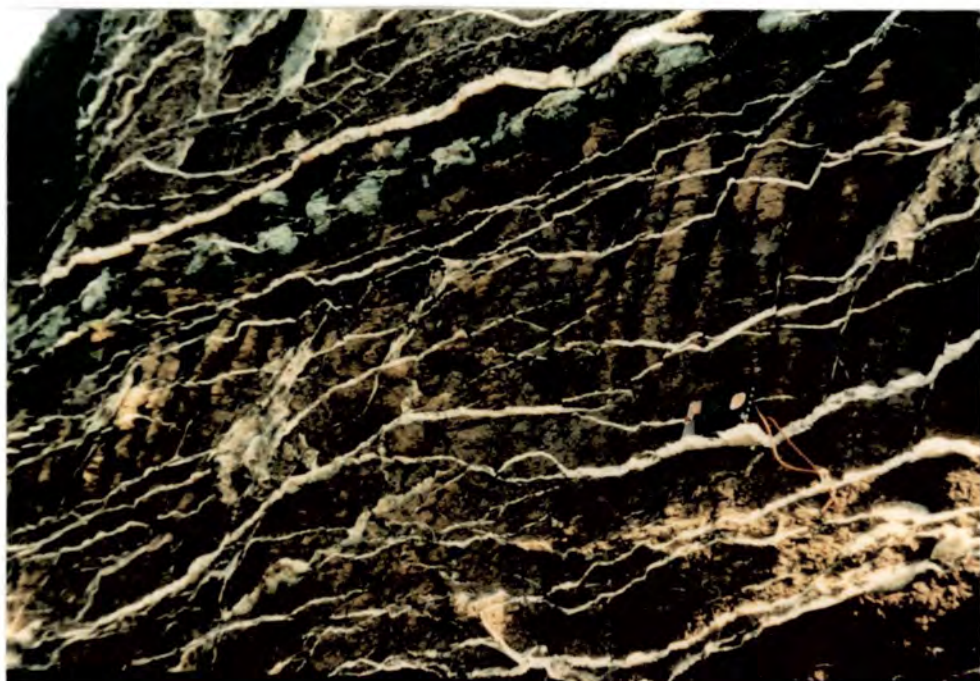


**Fig. 7.12** Nodular *vertisols* and anticlinal fractures infilled by fibrous gypsum in the Mercia Mudstone Group at Watchet, Somerset.



**Fig. 7.13** Mudstone-filled veins in the Mercia Mudstone Group in Blue Anchor Bay, Somerset. These are possibly of pedogenetic origin but in these veins the evidence is not conclusive. Similar veins are common in the Mercia Mudstone Group.

are difficult to distinguish from the surrounding red mudstones since they are similar in colour and composition. Underlying the nodular horizon is several metres of mudstones containing pseudoanticlinal *packages* up to several metres in height ( Fig 7.12 ). The geometry of the anticlines has been accentuated by the presence of fibrous gypsum. The lateral continuity of the *pedogenetic* horizon could not be estimated due to faulting. The *vertisols* preserved in the cliffs at Watchet are important in that they provide the only conclusive evidence of pedogenesis in the study area. The structures in the cycles are made prominent due mainly to the presence of gypsum within the anticlines. In Somerset the only structures which can be compared with the Watchet structures occur in a fault block of Mercia Mudstone Group of unknown age in Blue Anchor Bay ( Fig. 7.13 ). The anticlinal form of these fractures is not accentuated by gypsum and so their geometry is difficult to assess. There are no nodular structures and the fractures appear to be developed in one horizon. The similarity of the fractures to those west of Watchet Harbour indicates a similar method of formation, and it is possible that these beds represent a less intense period of *pedogenesis* or pedogenesis.

In Branscombe Cliffs in South Devon some 15 metres of mudstones containing abundant veins and nodular gypsum is exposed. There is also some evidence for brecciation of the mudstones in the bed. The veins of gypsum are anticlinal in nature ( Fig. 7.14 ) and very similar to those in Somerset. No nodular structures are present in the mudstones although these need not be present in a less mature *vertisol* profile. The *vertisol* profiles described by Wright et al. ( 1988a ) are all well developed, and less mature examples need not contain all of the elements of the mature examples. *Pedogenesis* has been proposed as a reason for the homogeneity of the mudstones. It is impossible to estimate the amount of pedogenesis which has taken place in the Mercia Mudstone Group since there are not necessarily any distinctive structures which will be present. There are some geochemical indications of the intensity of pedogenesis which has taken place. These will be discussed in Section 10.3 .

### 7.2.5 Aeolian Beds

In the cliffs west of Watchet Harbour, in a different fault block from that in

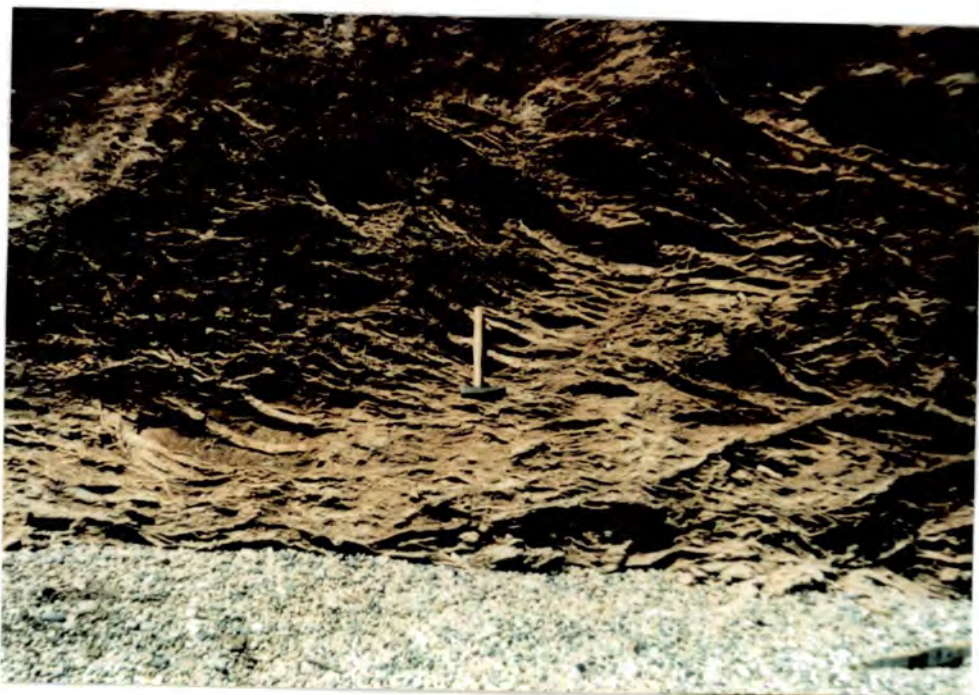


**Fig. 7.14** Abundant gypsum veins in the Mercia Mudstone Group in Branscombe Cliff, South Devon. These anticlinal forms are more likely to be of pedogenetic origin and are similar to those shown in Fig. 7.12 .



**Fig. 7.15** Aeolian sandstone in the Mercia Mudstone Group west of Watchet, Somerset. The beds have been affected by postdepositional deformation but primary cross-bedding can be seen in the centre of the photograph. The bed has been cemented by gypsum.

which the calcretes are exposed, a bed of white gypsum cemented sandstone up to one metre in thickness is present ( Figs. 7.15, 7.16 ). This bed is composed of a texturally mature but lithologically immature sandstone showing large scale cross bedding ( Fig. 7.15 ). The lateral continuity of the sandstone cannot be measured since it is cut out at both ends of the fault block. The thickness of the bed which is exposed is variable however, and it is likely that the bed was not more than several hundred metres long. The cross bedding is patchily well preserved but in places has been disturbed by post-depositional processes. Contacts with the surrounding red mudstones can be diffuse and the sand has in several places been injected into fractures up to 2 metres long above the bed ( Fig. 7.16 ). The very well rounded grains and nature of the cross bedding indicate an aeolian origin for the bed which probably formed an isolated barchan-type dune migrating across the peneplain during a period of increased aridity. The clasts in the sandstone are composed of quartz with some augite and plagioclase feldspar. This indicates that the sand was not being transported for a sufficient time to allow the mineralogically less stable grains to be removed. The sand was probably washed on to the peneplain in a flash flood event and then reworked rapidly by aeolian processes. At least 2 metres of burial by the red mudstones took place before the sandstone was modified by the processes which caused the disturbed bedding and injection structures, probably water escape movements. Although the exact position of the bed cannot be estimated it is not likely to be a correlative of the thicker and more laterally persistent Arden Sandstone of Carnian age.

No other distinctive aeolian units are exposed in the study area. Elliott ( 1961 ) and Arthurton ( 1980 ) proposed that much of the fine detritus in the Mercia Mudstone Group is the product of aeolian transport into the basin. This has been used to account for the lack of structure in the mudstones. The sandstone bed exposed in Somerset is evidence that at least at times in the Upper Triassic wind-derived detritus was carried into the basin. It is probable that there was a constant input of wind-derived fines into the basin during the Norian. The proportion of the mudstones which can be ascribed to aeolian rather than fluvial processes cannot, however, be estimated.



**Fig. 7.16** Vein of aeolian sandstone which has been injected into the overlying mudstones during post-depositional movement. Length of hammer 40 centimetres.

### 7.3 Conclusions

The Mercia Mudstone Group consists of up to 1200 metres of red dolomitic and calcareous mudstones and siltstones containing rare sandstone beds and some sulphate and halite units. In the Upper Triassic marginal successions exposed in Devon, Somerset and South Wales, there are no correlatable beds within the mudstone sequence underlying the Blue Anchor Formation, the base of which serves as a datum in all three areas.

Petrographically the Mercia Mudstone Group consists mostly of clay minerals, carbonates and quartz with minor iron minerals. The mudstones provide limited information to enable the depositional environment to be described. The majority of the mudstones are homogenous and contain no sedimentary structures. There is some evidence for the action of basinward currents and for local calcretisation. In one exposure an aeolian sandstone 1 metre in thickness is exposed. It is possible that pedogenesis and wind action were important processes in the formation of the mudstones but the extent to which each process had an effect cannot be estimated.

Sedimentary structures are more common in the Blue Anchor Formation and in the green dolomitic beds which occur 10 to 30 metres below the Blue Anchor Formation. These beds contain cross bedding and microbial lamination and their upper surfaces are desiccated. Asymmetric ripples indicate a current direction to the north into the North Somerset Basin. These beds formed during periods of increased continental runoff into the basins when less arid conditions more typical of the Blue Anchor Formation were established. They represent the initial incursion of Blue Anchor Formation conditions as the climate gradually became less arid in the Upper Triassic.

In South Wales where the relationship between the Mercia Mudstone Group and underlying basement can be seen there is evidence for the presence of a permanent water body during the Upper Norian. The mudstones in this area are not noticeably different from those in Devon and Somerset and do not contain any evidence themselves for lacustrine conditions. The lake in South Wales appears to have been restricted in its area and was not of a constant size but was reduced

in size periodically, during which time marginal sulphates formed in localised pools on the peneplain.

## **Chapter 8**

### **Clay Mineralogy of the Mercia Mudstone Group**

## Chapter 8

### Clay Mineralogy of the Mercia Mudstone Group

#### 8.1 Introduction

##### 8.1.1 Uses of Clay Mineralogy

The clay minerals within the Mercia Mudstone Group have been analysed by several authors as a means of gaining information on the depositional environment in which the mudstones formed. The clay mineral suite consists mostly of illite and chlorite, but variations in the proportions of the other clays present have been used as indicators of a change in the environment of deposition. Two studies in particular have used clay mineralogy as a means of subdividing the Mercia Mudstone Group. In Nottinghamshire, Taylor ( 1982 ) used variations in the amount of mixed-layer clays to divide the Norian Mercia Mudstone Group into two members. More relevant to this study, Jeans ( 1978 ) described changes in clay mineralogy in the Mercia Mudstone Group of South Devon. These studies were of much use in deciding which areas of outcropping Mercia Mudstone Group should be sampled in this project.

##### 8.1.2 Sampling

In this study, large scale differences in the mineralogy of the mudstones were sought rather than small variations. For this reason, where possible, red mudstones were sampled in preference to green or grey beds and coarse lithologies were avoided. In practice, it was necessary to sample all lithologies in the more variable upper Mercia Mudstone Group. In the Blue Anchor Formation, to preserve continuity of sampling with the underlying red beds, sampling was restricted where possible to mudstones. Coarser dolomite units were avoided.

Sampling was carried out on vertical cliff sections in three main areas in South-west Britain:—

- 1) South Wales: Penarth Cliffs, ST192718 - ST187694
- 2) North Somerset: St. Audrie's Bay, ST104433 - ST119437
- 3) South Devon: Seaton Cliffs, SY275895 - SY236893

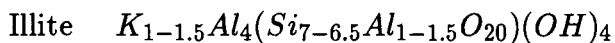
Some sampling was also carried out on the North Somerset coast at Watchet, 4 kilometres to the west of St. Audrie's Bay, and at Branscombe Cliffs, 6 kilometres southwest of Seaton Cliffs in Devon. The cliff sections in slightly folded and faulted Mercia Mudstone Group allowed continuous sampling of up to 150 metres of red mudstones, plus up to 20 metres of Blue Anchor Formation. In Somerset, where the Blue Anchor Formation is 40 metres in thickness, much of the upper part of the section has been obscured by landslipping. Despite this, a total of 170 metres of section were available for sampling. There is some minor faulting in the Somerset section but the displacement on the faults is less than 5 metres. They do not affect the continuity of the succession. In Devon, 90 metres of continuous section were sampled at Seaton Cliffs. Further exposures of red mudstones occur at Branscombe Cliffs separated from the Seaton section by a gap in outcrop estimated by Jeans (1978) as 55 metres. This estimate, however, is based upon borehole evidence from Lyme Regis 16 kilometres to the east. Lateral thickness changes in the Mercia Mudstone Group are rapid (Lott et al., 1982) and so Jeans' estimate of the thickness of the gap in the succession is not an exact figure. In South Wales, a total of 50 metres of section were available for sampling.

Given the continuous section available, samples were collected at one or two metres intervals. Samples of red mudstone were collected every 2 metres. In the Blue Anchor Formation and the upper red mudstones, where lithology is more variable, sampling took place every metre. In total, 213 samples were collected. During sampling, care was taken to avoid weathered rock and in some cases surficial material had to be removed from the cliff in order to collect fresh mudstone. Around 100 grams of rock were collected at each sample site. Before preparation, all weathered surfaces were removed from samples using a grinding wheel.

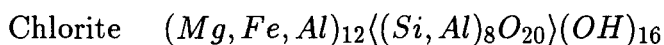
### 8.1.3 Methods and Interpretation

The methods of preparation of an orientated clay specimen and the operating conditions used in the X-ray diffraction analyses of the clays are given in Appendix 3 .

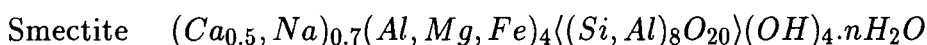
For each sample, 3 X-ray diffraction ( XRD ) traces were taken after different treatments of the clay using identical operating conditions, thus making the traces directly comparable, ( Fig. 8.1 ). The peaks on the chart and their movements after treatment could then be interpreted. Initial interpretations were made on the basis of standard charts in Henson ( 1973 ), Thorez ( 1975 ), Brown & Brindley ( 1980 ) and Hower ( 1981 ). From this the following basic clay species were identified ( descriptions adapted from Deer, Howie & Zussman, 1966 ):-



Illite is a disordered muscovite mica, predominantly dioctahedral and containing more  $Si^{4+}$ ,  $Mg^{2+}$  and  $H_2O$  and less interlayer  $K^+$  and tetrahedral  $Al^{3+}$  . Illites are common in argillaceous rocks derived from the weathering of silicates and from alteration of other clays. Authigenesis of illite is favoured by alkaline waters containing  $Al^{3+}$  and  $K^+$  .



Chlorite consists of regularly stacked trioctahedral sheets in a pseudo hexagonal pattern. Chlorite is common in low grade metamorphic rocks, as an alteration product of ferromagnesian minerals in igneous rocks and as both detrital and authigenic phases in sediments.



Smectites can contain both di- and trioctahedral layers, and consist of superimposed layers containing a plane of  $Al^{3+}$  ions sandwiched between two inward

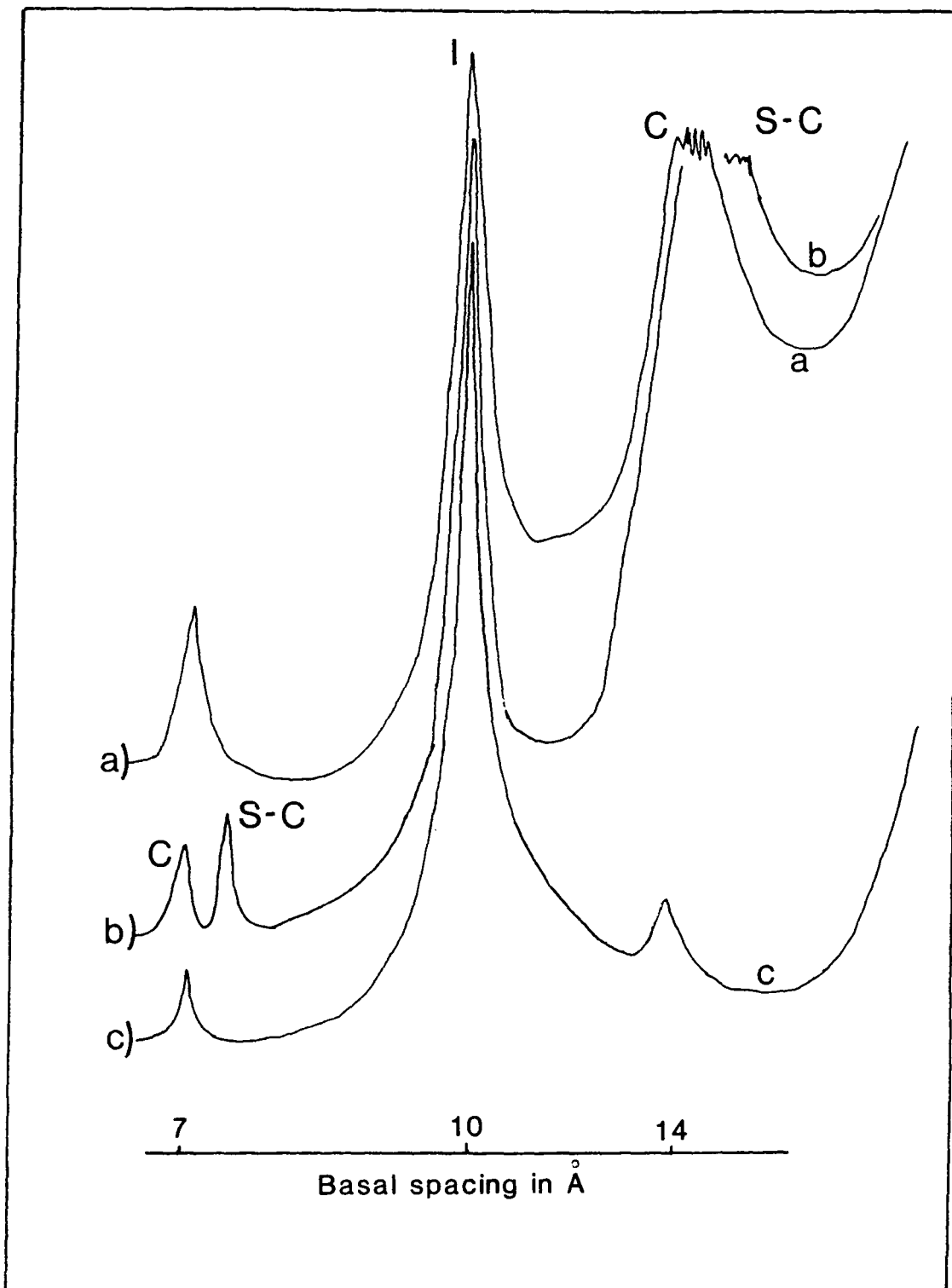
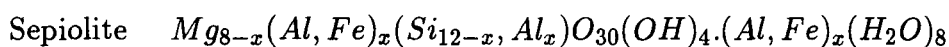
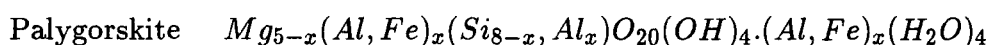


**Fig. 8.1** typical XRD traces from the lower red mudstones, Somerset. a - air-dried. b - after 4 hours in ethylene glycol. c - after 2 hours at 550°C . I - illite. C - chlorite. S-C - mixed-layer smectite-chlorite.

pointing sheets of  $\text{Si}^{4+}$  tetrahedra. Smectites most commonly form from the alteration of volcanic material and in soils associated with illite. Authigenic illite will form preferentially unless  $\text{Mg}^{2+}$  concentrations are high and  $\text{K}^+$  low.

Mixed layer smectite varieties consist of interlayers of smectite and other clay species. Interlayering can be regular or irregular. The chemistry of these clays is dependent on the type and amount of interlayer. These clay minerals will be discussed later in the section.



Both Palygorskite and Sepiolite contain sheets of tetrahedra of  $\text{Si}^{4+}$  and  $\text{Al}^{3+}$  with alternate tetrahedra pointing down. These are linked by sheets of octahedral  $\text{Mg}^{2+}$  and  $\text{Al}^{3+}$ . The mineral is characterised by a ribbon-like structure, as the octahedral layer is discontinuous, giving elongate sheets of limited lateral extent. Both minerals form in  $\text{Mg}^{2+}$  rich waters.

Individual clay species give rise to distinctive peaks on an XRD trace, ( Fig. 8.2, Table 8.1 ). Smectite varieties which contain layers of other clay types require more detailed examination. Upon treatment with ethylene glycol the smectite clays expand as the glycol enters the structure, giving rise to a different diffraction pattern. In a mixed-layer clay the amount of expansion will be related to the proportion of smectite in the structure. The movement of mixed-layer clay peaks on an XRD trace after treatment also depends upon the type of interlayer and its regularity within the structure. In this study both illite and chlorite layers occur in mixed-layer clays. The movement of the peaks of both interlayered clay types is similar and can only be resolved using all of the treatments available.

On the basis of air dried and glycolated XRD traces the smectite-illite and smectite-chlorite clay types cannot reliably be distinguished. After two hours at  $550^\circ \text{C}$ , the smectite-illite clay forms a peak around  $10\text{\AA}$  ( collapsed from the air dried  $14\text{\AA}$  peak ). The smectite-chlorite clay forms a diffuse peak over the 14 to  $10\text{\AA}$  area reflecting the chlorite present in the structure. This differentiation,

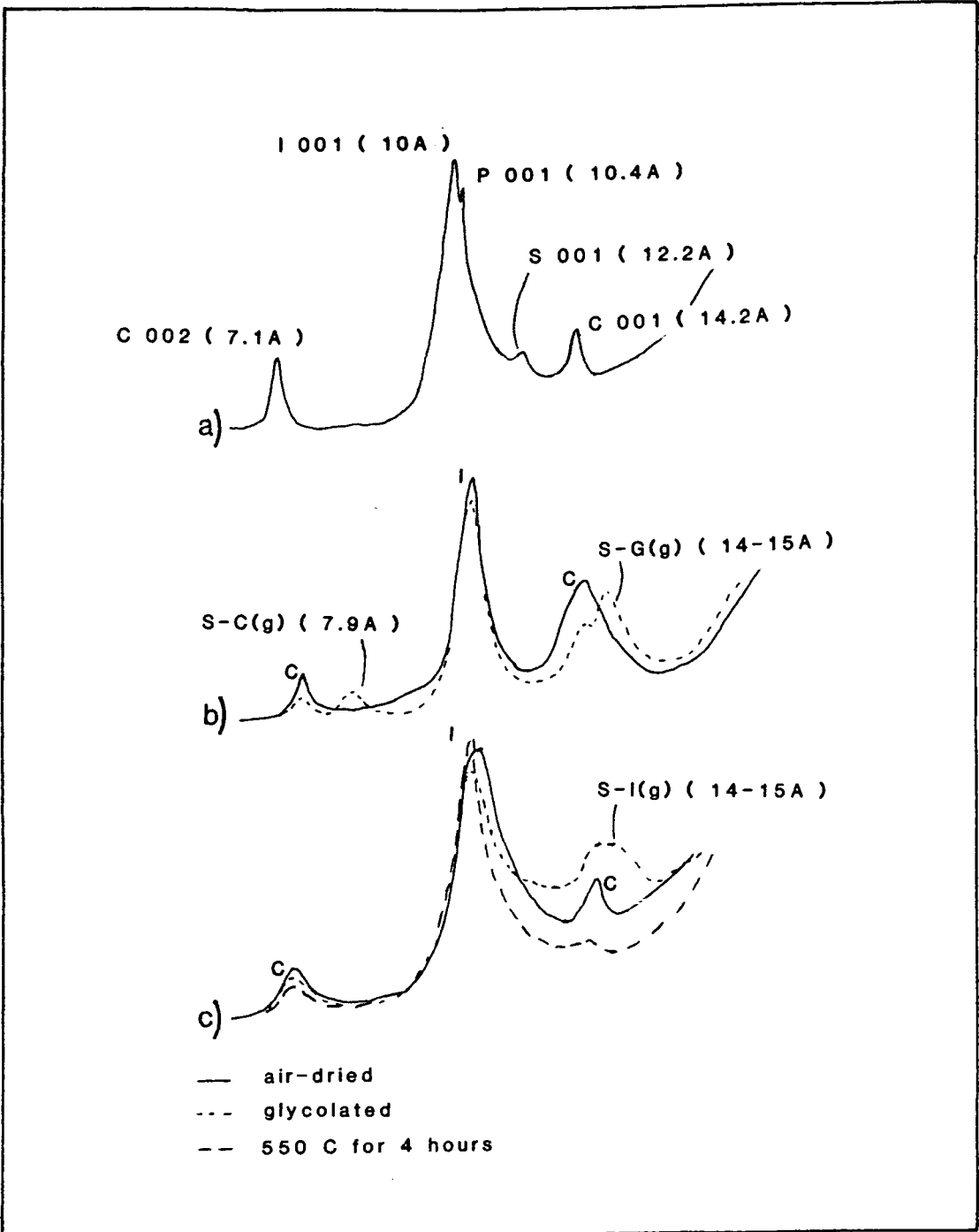


**Fig. 8.2** XRD peaks used in the identification of clay mineral species. I - illite. C - chlorite. P - palygorskite. S - sepiolite. S-C - mixed-layer smectite-chlorite. S-I - mixed-layer smectite-illite. (g) - ethylene glycol trace used in identification. a) illite, chlorite, palygorskite and sepiolite. b) smectite-chlorite. c) smectite-illite.

Table 8.1 Characteristics used for the identification of clay mineral species.

mineral	air-dried	ethylene glycol	550°C
illite	10Å	unaffected	sharpened
chlorite ( 001 )	14.2Å	unaffected	enhanced
chlorite ( 002 )	7.1Å	unaffected	diminished
smectite	14Å	17.5Å	10Å
smectite-chlorite ( 001 )	14.2Å	14-15Å	10-14Å
smectite-chlorite ( 002 )	7.1Å	7.5-7.9Å	7.1Å
smectite-illite	14Å	14-15Å	10Å
palygorskite	10.5Å	unaffected	10.3Å
sepiolite	12.2Å	unaffected	10Å

however, is difficult since the relative peak heights after treatments are of lowered intensity, and in samples containing small amounts of mixed-layer clay the peaks cannot be resolved from the background. The movement of the  $14\text{\AA}$  peak alone is often not diagnostic in the identification of mixed-layer clays. In samples containing a higher relative proportion of such clays, secondary peaks can be used. Smectite-chlorite clays in which the interlayers are relatively ordered show a peak at approximately  $7\text{\AA}$  ( the 002 reflection ). This peak is similarly affected by glycolation and heat treatment and can then be distinguished from the stable chlorite 002 peak which remains at  $7.2\text{\AA}$  . During glycolation the smectite-chlorite 002 peak will expand to between  $7.7$  and  $8.1\text{\AA}$  , depending on the proportion of chloritic layers and their regularity in the structure ( Weaver, 1956 ). Corrensite, the regular smectite-chlorite clay has a glycolated 002 peak at  $8.2\text{\AA}$  . In this study, none of the mixed-layer clays had a glycolated peak at this position and it is assumed that the smectite-chlorite varieties sampled are not fully ordered. The smectite-illite clay has no such 002 peak around  $7\text{\AA}$  . Movement of the  $7\text{\AA}$  peak, when observed, is considered as being diagnostic of the smectite-chlorite clay type.

In many samples, however, the proportion of mixed-layer clay was not large enough to permit identification of clay type. In these cases the mixed layer clay has been assigned to the species which has been positively identified in nearby samples. In practice this has involved assigning one particular mixed layer species to each of the sections studied. The method of Bradshaw ( 1975 ), which distinguished between different mixed layer-clays in one sample, was not found to be of use in this study since the XRD peaks could not be resolved with sufficient accuracy.

An additional potential complication in XRD analysis is the presence of a gypsum peak at  $7.6\text{\AA}$  . In theory this peak could interfere with the smectite-chlorite 002 peak. In practice it was found that the gypsum peak is sharper than the clay peaks and could be removed from the trace without difficulty.

After clay species had been identified in each specimen, semi-quantitative determinations of the amounts of each mineral were carried out using the methods advised by Taylor ( 1982 ). The 001 peaks were identified for each species on the

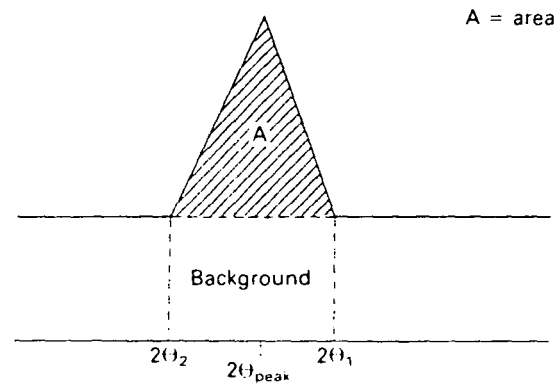
glycolated trace and were separated if overlap occurred. Peak areas were then measured using a base line which was taken as a horizontal line intermediate between the two peak-background intercepts ( Fig. 8.3 ). The relative intensities were then converted to semi-quantitative proportions using the following, ( after Taylor, 1982 ):-

Clay species	Peak used	Multiplication
Illite	10Å	×4
Chlorite	7Å	×2
Smectite	14-17Å	×1
Smectite-illite	14-15Å	×2 – 3
Smectite-chlorite	14-15Å	×1.25 – 1.75
Palygorskite	10.5Å	×6
Sepiolite	12.2Å	×8

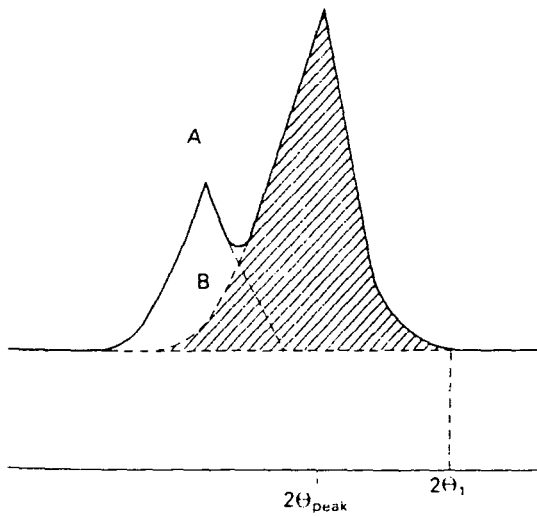
From this, the composition of the clay mineral suites can be calculated.

The clay minerals found in the Mercia Mudstone Group can be attributed to three modes of origin:-

- 1) Detrital - particulate matter transported into the basin and deposited without any chemical change taking place.
- 2) Transformed - clays which have been degraded during weathering and transport but which take up cations in the final stages of transportation and become regraded, either to form the original clay type or a new species. Both illite and chlorite are degradationally transformed during weathering and soil formation due to a leaching of cations from surficial rocks. These degraded clay lattices are unstable and in a cation-rich environment will undergo a regradational transformation. Chlorite can absorb  $Mg^{2+}$  during transportation and early diagenesis; illite absorbs  $K^+$  during diagenesis. Both clays will develop better crystallinity and order with progressive burial. Degraded smectites can absorb  $Mg^{2+}$  or  $K^+$



(a)



(b)

**Fig. 8.3** The method for measuring the intensity of an XRD peak by integration of area for a) a single peak and b) overlapping peaks. From Hardy & Tucker ( 1988 ).

to form mixed layers with chlorite or illite respectively ( Lucas & Ataman, 1968 ), ( Fig. 8.4 ).

3) Neoformed - clays which form directly from gels or solutions without the need for an existing clay lattice. Neoformalional clays can form at all stages of the sedimentary cycle. Smectites and kaolinities form during weathering and calcretisation. Smectite, palygorskite and sepiolite form during deposition and early diagenesis in evaporitic,  $Mg^{2+}$  rich environments. Neither illite nor chlorite form neoformalionally since they require  $Al^{3+}$  which is relatively insoluble. Also, both minerals consist of highly charged silicate sheets which cannot form at surface temperatures ( Lucas & Ataman, 1968 ).

#### 8.1.4 Previous Work

Many authors have studied the clay mineralogy of the Mercia Mudstone Group and have used clay suites to make statements on the palaeogeography and depositional environment of the mudstones . Early studies ( Lomas, 1907; Miskin, 1919; Honeybourne, 1951 and Lippman, 1956 ) concentrated on an identification and description of the clay mineral suites present. The first detailed descriptions of clay mineralogy in an attempt to provide a picture of mineralogical change over a wide area were given by Lucas ( 1962 ) and later in Lucas & Ataman ( 1968 ). Both papers describe a series of transformational reactions in the Jura Basin of eastern France beginning with detrital degraded illite varieties and ending with well crystallised clays at the basin centre ( Fig. 8.5 ). These transformations involve the uptake of cations from solution during transport in hypersaline waters or during early diagenesis. Dumbleton & West<sup>(1966)</sup> described a clay assemblage of illite, chlorite and swelling chlorite ( irregular smectite-chlorite ) with minor sepiolite and palygorskite in the Worcester and Midlands Basins. This assemblage was attributed to the transformational regradation of detrital illite. Jeans ( 1978 ) argued that a similar clay mineral series could be the result of neoformalional reactions and proposed that the interaction of brines and amorphous gels during early diagenesis gave rise to neoformalional clays as waters moved across an extensive evaporative platform, becoming more saline as they moved to the northwest, Mayall ( 1979, 1981 ) studied the clay mineralogy of the Blue Anchor (Fig. 8.5).

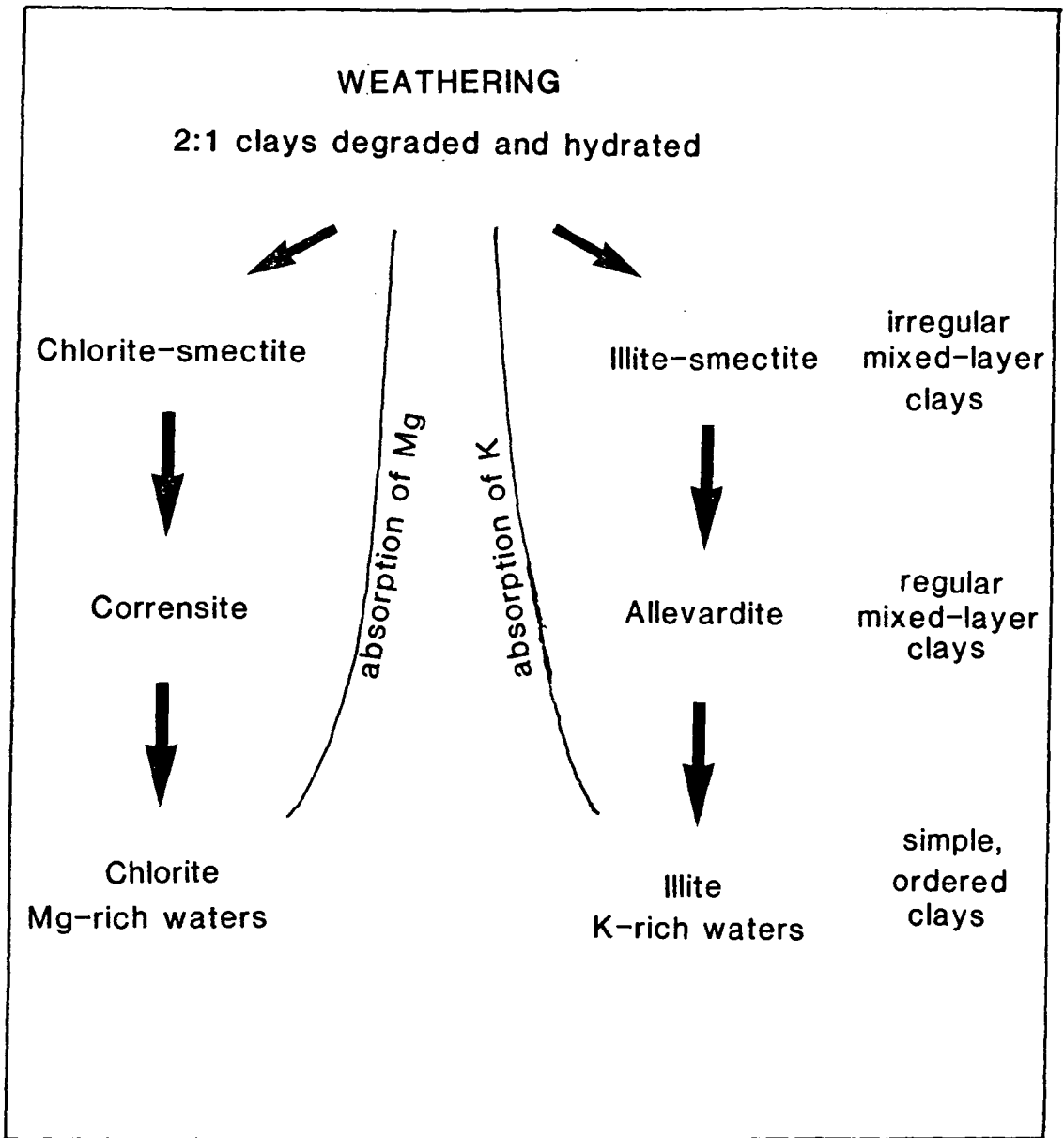


**Fig. 8.4** Transformational reactions involving smectite in  $Mg^{2+}$  and  $K^+$  rich environments. From Taylor (1982).

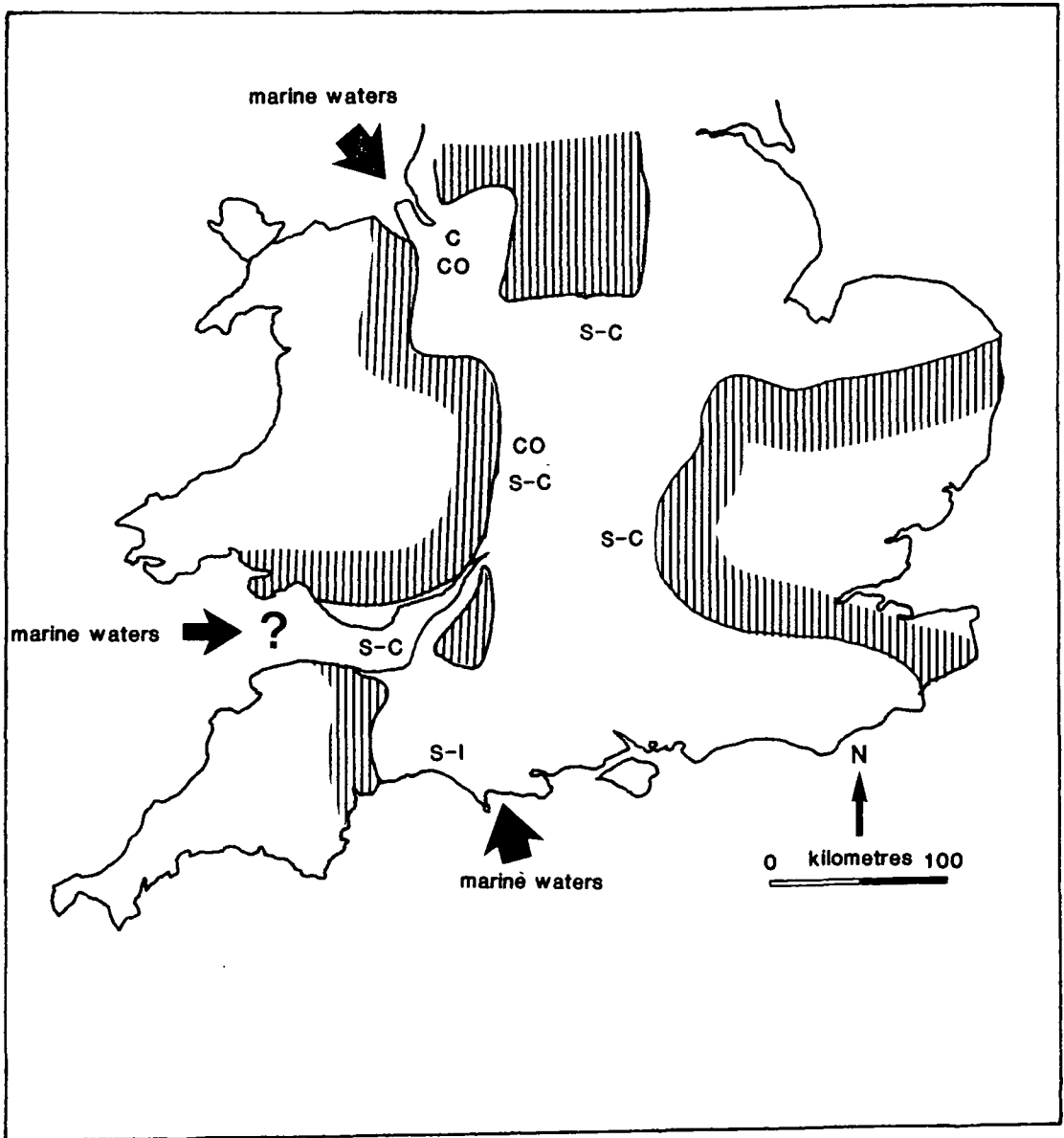


**Fig. 8.5** Distribution of regraded transformational clay mineral types in the Upper Triassic of Southern Britain. S-I - mixed-layer smectite-illite. S-C - mixed-layer smectite-chlorite. CO - corrensite. C - chlorite. Detrital illite and chlorite are not shown. From Jeans ( 1978 ) and Taylor ( 1982 ).

Formation in Devon, Somerset and South Wales. He described an assemblage of illite, chlorite and a number of 14Å clays using the methods of Bradshaw, ( 1975 ).

In the most recent study of Mercia Mudstone Group clay mineralogy, Taylor ( 1982 ) described the assemblages to be found in the Midlands Basins in Nottinghamshire where a thinner Mercia Mudstone Group succession was laid down in a series of small subbasins east of the Cheshire Graben. In this area the clays consist of illite, chlorite mixed layer smectite-chlorite and minor sepiolite and palygorskite. Taylor subdivided the upper ( Norian ) Mercia Mudstone Group into two members on the basis of changes in the clay mineral suite. The total amount of smectite-chlorite was used to distinguish between detrital and transformed suites, the boundary being set at 15% mixed-layer clay. Taylor also put forward various lines of evidence for the aggradational transformation of the non-detrital clay minerals, as opposed to a neoformational origin. Taylor cited the poor crystallinity of the mixed layer clay varieties and a variability in illite crystallinity to account for missing intermediate phases described by Lucas ( 1962 ). Jeans had used the lack of some phases in the transformational series as evidence for neoformation. The Mercia Mudstone Group is poorly exposed in parts of South-west Britain and the complete transformational sequence would not necessarily be present at outcrop.

Taylor also made some comments regarding the relative degradation of the detrital illite supplied to the basin and the crystallinity of the illite at present in the clay assemblage. A constant input of variously degraded illite and chlorite was proposed with differences in water composition being the primary influence on the final clay assemblage. During times of low  $Mg^{2+}$  input, all degraded illite absorbed  $K^+$ , while the small amounts of  $Mg^{2+}$  entered and regraded the detrital chlorite. If the  $Mg^{2+}$  input into the basin increased, then the most degraded illites absorbed Mg to become a mixed-layer ( smectite-chlorite ) while moderately to poorly degraded illites regraded to an ordered, crystalline form. Thus at times of low  $Mg^{2+}$  input, the crystallinity of illite is be more varied.

## **8.2 Clay Mineralogy, This Study**

### **8.2.1 Introduction**

In total, 65 samples of mudstones were studied. The principal objective was to identify major changes in the clay mineralogy suite in the vertical sections of mudstones in the three localities. Specific lithologies were also sampled in Devon and Somerset in order to look at specific aspects of sedimentology. The results of the analyses of the vertical sections are shown in Figs. 8.6-8.8. All of the samples contain a basic assemblage consisting of illite, chlorite and a mixed-layer clay. Smectite, palygorskite and sepiolite are present in minor quantities in some samples. The distribution of clays will be described from each area of outcrop in terms of the assemblage present and the relative proportions of the clays.

### **8.2.2 Clay Assemblages, South Devon**

Sixteen samples from the succession in Devon were analysed by XRD to establish vertical clay mineralogical variations in the sequence. A further four were collected from the Blue Anchor Formation. The clay mineral assemblage in the uppermost 120 metres of Mercia Mudstone Group below the Blue Anchor Formation consists mostly of illite and chlorite, containing relatively low proportions of other clay types ( Fig. 8.6 ). In the topmost 50 metres of red mudstones below the Blue Anchor Formation, illite and chlorite make up over 90% of the total clay mineral suite. These beds crop out to the east of Seaton. The Mercia Mudstone Group around Seaton itself is covered by recent alluvium, and there is a gap of 1.2 kilometres between exposures in Seaton east and west cliffs. From the limited information given in published maps and from observations made at outcrop, it is proposed that the gap in the section is no more than 20 metres. Jeans ( 1978 ) apparently did not sample from the cliffs west of Seaton, although this is not made fully clear.

The clay mineralogy of west Seaton Cliffs contains the same assemblage of minerals as is found in the east cliffs but differs in the relative proportions of clay species. In the east cliffs a mixed layer clay is present but cannot reliably be identified due to its low abundance ( 0-5% ). In the western cliffs, up to 30%

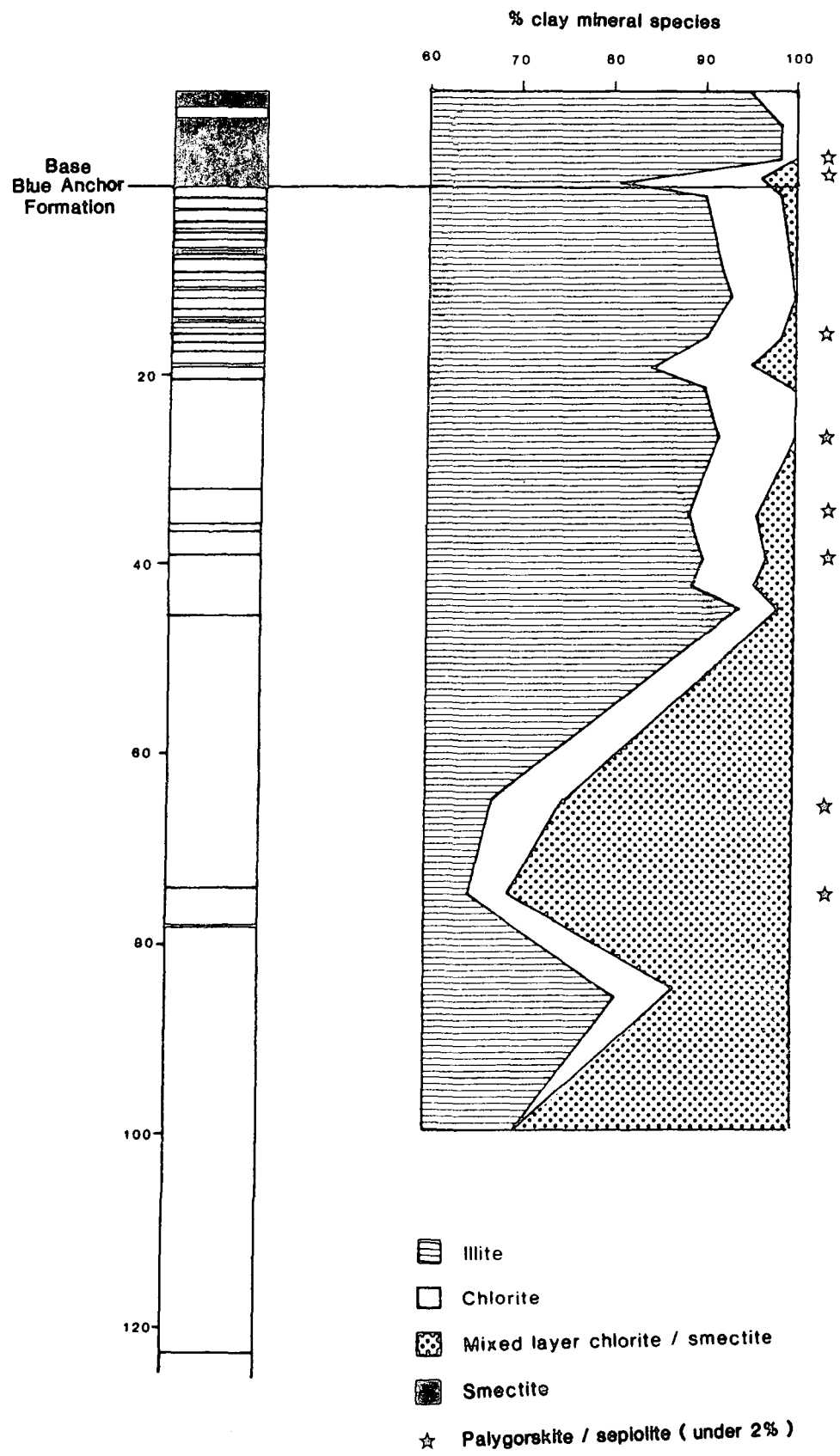


**Fig. 8.6** Vertical distribution of clay mineral types in the Upper Mercia Mudstone Group at Seaton and Branscombe Cliffs, Devon.

of the clay assemblage consists of a mixed-layer clay which can be identified as smectite-illite. The transition in the amount of illite and chlorite in the assemblage from 95-70% is likely to have taken place gradually over a period of time. Taking Taylor's hypothesis, the increase downwards in the mixed layer clay can be attributed to a greater availability of Mercia Mudstone Group. Further samples were collected from Branscombe Cliff but the poor exposure and extensive landslipping meant that a reliable stratigraphic position could not be established. Jeans ( 1978 ) drew a continuous outcrop section for Branscombe Cliff and placed the transition between low and high mixed layer clay assemblages in this section. No samples from Branscombe Cliff containing less than 15% mixed-layer clays were found in this study and it was found to be infeasible to construct a continuous section. The samples taken from Branscombe Cliff are assumed to be *in situ* and stratigraphically in the correct sequence. Also the Branscombe Cliff section is assumed to lie stratigraphically below the Seaton Cliff succession. Lithological evidence does not suggest any duplication of the succession and the thickness of the gaps in exposure are unlikely to differ from the estimates given in Fig. 8.6 by more than 10 metres. It is possible that the mixed-layer poor assemblages identified by Jeans from Branscombe Cliff are part of a landslipped block. The lowest sample collected in this study is from a distinctive gypsiferous unit estimated as being 140 metres below the base of the Blue Anchor Formation. This unit can be followed in Branscombe Cliff and is also present in landslipped blocks, although its lateral continuity is not known. The unit contains nodular and vein gypsum which commonly forms distinct anticlinal structures ( Fig. 7.14 ). Brecciated carbonate is also present in the unit. The very poor quality of outcrop and the uncertainty of the amount of landslipping were such that no further samples were collected below the gypsiferous unit.

The process of aggradational transformation is the most likely origin of the mixed layer 14Å clays in the lower red mudstones. The supply of detrital degraded illite and chlorite can be assumed to be relatively constant throughout the time period covered in this study ( Upper Norian ). The proportion of insoluble residue in the mudstones, which is effectively the detrital fraction, is variable but does not show any trend in the red mudstones, nor does it show any correlation with the proportion of mixed layer clays, ( Table 8.2 ). Thus the most important control

Table 8.2 The relationship between % insoluble residue and the composition of the clay mineral assemblage in the Upper Mercia Mudstone Group, Devon.

Mercia Mudstone Group	% insoluble residue	% mixed-layer clays
Blue Anchor Formation n=4	30.3	1.0
upper red mudstones n=11	63.9	1.9
lower red mudstones n=4	69.2	29.8

Table 8.3 Variation in the crystallinity of illite in the Upper Mercia Mudstone Group, Somerset.

Mercia Mudstone Group	illite crystallinity
Blue Anchor Formation n=5	3.8
upper red mudstones n=19	7.7
lower red mudstones n=11	8.4

The crystallinity value is a simple ratio of the height of the illite 001 peak over width of the base of the peak. Higher values indicate a more crystalline illite.

on final clay-mineral assemblage is the availability of suitable cations in solution in the depositional waters.

An estimate of relative illite crystallinity was made in the Mercia Mudstone Group succession in Devon. On average, the illite in the lower part of the red mudstones, associated with mixed-layer smectite-illite clays, is a better crystallised form ( ie. a sharper  $10\text{\AA}$  peak ) than the illite present within the upper assemblage. This supports the hypothesis that the illite associated with the mixed layer clays formed from a less degraded detrital precursor than those in the upper assemblage.

The relationship between the type of  $14\text{\AA}$  clay formed and the presence of evaporitic material found by Lucas & Ataman ( 1968 ) was not established in this study. There is no evidence of extensive halite having formed in the marginal environment exposed in South Devon, relative to the deeper western Wessex Basin 10 kilometres to the east in Dorset ( Lott et al., 1982 ).

Thus in the upper Mercia Mudstone Group of Devon a boundary can be drawn between two clay mineral suites which are distinguished by the relative abundance of the mixed layer smectite-illite clay species. The boundary cannot be identified at any particular horizon, and will almost certainly be gradational over several metres. The boundary most likely lies in the area of non-outcrop between Seaton east and west cliffs, some 45-65 metres below the base of the Blue Anchor Formation. The base of the mixed-layer clay-enriched unit was not reached in this study.

### 8.2.3 Clay Assemblages, North Somerset

In Somerset a continuous section of 150 metres of red mudstones was sampled without any major breaks in the succession. Thirty-six samples were analysed, of which five are from the Blue Anchor Formation and are considered in Section 8.2.5 . The Blue Anchor Formation on the Somerset coast consists of up to 40 metres of green and grey mudstones and dolomites ( Hamilton 1977 & Whittaker ). At St. Audrie's Bay, where the majority of sampling was done, much of the Blue Anchor Formation has been obscured by a rockfall.

The clay mineral assemblages in Somerset are basically similar to those on the South Devon coast ( Fig. 8.7 ). Illite, chlorite and mixed-layer clays make up the majority of the assemblage with minor amounts of smectite, palygorskite and sepiolite. In this case the mixed-layer clay has been interpreted as a smectite-chlorite type. The difference in interpretation of the mixed layer is due to differences in the behaviour of the 001 and 002 peaks after glycolation. In samples from Somerset, the 7Å peak splits into a stable ( chlorite ) component and an expandable mixed layer part, as described in Section 8.3 . This is diagnostic of a smectite-chlorite type clay. This distinction can only be made in samples containing over 10% of mixed layer clays. In the case of smectite-chlorites, the amount of chlorite in the clay can be estimated by measuring the displacement of the 7Å peak after glycolation. From the movement of this peak ( from 7.2Å to between 7.5 and 8.1Å ) the mixed-layer clay was assigned a composition of 25% ( 8.1Å ), 50% or 75% ( 7.5Å ) chlorite.

As in the Devon succession the clay mineral assemblage can be subdivided into upper and lower suites on the basis of the proportion of mixed layer clay present. The upper red mudstones contain more than 90% illite and chlorite, while in the lower mudstones there is at least 15% mixed-layer clay. The lower assemblage also contains palygorskite and sepiolite, making up no more than 3% of the total but occurring constantly in the section. This is in contrast to the Devon section where both minerals occur throughout the section. This is most probably a result of a failure to detect the very small amounts of palygorskite and sepiolite present, rather than an actual distribution in the mudstones. Both palygorskite and sepiolite are neoformal minerals, forming in silica-supersaturated solutions or gels and in high ( 8.5-9.0 ) pH conditions ( Wollast, Mackenzie & Bricker, 1968 ). These are the only truly neoformal clays identified in this study. Their mode of origin is supported by their fine ribbon-like form seen in SEM ( Section 8.5 ).

The boundary between the two clay mineral assemblages can be identified more readily in Somerset due to the more continuous exposure but is still gradational in nature ( Fig. 8.7 ). The transition takes place over 20 metres in which the proportion of smectite-chlorite increases downwards in the section from under 10% to over 15% . Taylor ( 1982 ) used the 15% mixed layer clay value as a

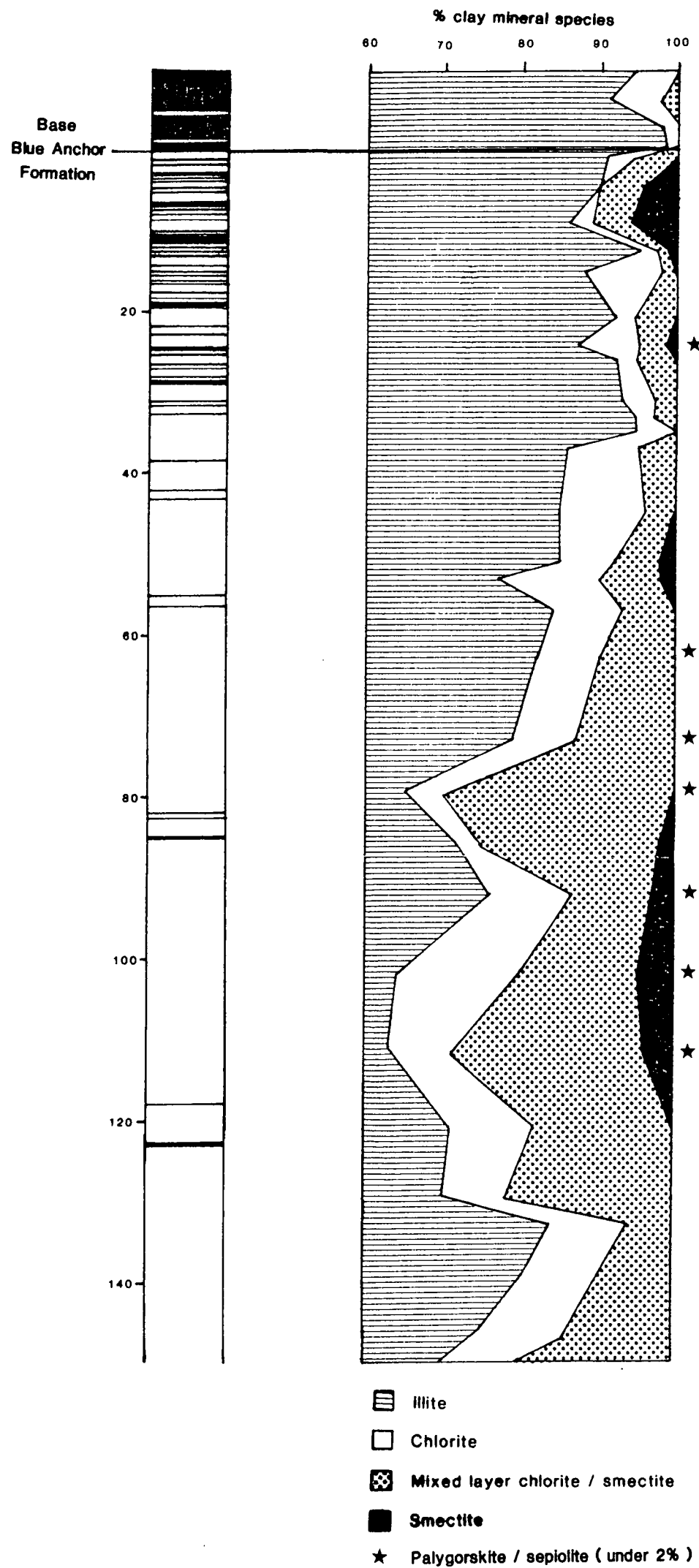


**Fig. 8.7** Vertical distribution of clay mineral types in the Upper Mercia Mudstone Group at St. Audrie's Bay, Somerset.

boundary to subdivide the Nottinghamshire Mercia Mudstone Group. In this study, the 15% value serves as a convenient marker. Using this value the boundary between upper and lower mudstones can be placed 75 metres below the base of the Blue Anchor Formation. As in Devon the crystallinity of the illite in the lower mudstones is relatively greater than that in the upper beds. This estimate of crystal order is purely qualitative, based on a measurement of the 10Å peak height to width at base ratio ( Table 8.3 ). The difference in the two groups is not great but does indicate a significant variation.

In the lowermost 75 metres of red mudstones in the Somerset Mercia Mudstone Group a relatively  $Mg^{2+}$  rich depositional environment can be proposed. The detrital illite was regraded to either a well crystallised illite or a smectite-chlorite depending on the state of the degraded illite. Detrital chlorite would similarly be regraded to a better crystallised form. The upper 75 metres of red mudstones, below the Blue Anchor Formation, consist of a regraded illite and chlorite suite in which in the  $Mg^{2+}$  poor environment, both clays were able to absorb the appropriate cation, becoming more ordered in the process.

#### 8.2.4 Clay Assemblages, South Wales

Nine samples were collected from the Mercia Mudstone Group in South Wales, three from the Blue Anchor Formation and six from the red mudstones. Some 25 metres of red mudstones underlying the Blue Anchor Formation are exposed in Penarth Cliffs, 3 kilometres south of Cardiff. The small vertical section made the identification of changes in clay mineralogy such as those seen in Devon and Somerset unlikely. The South Wales succession is almost certainly too thin to contain such changes ( Penn, 1987 ).

The clay mineral suite in South Wales consists of illite, chlorite and minor amounts ( under 10% ) of a mixed-layer clay, almost certainly smectite-chlorite ( Fig. 8.8 ). This assemblage can be ascribed to formation in a  $Mg^{2+}$  poor environment, similar to the upper parts of the succession in Devon and Somerset. Neither palygorskite nor sepiolite were identified in this section.

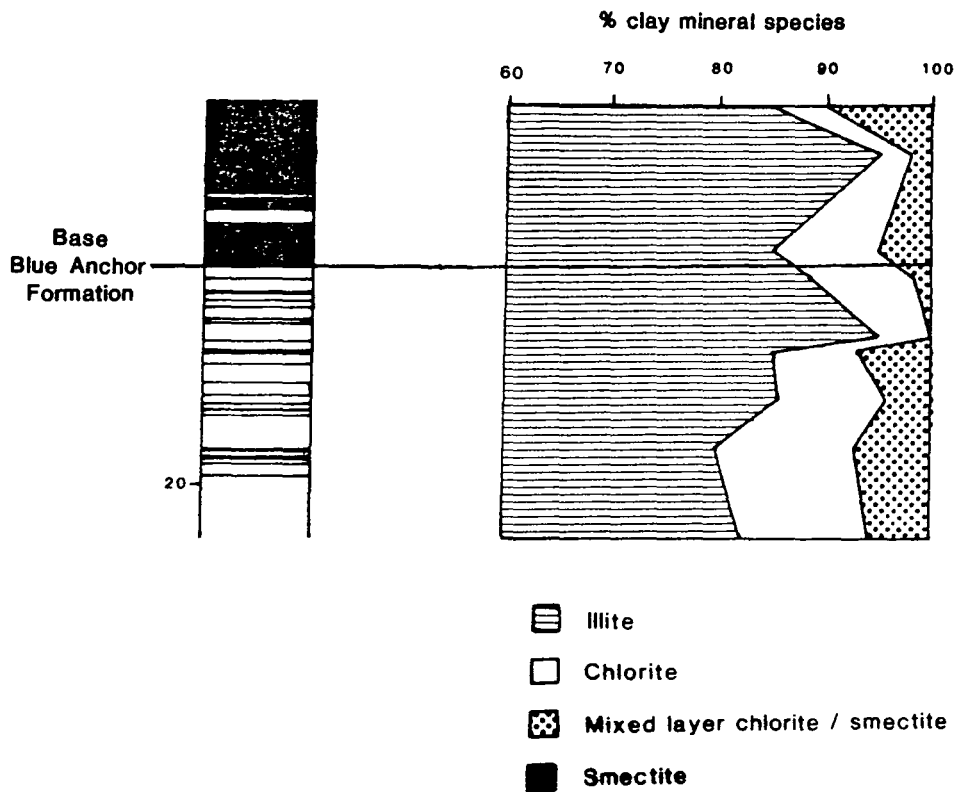


**Fig. 8.8** Vertical distribution of clay mineral types in the Upper Mercia Mudstone Group at Penarth Cliffs, South Wales.

### 8.2.5 Clay Assemblages, Blue Anchor Formation

The Blue Anchor Formation consists of between 15 and 38 metres of green and grey mudstones and dolomites, overlying the red mudstones. Some limited sampling was carried out to assess the changes in clay mineralogy, if any, across the basal boundary of the Blue Anchor Formation. In total, twelve samples were collected from the Formation in the three field areas.

In this study no new clay mineral types were identified in the Blue Anchor Formation. The clay assemblage consists of over 95% illite and chlorite, with minor mixed-layer clays and in two samples from Devon, palygorskite, ( Figs. 8.6-8.8 ). This indicates a continuation of the  $Mg^{2+}$  poor environment of deposition seen in the upper red mudstones. The incoming of more magnesian clays associated with the Rhaetian marine transgression occurs in the topmost Blue Anchor Formation ( Mayall 1981 ) and was not covered in this study.

Mayall, ( 1979, 1981 ) analysed the clay mineralogy of the Blue Anchor Formation in all three areas and identified a different clay assemblage to that found in this study, both in terms of clay types present and of the relative proportions of each clay species ( Fig. 8.9 ). The reasons for this difference are not fully appreciated. Mayall was able to subdivide the mixed-layer component of his clays into smectite-illite and corrensite. On the basis of the traces shown in Mayall ( 1979, fig. 2 ), this would appear to be overly optimistic. In this study it was possible to subdivide the  $14\text{\AA}$  peaks into smectite and mixed-layer components, but the mixed-layer clays themselves could not be further divided.

The relative amounts of each clay type are also interpreted differently in this study and in Mayall ( 1979 ). This can be attributed to a difference in processing technique. Mayall used the method of Bradshaw ( 1975 ) in order to calculate relative abundances of the different clay species. In this the ratio of peak area of illite and smectite ( and thus mixed-layer varieties ) is taken directly as a ratio of clay abundances. In this study, following the method used in Taylor ( 1982 ), the smectite peak area is multiplied by 0.25 relative to that of illite. This process gives a more realistic relative proportion of clays and has been retained in this

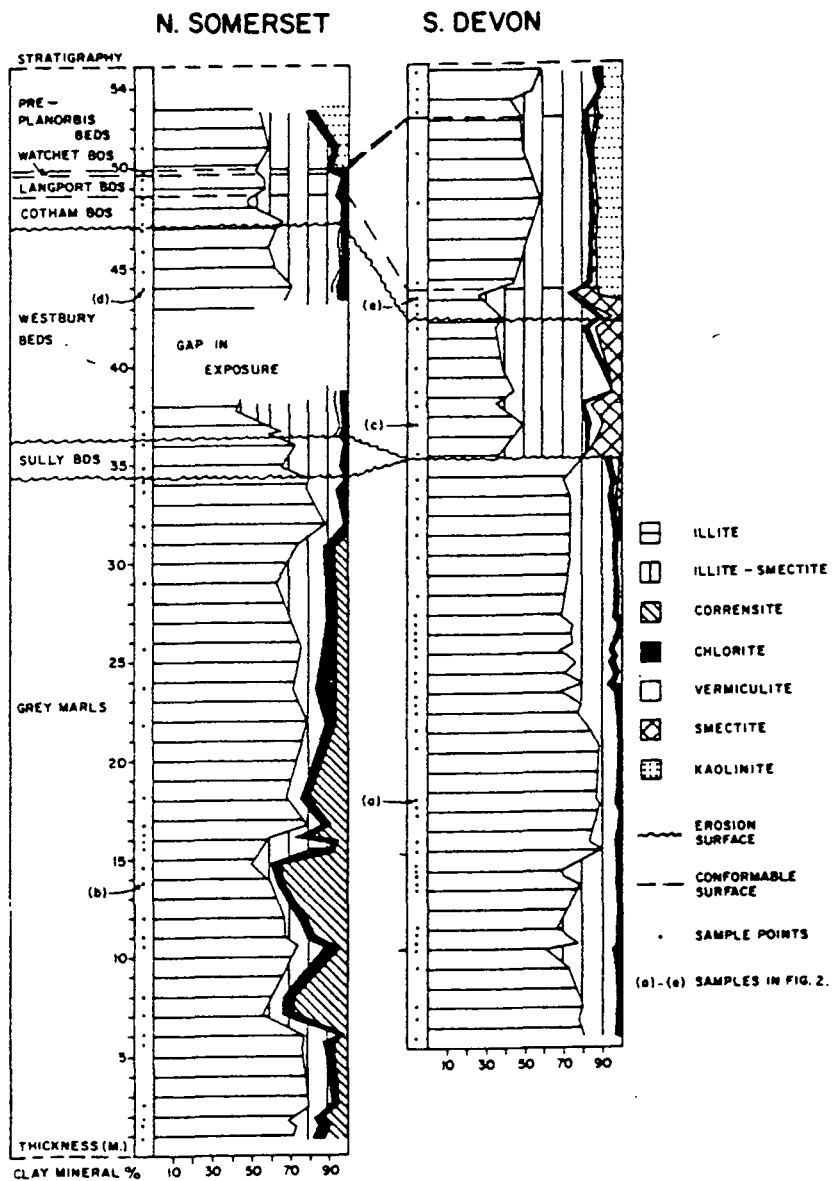


**Fig. 8.9** Clay mineral assemblages in the Blue Anchor Formation and overlying beds in Somerset and Devon. From Mayall ( 1979 ).

study in order to preserve the continuity of the assemblages throughout the section.

### 8.3 Scanning Electron Microscopy

Fractured surface stubs of selected Mercia Mudstone Group samples were prepared by the method described in Appendix 3.3. Most clay mineral species could not be distinguished using SEM. Illite, chlorite and mixed layer clays all form irregular platy or massive crystals ( Fig. 8.10 ), often forming flocculated aggregates. Carbonate and iron oxide coatings tend to obscure the surface details of the clay particles. In some specimens in the lower red mudstones, an irregular network of long fibres was seen ( Fig. 8.11 ). These are interpreted as authigenic palygorskite, possibly grown in microcavities in the mudstones ( Welton, 1983 ). The delicate fibrous habit precludes a detrital or aggradational origin. The SEM analysis confirmed the XRD traces which had indicated the presence of palygorskite. The two clay mineral suites could not be distinguished using SEM, since the main clay minerals have the same aggraded form. Rhombic dolomite was identified, and in some samples gypsum was present as a well crystalline mineral.

### 8.4 Conclusions

Clay mineralogy can be used to subdivide the Norian Mercia Mudstone Group into two groups on the basis of mixed-layer clay content. A lower group, containing over 15% of mixed-layer clays has been identified in outcrop sections in Devon and Somerset. The upper group contains under 10% mixed-layer clays and is composed of regraded illite and chlorite. All of the main clay varieties formed by the process of aggradational transformation, as degraded detrital clays absorbed cations during transport and early diagenesis. The rate of supply of detritus into the basin is assumed to have been relatively constant during the Norian. Thus the difference in clay mineral assemblage can be related to changes in the chemistry of the depositional waters. Palygorskite and sepiolite, which occur in minor amounts in the Mercia Mudstone Group, precipitated directly

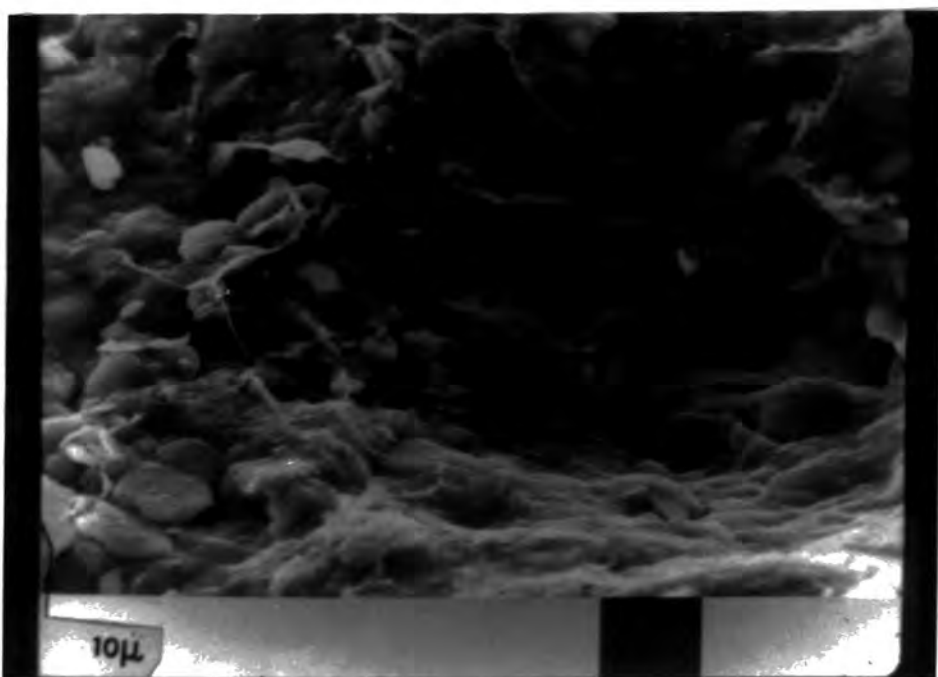


**Fig. 8.10** SEM photograph of irregular, platy crystals which comprise the majority of the clay minerals in the Mercia Mudstone Group. Lower red mudstones, Somerset. The clay mineral species could not be distinguished using SEM.

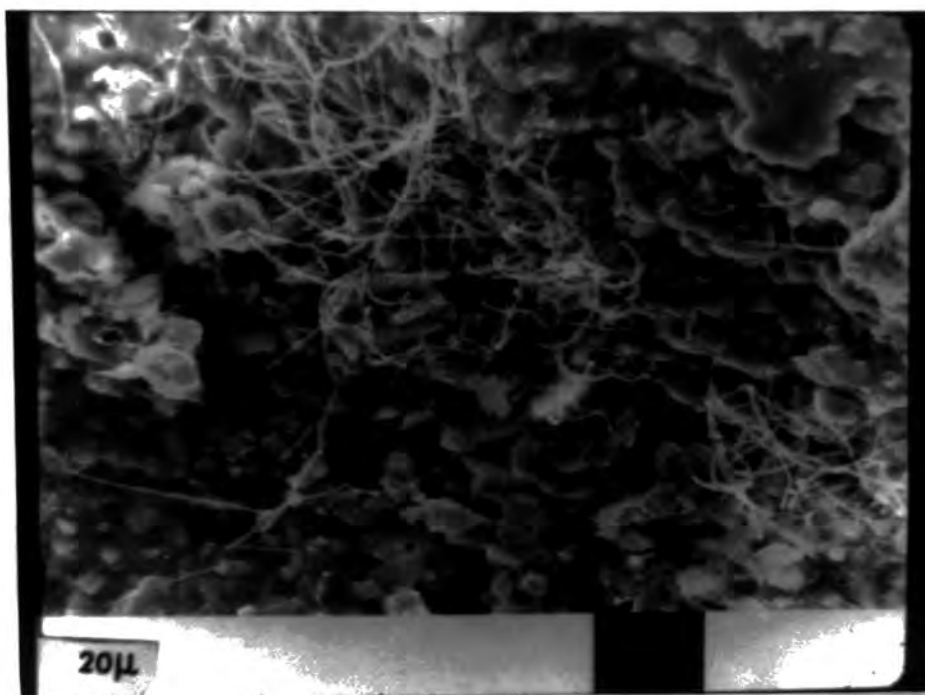


**Fig. 8.11** SEM photograph of elongate fibrous palygorskite in the lower red mudstones, Devon.

from solution. This is the only evidence for authigenesis of clays found in this study.

The clay mineral species present in Southwest Britain Mercia Mudstone Group can be related to the series of transformations proposed by Lucas ( 1962 ) and are influenced primarily by the chemical composition of the waters in which the transformation of detritus took place. In Devon and Somerset, the lower clay mineral suite formed in a relatively  $Mg^{2+}$  rich environment, whereas in the upper assemblage most of the degraded detritus absorbed  $K^+$  to form illite. This difference in water composition has been attributed to incursions of marine derived brines into the Triassic basins. The clay mineralogy in Devon and Somerset reflects the gradual reduction in marine brine influence in the red mudstones, until the upper mudstones are composed primarily of regraded detritus. The boundary between the two units is transitional over 20 metres, and occurs between 50 and 70 metres below the base of the Blue Anchor Formation. The section in South Wales contains only the upper assemblage, mixed layer clays making up under 10% of the total clay fraction.

In the lower Blue Anchor Formation the clay assemblage is similar to that of the underlying red mudstones, indicating a continuation of the  $Mg^{2+}$  poor depositional and diagenetic environments. The gradual incursion of marine waters into the basin is reflected in a change in clay mineralogy in the upper Blue Anchor Formation and the overlying Penarth Group.

## **Chapter 9**

### **Gamma-Ray Spectrometry of the Mercia Mudstone Group**

## Chapter 9

### Gamma-Ray Spectrography of the Mercia Mudstone Group

#### 9.1 Gamma-Ray Spectrometry, Introduction

##### 9.1.1 Background

Although gamma-ray measurements are almost always taken during drilling of a sedimentary sequence, use of the technique in the examination of rocks at outcrop has only recently become recognised as a valuable addition to more conventional field methods. There are only a limited number of minerals which are a source of gamma-rays. Variations in gamma-ray count can thus be attributed to specific changes in the mineralogy of the rock being analysed. Machines which provide spectrometric data on the abundances of potassium, uranium and thorium in the rock are of greater use in the analysis of sedimentary environments. After initial work in the United States of America in the 1960's, little use was made of gamma-ray spectrometry in sedimentology at outcrop until the work of Myers ( 1987 ) and Southworth ( 1987 ) who attempted correlation of exposures on land with borehole sequences.

The use of gamma-ray spectrometry in the outcrop analysis of sedimentary rocks is a relatively recent technique, although it is used commonly in borehole studies. The first use of gamma-ray spectrometry in studying U and Th distribution in shale ( Pliler & Adams, 1962 ) did not lead to a widespread use of the technique. In the last ten years, however, several studies have led to a more widespread appreciation of gamma-ray spectrometry , and the procedures necessary to acquire meaningful field data have become more firmly established. The statistical methods involved in the reduction of field data are presented in Lovborg & Mose ( 1987 ) and have been summarised in Appendix 4 . Myers ( 1987 ) gave a detailed account of field procedures using a portable gamma-ray spectrometer which is summarised in Section 9.1.3 .

Little work in this field has been carried out on the Mercia Mudstone Group at outcrop, although a large volume of data has recently been published using

borehole readings ( Lott et al., 1982; Penn, 1987 ). Southworth ( 1987 ) correlated part of the southern North Sea Triassic with Mercia Mudstone Group in quarries in Nottinghamshire using a hand held gamma-ray meter. The machine used, however, did not provide any spectroscopic information and was not designed for use in field studies.

### 9.1.2 Field Methods

Details of the gamma-ray spectrometer used in this study and the calculations made in order to convert raw data into elemental abundances are given in Appendix 4 . This section is concerned with the practices adopted in the field in order to avoid errors in measurement.

Ideally, in order to measure an effective constant sample size, a planar area of outcrop at least 1 metre in diameter is required. In the cliff sections studied, a surface perpendicular to bedding was also necessary. In practice, this quality of outcrop was not always available. The mudstones of the Mercia Mudstone Group are very prone to fracturing and cliff faces are unstable, particularly after rain. Thus planar surfaces with an area of one square metre are not common. Jointing in the mudstones can provide good surfaces, however, and often on a superficially rough surface the detector could be placed on the highest irregularity, maintaining the required geometry ( Fig. 9.1 ). At higher detector elevations the area sampled is on average shallower, leading to the inclusion of possible weathering effects. It was not possible to avoid weathered surfaces entirely during the study. Obviously weathered faces were avoided, but the fracturing in the mudstones penetrates up to one metre into the cliff and weathering effects are likely to extend at least as far. In extreme cases, faces were cleared to provide a suitable surface. The effective mass of rock sampled, 47 kilograms, is such that the weathered veneer does not significantly alter the gamma-ray count.

Sample points were spaced 1-4 metres apart depending on outcrop continuity and the availability of suitable surfaces. In all, 139 sites were measured in the vertical sections. 36 other sites, representing lithologies of interest in the Mercia Mudstone Group, were also sampled.

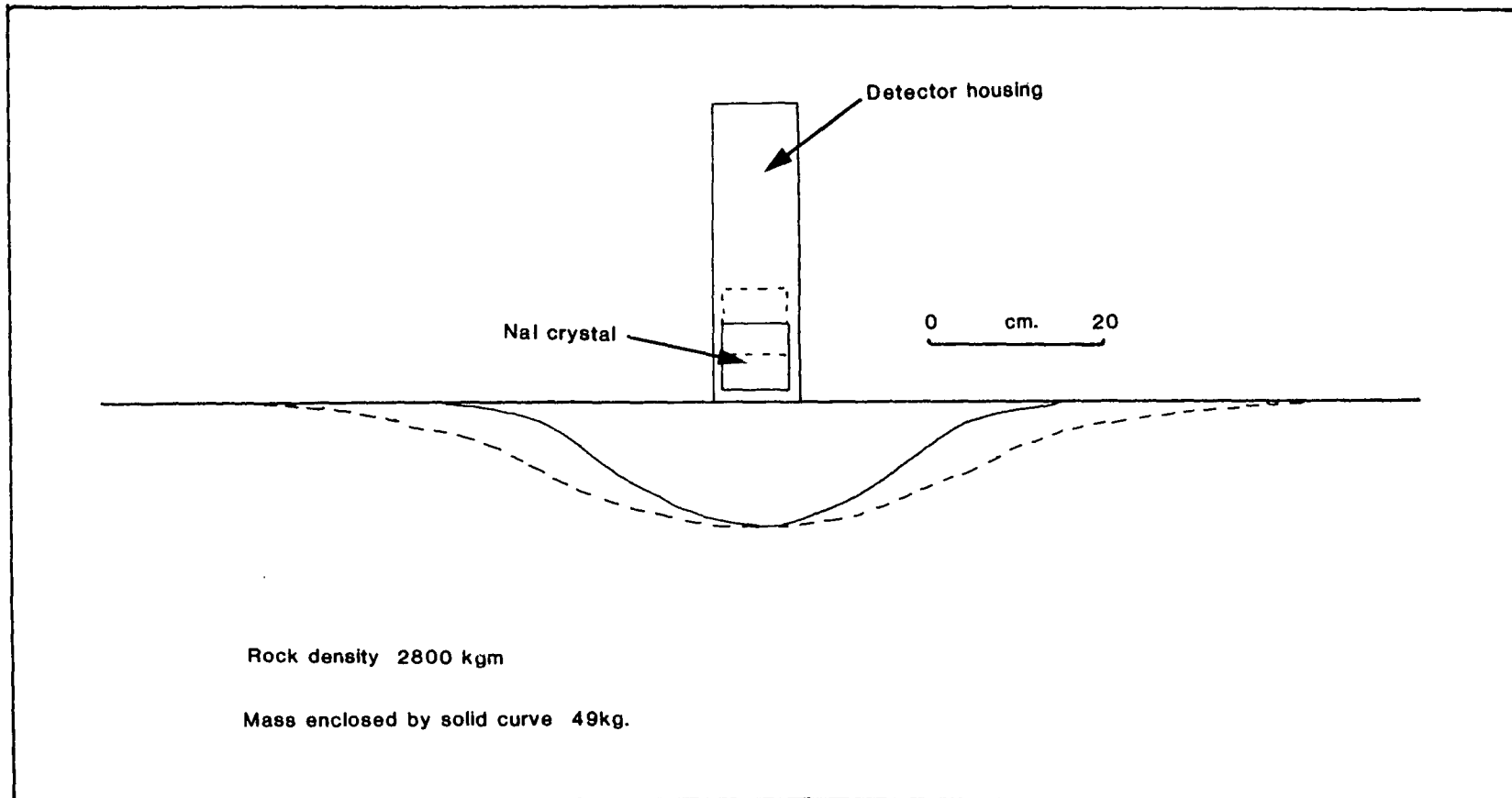


**Fig. 9.1** Vertical cross-section showing the dimensions of 'effective' sample for detector placed directly on a  $2\pi$  surface ( solid curve ) and 5 centimetres above the surface ( dashed curve ) for 2.62 MeV gamma-rays ( Th ).

### 9.1.3 Gamma-Ray Sources

There are a limited number of sources of natural gamma radiation in a mudstone. The most important source in this study is potassium, which is present in a limited number of minerals ( Reverdsky et al., 1983 ). There is no evidence for the presence of alkali feldspar, either as a detrital or authigenic component, within the Mercia Mudstone Group. XRD analysis would not detect small amounts of the mineral ( under 1% ), and so it is possible that there is a small input of feldspathic  $K^+$  into the gamma-ray spectrum. This is of more importance in Devon where the mudstones are derived from feldspar-bearing Devonian rocks to the west. In a mudstone where between 15 and 60% of the rock is illite, however, the detrital alkali feldspar input can be discounted as a significant source of potassium. The other components in the mudstones, quartz, carbonate and non-illitic clays are essentially non radioactive. Given this, the origin of the potassium radiation in the mudstones can be ascribed to illite or mixed-layer clays containing illite sheets. The presence of uranium and thorium in the mudstones is due to transport into the basin as particulate matter and as ions in solution. The amounts of detrital heavy minerals within the mudstones are small. Analyses of concentrates of heavy minerals have not identified any radiogenic minerals. Al-Kattan ( 1976 ) described a heavy mineral suite containing zircon from South Wales. The amount of zircon in the sample was not specified and in this study no zircon was identified using XRD analysis of heavy mineral concentrates.

### 9.1.4 Gamma-Ray Correlation with Borehole Data

In order to correlate outcrop and borehole results, a datum was required which could be traced across the area covered in this study and which could be identified both in boreholes and at outcrop. The only subdivision of the Mercia Mudstone Group which can be made at outcrop is a separation into the upper Blue Anchor Formation and the lower undifferentiated red mudstones. This boundary can be followed at outcrop throughout the British Triassic ( Fig. 7.5 ) and can also be identified in boreholes on the basis of gamma-ray and sonic velocity logs, (Lott et al., 1983).

At outcrop the boundary between the Blue Anchor Formation and the underlying red mudstones is relatively sharp. The base of the Blue Anchor Formation has

been defined as the position of the highest prominent red mudstone bed ( Mayall, 1981 ). Although beds of red mudstone are present within the Blue Anchor Formation, the boundary can be identified without difficulty. For the purposes of this study, the base of the Blue Anchor Formation is treated as a time line. The Blue Anchor Formation is variable in thickness but this is proportional to total thickness changes in the Mercia Mudstone Group ( Fig. 9.2 ), suggesting that the differences are a result of constant sedimentation / subsidence rates rather than diachrony of the formation. The Rhaetian transgression is assumed to be a simultaneous event in Southwest Britain ( Balchin & Ridd, 1970 ). The lithological change at the base of the Blue Anchor Formation represents a similar change, in this case reflecting both climatic change and the initial effects of transgression. The base of the Rhaetian was not chosen as the datum for the following reasons:-

- 1) The shales of the lowest Rhaetian are highly weathered at outcrop and the gamma-ray measurements are very variable ( Fig. 9.2 ). The boundary is not distinct and the difference in the intensity of weathering above and below the change is not directly comparable with borehole conditions. The change at the base of the Blue Anchor Formation does not involve a marked change in the intensity of weathering and readings can be made on relatively fresh sample.
- 2) In Devon and Somerset the Blue Anchor Formation is not constantly exposed but is affected by landslipping and faulting. In order to preserve a continuous section, the base of the Blue Anchor Formation was used as a reference point.

## **9.2 Gamma-Ray Total Count Results**

### **9.2.1 Introduction**

No gamma-ray spectrometric data have been published on the Mercia Mudstone Group to date and so the most useful aspect of the gamma-ray studies has been the correlation of the total count results with borehole gamma-ray logs. Borehole gamma-ray data are presented in API units ( Schlumberger, 1972 ). The raw total count data from outcrop analyses range from 500 to 1700 units, with 85% of

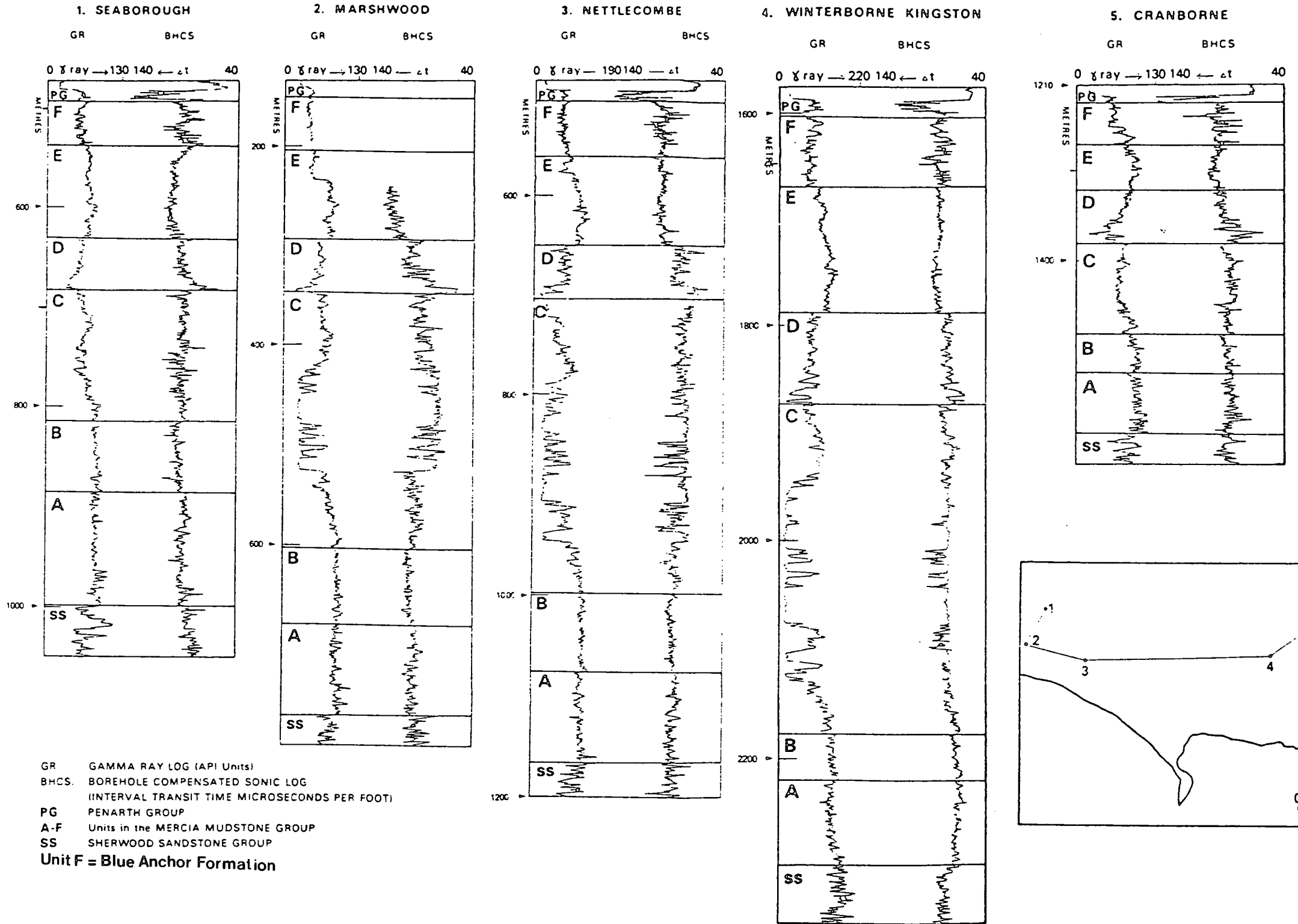


Fig. 9.2 Gamma-ray correlation of the Mercia Mudstone Group in the Dorset - Devon Basin ( from Lott et al., 1982 ).

the results lying between 1000 and 1500. This data set has been calibrated such that the range in outcrop measurements is directly comparable with API units. No absolute values have been ascribed to the outcrop data; they have been used in a purely qualitative way as a comparison with other data sets. For this reason, background count was not removed from the total count data since it is assumed to be constant.

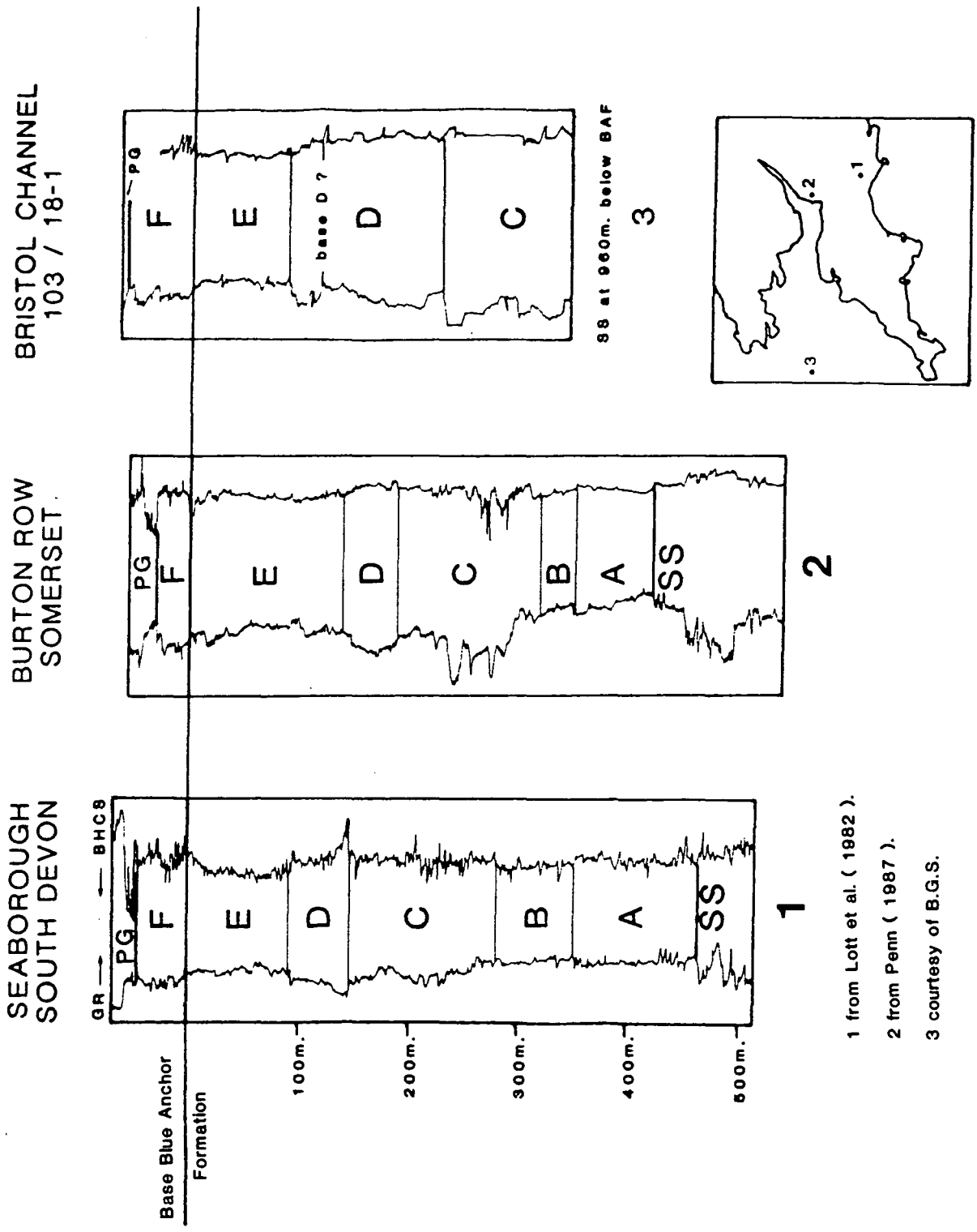
The exposures on which gamma-ray measurements were made are the same cliff sections as those described in Section 8.1.2 . As in the mudstone sampling, measurements were taken at intervals of between 1 and 4 metres. The two sample sets are not directly equivalent due to the problems of finding suitable sample geometry for gamma-ray analysis. Samples taken 1 metre apart will have an area of overlap ( Fig. 9.1 ), but since the borehole data are collected using continuous measurement this is not considered to be a problem.

The total gamma-ray count results from the three cliff sections are shown in Figs. 9.4-9.6 . Raw and processed results are listed in Appendix 4 .

### **9.2.2 Total Count Results, South Devon**

In Devon 65 metres of continuous section below the Blue Anchor Formation were measured in Seaton Cliffs, as well as several samples from Branscombe Cliffs. Only 12 metres of Blue Anchor Formation are exposed in Seaton Cliffs but this is sufficient to allow correlation of the outcrop section with borehole data.

The characteristic 'waisted' signature shown by the gamma-ray and sonic velocity logs in the upper red mudstones has been noted by Lott et al. ( 1982 ) and Penn ( 1987 ) and can be seen in the outcrop gamma-ray results from Seaton Cliffs ( Figs. 9.3, 9.4 ). This variation indicates an increase in the proportion of potassium towards the middle of the red mudstones which corresponds to unit E of Lott et al. ( 1982 ) and Penn ( 1987 ). The gradual decrease in gamma-ray value towards the base of the outcrop section is evidence that the boundary between units E and D is within or close to the Branscombe Cliffs section. The boundaries shown in the borehole sections ( Fig. 9.3 ) are arbitrary points in transitional changes which take place continuously in the section. This particularly applies to the E/D transition which has no obvious point at which values change markedly.



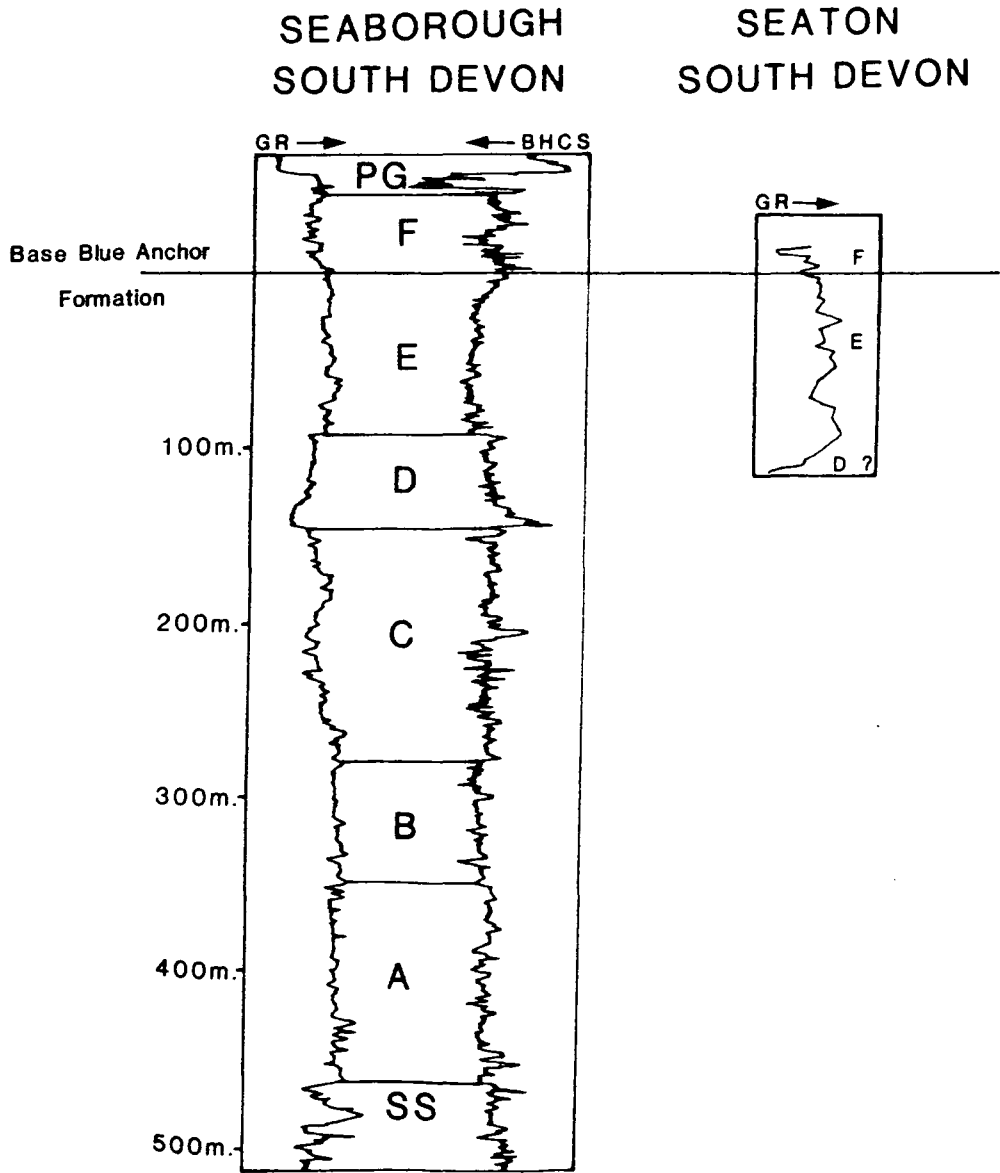
- 1 from Lott et al. ( 1982 ).
- 2 from Penn ( 1987 ).
- 3 courtesy of B.G.S.

Fig. 9.3 Regional correlation of the Mercia Mudstone Group over South West Britain from the Dorset - Devon Basin to the Outer Bristol Channel Basin.

At outcrop, there is no indication of a boundary at all in the lower mudstones. The gradual variations are of use in indicating areas which can be sampled in order to apply sedimentological constraints to the gamma-ray changes.

In the topmost part of the section the base of the Blue Anchor Formation is shown up by a decrease in total gamma-ray count from over 1100 to 1000 counts per 2 minutes. This increase, however, takes place over 40 metres ( Fig. 9.4 ) and on the basis of gamma-ray variations the base of the Blue Anchor Formation cannot be accurately located.

The interpretation of Lott et al. ( 1982 ) implies a thinning of the total Mercia Mudstone Group sequence in the western Wessex Basin from 600 metres in central Hampshire to under 500 metres on the Dorset-Devon boundary. Most of this thickness change is taken up by the halite-bearing beds ( Unit C of Lott et al. ) which occur in the middle of the Mercia Mudstone Group sequence. In units D, E and F which are covered by this study there is a less pronounced thickness change. In the borehole closest to the outcrop section, unit E is 100 metres in thickness. In the 14 kilometres between this borehole and the outcrop section at Seaton, thickness changes in the unit should not be large. If the thickness of the unit is similar in the two sequences, then the boundary between units E and D should be exposed in Branscombe Cliffs. This fits well with the data collected at outcrop. The gamma-ray values recorded in Branscombe Cliffs are lower than those from west Seaton Cliffs but slightly higher than those of the Blue Anchor Formation. The gamma-ray values at the E/D boundary of Lott et al. are slightly higher than those of the basal Blue Anchor Formation. Unit D itself contains highly variable but generally low gamma-ray values. This is interpreted as being due to an intercalation of sulphate and dolomite beds within the mudstones. In this case the sulphate-rich unit which forms the base of the sampled section would be part of unit D. At outcrop the sulphate-rich beds record lower gamma-ray values than the overlying red mudstones. These beds are some 15 metres in thickness and would be conspicuous if seen in borehole logs. In fact such low gamma-ray intervals do occur within unit D in Dorset. Using the outcrop gamma-ray measurements the boundary between units E and D can be placed within the Branscombe Cliffs section and lies above the sulphate and carbonate-rich beds which are the lowest rocks sampled in this study.



**Fig. 9.4** Correlation of outcrop gamma-ray measurements taken at Seaton and Branscombe Cliffs, Devon with a borehole log from the Dorset - Devon Basin ( from Lott et al., 1982 ).

### 9.2.3 Total Count Results, North Somerset

In Somerset the six-fold subdivision of the Mercia Mudstone Group has been established in the Burton Row Borehole ( Penn, 1987 ). Unit F is again interpreted as the Blue Anchor Formation and unit E shows a distinct 'waisted' form with the highest gamma-ray values in the middle of the unit ( Whittaker et al., 1985 ). The Burton Row Borehole was drilled in the centre of the Central Somerset Basin and unit C contains some 50 metres of halite-bearing mudstones ( Whittaker, 1980 ). At St. Audrie's Bay, both the lower and upper parts of the Blue Anchor Formation are exposed, although much of the formation is obscured by landslipping. The base of the Blue Anchor Formation, clearly distinguished at outcrop, is not obvious in the gamma-ray measurements ( Fig. 9.5 ). There are a number of possible reasons for this:-

- 1) The base of the Blue Anchor Formation in Somerset is composed mostly of mudstones as opposed to the more dolomitic beds in Devon. Thus the actual amount of illite in the rock will not change appreciably over the boundary ( see Section 9.1.5 ).
- 2) The section of red mudstones directly underlying the Blue Anchor Formation in Somerset contains a number of dolomitic beds ( Fig. 7.7 ), and so the total illite in the rock was already less in the beds below the Blue Anchor Formation, thus diminishing the difference at the actual boundary.

Although the number of sample points is low, the spread of values in the Blue Anchor Formation is greater than in the underlying red mudstones ( $\sigma = 21.2$  in the Blue Anchor Formation as opposed to  $\sigma = 8.6$  in the red mudstones, taking 15 data points above and below the boundary ). This indicates that the Blue Anchor Formation is lithologically more variable. In the Burton Row Borehole the Blue Anchor Formation boundary is more prominent but since the amount of dolomite in the Mercia Mudstone Group can vary widely on a kilometric scale, the variation in gamma-ray values is acceptable. The gamma-ray value increases to a maximum between 20 and 50 metres below the base of the Blue Anchor Formation and then falls to a level equivalent to those in the

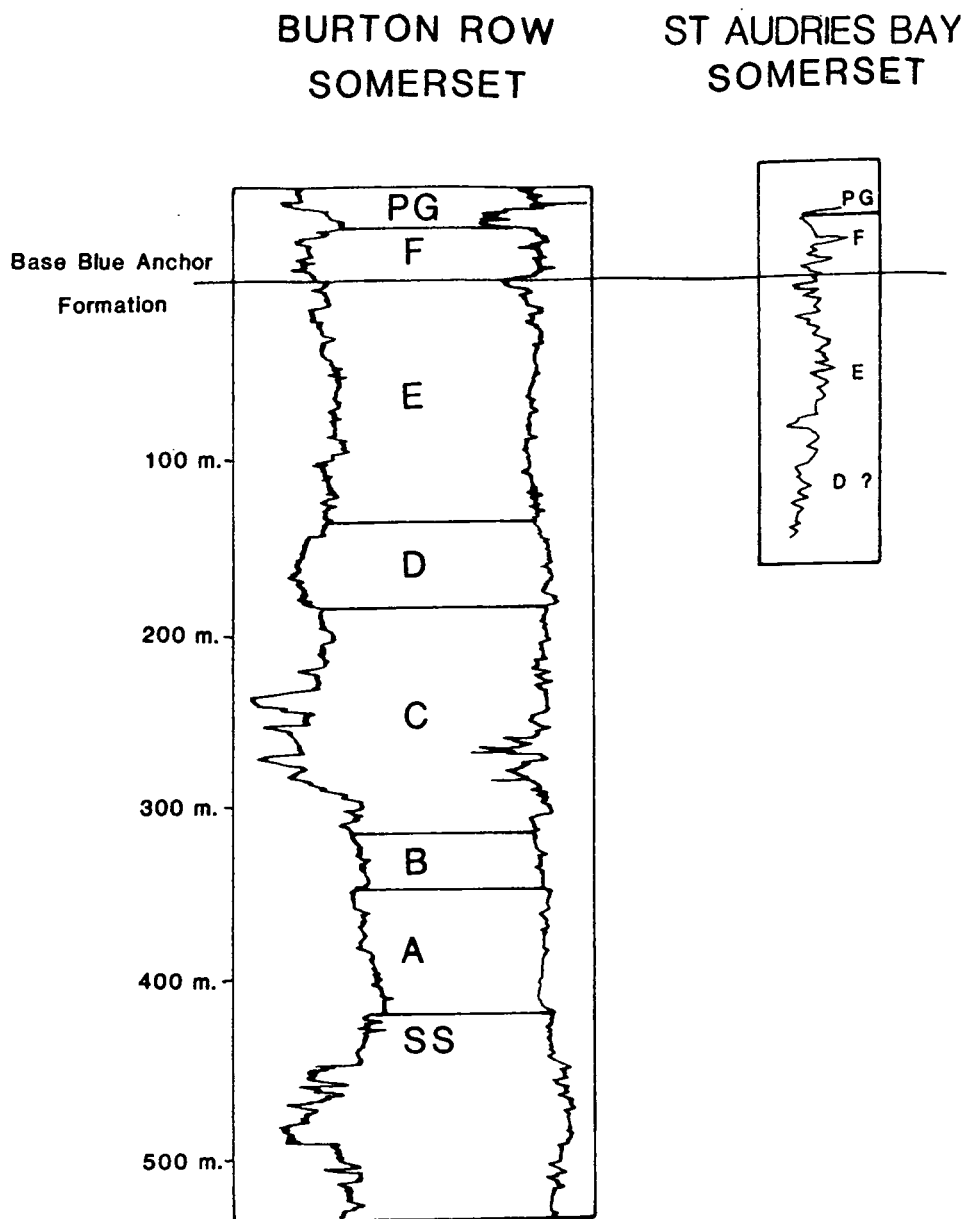


**Fig. 9.5** Correlation of outcrop gamma-ray measurements taken at St. Audrie's Bay, Somerset with a borehole log from the Somerset basin ( from Penn, 1987 ).

Blue Anchor Formation in the lowest samples measured. This variation is similar to that seen at outcrop in Devon and in the Burton Row Borehole ( Fig. 9.5 ). This indicates that the subdivisions applied to borehole variations in Somerset can be extended to the outcrop sections. Unit E in the borehole is 140 metres in thickness, although the boundary is again an arbitrary one ( Penn, 1987 ). Assuming a constant thickness of Mercia Mudstone Group throughout the basin, the E/D boundary would be crossed near the end of the section in St. Audrie's Bay. The gamma-ray values at the E/D boundary are slightly higher than those at the base of the Blue Anchor Formation. Using this control the base of unit E occurs 120 metres below the base of the Blue Anchor Formation. This gives a thinning of 20 metres between Burton Row and St. Audrie's Bay, a distance of 35 kilometres. The difference is very little considering the change from basinal to marginal environments, since the St. Audrie's Bay section is under 5 kilometres from the Palaeozoic basement of the Brendon Hills ( Thomas, 1940 ). This would indicate that active faulting would not take place within the basin in the Norian.

#### **9.2.4 Total Count Results, South Wales**

The relatively small section in Penarth Cliffs was measured to ensure that the change between the red mudstones and the Blue Anchor Formation was visible in the gamma-ray results ( Fig. 9.6 ). The boundary is indicated by a more localised increase in total gamma-ray count than is seen in Somerset. There is a more obvious lithological change across the Blue Anchor Formation boundary in South Wales between the mudstones and the more dolomitic green beds, giving rise to a sharper change in gamma-ray values.

In the St. Fagan's Borehole, 10 kilometres to the northeast of the Penarth Cliffs section, a total of 55 metres of red mudstones were drilled and are placed in unit E ( Penn, 1987 ). There is no evidence from boreholes or outcrop to indicate the presence of unit D in South Wales, where a maximum of 100 metres of mudstones are present.

103 / 18-1                      PENARTH  
BRISTOL CHANNEL      SOUTH WALES

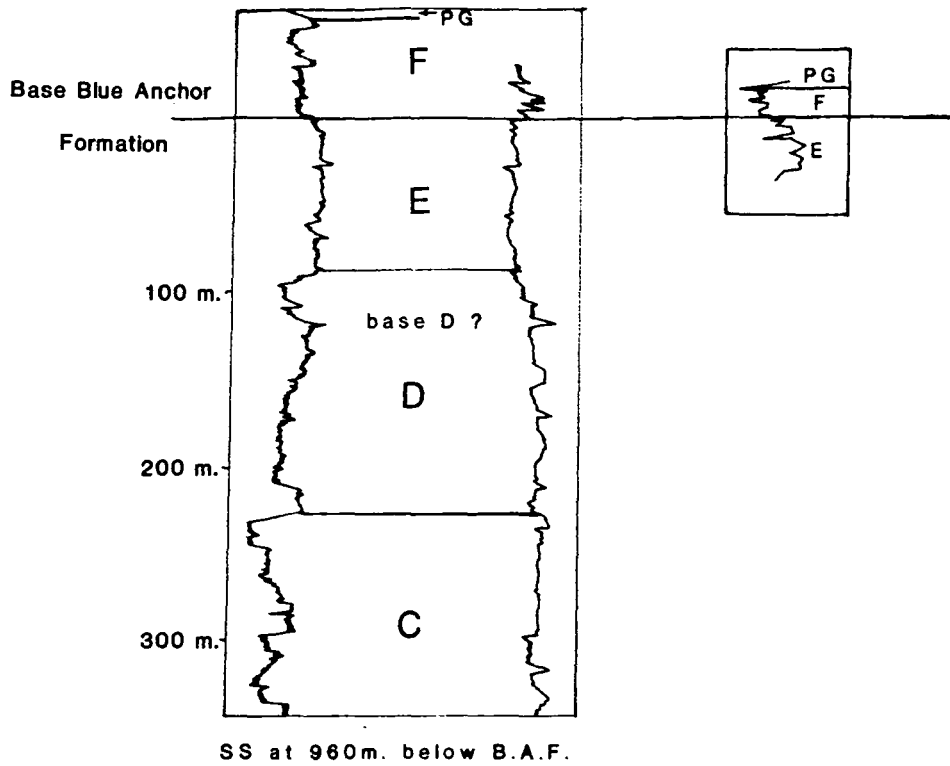


**Fig. 9.6** Correlation of outcrop gamma-ray measurements taken at Penarth Cliffs, South Wales with a borehole log from the Outer Bristol Channel Basin.

## **9.3 Gamma-Ray Elemental Analyses**

### **9.3.1 Introduction**

The Geometrics 410 instrument provides not only a total gamma-ray count of a sample but also information on the amounts of potassium, uranium and thorium present in the rock. This information can then be reduced to present the data in the form of % K and ppm U and Th . This procedure is described in Appendix 4 . The elemental analyses will be discussed in terms of individual elements and the three areas of outcrop will not be treated separately.

### **9.3.2 Correlation of Gamma-Ray Spectrometric Results**

The gamma-ray spectrometer was calibrated before this field study using control stations set up by other workers ( Cassidy, 1979 ). Similarly, during this study, several sample sites were chosen as control stations with a view to later calibration of the gamma-ray spectrometric results with other laboratory-based geochemical techniques, as described in Appendix 4 . The results of this calibration are shown in Table 9.1 .

All of the results obtained using gamma-ray spectrometry are less than those found using other techniques. This suggests that there has been a general loss of sensitivity in all counting channels and that the corrections applied to the calibration equations ( Appendix 4 ) did not account for the decay of the counting crystal. In this study, qualitative elemental comparisons are sufficient for interpretations to be made. However, the instrument requires a thorough recalibration as described by Myers ( 1987 ) and possibly the replacement of the detector crystal before further studies are carried out.

The gamma-ray values obtained at each control station do not correlate well with the neutron activation and x-ray fluorescence elemental analyses. Furthermore, the data taken from the two neutron activation analyses contain discrepancies, particularly in the U measurements ( Table A.4.4 ). The reasons for the difference between the two neutron activation runs are not certain. The same samples were used, the only difference being time of decay after irradiation which is taken into

Table 9.1 The uranium and thorium content of the nine control samples from Devon, Somerset and South Wales as determined by gamma-ray spectrometry ( GR ), neutron activation analysis ( NA ) and x-ray fluorescence ( XRF ).

Sample	U ( GR )	Th ( GR )	U ( NA )	Th ( NA )	U ( XRF )	Th ( XRF )
Wales 1	4.9	4.3	2.2	6.3	3	10
Wales 2	6.3	6.9	2.7	10.2	0	8
Wales 3	6.8	8.4	2.5	14.0	2	10
Somerset 1	4.6	5.5	5.4	6.9	3	11
Somerset 2	5.7	7.8	3.2	10.5	2	10
Somerset 3	5.7	7.8	2.2	10.0	2	11
Devon 1	3.3	5.4	2.3	3.0	3	11
Devon 2	4.4	11.6	2.6	14.0	2	11
Devon 3	2.5	8.8	1.8	8.1	0	0

account by the on line computer program. The accuracy of the spectrometric data can thus be questioned and its use in this study is reduced.

It can be seen from Table 9.1 that there is at least a relative correlation between the data sets. If two of the measurements are accepted as being anomalous ( Wales 1, U, gamma-ray and Devon 1, Th, neutron activation ) and are rejected, then the relative correlation is acceptable in terms of U and Th values although no quantitative figures can be assigned to the data.

The % K values derived from the gamma-ray measurements were calibrated with data from the x-ray fluorescence analyses and also roughly with estimates of illite content of the mudstones made on the basis of XRD and insoluble residue results. The results of this correlation are given in Table 9.2 . Again, the quantitative correlation is poor but qualitative statements can be made about the distribution of K in the Mercia Mudstone Group.

### 9.3.3 Potassium

The potassium values of the Mercia Mudstone Group samples measured by gamma-ray spectrometer range from 0.6 to 3.7% K , equivalent to 0.7 to 4.5%  $K_2O$  . This gives a range in the amount of illite in the mudstones of 10-58% , which is probably an underestimate of 5-10% , given the poor sensitivity of the gamma-ray spectrometer. Due to this, no other quantitative statements will be made concerning elemental abundances within the mudstones.

In general, the abundance of K in the mudstones closely follows variations in the proportion of illite in the clay fraction ( Table 9.2 ). Total illite in the rock can be calculated by multiplying the amount of illite in the clay fraction with the percentage of insoluble residue in the rock. This involves several assumptions:-

- 1) The non clay fraction of the insoluble residue is a constant component within the mudstones. The non-clay fraction is composed almost entirely of quartz which can be assumed to be a detrital mineral. No evidence of authigenic quartz has been found in SEM studies. As stated in Section 9.1.3 , no other major detrital phases have been found and the heavy minerals described by Al-Kattan ( 1976 ) are not volumetrically important, indeed most of the heavy minerals described by

Table 9.2 Correlation of the % illite as a fraction of the whole rock with % K<sub>2</sub>O as determined by gamma-ray spectrometry ( GR ) and x-ray fluorescence ( XRF ).

Sample	% illite	% K <sub>2</sub> O ( GR )	% K <sub>2</sub> O ( XRF )
Wales 3	54.2	2.07	5.2
Somerset 3	48.0	2.26	5.1
Devon 1	20.9	1.79	3.1
Devon 2	31.8	1.92	5.2
Devon 3	60.8	2.35	4.1

Al-Kattan were not identified in this study. The input of total detrital material into the basin is also assumed to have been constant throughout the Norian.

2) During removal of the soluble fraction of the mudstones using 10% HCl ( Appendix 5.2 ) the clay minerals were not attacked by the acid. Schultz ( 1964 ) used treatment with hot HCl to remove chlorite from a clay assemblage. The conditions required are far more extreme ( 6M HCl at 60°C for 16 hours ) than those used in this study. Several whole rock samples were analysed by XRD at standard operating conditions before and after digestion of the carbonate using HCl . There was no change in the relative intensity of the 002 chlorite peak after treatment, and so it is assumed that the chlorite was not attacked by the weaker HCl used.

The Blue Anchor Formation contains on average less K than the underlying red mudstones ( Fig. 9.7 ). This can be attributed to an increase in the total percentage of carbonate in the Blue Anchor Formation, since the illitic fraction of the clay assemblage is unchanged. The reduction in the amount of K in the Blue Anchor Formation can be seen in all three sections studied. The difference is least obvious in Somerset where, as has already been discussed, the lithological change at the Blue Anchor Formation boundary is less pronounced. In the Devon and Somerset sections, there is also a reduction in the total amount of K in the lower red mudstones which correlates with the increase in mixed-layer clays. As in the total gamma-ray count results, this transition takes place over 50 metres. In Devon this boundary is less pronounced since the mixed-layer clay in the assemblage is a smectite-illite which will contribute to the gamma-ray spectrum. The smectite-chlorite in the Somerset mudstones is not a gamma-ray source and so the change in both total count and K gamma-ray values is more marked.

The abundance of K in the mudstones is therefore a direct correlative of the amount of illite ( and the mixed layer smectite-illite ) in the rock. The relative differences in the K channel are less than those of the total count results. If K is the main control on total count variations, then the K channel itself might be expected to show relatively greater changes. The K window actually records a small part of the total K gamma-ray spectrum. If K is the most important source of gamma-rays, then the whole K spectrum, making up the majority of

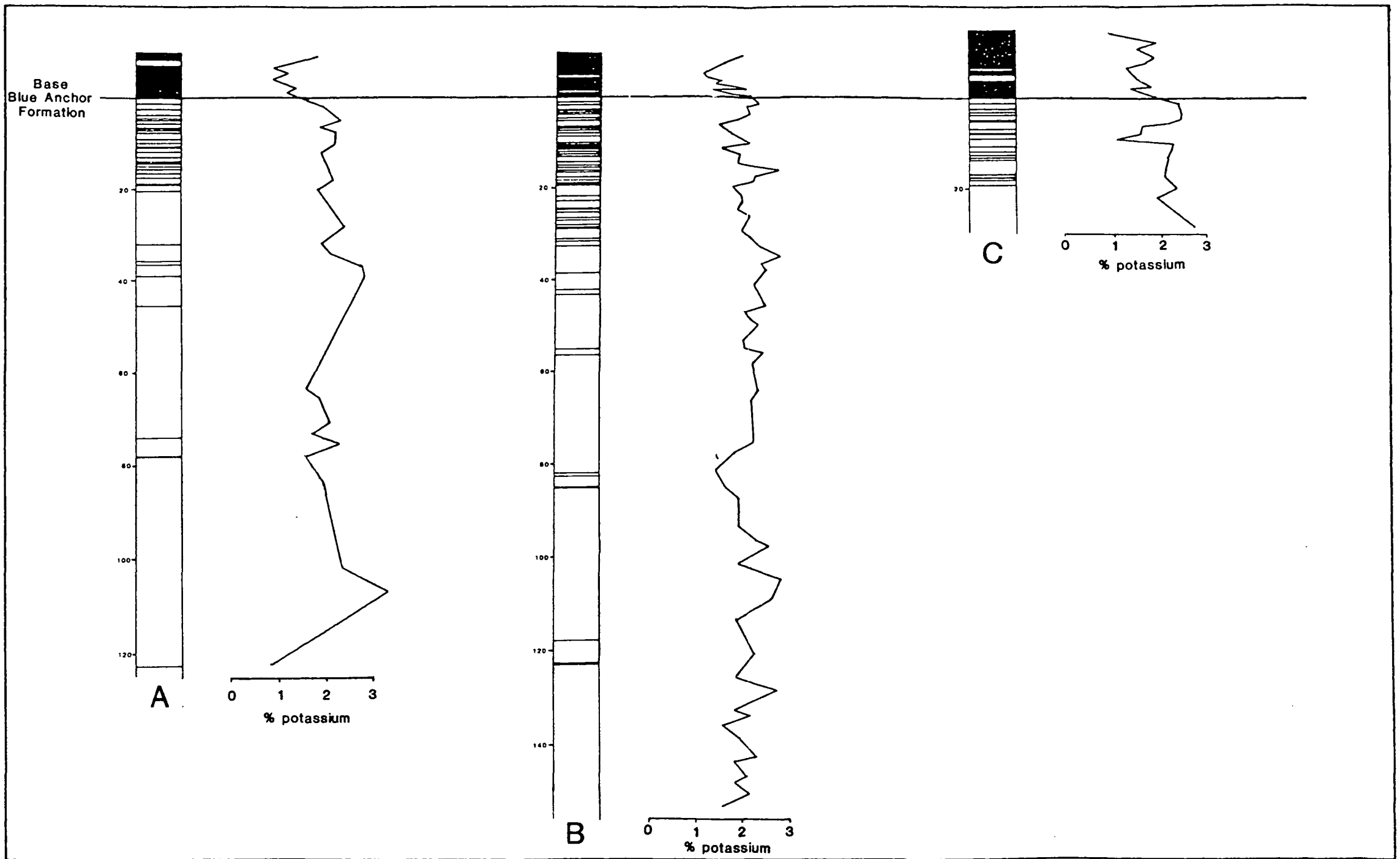


Fig. 9.7 Variations in potassium content of the Upper Mercia Mudstone Group from A - Seaton and Branscombe Cliffs, Devon. B - St. Audrie's Bay, Somerset. C - Penarth Cliffs, South Wales. The topmost 20 metres of the Blue Anchor Formation in the Somerset section are not shown.

the total count readings, will have as great an influence on total count variations as on the K channel. It is possible that the variations in the K channel have been suppressed by the processing, since it is known that the total K value has been reduced in the calculation.

#### 9.3.4 Uranium / Thorium

In this case the two elements will be considered together. Neither element is present as a major component in any of the common minerals in the Mercia Mudstone Group. Both were introduced into the depositional system in solution, adsorbed on to the charged surfaces of degraded clays or as detrital heavy minerals. The heavy mineral input has already been discussed and U and Th bearing minerals have not been detected. The detrital input for the purposes of this study is assumed to be constant and so variations in U and Th cannot be attributed to heavy mineral variations.

In all three areas the relative abundances of U and Th are less in the Blue Anchor Formation. This is the result of the increase in carbonate in the green beds and indicates that the elements are not contained predominantly within the carbonate fraction. The variation in U is less than that of Th, however, indicating that the more soluble  $U^{5+}$  ion may have been more available to enter the carbonate lattice than Th, which is more likely to have been transported adsorbed on to clay surfaces, ( Piler & Adams, 1962 ).

Within the red mudstones underlying the Blue Anchor Formation, U and Th are roughly covariant ( Fig. 9.8 ), indicating a similar origin for the two elements. In the upper red mudstones there is a very slight decrease in U and Th upwards. This is possibly due to an increase in total carbonate in the rock towards the Blue Anchor Formation. This decrease is best seen in Somerset where the amount of carbonate in the section increases gradually over 50 metres rather than showing a sharp change at the base of the Blue Anchor Formation. In the lower red mudstones in both Devon and Somerset, there is a subtle difference in the elemental distributions ( Fig. 9.8 ). 50 metres below the base of the Blue Anchor Formation in Devon and 70 metres below in Somerset, the relative abundances of both U and Th decrease. This distribution is most clearly seen in the Devon section,

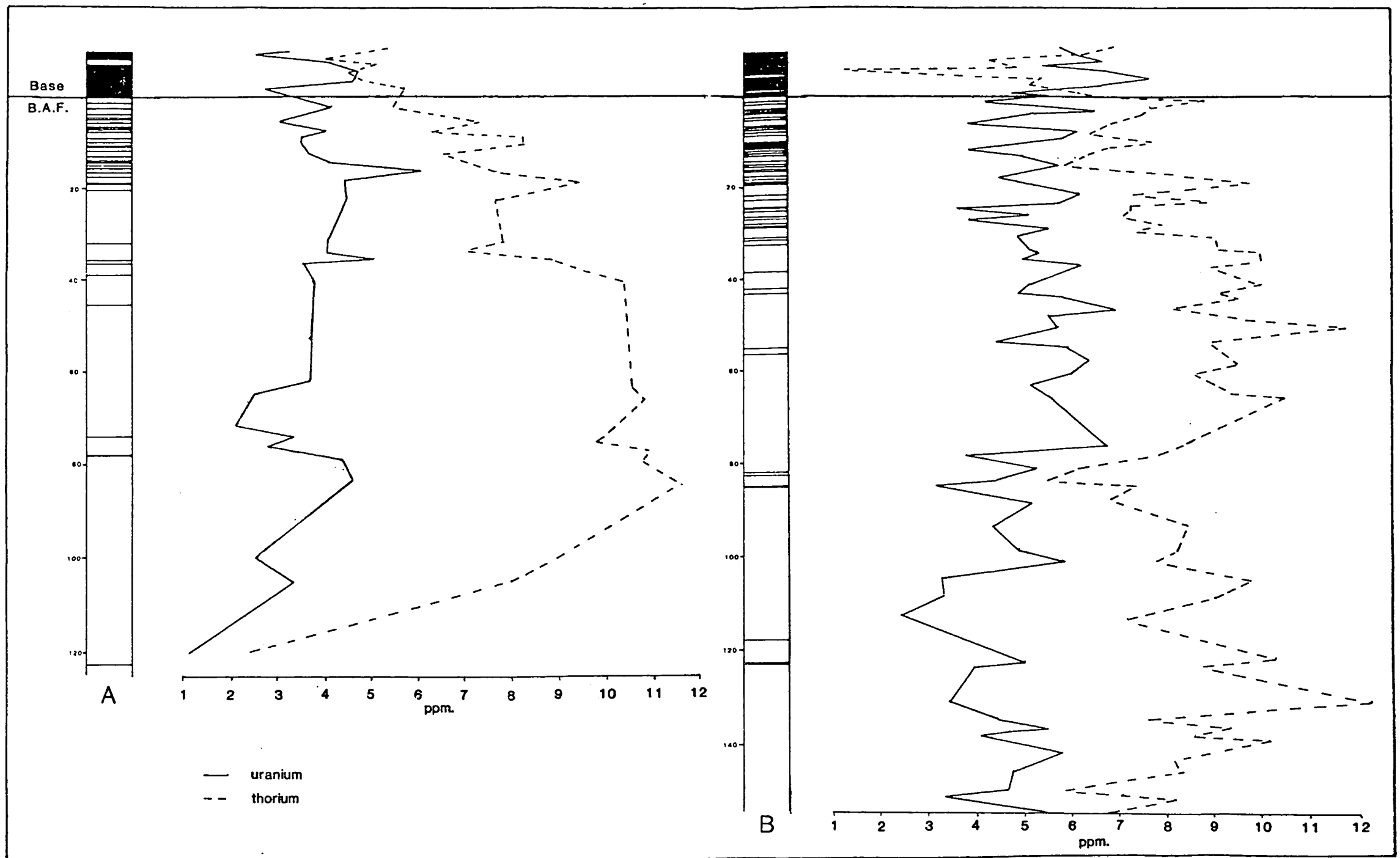


Fig. 9.8 Variation in the uranium and thorium content of the Upper Mercia Mudstone Group from A - Seaton and Branscombe Cliffs, Devon. B - St. Audrie's Bay, Somerset. The topmost 20 metres of the Blue Anchor Formation in the Somerset section are not shown.

where the transitional zone is present in the gap in outcrop between Seaton east and west Cliffs. There are a number of possible reasons for these variations:-

- 1) The environment of deposition and early diagenesis of the lower red mudstones was one in which less U was present. The clay mineralogy suite implies a relatively  $Mg^{2+}$  rich,  $K^+$  poor environment. These magnesian waters may have been less able to carry U in solution, leading to a preferential precipitation of U in proximal deposits. The Mercia Mudstone Group in the Devon succession is the most distal of the three areas of study and if significant this would have most effect on the Devon succession. The less soluble Th ions would not be affected to the same extent by a change in water chemistry.
- 2) The lower red mudstones may represent a more proximal environment in which the less soluble Th was deposited in the clastic fraction while U was carried into the more distal parts of the basin. A similar relationship has been described in the Cretaceous Mancos Shale in the central U.S.A. by Pfler & Adams ( 1962 ).
- 3) There was a change in source area for the detritus entering the basin, which altered the composition of the detrital fraction.

It is unlikely that the reduction of the U/Th ratio in the lower mudstones is the result of either a change in source area or variations in the proximal / distal relationship of the beds. The obviously more proximal South Wales succession contains high U/Th ratios similar to the upper parts of the Devon and Somerset sections. Also, during the Norian, there was little tectonic activity and changes in basin geometry or source area would not be expected to occur. The most likely cause of the difference in U/Th ratios is a change in the waters in which the mudstones were deposited. The waters responsible for the formation of mixed layer clays caused a reduction in the amount of U in the mudstones. Uranium is most effectively leached by alkaline oxidising solutions (Weigel, 1986 ). The formation of palygorskite and sepiolite also requires such conditions. It is likely that the authigenic and transformed clay minerals formed in waters in which precipitation of U was inhibited while the detritally influenced Th was unaffected.

It must be stressed that the differences in the U/Th ratio are very small and are at the limits of statistical significance ( Table 9.3 ).

#### 9.4 Conclusions

The application of gamma-ray spectrometry to sedimentary sequences is a technique of which the full potential has still to be recognised. In this study the most useful aspect of the gamma-ray survey has been the correlation of total count values with variations observed in boreholes. The topmost three subdivisions applied in boreholes to the Mercia Mudstone Group have been identified at outcrop, despite the fact that the lower boundary identified has no visible lithological expression. Using the gamma-ray survey it was possible to sample the mudstones on either side of the subtle boundary in order to define lithologically the reasons for the changes in gamma-ray value. The total gamma-ray count variations can be related to changes in the amount of illite in the mudstones. Similarly the amount of K is directly comparable with illite distribution. The variations in the amounts of U and Th in the mudstones appear to be related to the greater solubility of U , although both elements can be correlated with the amount of detritus entering the basin.

Table 9.3 Variation in the uranium and thorium content of the Upper Mercia Mudstone Group in Devon and Somerset. The figures are quoted plus or minus one standard deviation.

Table 9.3a U and Th variations, Seaton and Branscombe Cliffs, Devon.

Mercia Mudstone Group	U	Th
Blue Anchor Formation n=6	3.73±0.88	4.82±0.85
upper red mudstones n=16	4.11±0.71	8.64±1.39
lower red mudstones n=9	2.97±1.04	9.28±2.66

Table 9.3b U and Th variations, St. Audrie's Bay, Somerset.

Mercia Mudstone Group	U	Th
Blue Anchor Formation n=18	5.96±1.34	5.88±1.65
upper red mudstones n=37	5.22±0.80	8.34±1.35
lower red mudstones n=24	4.45±1.00	7.78±2.15

## **Chapter 10**

### **Geochemistry of the Mercia Mudstone Group**

## Chapter 10

### Geochemistry of the Mercia Mudstone Group

#### 10.1 Introduction

##### 10.1.1 Reasons for Analysis of the Carbonate Fraction

In mudstone sequences such as those in the Upper Triassic where sedimentary structures are rare geochemical analyses are of more importance in helping to describe depositional environments. The Mercia Mudstone Group contains very few obvious features visible at outcrop and so geochemical analyses have been used to provide information on the deposition and early diagenesis of the mudstones. For this reason the geochemistry of the carbonate fraction was analysed since it can be shown to be almost entirely authigenic in origin. Stable isotopic and trace elemental geochemistries have been widely used in sedimentology to provide information on the chemistry of the waters in which the carbonates precipitated and the depth at which formation of diagenetic phases took place. In the Triassic there have been relatively few geochemical studies. Taylor ( 1982, 1983 ) described the stable isotopic composition of the Upper Mercia Mudstone Group in Nottinghamshire, attributing the changes in  $\delta^{18}O$  to the influences of two different water bodies.

##### 10.1.2 Sampling

In almost all cases geochemical analyses were carried out on the carbonate fraction of the mudstones. This component of the rock is relatively easy to isolate using phosphoric or hydrochloric acid and provides information about the depositional and diagenetic solutions present during mudstone formation. Since the majority of the non-carbonate fraction is detrital in origin and composed of essentially the same elements, Si, Al, Fe, Mg, Ca and Mg, whole rock analysis would not provide any additional useful information. The nine samples used for calibration of gamma-ray data were analysed by XRF to provide information on

K, U and Th whole rock distributions. Other than this, whole rock geochemical analyses were not used in this study.

The samples collected for clay mineral analysis were also used for the geochemical studies. Details of the sample sites in the three areas of study are given in Section 8.1.1 .

### **10.1.3 Methods**

The methods of preparation for the two geochemical techniques are different and will be discussed separately. The basic concept of removing a part of the carbonate within the rock, either as a liquid or a gas, in order to analyse its chemistry is similar.

The reaction of carbonate with phosphoric acid and the collection of the CO<sub>2</sub> gas evolved are described in Appendix 2 . Since the CO<sub>2</sub> gas is the product which is analysed in stable isotope studies, reaction of the non carbonate fraction with the acid is not important.

Trace elemental analysis involves the digestion of the carbonate in dilute hydrochloric acid as described in Appendix 1 . In this case the solution of acid and dissolved cations is analysed, raising the possibility of contamination due to reaction of the acid with the non-carbonate fraction. Leaching of Fe and Mn ions by weak acetic acid solutions has been reported ( Boyle, 1981 ). In this study, however, there is no detectable relationship between the proportion of non-carbonate in the mudstones and trace elemental values ( Fig. 10.1 ).

## **10.2 Carbonate in the Mercia Mudstone Group**

### **10.2.1 Origin of the Carbonate**

The carbonate fraction ( dolomite and calcite ) in the Mercia Mudstone Group can be attributed to several sources:—

1) Detrital - in areas where the Palaeozoic basement contains carbonate the detrital input into the Mercia Mudstone Group could contain significant amounts

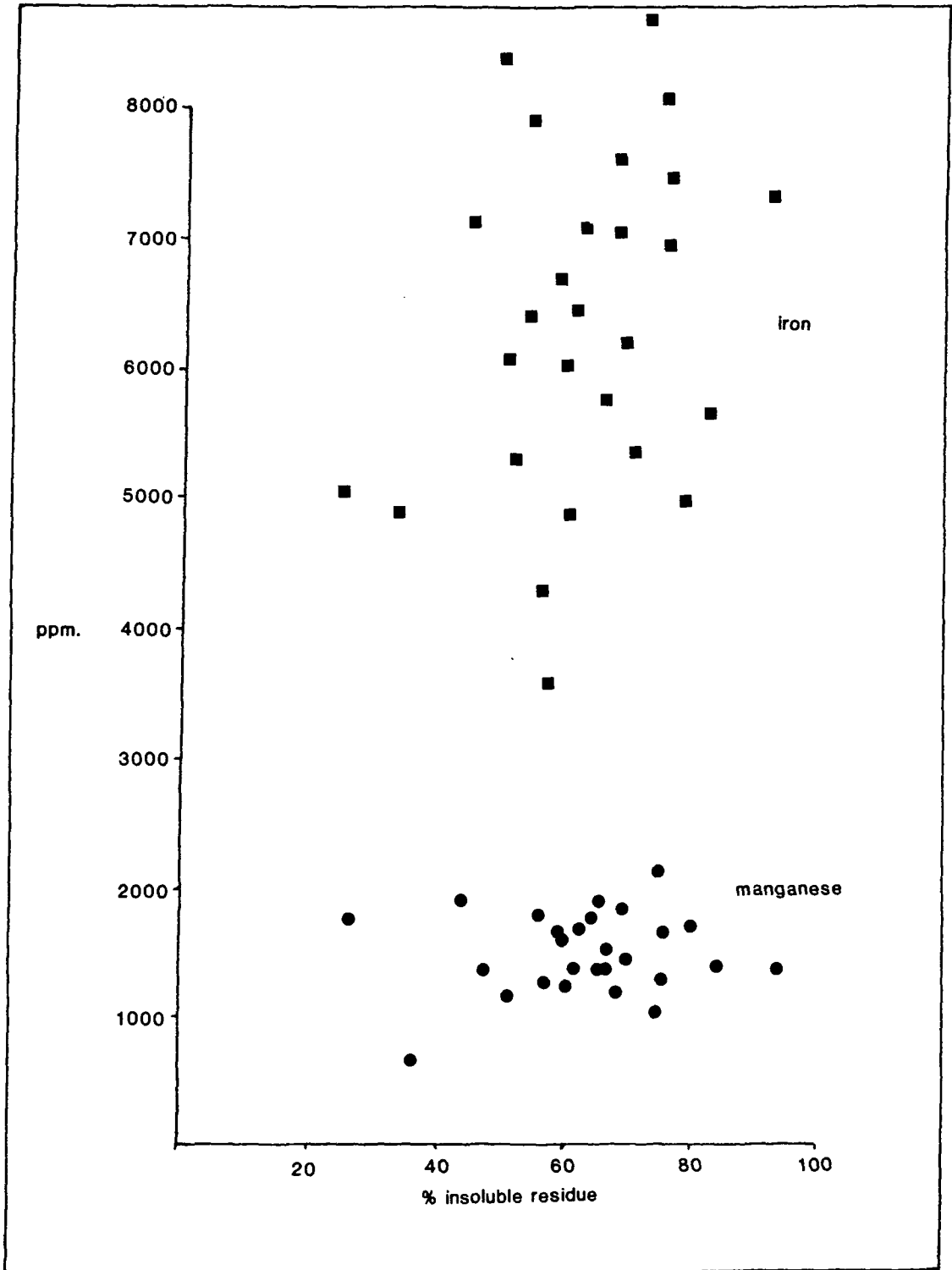


**Fig. 10.1** % insoluble residue plotted Fe ( squares ) and Mn ( circles ) in the carbonate fraction of the Mercia Mudstone Group in Devon.

of calcite or dolomite.

2) Syndepositional / Early Diagenetic - in an evaporitic playa-alluvial environment, precipitation of carbonates is a common occurrence. A number of carbonate phases can be precipitated initially. During early diagenesis ( often within the first few metres of burial ) these carbonates will recrystallise to the more stable forms of dolomite and calcite.

3) Deep ( Burial ) Diagenetic - recrystallisation of carbonates during deep burial and further carbonate precipitation in any pore space is common in most sedimentary rocks. Burial dolomitisation in particular is common.

In both South Wales and Somerset, carbonates of the Carboniferous Limestone Series were exposed and were being eroded during the Norian ( Fig. 10.2 ). In South Wales the basement topography is complex and the input of carbonate detritus into the relatively proximal Penarth Cliffs section is likely. However the range of lithologies within the Carboniferous Limestone ( Waters & Lawrence, 1987 ) precludes any attempt to ascribe a particular geochemical value to the detrital carbonate input. In Somerset the carbonates of the Mendip Hills are at a greater distance from the section at St. Audrie's Bay. The Mendips lie on the north side of the Central Somerset Basin and are less likely to contribute detritus to marginal beds to the south of the main basin axis. Current directions in the dolomitic beds within the Mercia Mudstone Group in Somerset indicate transport from the south and southwest, where the basement is composed of Devonian clastics ( Fig. 10.2 ). The clastic carbonate input into the Mercia Mudstone Group in Somerset during the Norian will therefore be less than that in South Wales, although this does not preclude any clastic input from the northeast. In Devon the most proximal basement lies to the west and is composed of Devonian siliciclastics. The input of clastic carbonate into the Mercia Mudstone Group at Seaton Cliffs will have been minimal.

The majority of the carbonate in the Mercia Mudstone Group formed in a depositional or early diagenetic environment. Precipitation from the evaporitically enriched waters took place in the topmost few metres of mudstone, as coatings on clastic grains and within cavities. SEM examination of the mudstones has

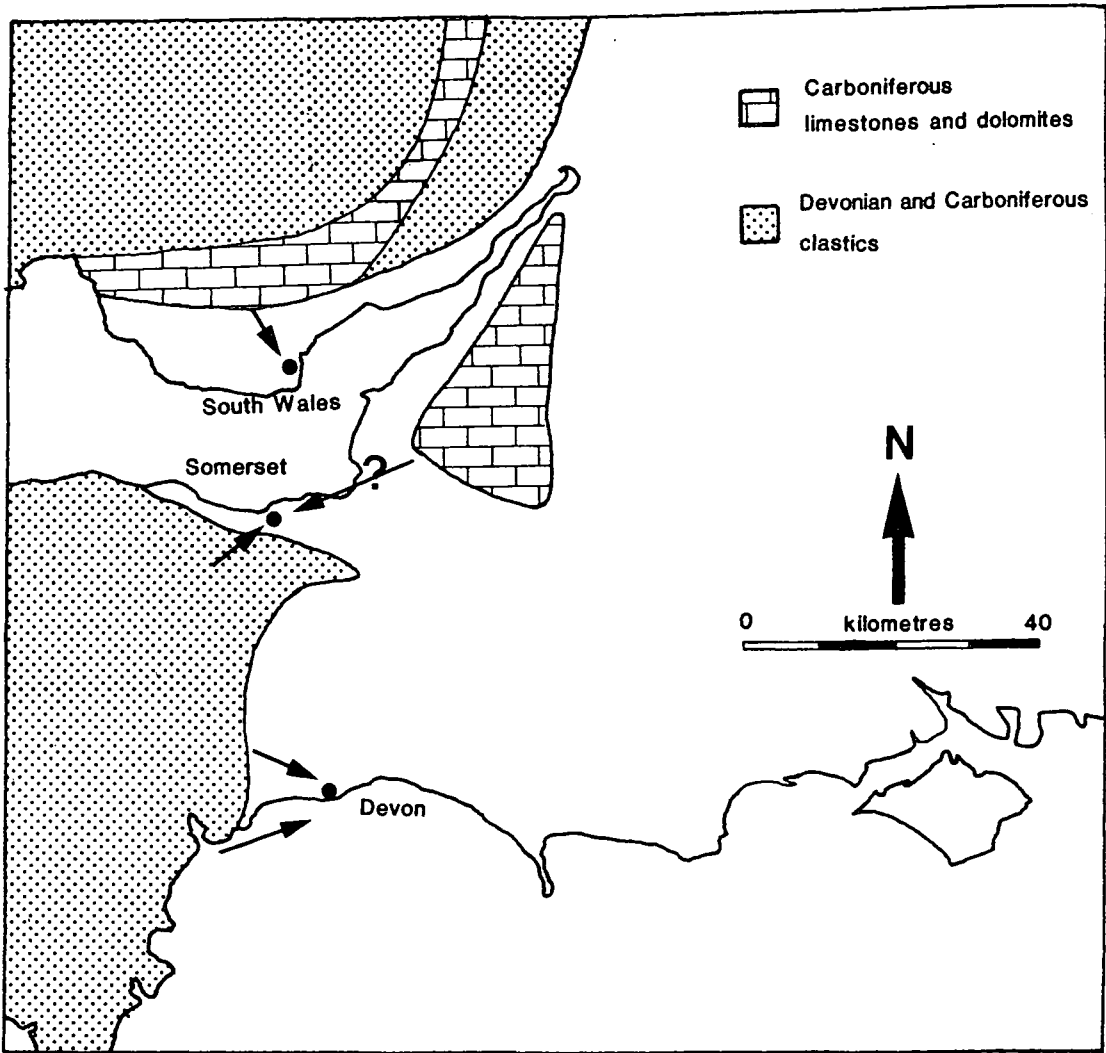


**Fig. 10.2** Map of Southwest Britain showing the location and lithologies of the Palaeozoic basement as sources of clastic material for the Upper Mercia Mudstone Group.

revealed few well developed carbonate crystals ( Fig. 10.3 ). EDAX analysis of most detrital grains indicates the presence of carbonate as a coating around clasts.

There is no evidence for the crystallisation of a late diagenetic carbonate such as baroque or saddle dolomite. The formation of a stable, ordered carbonate assemblage can take place during early diagenesis ( Rosen et al., 1988 ), in the presence of effectively depositional waters. The dolomitic beds present in the red mudstones in Somerset and throughout the Blue Anchor Formation are more porous and might be expected to be affected by later diagenetic events ( Mayall, 1981 ). However the texture of the dolomite within these beds does not suggest late recrystallisation and some microbial fabrics and cross lamination are preserved ( Section 7.2 ). There is no evidence, therefore, for late diagenetic recrystallisation in the dolomitic beds.

### 10.2.2 Dolomite - Calcite Cogenesis

The carbonate fraction in many of the mudstones contains both dolomite and calcite, ( Fig. 10.4 ). In general, the Blue Anchor Formation contains only dolomite whereas the red mudstones can have a mixture of both carbonates. There is a complete range in the proportion of the carbonates from 0-100% dolomite, although rocks containing over 50% calcite are rare.

It is probable that the carbonates formed during early diagenesis ( Section 10.2.1 ). Whether both dolomite and calcite can form at the same time and in equilibrium has been the subject of some discussion, ( Degens & Epstein, 1964; Veizer & Hoefs, 1976; Anderson & Arthur, 1983 and others ). The subject was reviewed by Land ( 1980 ), who concluded that in terms of isotopic composition of dolomite-calcite pairs precipitated in equilibrium, no one model could be universally applied, although there was likely to be some enrichment in  $^{18}\text{O}$  in dolomite relative to calcite. In this study there is insufficient petrographic information to allow the separation of the carbonate into two phases. It is probable that dolomite and calcite both stabilised in essentially depositional waters.

Assuming that the two carbonate phases formed in the same hydrochemical environment, then an estimate of the enrichment of  $^{18}\text{O}$  in dolomite relative to calcite

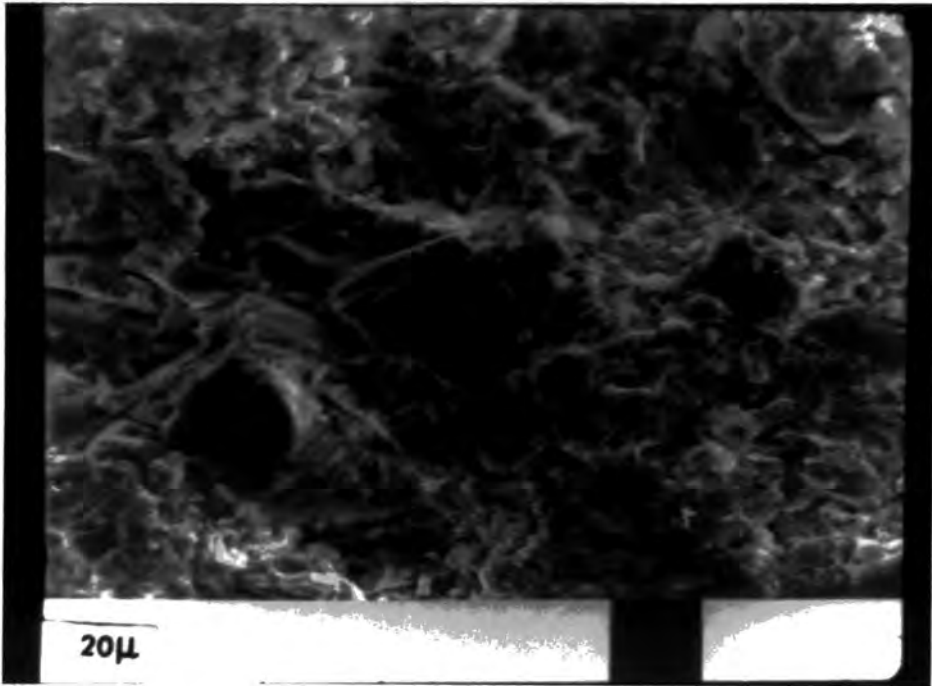


**Fig. 10.3** SEM photograph of carbonate in the upper red mudstones in Somerset showing rhombic dolomite crystals. The majority of carbonate in the Mercia Mudstone Group occurs as coatings around clay and quartz.

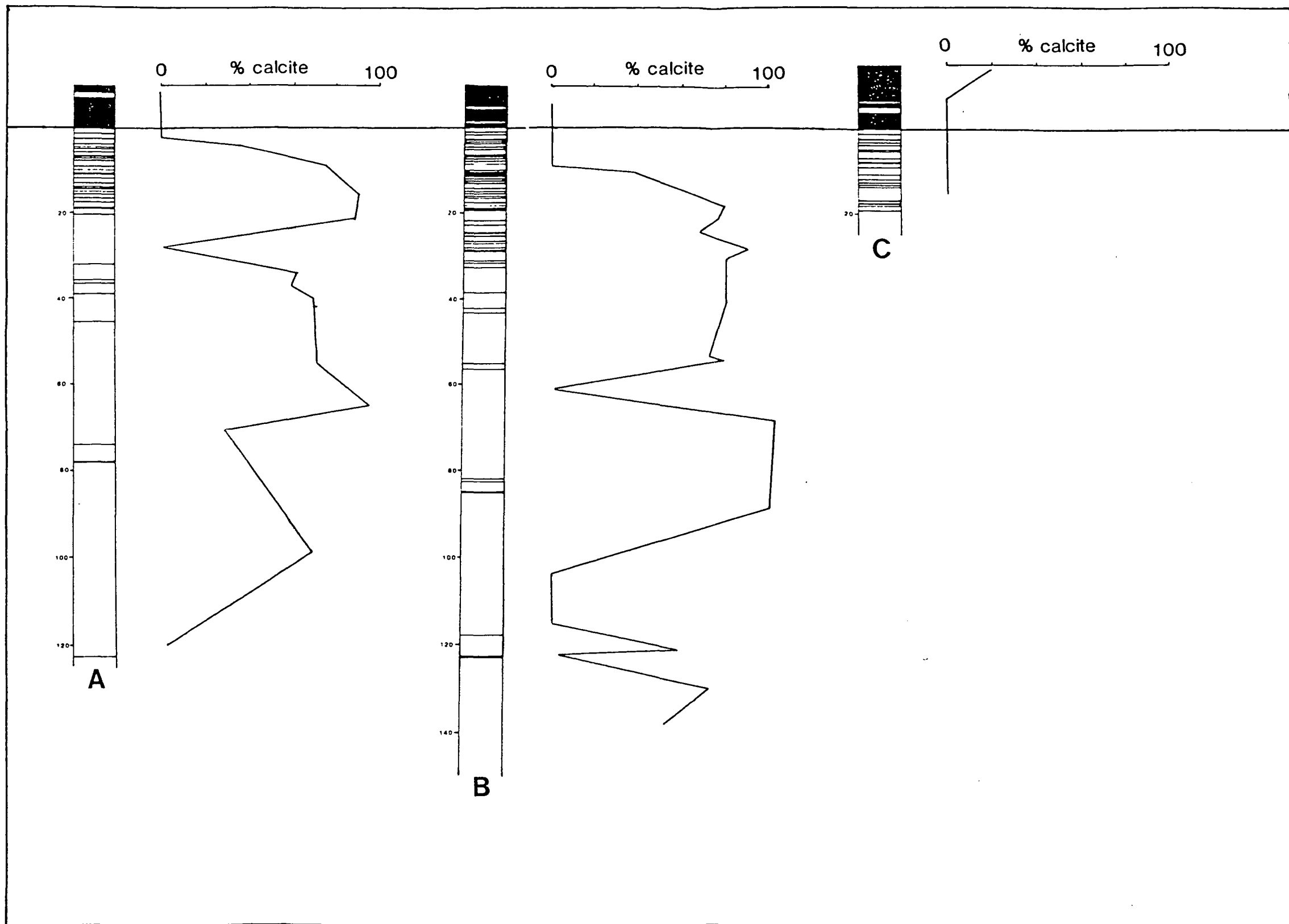


Fig. 10.4 Dolomite - calcite ratios in the Mercia Mudstone Group. A - Seaton and Branscombe Cliffs, Devon. B - St. Audrie's Bay, Somerset. C - Penarth Cliffs, South Wales.

can be made. Land ( 1980 ) quotes values ranging from +1.0 to +7.0‰ . The 1.0‰ value assumes no difference in fractionation factor, the enrichment being the result of fractionation during reaction with the acid. The  $\delta^{18}O$  values plotted against dolomite / calcite ratios do not reveal any significant trend ( Fig. 10.5 ). If samples containing over 90% and under 10% dolomite are plotted, representing near end member values, then a significant difference is found ( Table 10.1 ). This figure indicates an enrichment in  $^{18}O$  of +2.8‰ in dolomite relative to calcite, which lies within the range given by Land ( 1980 ). Given this fractionation factor, a correction can be applied to the mixed dolomite-calcite samples. The isotopic values are corrected to a 100% dolomite value to enable comparisons with the data presented by Taylor ( 1982 ), who analysed dolomitic Mercia Mudstone Group samples from Nottinghamshire.

The distribution of dolomite and calcite in the Mercia Mudstone Group suggests that the variations may be the result of sedimentological factors. It is possible that changes in water chemistry gave rise to changes both in isotopic composition and in the dolomite-calcite ratio. Thus the enrichment of +2.8‰ in the dolomites may be a result of changes in actual water chemistry, not simply a fractionation. For this reason, the stable isotopic results plotted in Figs. 10.5-10.6 and 10.8 contain both the original and the corrected  $\delta^{18}O$  results.

Similarly, for  $\delta^{13}C$  , different fractionation factors have been quoted for dolomite and calcite. Sheppard & Schwarcz ( 1970 ) extrapolated high temperature results to predict a 2‰ enrichment in  $\delta^{13}C$  in dolomite relative to cogenetic calcite. The  $\delta^{13}C$  of samples containing over 90% dolomite or calcite were averaged but in this case no conclusions could be drawn from the results ( Table 10.2 ). Although a fractionation factor of +0.9‰ can be inferred for dolomite, the range of values is such that the results are not significant. A far greater number of samples than was feasible in this study would be required to derive a reliable  $\delta^{13}C$  fractionation factor for dolomite. The  $\delta^{13}C$  in this study are quoted in their original form.

For trace elements an average composition for dolomite and calcite has been published in Veizer ( 1983 ). The technical problems of synthesising ordered dolomite at low temperatures are such that reliable partition coefficients for dolomite relative to calcite have not been published. The structural and geo-

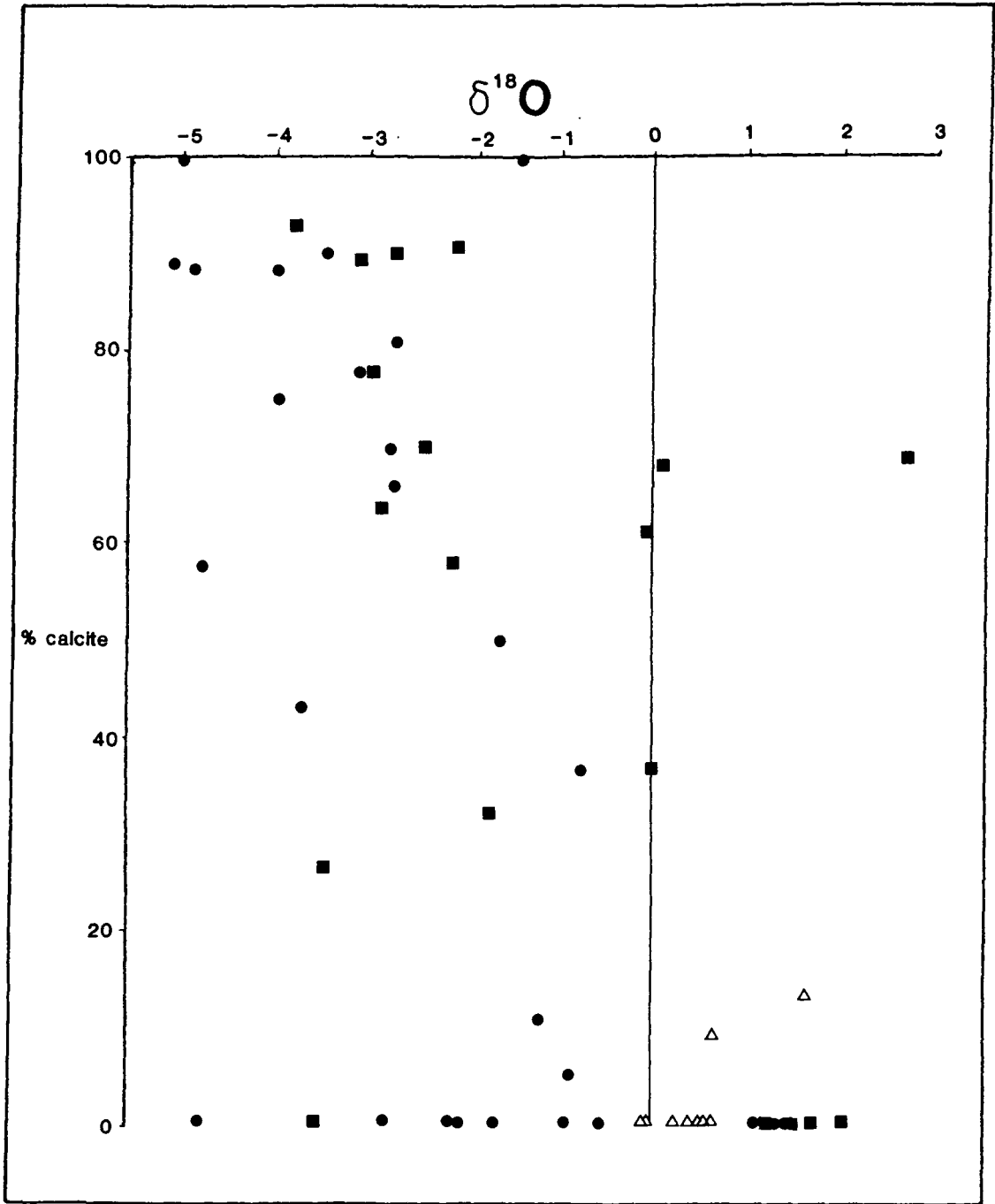


**Fig. 10.5** Relationship between dolomite - calcite ratio and  $\delta^{18}O$  composition in the Mercia Mudstone Group. Squares - Seaton and Branscombe Cliffs, Devon. Circles - St. Audrie's Bay, Somerset. Triangles - Penarth Cliffs, South Wales.

Table 10.1 Average  $\delta^{18}O$  composition of dolomitic and calcitic samples from the Mercia Mudstone Group. Errors quoted are plus and minus one standard deviation.

Mineralogy	Average $^{18}O$
dolomite n=24	-0.10±1.76
calcite n=6	-3.1±1.23

Table 10.2 Average  $\delta^{13}C$  composition of dolomitic and calcitic samples from the Mercia Mudstone Group. Errors quoted are plus and minus one standard deviation.

Mineralogy	Average $^{13}C$
dolomite n=24	0.62±1.20
calcite n=6	-0.62±2.07

chemical variability of dolomite further complicates the interpretation of trace elemental analyses. The data quoted in Veizer ( 1983 ) for marine carbonates does not specify cogenetic precipitation, and is therefore not of use in this study. Hird ( 1985 ) derived partition coefficients for Mn and Sr for dolomites of various types. His samples are diagenetic dolomites which are not in equilibrium with the calcite being replaced, and are not comparable with the dolomite calcite pairs formed cogenetically in the Mercia Mudstone Group.

The technique of separating dolomite and calcite phases in order to carry out separate geochemical analyses has been used widely ( see Fairchild et al., 1988, page 330 for refs. ). The carbonate phases can be separated using heavy liquids and then analysed individually. This method requires a reasonable crystal size and in this study most carbonate exists as detrital grain coatings, thus making separation of dolomite and calcite on the basis of density differences impossible. In stable isotopic analyses, separation on the basis of different reaction rates has been carried out in stable isotopic studies where the first  $\text{CO}_2$  evolved is assumed to be derived from the more reactive calcite, while later gas production is attributed to dolomite reaction. This technique was not employed in this study for the following reasons:

- 1) Both dolomite and calcite are fine grained and as such the difference in rate of reaction will be small, particularly if the carbonate is present as coatings around detrital grains with a large surface area.
- 2) The dolomites in the Mercia Mudstone Group contain 52-56%  $\text{Ca CO}_3$  . Calcian dolomites are less stable during reaction with acid, reducing the difference in reaction time between dolomite and calcite.

### **10.3 Stable Isotopic Analysis, Results**

#### **10.3.1 Introduction and Previous Work**

In total, 54 stable isotopic analyses were carried out on the Mercia Mudstone Group. Samples were collected from the Blue Anchor Formation and the underlying mudstones. In order to detect changes in stable isotopic composition

on a scale of tens of metres without interference from lithological variations, red mudstones were preferentially analysed, although in practice all lithologies were sampled. Due to the small number of analyses which could be carried out in the laboratory time available, samples were widely spaced in the vertical sections, occurring every 5 metres on average in Devon and Somerset. In South Wales samples were spaced every 2.5 metres apart. This limited the number of samples of different lithologies which could be analysed and these were collected only in the Somerset section. In almost all cases marls associated with sulphates were not sampled, to avoid the analysis of carbonates with different isotopic composition as a result of more intense evaporative effects which might obscure the larger scale variations.

Only one study of the stable isotopic composition of the Mercia Mudstone Group has been carried out ( Taylor, 1982, 1983 ). In this, changes in clay mineralogy and in stable isotopic composition of the carbonates were attributed to variations in the composition of the depositional waters. Triassic stable isotopic values have been published as part of larger studies of secular variations through the Phanerozoic ( Pilot et al., 1972; Veizer & Hoefs, 1976 ) but these are on too large a scale to be of use in studies of the Norian within the Upper Triassic, and they are primarily concerned with variations in normal marine trends, not relevant to this study.

### 10.3.2 Stable Isotopic Results, Devon

Seventeen samples from the Devon succession were analysed, two from the Blue Anchor Formation and fifteen from the underlying red mudstones in Seaton and Branscombe Cliffs. In Devon, red sulphate-free mudstones were analysed below the Blue Anchor Formation with the exception of the lowest sample which contained gypsum. This sought to avoid geochemical changes as a result of lithological variations. The carbonates analysed were therefore precipitated in the same depositional-early diagenetic environment.

The vertical variations in  $^{18}\text{O}$  and  $^{13}\text{C}$  are shown in Fig. 10.6 . Oxygen and carbon are not closely covariant. Carbon shows a constant trend of enrichment from  $-2.0\text{‰}$  at the base of the section to  $+1.5\text{‰}$  in the lower Blue Anchor

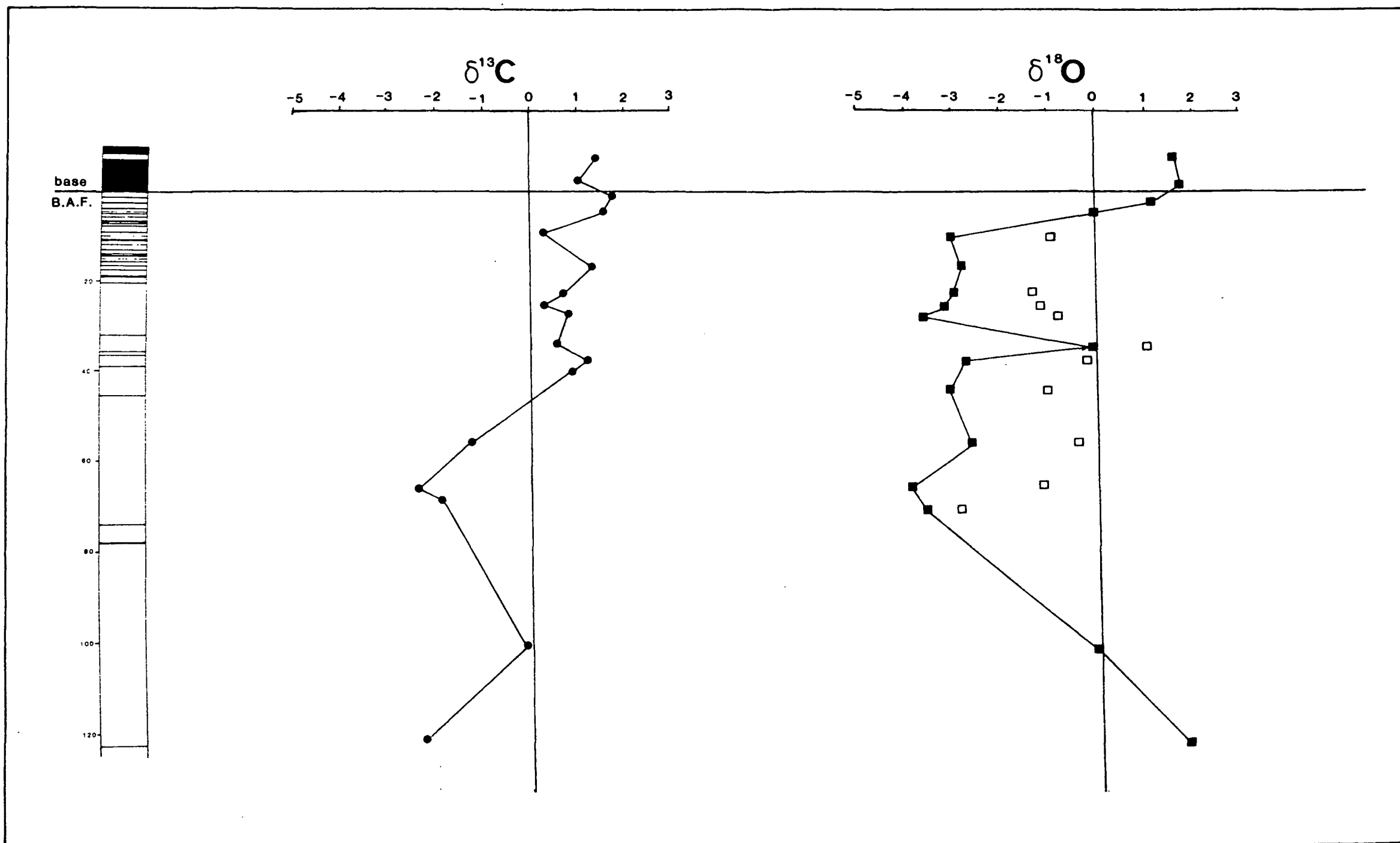


Fig. 10.6  $^{13}\text{C}$  and  $^{18}\text{O}$  variations in the Mercia Mudstone Group. Seaton and Branscombe Cliffs, Devon. Circles -  $\delta^{13}\text{C}$ . Squares -  $\delta^{18}\text{O}$ . Open squares - corrected  $\delta^{18}\text{O}$  for 100% dolomite.

Formation. Oxygen displays a more complex pattern which can be related to a number of influences. The  $\delta^{13}C$  variations can be related to a number of factors:-

- 1) A decrease in the influence of organic CO<sub>2</sub> in the mudstones upwards in the succession. This could be caused by an change in the rate of production of organic material or a variation in the rate of burial of the sediments.
- 2) A reduction in soil CO<sub>2</sub> influence, or less intense calcretisation in the upper mudstones ( Allen & Matthews, 1982 ).
- 3) A secular trend in  $\delta^{13}C$  values worldwide which has an expression in the waters forming the carbonates in the Mercia Mudstone Group.
- 4) The influence of a mixing zone of two water types of different composition in which a more <sup>13</sup>C rich marine water becomes more influential upwards in the succession ( Hudson, 1977 ).

An upward decrease in the amount of organic material in the Devon Mercia Mudstone Group is not a likely cause of  $\delta^{13}C$  variations. The Blue Anchor Formation contains a sparse fauna of micro and macrofossils ( Warrington, 1976 ) and the red mudstones contain no evidence of biological activity. The influence of calcretisation and soil CO<sub>2</sub> on the  $\delta^{13}C$  composition of the mudstones is difficult to estimate. The homogenous mudstones contain very little obvious evidence of calcretisation. Pedogenic processes have been used to account for the lack of structure in the mudstones and are likely to have played a part in the formation of the Mercia Mudstone Group . Vertical variations in the effects of calcretisation however cannot be estimated due to lack of evidence at outcrop.

A gradual change in the chemistry of the waters precipitating the carbonate is the most likely reason for the variations in  $\delta^{13}C$  . Evidence for changes in the chemistry of the depositional waters has already been presented in Chapter 8 . These changes involve a gradual reduction in the amount of Mg<sup>2+</sup> in the waters, representing a progressive change from waters of a mixed marine / continental origin to those of a predominantly continental-derived composition in the upper

red mudstones before deposition of the Blue Anchor Formation . Secular trends in  $\delta^{13}C$  have not been described for the Triassic in detail, although between the Permian and Jurassic there is a progressive depletion in  $^{13}C$  ( Veizer & Hoefs, 1976 ). Their average value for Triassic dolomite,  $\delta^{13}C +3.0\text{‰}$  , is derived from replaced marine carbonates which are not relevant to this study. In the continental 'Keuper' of Southeast Spain, beds of Carnian age have a  $\delta^{13}C$  value of between  $+2.0$  and  $+4.0\text{‰}$  ( M. Tucker, pers comm. ). These beds are of more importance although they are most likely derived from evaporative marine-derived waters. None of the carbonates analysed in this study were precipitated from purely marine waters. Any secular trend in marine waters has been obscured by the effects of the mixing of two water types, both of which are evaporative.

The pattern of oxygen isotope variations is more complex than that of carbon, ( Fig. 10.6 ). Correction for fractionation between dolomite and calcite has reduced the intensity of the variations in the  $\delta^{18}O$  values but has not removed any of the trends. The majority of the mudstones are relatively depleted in  $^{18}O$  (  $-1.0$  to  $-3.0\text{‰}$  ) while the lowest red mudstones and the beds approaching the Blue Anchor Formation are more enriched. There are three main factors which can influence  $\delta^{18}O$  in an environment such as that in which the Mercia Mudstone Group formed:—

- 1) The temperature at which the carbonate was precipitated.
- 2) The intensity of evaporation of the waters from which carbonate formed.
- 3) The original stable isotopic composition of the waters entering the basin.

Beds of nodular sulphate, or their dissolution residues, are found throughout the red mudstones and lower Blue Anchor Formation. There is no direct evidence for the presence of major beds of halite although some dissolution casts of individual crystals occur on bedding planes. The presence of sulphate is evidence for continuous relatively intense evaporative effects and therefore a constant oxygen isotopic enrichment throughout the period of study is likely. In the Devon section, to avoid any locally intense evaporitic enrichments, mudstones associated with sulphates were not sampled.

Thus the most important influence in the  $\delta^{18}\text{O}$  composition of the carbonate in the mudstones is likely to be the chemical composition of the waters entering the basin. On this basis, Taylor ( 1982, 1983 ) was able to subdivide the Nottinghamshire Mercia Mudstone Group into two units below the Blue Anchor Formation using changes in stable isotopic composition. He followed these changes from basinal areas in the Cheshire Graben onto reduced sequences deposited on uplifted fault blocks to the east. In Devon similar variation in stable isotopic composition is observed and is accompanied by a change in clay mineralogy which suggests variations in both the isotopic and cation chemistry of the depositional waters.

In the Devon succession the lowest samples analysed, from Branscombe Cliffs, are enriched in  $^{18}\text{O}$  relative to the overlying red mudstones from Seaton Cliffs which with one exception lie between  $-2.0$  and  $-4.0\text{‰}$  ( Fig. 10.5 ). These are depleted values considering the known evaporative effects which occurred during deposition, and indicate an initially depleted water source. In the Blue Anchor Formation there is a relative enrichment in the  $\delta^{18}\text{O}$  values, indicating the incoming of more enriched waters in the latest Norian.

One sample which lies 33 metres below the base of the Blue Anchor Formation has an anomalous  $\delta^{18}\text{O}$  value. This sample has a  $\delta^{18}\text{O}$  of  $-0.0\text{‰}$ , more enriched than the surrounding values. There is no lithological evidence to indicate the reason for the change in chemical composition. However, this does not preclude the original presence of evaporites within the mudstones. Surficial halite deposits are markedly unstable and their preservation potential is very low ( Kendall & Warren, 1988 ). It is possible that intensive evaporation of a temporary body of standing water took place accompanied by the precipitation of halite, the evidence for which has now been removed. This would give rise to anomalously enriched  $^{18}\text{O}$  values in a mudstone containing no other evidence for a change in depositional ( or early diagenetic ) environment. This event would give rise to a small excursion in the stable isotopic pattern. An incursion of marine waters into the basin would be likely to cause variations on a larger scale, affecting a greater thickness of mudstones.

Thus variations in  $^{18}\text{O}$  in the Mercia Mudstone Group in Devon can be attributed

to the mixing of two water bodies of different chemical composition. In the lowest beds sampled and in the Blue Anchor Formation, the carbonate is enriched in  $^{18}\text{O}$ , indicating a water of more marine composition, while the majority of red mudstone samples formed in waters relatively depleted in  $^{18}\text{O}$ .

### 10.3.3 Stable Isotopic Results, Somerset

#### 10.3.3.a General Trends

Twenty seven samples from St. Audrie's Bay on the North Somerset coast were analysed for stable isotopic composition. The sampling method in Somerset was different from that in Devon. As well as sampling the Blue Anchor Formation and underlying red mudstones, various lithologies within the mudstones were sampled specifically in order to find any geochemical differences between the different rock types. These differences will be discussed in Section 10.3.3.b.

In Somerset the pattern of stable isotopic variations within the red mudstones is roughly similar to that in Devon ( Fig. 10.7 ). The majority of  $\delta^{13}\text{C}$  values show an increasing trend of enrichment upwards in the Mercia Mudstone Group. As in Devon this can be attributed to changes in water chemistry during deposition. This general pattern is disrupted by three excursions in which the  $^{13}\text{C}$  values are more depleted. One of these, towards the top of the Blue Anchor Formation, has possibly been affected by waters from the overlying Rhaetian shales, and may not represent early diagenetic reactions. This excursion, which includes the most depleted  $^{13}\text{C}$  value, will therefore not be discussed. The other excursions occur within the red mudstones and are therefore not likely to have been affected by later diagenetic solutions. If they represent a depositional or early diagenetic effect, the most likely cause of the depletion in  $^{13}\text{C}$  is an increase in the effects of soil  $\text{CO}_2$ . Calcretes within the Mercia Mudstone Group have been described but they are subtle structures and their identification is often difficult ( Wright et al., 1988a ). The calcretes described from Watchet in Somerset ( Section 7.2 ) have  $\delta^{13}\text{C}$  values between 0.0 and  $-1.8\text{‰}$ . Similarly the calcrete related structures in Branscombe Cliffs have a value of  $-2.3\text{‰}$ . These are more depleted than the majority of the mudstone samples and suggest that calcretisation does have an effect on  $\delta^{13}\text{C}$  values. The lack of calcrete structures within the mudstones is

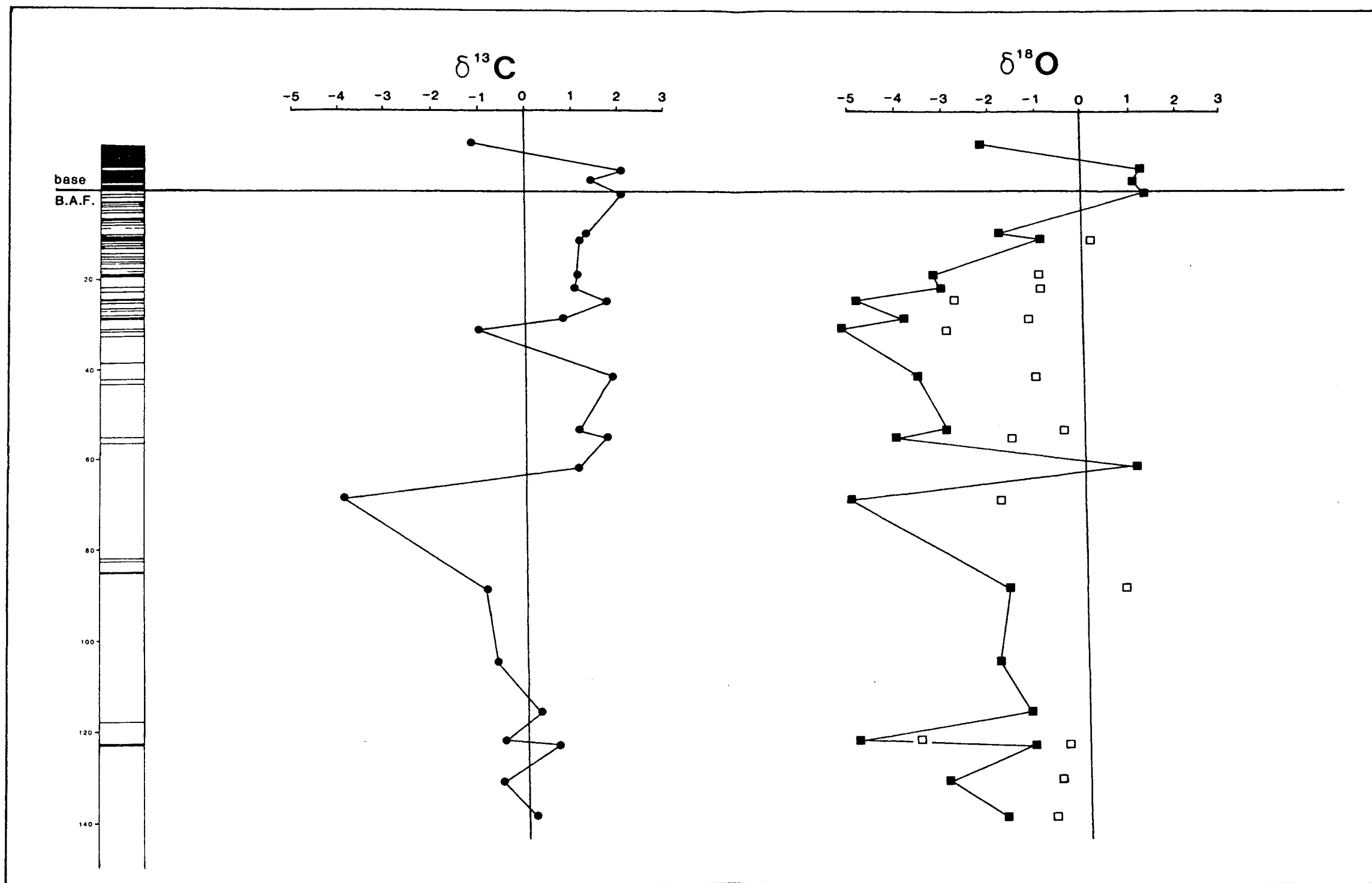


Fig. 10.7  $^{13}\text{C}$  and  $^{18}\text{O}$  variations in the Mercia Mudstone Group, St. Audric's Bay, Somerset.  
 Circles -  $\delta^{13}\text{C}$  . Squares -  $\delta^{18}\text{O}$  . Open squares - corrected  $\delta^{18}\text{O}$  for 100% dolomite.

not proof that no calcretisation occurred. Pedogenetic processes have been cited as one of the reasons for the lack of structure in the mudstones ( Wills, 1970 and others ).

The oxygen isotope variations in the St. Audrie's Bay section are similar to those in Devon ( Fig. 10.7 ). The lowest red mudstones sampled and those immediately below the Blue Anchor Formation are enriched in  $^{18}\text{O}$  relative to the central section of red mudstones. In Somerset the trend towards more enriched  $^{18}\text{O}$  values in the Blue Anchor Formation is a progressive one which commences some 25 metres below the base of the green beds. It has already been noted that the lithological transition at the base of the Blue Anchor Formation in Somerset is not abrupt. The trend towards more enriched values commences at the same time as green dolomitic beds appear within the red mudstones. In Devon, both the lithological and stable isotopic changes are more abrupt, although the magnitude of the change is similar in both areas (  $+4.0\text{‰}$  ). The enrichment of  $^{18}\text{O}$  towards the base of the section in Somerset is not as pronounced as in Devon. In the red mudstones there is a difference between the upper samples which lie between  $-2.5$  and  $-5.0\text{‰}$  and the lower mudstones,  $-0.5$  and  $-2.8\text{‰}$  . This indicates the input of a more  $^{18}\text{O}$  enriched water type in the lower mudstones, although less so than in Devon.

As in Devon, one red mudstone sample is anomalously enriched in  $^{18}\text{O}$  ( Fig. 10.7 ). This sample occurs in a part of the section devoid of any sedimentary structures. There is no evidence for the original presence of evaporites. The magnitude of the enrichment suggests the possibility of a spurious result, but it is probable that this sample represents a period of more intense evaporation of a standing body of water, as in the sample from Devon. The enriched sample occurs 61 metres below the base of the Blue Anchor Formation in Somerset, whereas in Devon the excursion lies 33 metres below the green mudstones. The events are not related and are more likely to be the result of local variations in runoff which gave rise to temporary bodies of standing water and a local enrichment in the  $\delta^{18}\text{O}$  of the carbonates precipitated. Both samples contain 100% dolomite in the carbonate fraction, which has contributed to the apparent extremity of the excursions. However in the corrected values both excursions are still significantly enriched in  $^{18}\text{O}$  .

### 10.3.3.b Lithological Variations

As well as analysing the Somerset section in terms of large scale trends in the data, different lithologies in the mudstones were sampled to see if there was a relationship between stable isotopic composition and rock type. The stable isotopic values for the different lithologies present are plotted in Fig. 10.8 , which includes some data which were not included in the vertical section. In this diagram, the uncorrected  $\delta^{18}O$  values have been used in order to clarify trends in the data. On the basis of the stable isotopic values the green dolomitic beds within the red mudstones can be differentiated and several trends in the data are present. The green dolomites are the most depleted in  $\delta^{18}O$  composition whereas beds of similar lithologies in the Blue Anchor Formation are more enriched than the majority of the red mudstones. The red mudstones themselves show two trends. The first involves a covariance of  $^{13}C$  and  $^{18}O$  . Samples from the Blue Anchor Formation and the lowest red mudstones form the enriched end member, while the samples most depleted in  $^{18}O$  and  $^{13}C$  occur in the centre of the section. This covariant trend is evidence of the mixing of the two water types ( Hudson, 1977 ).

The second trend involves a variation of  $\delta^{18}O$  with a relatively constant  $\delta^{13}C$  . The  $^{18}O$  rich end member of this trend is the same as that of the covariant relationship and includes the samples from the Blue Anchor Formation. At the depleted end of this trend are the green dolomitic beds which occur within the red mudstones. The  $\delta^{13}C$  value in this trend remains relatively constant at between 0.0 and  $+2.0\text{‰}$  . The green dolomitic beds, from lithological evidence, were formed during periods of high runoff. Their position within the upper red mudstones suggests that they were formed during a period of predominantly continental water input into the basin, with a gradual incursion of marine waters occurring from this point into the Blue Anchor Formation. The composition of the green dolomites implies formation in an  $^{18}O$  depleted water similar to that in which the surrounding red mudstones formed. The  $\delta^{13}C$  values in the dolomites are more enriched than in the surrounding red mudstones and suggest an input of organic  $CO_2$  . It is not likely to be the result of an incursion of marine waters which would form beds of a thickness greater than one metre. The dolomites do contain evidence for the original presence of microbial structures,

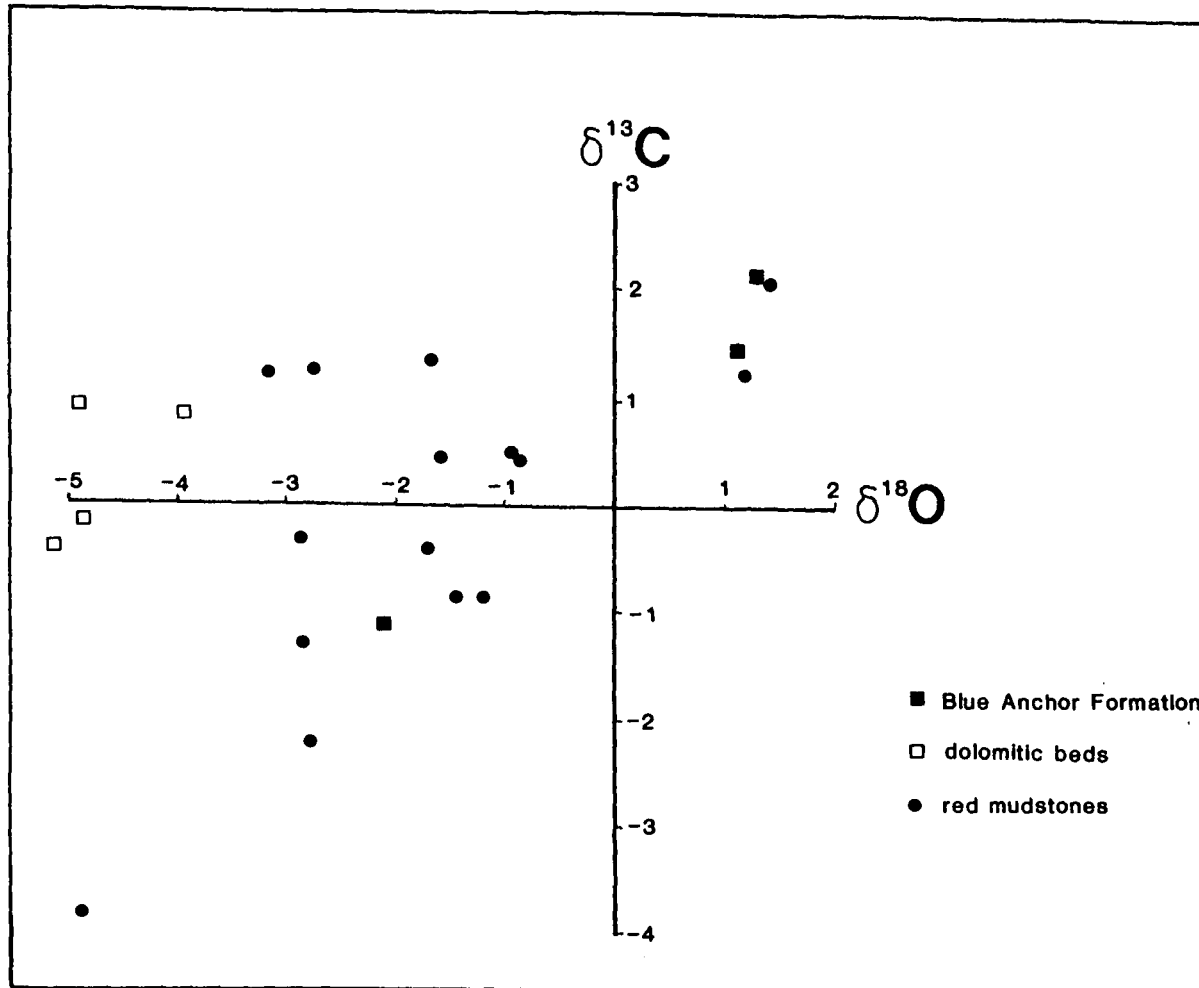


Fig.10.8  $\delta^{13}C - \delta^{18}O$  cross-plot of the Mercia Mudstone Group samples from St. Audrie's Bay, Somerset.

and palynomorphs and microfossils have been found ( M. Talbot, pers comm. ). The lack of soil CO<sub>2</sub> input into the green dolomites also serves to increase the enrichment in  $\delta^{13}C$  value relative to the red mudstones. Thus the stable isotopic composition of the green dolomites suggests formation in continental-derived waters with some organic input. The trend between the green dolomites and the Blue Anchor Formation also contains some red mudstone samples. This suggests that there may have been some residual organic input into the red mudstones overlying the dolomite beds.

#### 10.3.4 Stable Isotopic Results, South Wales

The stable isotopic values from South Wales show a different pattern to those from the Devon and Somerset successions ( Fig. 10.9 ). The Blue Anchor Formation samples are less enriched than those in the red mudstones. In the 15 metres of red mudstone sampled, there is little variation in stable isotopic composition. The carbonate is enriched in <sup>18</sup>O relative to the other areas and indicates a different hydrological environment. In Devon and Somerset, positive isotopic excursions have been related to periods when surface waters were affected by evaporation to a greater than normal extent during deposition. Stable isotopic results suggest that in South Wales there was a more permanent but evaporative standing body of water during the late Norian.

The input of more enriched waters into the South Wales Mercia Mudstone Group with the commencement of Blue Anchor Formation deposition is not as marked as in Devon or Somerset. This is a result of the already evaporatively enriched waters present during the deposition of the red mudstones. The stable isotopic data show a strong covariance, suggesting that there was a mixing of two water types. The composition of these waters was not as different as in Devon and Somerset, giving rise to a less obvious mixing trend.

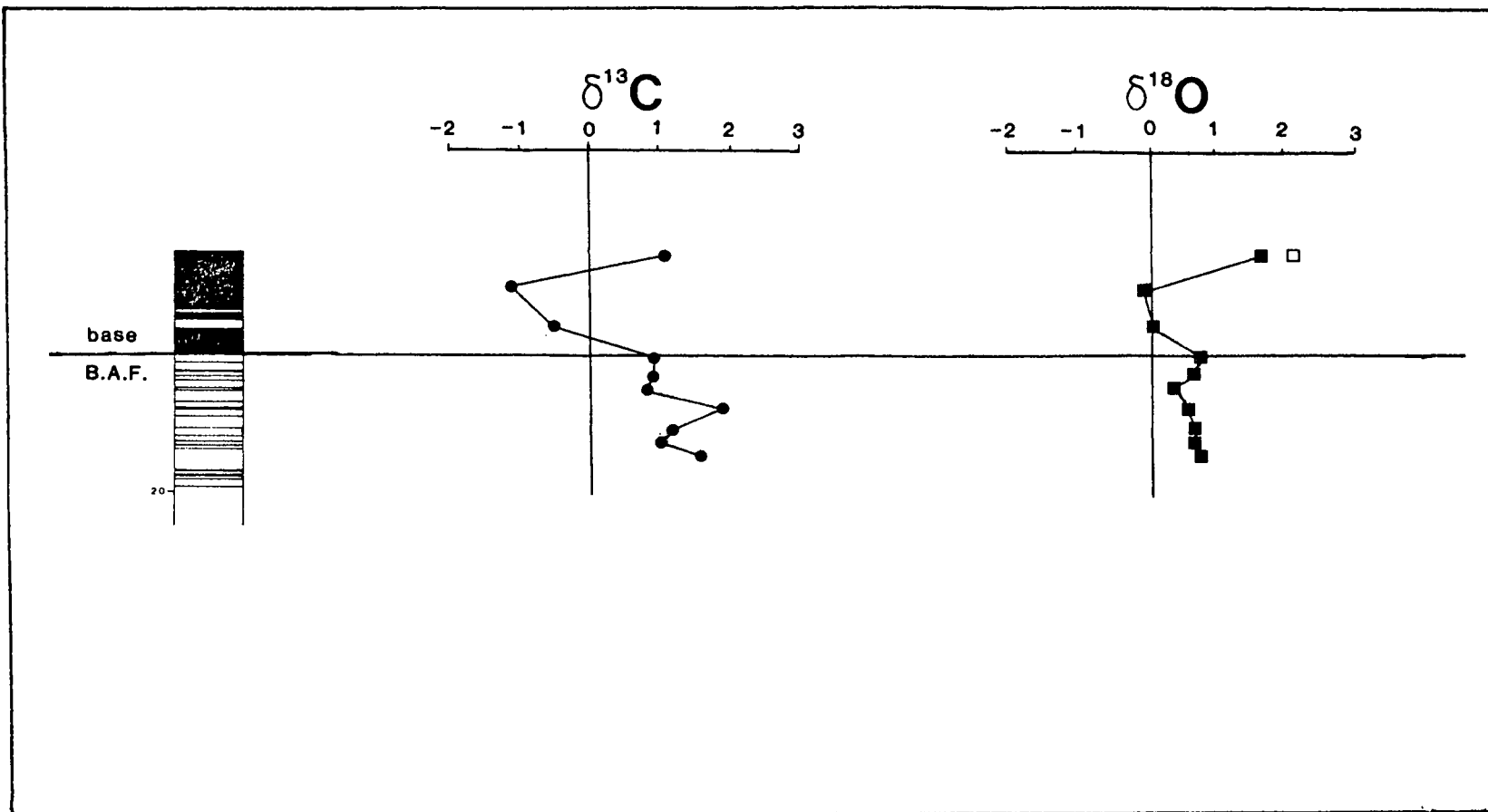


**Fig. 10.9**  $^{13}C$  and  $^{18}O$  variations in the Mercia Mudstone Group. Penarth Cliffs, South Wales.  
 Circles -  $\delta^{13}C$  . Squares -  $\delta^{18}O$  . Open squares - corrected  $\delta^{18}O$  for 100% dolomite.

### 10.3.5 Discussion

The mudstones of the Mercia Mudstone Group can be subdivided both in vertical sections and on the basis of lithology using carbon and oxygen stable isotopic variations. In Devon the sampling of one lithology throughout the section allowed large scale variations in the hydrogeochemical environment to be identified. In these samples a mixing between two water types of different chemistry is proposed to account for the difference in stable isotopic composition which shows a general covariance ( Fig. 10.6 ). In the central sections of both the Devon and Somerset successions, carbonate precipitated from an  $^{18}\text{O}$  depleted water type. In the lowest samples analysed and in the Blue Anchor Formation and immediately underlying red mudstones, the influence of a relatively  $\delta^{18}\text{O}$  enriched water is seen, ( Figs. 10.6, 10.7 ). This large scale pattern in the red mudstones is interrupted locally by samples which are anomalously enriched in  $^{18}\text{O}$ , the result of intense evaporation of ephemeral bodies of standing water. The large scale variations in  $\delta^{13}\text{C}$  values are overprinted by periods of more intense calcretisation or pedogenesis giving rise to depleted values. In South Wales the stable isotopic values indicate the presence of a more permanent body of standing water which gave rise to more enriched  $^{18}\text{O}$  values. The covariance of the oxygen and carbon isotopic values again suggests mixing of two water types, albeit of a more similar composition than those which were present in Devon and Somerset.

Taylor ( 1982, 1983 ) attributed the variation in  $\delta^{18}\text{O}$  to the varying input of marine and continental derived waters in the Nottinghamshire Triassic. In Devon and Somerset there is a similar pattern of stable isotopic variation in the Norian Mercia Mudstone Group to that described from Nottinghamshire. In both Devon and Somerset, large thicknesses of halite have been proved in boreholes in the deeper parts of the basins ( Warrington, 1974 ). Periods of deposition of halite during the Triassic have been attributed to times of marine incursions into the main basins ( Audley-Charles, 1970a; Warrington, 1974 ). In both Devon and Somerset it is estimated that halite mudstones lie some 100 metres below the outcrop sampled in this study. The *depletion* of  $^{18}\text{O}$  in the lowest samples in both areas represent the gradual regression of marine derived waters, giving a time of continental water-dominated carbonate precipitation

until, in the samples underlying the Blue Anchor Formation a gradual incursion of  $^{18}\text{O}$  enriched marine waters can be seen.

The samples from South Wales, taken from a smaller section, are enriched in  $^{18}\text{O}$  relative to those in Devon and Somerset. The total Mercia Mudstone Group sequence in South Wales is 100 metres ( Penn, 1987 ). The enriched  $^{18}\text{O}$  values do not represent a widespread marine incursion, since waters reaching the marginal region of South Wales during deposition of the uppermost 25 metres of red mudstone would also have been present in Devon and Somerset. Several exposures in South Wales show the contact of the Mercia Mudstone Group with the underlying Carboniferous Limestone basement. Tucker ( 1977, 1978 ) described a series of Triassic wave cut platforms and cliffs at Barry Island, 7 kilometres to the southwest of Penarth Cliffs. Well sorted beach sands and gravels are exposed at Sully Island, 3 kilometres south of Penarth. These sedimentary rocks are strong evidence for the existence of a standing body of water in the late Norian. The wave cut cliffs at Barry Island are laterally equivalent to mudstones 10 metres below the base of the Blue Anchor Formation, and therefore the Penarth Cliffs section. Thus it is probable that the Mercia Mudstone Group in South Wales was laid down in a different depositional environment than the equivalent beds in Devon and Somerset.

The enriched  $^{18}\text{O}$  values in South Wales could also be the result of an input of clastic carbonate from the Carboniferous Limestone basement. Coarse beds within the mudstones do contain clasts of Carboniferous Limestone but the mudstones themselves contain very few visible clasts which are mostly composed of quartz. The few carbonate clasts which can be identified are either dolomitic or calcitic. The stable isotopic composition of dolomites within the Carboniferous Limestone has been analysed by Hird ( 1985 ) who described a variable composition of both  $\delta^{18}\text{O}$  and  $\delta^{13}\text{C}$  . It is not possible to ascribe a particular stable isotopic composition to the detrital carbonate input. Since the mudstones in South Wales contain between 40 and 80% carbonate, the minor input of detrital carbonate will not significantly alter the stable isotopic composition of the samples.

The  $\delta^{18}\text{O}$  and  $\delta^{13}\text{C}$  of all of the samples from the three areas of study have been

plotted ( Fig. 10.10 ). The two trends present in Somerset are also shown by the Devon data, indicating that the mixing and evaporative trends were present in both areas. The South Wales data show a mixing trend involving two water bodies of more similar composition.

## 10.4 Trace Elemental Analysis, Results

### 10.4.1 Introduction and Previous Work

In total, 106 samples of Mercia Mudstone Group were analysed by ICPAES for the following trace elements : Fe, Mn, Zn and Sr . Ca and Mg were also analysed in order to enable the absolute concentration of trace elements in the carbonate fraction to be calculated. Unfortunately, using the ICP-AES it was not possible to analyse for Na , which may be of use as a salinity indicator ( Veizer et al., 1977 ). The larger number of samples analysed for trace element concentrations allowed a more complete coverage of the sections in Devon and Somerset so that all lithological types were sampled and some mudstones immediately adjacent to sulphates were analysed. In South Wales and Devon samples containing celestite and strontianite were analysed. In these samples, digestion of the strontianite led to the input of excess Ca and Sr into the solution to be analysed, thus invalidating the other trace element results. The presence of Sr bearing carbonate is limited to a few horizons and does not affect the majority of samples. To date, no papers have been published on the trace element geochemistry of the Mercia Mudstone Group in Britain. Aljubouri ( 1972 ) and Al-Kattan ( 1976 ) both produced theses describing aspects of the trace element chemistry of the mudstones, but neither specifically studied the carbonate fraction. Their analyses were mostly concerned with a correlation of elemental abundances with clay minerals. Since the carbonate fraction is effectively authigenic in origin, it was considered to be of more use than whole rock analysis in detecting changes in the depositional or early diagenetic environments.

The four minor elements analysed in detail, Fe, Mn, Zn and Sr, provided information on larger scale changes in water chemistry in the 120 metres of Upper Norian Mercia Mudstone Group covered in this study.

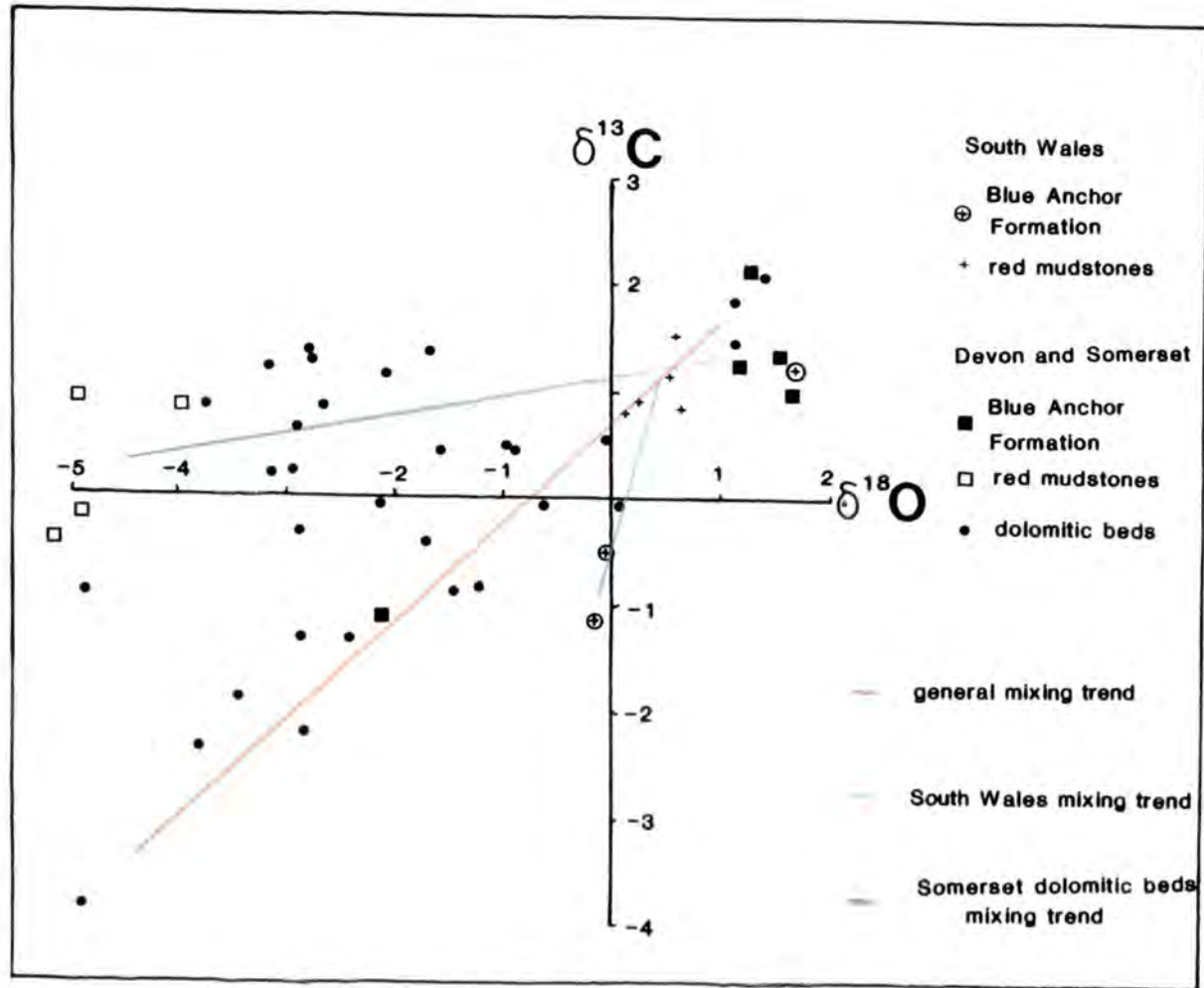


**Fig. 10.10**  $\delta^{13}\text{C} - \delta^{18}\text{O}$  cross-plot of the Mercia Mudstone Group samples from Devon, Somerset and South Wales showing the covariant mixing trends of the red mudstones and the  $^{13}\text{C}$  enriched trend of the green mudstones in Somerset.

#### 10.4.2 Trace Elemental Results, Devon

Thirty-four samples from the Devon succession, including Branscombe Cliffs, were analysed. The results are shown in Figs. 10.11 and 10.12. The variation between individual samples is large but does not obscure the large scale variations which take place over 10's of metres in the section. The boundary between the Blue Anchor Formation and the underlying red mudstones is not shown by the trace elemental variations. There are slight increases in Zn and Sr in the 10 metres below the boundary but Mn and Fe show no change associated with the Blue Anchor Formation. In the red mudstones in east Seaton Cliffs, there is a gradual increase down section in all four trace element abundances ( Table 10.3a ). This increase of between 1.5 and 3 times occurs in the first 50 metres of the section. In the west Seaton Cliffs and in Branscombe Cliffs the trace elemental distributions are different. The relative proportions of Mn and Sr fall to values similar to those of the topmost red mudstones, while the concentrations of Zn and Fe remain constant throughout the lower red mudstones. The distributions of the four trace elements are controlled by different processes acting on the mudstones. The variations in the values of Mn and Sr are similar to the distribution of  $\delta^{18}O$ , suggesting that the control on these trace elements was the composition of the waters from which the carbonate precipitated. The variations in Zn and Fe distribution suggests that other factors were important in controlling these trace element abundances. Iron can be enriched in a sediment during calcretisation and it is possible that the pedogenesis taking place in the lower red mudstones as indicated by some anomalous  $\delta^{13}C$  values led to the precipitation of a more ferroan carbonate. In the lower mudstones, Zn follows Fe distribution more closely than Mn. This may be the result of the interaction of two opposing influences in the carbonate precipitation such that the enrichment of Mn during calcretisation is counteracted by a reduction of total Mn in the depositional waters. Perhaps more likely is the preferential concentration of Fe relative to Mn due to the more oxidising environment during pedogenesis.

The data presented in Veizer ( 1983 ) are of limited use in this discussion. In his study of marine dolomites and calcites, Fe and Zn are enriched while Mn and Sr are depleted in dolomite. The correlation between the composition of

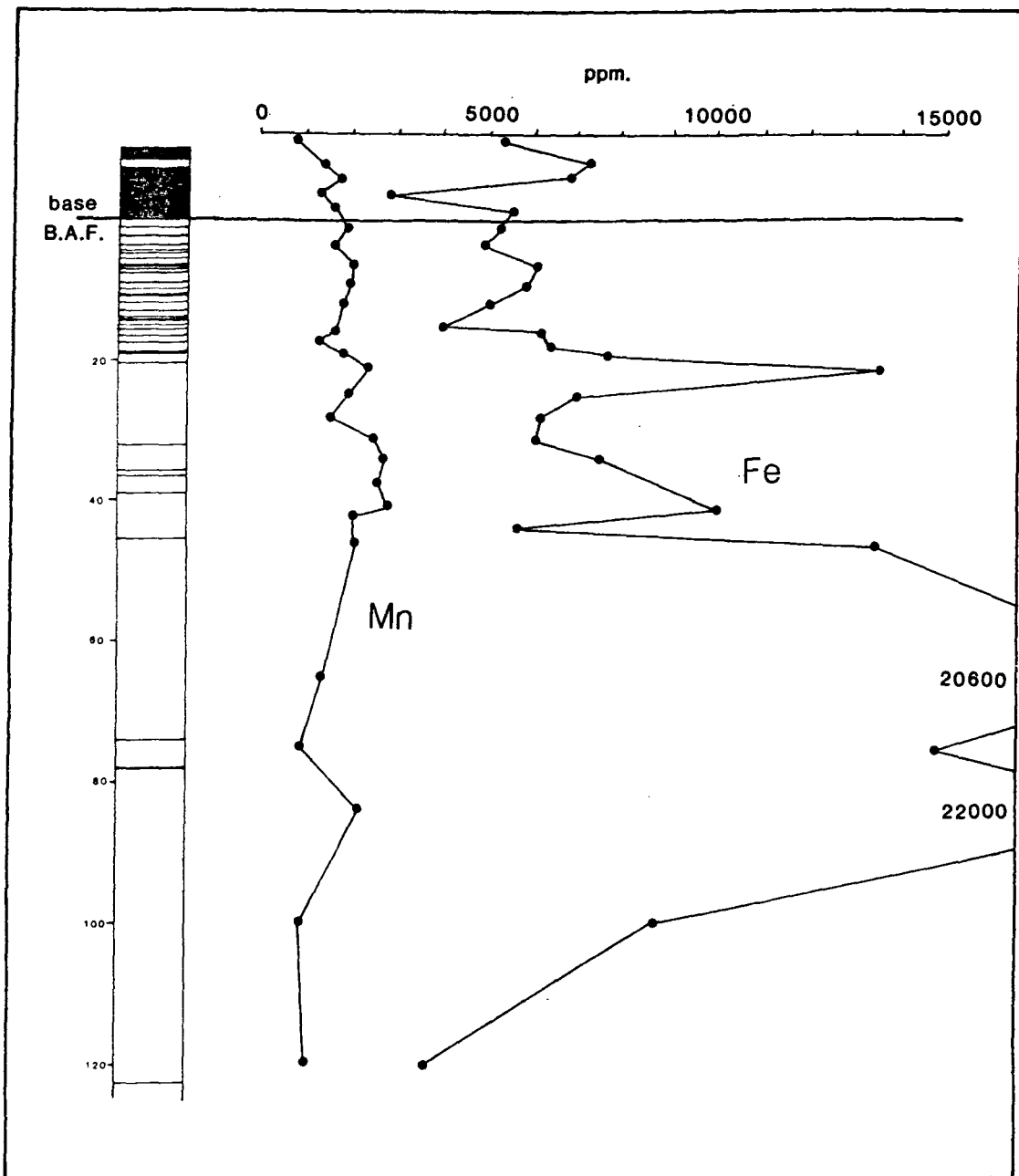


**Fig. 10.11** Distribution of Fe and Mn in the carbonate fraction of the Mercia Mudstone Group, Seaton and Branccombe Cliffs, Devon.

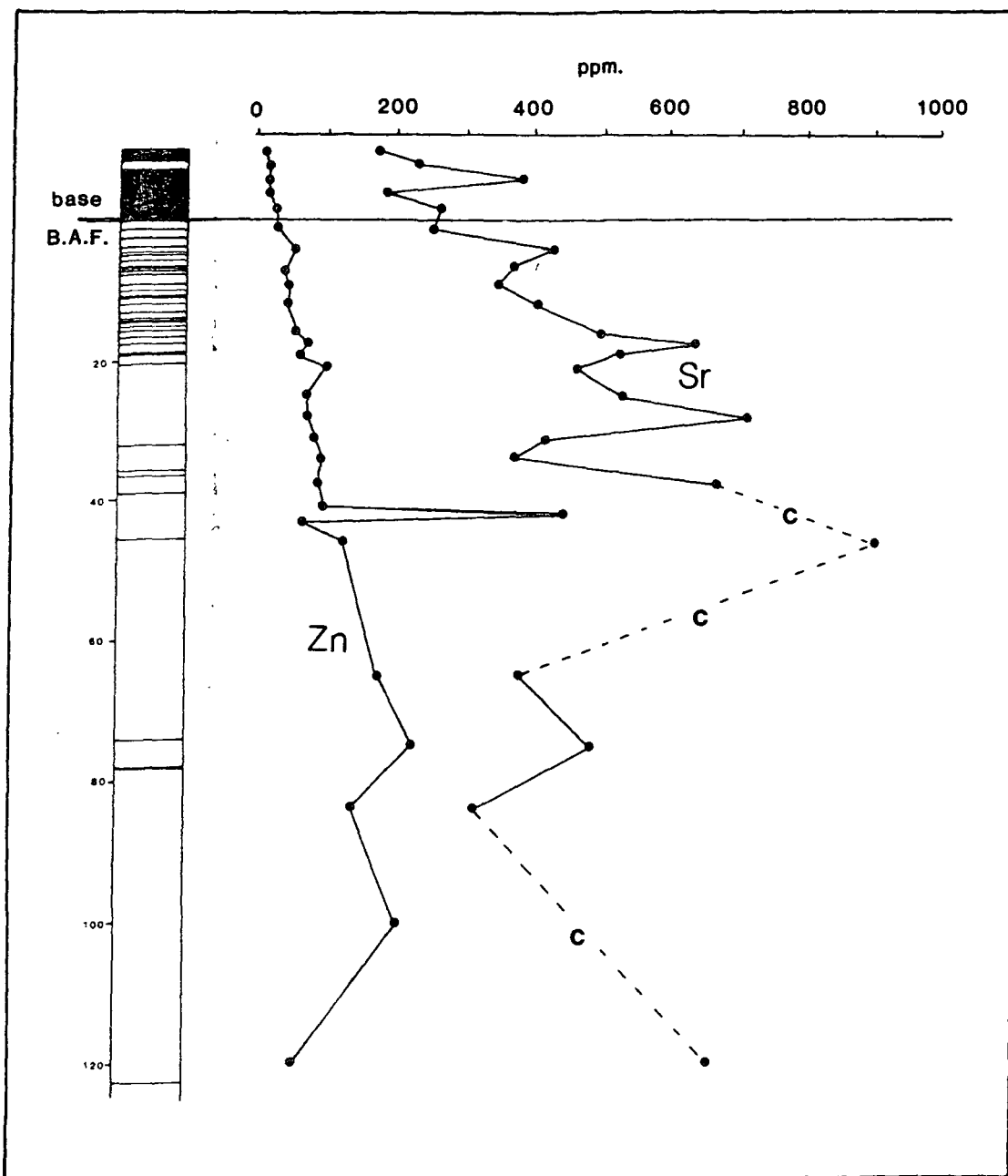


**Fig. 10.12** Distribution of Zn and Sr in the carbonate fraction of the Mercia Mudstone Group, Seaton and Branscombe Cliffs, Devon. C - samples containing celestite (  $\text{SrCO}_3$  ) giving rise to anomalous values.

Table 10.3 Average trace elemental concentrations of the Blue Anchor Formation and upper and lower red mudstones in the three sections of Mercia Mudstone Group studied. The boundary between the upper and lower red mudstones is based on the clay mineralogy and stable isotopic analyses. The limits given for each value represent one standard deviation above and below the average value. The Sr values in the South Wales section are influenced by the presence of celestite in the mudstones.

Table 10.3a Trace Elemental Distributions, Devon.

element	Blue Anchor Formation	upper red mudstones	lower red mudstones
Fe	5816±749	7440±405	13885± 7502
Mn	1270±281	2003±391	1462±290
Zn	22±14	84±77	168±150
Sr	251±203	737±619	468± 433

Table 10.3b Trace Elemental Distributions, Somerset.

element	Blue Anchor Formation	upper red mudstones	lower red mudstones
Fe	10950±5033	8700±3570	14064± 5426
Mn	1961±1162	2020±799	2323±811
Zn	42±12	97±35	118± 40
Sr	421±85	507±172	240±83

Table 10.3c Trace Elemental Distributions, South Wales.

element	Blue Anchor Formation	upper red mudstones
Fe	10060±5188	14500±19454
Mn	1283±536	2232±568
Zn	51±29	132±96
Sr	10060±13423	3610±4268

the carbonate phase and trace element distribution is poor and there is no evidence that the trace element composition is related to the dolomite / calcite ratio. The variations in trace element composition can therefore be related to the composition of the waters in which the carbonate precipitated.

#### **10.4.3 Trace Elemental Results, Somerset**

In total 45 samples of Mercia Mudstone Group were analysed from the Somerset section in St. Audrie's Bay. The pattern of trace element variation in Somerset is similar to that in Devon but some smaller scale differences were distinguished due to the larger sample number ( Figs. 10.13, 10.14 ). As in Devon all four trace elements increase in abundance downwards in the section to a point between 60 and 70 metres below the base of the Blue Anchor Formation. There is no sharp change at the Blue Anchor Formation boundary itself. Below 70 metres, the level of Sr in the carbonate fraction decreases, Fe values increase and the Zn and Mn abundances remain relatively constant. The variability between individual samples is such that trends in the data are difficult to make out ( Table 10.3b ). The most obvious trends are shown by Sr ( Fig. 10.14 ). Within the overall increase in Sr composition in the upper red mudstones, there are some smaller variations in Sr value. Between 5 and 25 metres below the base of the Blue Anchor Formation Sr values are slightly enriched. This section of the mudstone succession includes the prominent green dolomite beds which have been interpreted as being the result of periods of increased runoff. Within this area of increased Sr composition, there appears to be no difference between the green beds and red mudstones. Near the base of the St. Audrie's Bay succession there is a second area of slightly increased Sr values, in this case occurring within beds of lower total Sr content. Both of these minor excursions do not obscure the larger scale pattern of variations within the Mercia Mudstone Group.

#### **10.4.4 Trace Elemental Results, South Wales**

Seventeen samples from the section at Penarth Cliffs were analysed, ( Figs. 10.15, 10.16 ). The small size of the section is not sufficient to allow the identification of large scale trends. In general Zn and Mn increase in abundance downwards

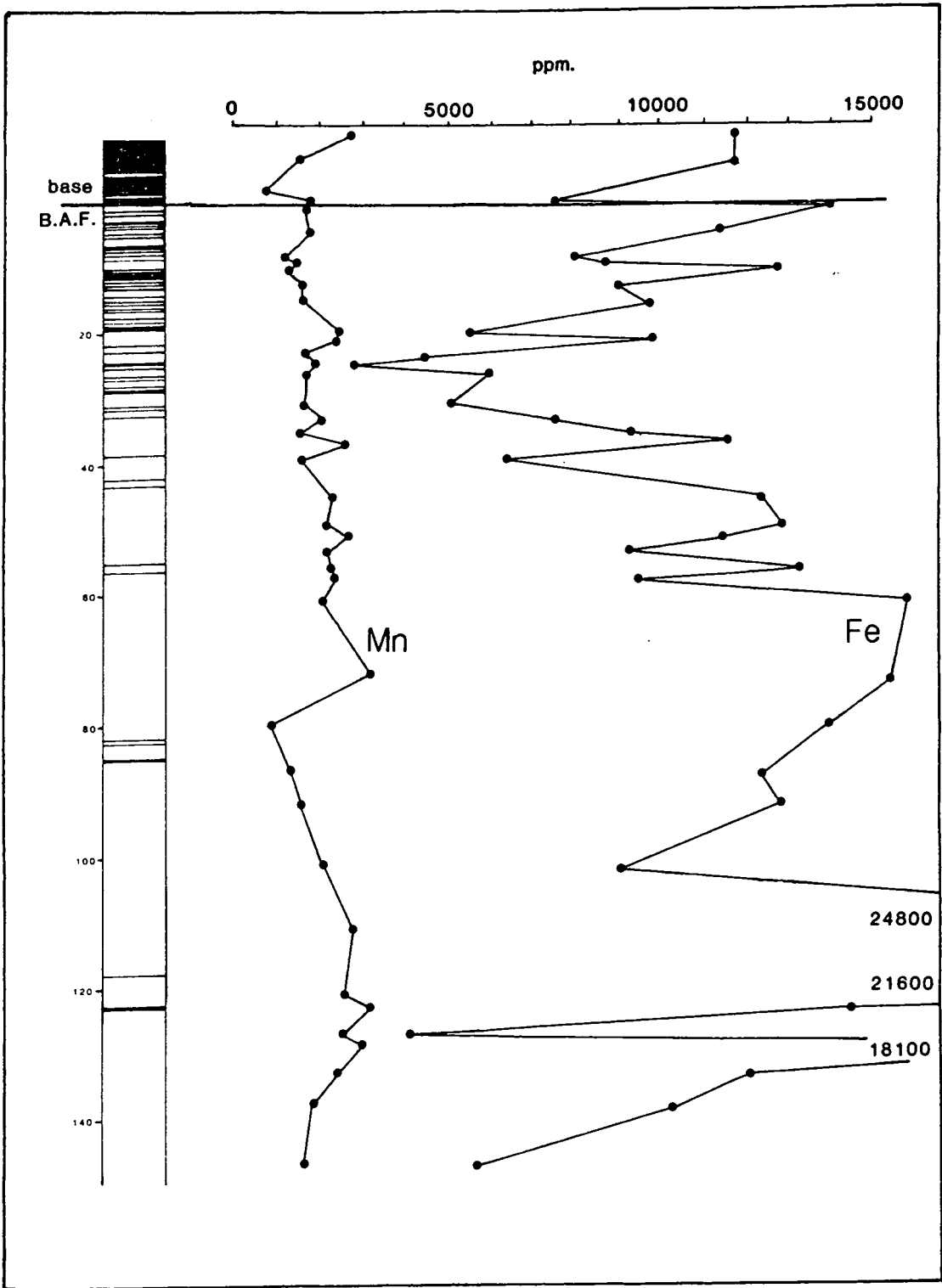


**Fig. 10.13** Distribution of Fe and Mn in the carbonate fraction of the Mercia Mudstone Group, St. Audrie's Bay, Somerset.

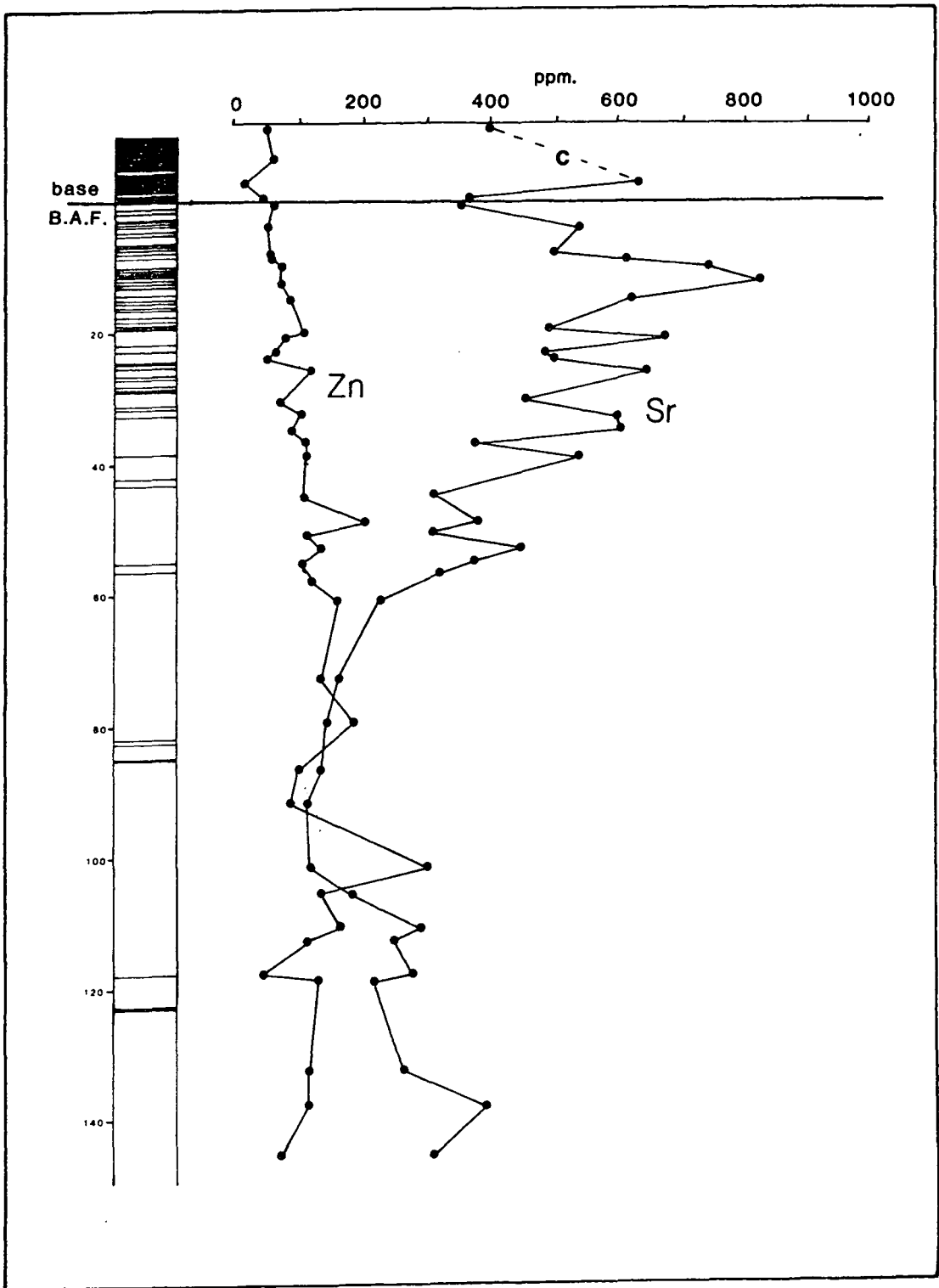


**Fig. 10.14** Distribution of Zn and Sr in the carbonate fraction of the Mercia Mudstone Group, St. Audrie's Bay, Somerset. C - samples containing celestite ( SrCO<sub>3</sub> ).

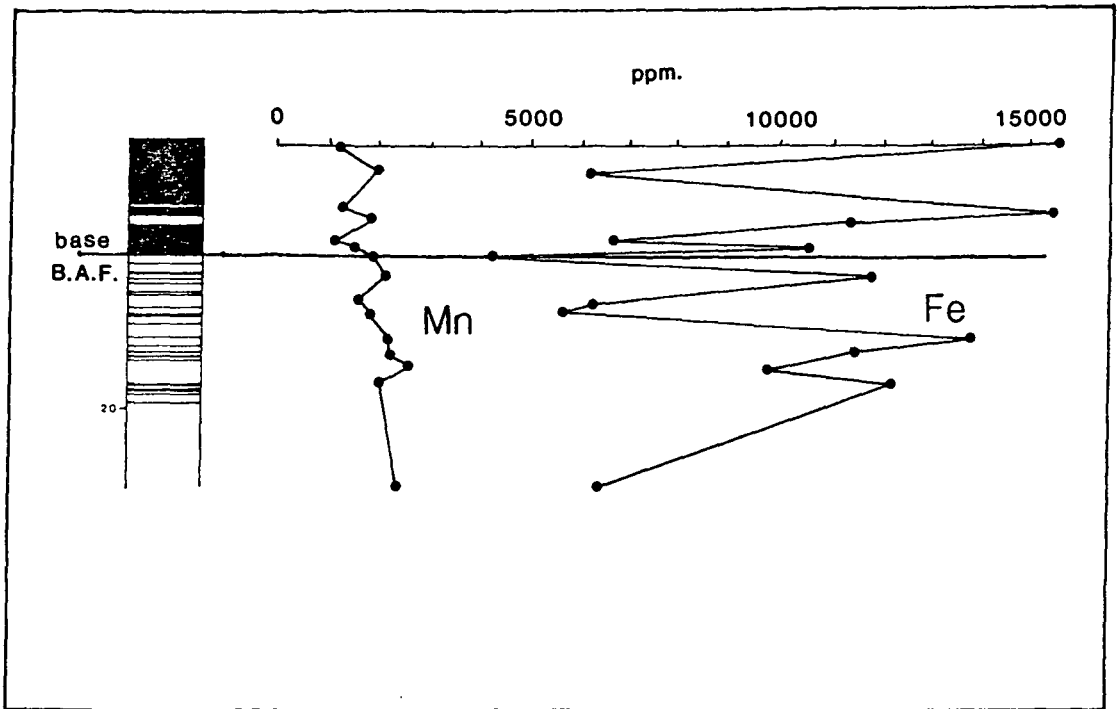


**Fig. 10.15** Distribution of Fe and Mn in the carbonate fraction of the Mercia Mudstone Group, Penarth Cliffs, South Wales.

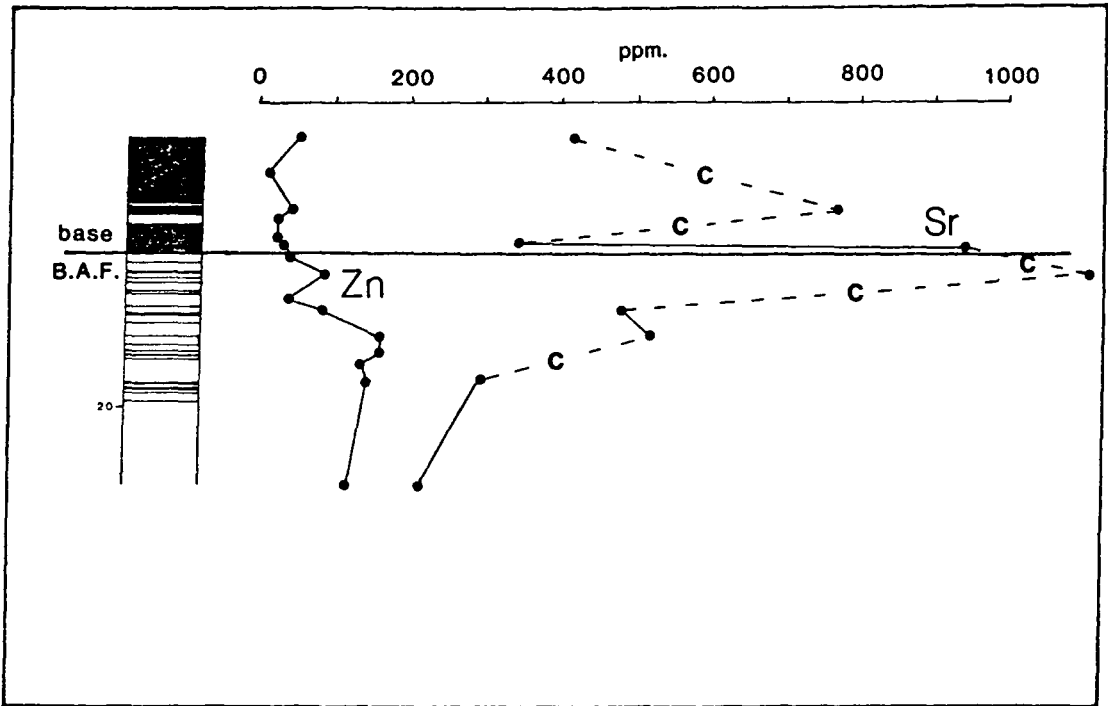


**Fig. 10.16** Distribution of Zn and Sr in the carbonate fraction of the Mercia Mudstone Group, Penarth Cliffs, South Wales. C - samples containing celestite ( SrCO<sub>3</sub> ). In South Wales most of the samples contain some celestite.

in the section, a similar trend to those in Devon and Somerset. The variation between samples means that trends in Fe and Sr data cannot be seen. However the Sr abundances are overprinted by the presence of celestite in several samples ( Table 10.3c ).

#### 10.4.5 Trace Elemental Correlations

The positive correlation of the variations in abundances implies a common origin for the four trace elements studied. The high variability of individual samples is such that any difference in composition between green and red beds is obscured and trends in the data are vague ( Table 10.3 ). Despite this there is a positive correlation between the four trace elements ( Figs. 10.17 - 10.18 ). The relationship between Fe and Sr is further complicated by the preferential enrichment of Fe during calcretisation ( Fig. 10.17 ). The beds in the mudstones which show evidence of calcretisation or pedogenesis contain some of the highest Fe values. The majority of the samples in the Fe / Sr plot show the positive correlative trend, reflecting the effect of the chemical composition of the waters. In the lower mudstones this trend is overprinted by the relative increase in Fe due to pedogenesis, which is shown by a movement towards more Sr depleted compositions with high Fe. This positive trend, displayed by the four trace elements, indicates the effects of mixing of two water types. The mudstones in the centre of the sections in Devon and Somerset were formed in waters relatively enriched in minor elements. During formation of the Blue Anchor Formation and the lower red mudstones, waters were depleted in trace elements.

Continently-derived waters are generally held to contain more Fe than those of marine origin. The distribution of Fe and of Mn can therefore be attributed to the mixing of marine and continentally-derived waters. The variations in Sr distribution would not normally display this marine / continental trend so strongly. In fact Sr is normally relatively depleted in continental waters. The reason for the distribution of Sr can be related to the diagenetic history of the basement in the area during the Upper Norian. Celestite occurs in large quantities in the Upper Triassic near Bristol ( Nickless et al., 1975 ). The input of a large amount of Sr into the mudstones has been attributed to the calcification of aragonite in

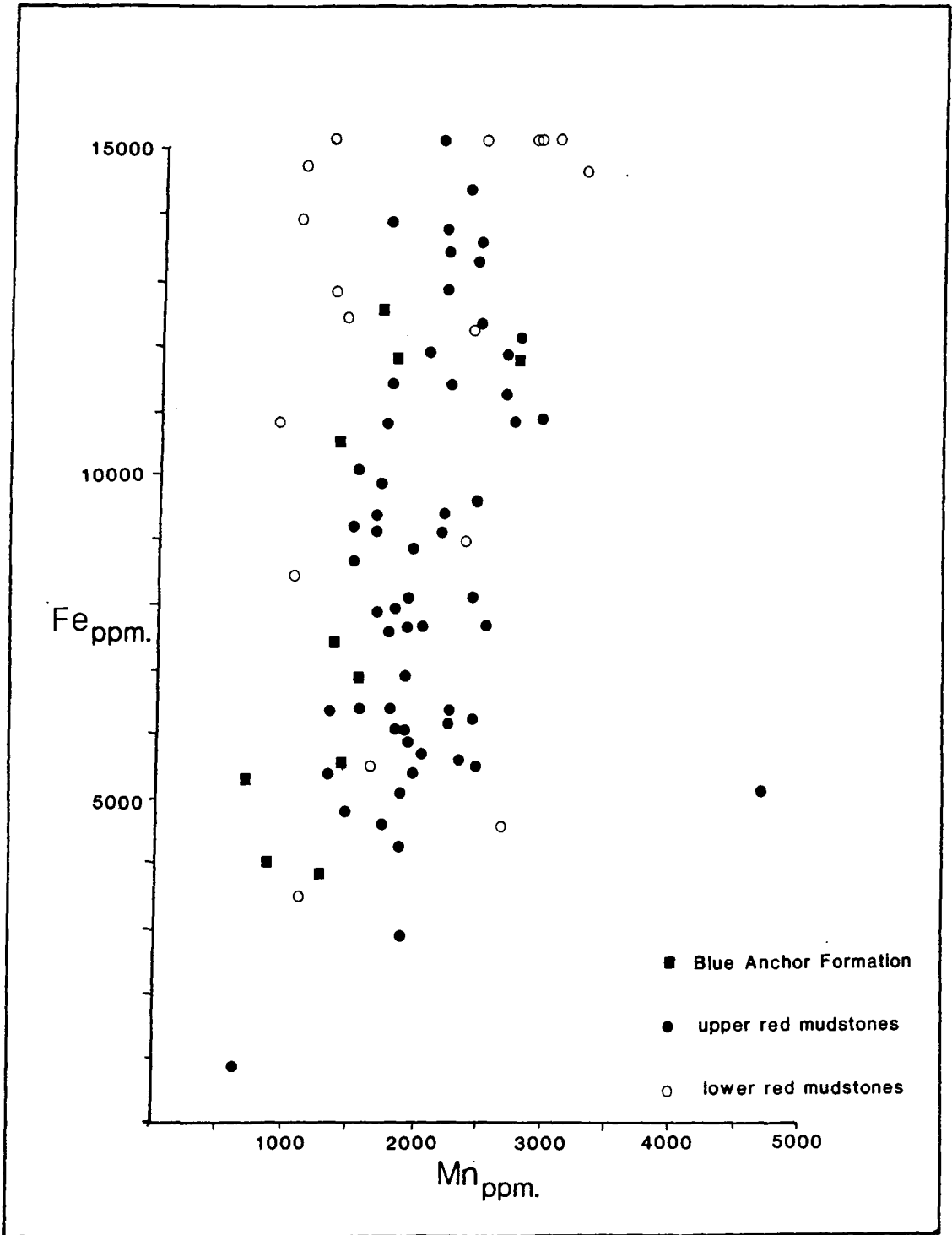


Fig. 10.17 Cross-plot of Fe against Mn in the carbonate fraction of the Mercia Mudstone Group, Devon, Somerset and South Wales.

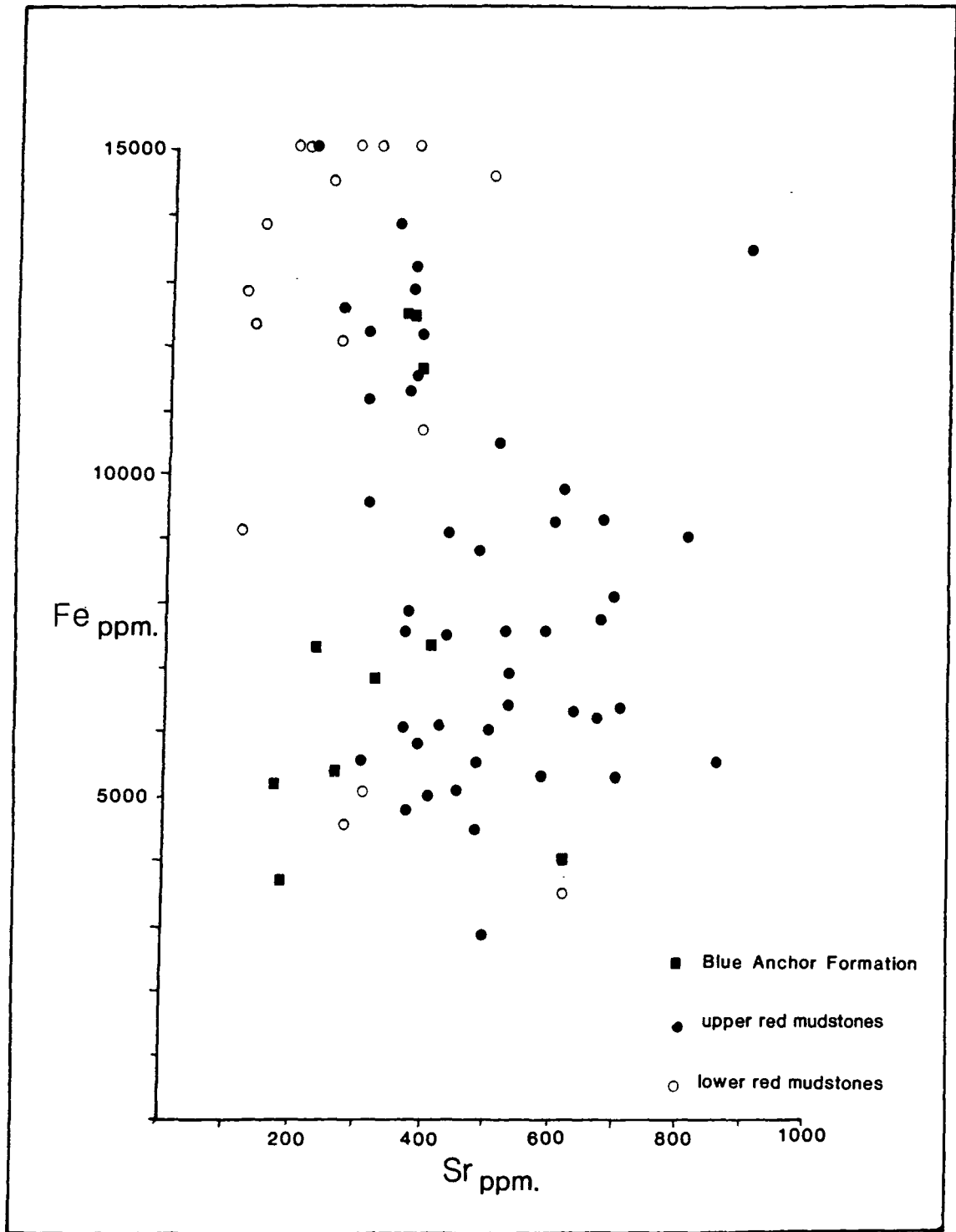


Fig. 10.18 Cross-plot of Fe against Sr in the carbonate fraction of the Mercia Mudstone Group, Devon and Somerset.

the Carboniferous Limestone. If this calcification took place throughout the Upper Triassic, then the continental runoff in areas where Carboniferous Limestone was present as basement would be enriched in Sr. This would explain the high Sr values in the continental derived carbonate and the minor variations in Sr abundance seen in Somerset can thus be related to periods of increased continental runoff. The distribution of Sr is such that it is unlikely to be the result of the input of marine waters. Strontium is generally more abundant in marine waters relative to those of continental origin. The highest Sr values, however, are found in beds which have the least marine-water input according to the clay mineralogy and stable isotopic variations. Thus the distribution of Sr in the mudstones is not simply due to the difference in input of the two water types. The South Wales succession is proximal to basement which is almost entirely composed of Carboniferous Limestone. This explains the generally higher Sr values in South Wales and the occurrence of beds of celestite and strontianite. In Devon and Somerset the abundance of Sr is lower but the occurrence of beds of celestite and strontianite suggests that Sr rich continental water runoff was in contact with some Carboniferous Limestones ( possibly those in the Mendip Hills ? ) during transport.

## 10.5 Conclusions

The variations in the geochemical composition of the carbonate fraction of the Mercia Mudstone Group can be related to changes in the composition of the depositional waters, in the volume of water entering the basins at any one time and to processes occurring during deposition and early diagenesis ( Fig. 10.19 ).

The carbon and oxygen stable isotopic composition of the carbonate in the mudstones can be used to subdivide the Mercia Mudstone Group into zones of continental and of mixed continental / marine water composition. A well defined covariant mixing trend is shown by the stable isotopic data. The waters in the basin were derived from continental runoff during much of the time period covered by this study. In the Blue Anchor Formation and in the lowermost mudstones sampled there is evidence for the incursion of marine-derived waters which transgressed into the basins from the English Channel and Celtic Sea areas. The

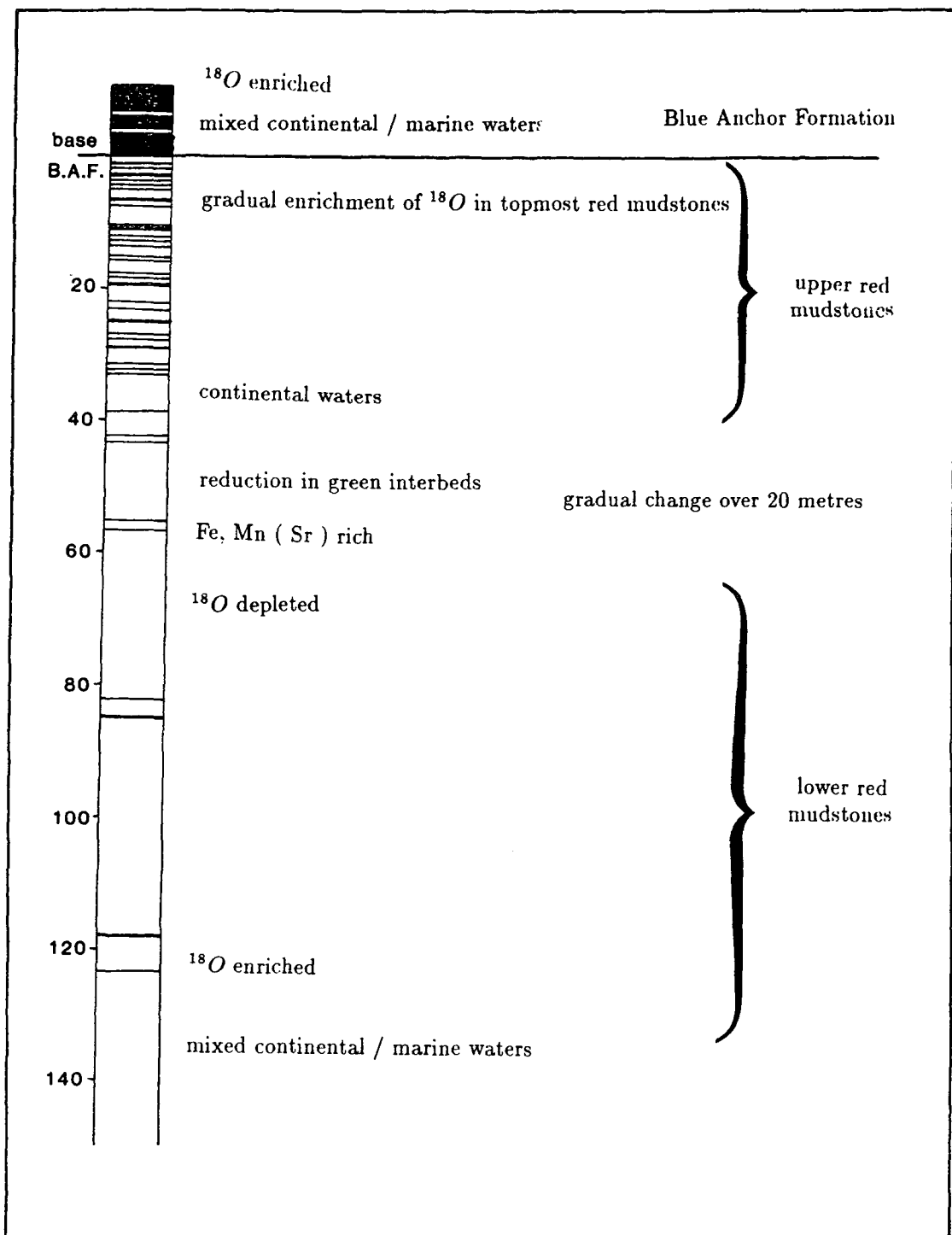


**Fig. 10.19** Summary geochemistry diagram for the Upper Mercia Mudstone Group in South-west Britain.

marine incursions gave rise to extensive halite deposits during the Carnian. The lowest mudstones sampled in this study lie stratigraphically 100 metres above the level of the halite and record the gradual reduction of marine water influence during the Norian. In the Blue Anchor Formation the carbonate precipitation records the first indications of the Rhaetian transgression.

The general variations in the stable isotopic values have been locally overprinted by syndepositional effects.  $\delta^{13}\text{C}$  values are in some samples anomalously depleted, the result of the influence of soil  $\text{CO}_2$  during periods of more intense calcretisation and pedogenesis. The influence of organic  $\text{CO}_2$  is most noticeable in the green dolomitic beds exposed within the upper red mudstones in Somerset. These  $^{13}\text{C}$  enriched beds form another trend of stable isotopic values of which the green dolomites form one end member. In this trend, some of the upper red mudstones also show the effects of organic  $\text{CO}_2$ .

$^{18}\text{O}$  values deviate from the mixing trend as a result of the periodic intensification of evaporative effects caused by the evaporation of ephemeral standing bodies of water. This evaporative enrichment of  $^{18}\text{O}$  can be seen in individual samples in Devon and Somerset and throughout the South Wales section where there is evidence for the presence of a more permanent water body.

The variations in the trace element data are less distinct than those in the stable isotopic results due to the wide spread of values. The element strontium is the most useful indicator of trends in the data and its abundance can be correlated with changes in water composition ( Fig 10.19 ). All of the trace elements studied tend to be more abundant in carbonate precipitated from continental waters. This trend is most clearly seen in the beds underlying the Blue Anchor Formation where there is a gradual increase in trace element values. In the lower red mudstones the trace elemental variations are more complex. The spread of values makes the identification of trends difficult. The presence of marine waters is indicated by the Sr and Mn variations. Both Fe and Zn values appear to have been enriched by pedogenesis, overprinting the variations due to changes in water chemistry.

Nowhere in the sections studied have carbonates derived from fully marine waters been analysed. The transgression at the end of deposition of the Mercia Mudstone

Group was completed during the latest Norian and is represented in the topmost few metres of the Blue Anchor Formation. The Carnian transgression which gave rise to the halite deposits in the western Wessex and Somerset Basins was by Norian times in the final stages of retreat. This retreat of marine-derived waters is recorded in the lowermost few 10's of metres in the Devon and Somerset sections.

## **Chapter 11**

### **The Mercia Mudstone Group in Southwest Britain: Conclusions**

## Chapter 11

### The Mercia Mudstone Group in Southwest Britain: Conclusions

#### 11.1 Problems of the Mercia Mudstone Group

The Mercia Mudstone Group is a problematical group of sedimentary rocks for several reasons. Apart from the boundary with the Blue Anchor Formation and the prominent sandstone beds in the centre of the Mercia Mudstone Group there are no correlable beds in the upper mudstones. No fossils of any use in stratigraphic correlations have been recorded and the mudstones themselves are structureless. The 100 to 200 metres of mudstone between the Blue Anchor Formation and the sandstone units have not been subdivided at all in Southwest Britain. For the purposes of this study the beginning of the deposition of the Blue Anchor Formation is seen as a synchronous event in all three study areas. The extent of peneplanation which had taken place by the Upper Norian is such that any change in overall climatic conditions would be seen simultaneously throughout the region. Similarly any marine incursion would transgress rapidly across the peneplain. Apart from the topmost 30 metres of red mudstones which contain a greater number of green beds, the sequence studied is almost entirely composed of red mudstone. In both Devon and Somerset 140 metres of continuous section of red mudstone underlying the Blue Anchor Formation were sampled for later laboratory study. In South Wales a section of 30 metres underlying the Blue Anchor Formation was available.

In Somerset some green dolomitic beds 10 to 30 metres below the Blue Anchor Formation indicate a temporary incursion of less arid conditions before the marginal lacustrine environment became fully established ( Stevenson & Warrington, 1971; Hamilton & Whittaker, 1977 ). Calcretised and aeolian beds are also exposed in the Mercia Mudstone Group in Somerset and Devon. Neither feature is laterally persistent and it is likely that they formed locally.

The exact depositional environment in which the Mercia Mudstone Group was laid down has also been a source of controversy. On the basis of sedimentary

structures in the mudstones, the Mercia Mudstone Group in the Cheshire Graben and Midlands Basins have been subdivided into units formed in fluvial/alluvial, aeolian, sabkha and hypersaline lacustrine environments ( Elliott, 1961; Klein, 1962; Audley-Charles, 1970b; Arthurton, 1980 and others ). The Upper Mercia Mudstone Group covered in this study is generally lacking in the structures described by these authors which makes description of the depositional environment more difficult. The structures exposed in the mudstones in Devon and Somerset indicate that a distal playa-alluvial environment with detrital input from aeolian and fluvial sources is the most appropriate model. The marginal environments exposed do not seem to be different from those in the basin centres since the succession in the Burton Row Borehole in the centre of the Somerset Basin is comparable with that exposed on the North Somerset coast ( Whittaker & Green, 1983 ).

The fact that the mudstones contain only a small silt-sized fraction in exposures which in Somerset are only 3 kilometres from basement is indicative of the extent of peneplanation which had occurred by the Upper Triassic. Little coarse material is present other than that directly adjacent to the basement ( Thomas, 1940 ).

In South Wales the Carboniferous Limestone basement has been cut into platforms and cliffs indicating that there was a relatively permanent water body present in the Upper Triassic. The lake level fluctuated but was stable enough at certain times to cut four platforms which would each take several thousands of years to form ( Tucker, 1978 ). There is no petrographic evidence in the mudstones to suggest a different depositional environment in South Wales compared to that in Somerset and Devon.

## **11.2 Clay Mineralogy**

Since petrographic studies are of limited use in the examination of the Mercia Mudstone Group both at outcrop and in thin section, other techniques were used. Several authors have studied the clay mineralogy of the Mercia Mudstone Group. In these studies although the same clay assemblages were found, interpretations differed. In this study two clay mineral suites were defined on the basis of the

amount of mixed-layer clay in the sample. This has been related to the input of marine-derived waters into the basin ( Taylor, 1982 ).

An increase in the proportion of smectite-illite or smectite-chlorite, which are of transformational origin and of palygorskite/sepiolite which are truly authigenic ( neoformalional ) indicates the presence of more magnesian depositional waters. Such an increase can be seen in the continuous sections in Devon and Somerset between 50 and 70 metres below the Blue Anchor Formation. The boundary is transitional over 20 metres, indicating the gradual retreat of marine-derived waters. The upper clay assemblage is composed of detritally-derived illite and chlorite with relatively little ( under 15% ) mixed-layer clays. The more magnesian clay assemblages present in the lower mudstones represent the last influence of the marine waters which were responsible for the precipitation of halite in the central parts of the basin in the latest Carnian.

Only the lower Blue Anchor Formation was sampled in this study and the clay assemblages do not show the gradual incursion of marine waters which took place in the Rhaetian. The clay mineralogy of the entire Blue Anchor Formation has been examined by Mayall ( 1979, 1981 ) who described the increase in mixed-layer clays in the Upper Blue Anchor Formation as a result of the marine incursion.

The lateral distribution of clay minerals in the Mercia Mudstone Group has been described by Lucas & Ataman ( 1968 ) in terms of a progressive aggradational sequence such as that found in the Triassic of the French Jura Basin. This sequence commences with detritally-derived degraded illite and chlorite and proceeds through various mixed-layer types to a regraded, well crystallised chlorite. The lateral distribution of mixed-layer clays in the British Upper Triassic ( Fig. 8.5 ) suggests the presence of such a sequence in the marine-derived parts of the succession. If this sequence existed in the British Triassic then a permanent water body would be required to extend from Devon to Cheshire with a constant movement of progressively more evaporated water northwards. Such an extensive water body of sufficient depth to permit a constant movement of fine detritus is unlikely to have been stable. The constant northwards flow would be disrupted by the input of continental runoff. Furthermore, the halite beds of the Cheshire Graben can be correlated with units in the Irish Sea. The source of marine-

derived waters into the Cheshire and Midlands areas is most likely through the Celtic and Irish Seas rather than from the south. It is more probable that the distribution of the mixed-layer clays is the result of different conditions within individual basins. In the Cheshire and North Worcester Grabens where thick halite is present the mixed-layer clay corrensite ( regular mixed-layer smectite-chlorite ) is present whereas in the more marginal mudstones of the Nottinghamshire and North Somerset Basins irregular smectite-chlorite formed. This probably represents a sequence from the margins of local basins to the centres, rather than one which took in all of the basins in southern Britain. The Devon section contains smectite-illite, a mixed-layer clay which occurs earlier in the sequence of Lucas & Ataman than the smectite-chlorites of Somerset. In this case the mineral corrensite would be expected to occur between the Devon and Somerset successions. Some of the mixed-layer clays in Somerset are approaching the order of corrensite and the fully ordered mineral is probably present to the south of the exposures on the Somerset coast. This implies that the movement of waters was northwards from the Devon and Dorset area into Somerset. The movement of waters eastwards through the Bristol Channel Basin is unlikely since the Mid-Bristol Channel High contains a condensed sequence of Mercia Mudstone Group and movement of marine waters eastwards from the Celtic Sea in the Carnian would not have been possible.

The presence of the marine influenced clay minerals does not imply a permanent water body throughout the Upper Triassic, although the amount of salt present implies a large scale transgression which may well have taken place in pulses. In the Norian mudstones covered in this study, the retreating marine brines may well have existed as ponds and groundwaters which were gradually diluted by the constant input of continental runoff.

### **11.3 Gamma-Ray Correlations**

Although the Mercia Mudstone Group has not been subdivided at outcrop gamma-ray and sonic measurements in boreholes have been used to subdivide the mudstones into six units, the topmost being the Blue Anchor Formation ( Lott et al., 1984; Penn, 1987 ). Using a portable gamma-ray spectrometer at outcrop

the topmost three units including the Blue Anchor Formation were recognised. The boundary between the lower two units of red mudstone could not be identified at outcrop other than by gamma-ray variations. These changes are the result of variations in the amount of potassium in the mudstones of which illite is the most important source. The gamma-ray unit boundary is the result of a reduction in the total amount of illite in the mudstones as the proportion of mixed-layer clays increases. The gamma-ray boundary, like that shown by clay mineral variations, is transitional over 20 metres. The gamma-ray units do not show great thickness changes in the basins. The marginal section exposed on the North Somerset coast is only 10 metres thinner than the fully basinal sequence in the Burton Row Borehole. In the Norian there was little active faulting and the Mercia Mudstone Group passively overlapped the basement which formed an extensive peneplain with little or no relief. The boundary at the base of the Blue Anchor Formation is the result of an increase in the amount of dolomite in the mudstones. The boundary is therefore shown more clearly in Devon where the lithological change is more marked than in Somerset, where there is a more transitional increase in dolomite over 10 metres.

As well as total gamma-ray count data the spectrometer also provided information on the distribution of potassium, uranium and thorium in the mudstones. As has already been stated the amount of K in the mudstones is related to the presence of illite. U and Th do not occur in any of the major mineral phases. Unfortunately calibration of the U and Th gamma-ray data with other techniques proved difficult and no quantitative statements could be made about the U and Th distributions. In general, the distribution of U and Th are related to the input of detrital material into the basins. The more alkaline marine waters in which formation of mixed-layer and authigenic clays was favoured tended to leach U in preference to the less mobile Th.

The most important use of the gamma-ray data was the correlation of outcrop sections with measurements taken in boreholes. This has enabled subtle lithological variations in the muds to be correlated with variations seen in borehole logs which can be followed across much of Southern Britain.

## 11.4 Geochemical Variations

The carbonate fraction of the Mercia Mudstone Group which consists of dolomite and calcite was examined in terms of its stable isotopic and trace elemental geochemistry. The stable isotopic results show a general trend controlled by the relative inputs of continental and marine-derived waters. This trend is at times overprinted by a local intensification of other effects. The  $\delta^{18}\text{O}$  isotope results show a trend in which there is an enrichment in  $^{18}\text{O}$  at the base and top ( within the Blue Anchor Formation ) of the sections in Devon and Somerset, which is indicative of the influence of marine-derived waters which themselves are enriched in  $^{18}\text{O}$ . In the upper 60 metres of red mudstone the  $^{18}\text{O}$  values are more depleted by 2 to 3‰ indicating a continental water source. This basic trend, which can be correlated with the variations in clay mineralogy and gamma-ray intensity, is overprinted in several samples which are anomalously enriched in  $^{18}\text{O}$ . This is most likely to be the result of more intense evaporation of the depositional waters. If the oxygen and carbon stable isotopic values are plotted together several trends are seen ( Fig. 10.9 ). A prominent mixing trend involving covariance of  $^{18}\text{O}$  and  $^{13}\text{C}$  is present. This is the result of the mixing of the two water types. The samples taken from the Blue Anchor Formation and the lowest red mudstones plot at the enriched end of the trend while the upper red mudstones which show the least marine water influence are depleted in both  $^{18}\text{O}$  and  $^{13}\text{C}$ . Also present especially in Somerset is a trend with constant  $^{13}\text{C}$  and varying  $^{18}\text{O}$ . This trend is the result of the evaporation of a continentally derived water which has been enriched in  $^{13}\text{C}$  by organic material. The trend represents the progressive evaporation of this water. In Somerset the depleted end-member of this trend is represented by a number of green, dolomitic beds which contain microbial laminae. These beds are the result of a temporary amelioration of the climate in Norian times before the permanent change took place in the Rhaetian. The  $^{13}\text{C}$  values themselves show a trend which can be related to the influence of the two water types. The overprinting of this general trend is seen in several samples which are depleted in  $^{13}\text{C}$ . These beds are interpreted to be the result of the influence of soil  $\text{CO}_2$  during periods of increased pedogenesis or calcretisation.

The pattern of stable isotopic values in the South Wales area is different to

that from Devon and Somerset. The carbonate is more enriched in  $^{18}O$  and the samples plot on a different mixing line ( Fig. 10.9 ). This is the result of an enrichment of the continental derived water due to increased evaporation of a relatively permanent lake. The South Wales Mercia Mudstone Group can thus be distinguished geochemically from the sections in Devon and Somerset where intense evaporation of the depositional waters occurred at certain horizons.

The trace elemental trends are more difficult to interpret since variation between individual samples is such that large scale changes are masked. In general the trace elemental abundances within the carbonate increase downwards from the Blue Anchor Formation boundary into the upper red mudstones. The corresponding decrease of trace element abundances in the lower red mudstones is less obvious but is shown by the strontium variations which are the most sensitive of the trace elements analysed in this study. The trace elemental composition of the carbonate in the mudstones can also therefore be related to the composition of the depositional waters. Iron and zinc distributions appear to have been affected by an increase in pedogenesis or calcretisation in the mudstones. The strontium distributions show smaller scale variations as well as the overall pattern which is related to water composition. This is most likely to be the effect of slight changes in the volume of runoff entering the basin.

### 11.5 Conclusions

The Mercia Mudstone Group consists of up to 1200 metres of mudstones of which the topmost 170 metres were examined at outcrop as part of this study. The topmost 20 metres of mudstones consist of green dolomitic beds which make up the lower part of the Blue Anchor Formation. The base of the Blue Anchor Formation is sharp and has been used as a datum in this study. The underlying red mudstones contain few sedimentary structures, none of which are of use in correlation. Calcretes and aeolian beds are locally developed. The topmost 20 metres of red mudstones contain interbedded green mudstones and some dolomites which formed in less arid conditions more typical of the overlying Blue Anchor Formation.

Gamma-ray variations measured at outcrop have been correlated with borehole logs which themselves contain changes in gamma-ray and sonic values which can be seen in boreholes across much of Southern Britain. The <sup>total</sup> gamma-ray variations are the result of changes in the amount of illite in the rock. Changes in the clay mineral suite are caused by incursions of magnesian marine-derived waters into the basins. In Devon and Somerset the lower 70 metres of red mudstones record the gradual retreat of marine-derived waters from the basins in the Norian as the brines responsible for the formation of the Carnian halite were progressively diluted by continental runoff. The varying influence of marine and continental waters is also shown by changes in the geochemistry of the carbonate phases in the mudstones. Lithological constraints can thus be put upon subdivisions which previously had only been seen in geophysical logs from boreholes. In Nottinghamshire these variations have been used to subdivide one of the upper Formations in the Mercia Mudstone Group into two Members ( Taylor, 1982 ). In this study it was felt that the lithological and geochemical variations, which were continuous over some 50 metres of section, were not distinct enough to allow the formal subdivision of the Mercia Mudstone Group at outcrop.

The much smaller section in South Wales does not contain evidence of marine brine influence in the red mudstones but the stable isotopic values in particular indicate that waters in the area were affected by more intense evaporation than those in Devon and Somerset. There is evidence at outcrop in South Wales for the presence of a permanent standing body of water during deposition of the mudstones. The Mercia Mudstone Group in South Wales was therefore laid down in a different depositional environment from that 10 kilometres to the south in Somerset.

## **Chapter 12**

### **The Upper Triassic Mercia Mudstone Group in Southwest Britain: Conclusions**

## Chapter 12

### The Upper Triassic Mercia Mudstone Group in Southwest Britain: Conclusions

#### 12.1 The Sully Island Succession

The sequence of sedimentary rocks in the Upper Triassic marginal deposits on Sully Island in South Wales is the result of the interaction of a number of factors including the palaeohydrology and palaeogeography of the area. The sequence was formed in a marginal lacustrine environment and is laterally equivalent to clastic beds which comprise the majority of the marginal deposits in South Wales. The series of carbonates overlies a wedge of clastic material which formed in a perilittoral environment. Well-sorted beach-type gravels overlie a <sup>near-</sup>planar surface of Carboniferous Limestone.

The onset of carbonate deposition as opposed to clastic beds containing carbonate detritus, is indicated by a bed of fenestral dolomite 0.2 metres in thickness, which represents the establishment of a mudflat environment at the lake shoreline. The dolomite has been replaced in the east of the Sully Island area by an iron-rich calcrete. This fenestral bed is overlain by up to 8 metres of dolomite containing replaced sulphate nodules. In general the dolomite represents a cycle of regression and transgression of the hypersaline lake shoreline with an increase in the influence of meteoric waters in the upper part of the unit. Perilittoral conditions in the upper and lower sections of the unit are indicated by the presence of rippled and laminated beds. The central part of the dolomite contains several horizons of replaced sulphate nodules, in the middle of which is a sabkha-type bed consisting of several bands of coalescing nodules. This bed also contains evidence of pedogenesis within the sediment and represents the period of greatest regression of the shoreline. The general transgression of the lake in the upper part of the unit has been overprinted by an influx of meteoric water during a temporary regression during which time a groundwater calcrete was formed. At this time the sulphate in the nodules was replaced by calcite and quartz. Subsequent dolomitisation of the calcite in the groundwater calcrete indicates a return

to the hypersaline perilittoral conditions during deposition of the topmost beds of the dolomite unit.

The subsequent regression of the lake shoreline and the formation of a meteoric water-dominated depositional environment took place over a long period of time during which the uppermost dolomite was calcretised and then partially removed by erosion to leave a bed 1 metre in thickness. This massive calcrete was modified by at least two phases of karstification and was originally part of a much thicker profile.

Overlying the karstic surface of the basal calcrete is up to 7 metres of partially dolomitised limestone. This was laid down in a perilittoral depositional environment which was the result of a locally high input of meteoric water into the Sully Island area as opposed to the perilittoral hypersaline conditions at the margin of the larger-scale Mercia Mudstone Group lake in South Wales. The limestones in the Sully Island area are therefore part of a subbasin with a very different palaeohydrology to the main South Wales - Bristol Channel Basin. Meteoric waters derived from the surrounding uplands to the north were channeled into the Sully Island area and moved upwards in response to the basinal topography of the basement. There is abundant evidence in the limestones for the emergence of groundwaters at the surface during deposition of the unit. Spring deposits are locally developed throughout the limestones and in the upper part of the unit polygonally-arranged fissures acted as conduits for the upward-moving waters. The upwelling groundwaters were responsible for rapid fluctuations in the water table which gave rise to early lithification of the limestones by vadose diagenetic cements. The topmost limestones have been deformed into tepee and saucer structures which indicate the continuation of the upward movement of waters with a reduction in the input of intraclastic material into the area as the limestone surface became exposed for an extended period of time.

In terms of geochemistry the two units in the Sully Island succession can be distinguished by their mineralogy. There does not appear to have been a great difference in the chemistries of the waters involved in the diagenetic replacement of the dolomite unit and the precipitation of primary carbonate in the limestone unit. None of the beds show an evaporitic marine signature and it is unlikely that

the hypersaline lake waters were of marine origin. Variation in the chemical composition of the emergent groundwaters is shown by the small-scale fluctuations in  $^{18}\text{O}$  and  $^{13}\text{C}$  in the flowstones. The gradual reduction in input of meteoric waters into the red mudstones overlying the limestones is shown by the trend of stable isotopic composition towards that of the Mercia Mudstone Group samples.

## 12.2 Correlation of the Mercia Mudstone Group

The Mercia Mudstone Group covered in this study consists of the lower part of the Blue Anchor Formation and up to 150 metres of underlying red mudstones. The succession is Norian or Rhaetian in age, the sandstone beds which form the top of the Carnian were not examined in this study. The Mercia Mudstone Group is composed of red and green dolomitic-calcareous mudstones which contain few sedimentary structures. Locally developed nodular sulphate horizons are common although they are not laterally persistent and cannot be used in correlation of the mudstones. Likewise the sedimentary structures which are present are restricted in their lateral distribution.

Geochemically, however, variations in the mudstones can be picked out and correlated over extensive areas. In particular, gamma-ray logging of boreholes has revealed variations in the Mercia Mudstone Group which can be correlated over large areas of Southwest Britain for which there is no obvious surface expression. These variations in gamma-ray value can be identified at outcrop and related to the presence of the clay mineral illite. Using these variations the successions of upper Mercia Mudstone Group studied in Devon and Somerset have been subdivided into an illite-rich upper section and a lower section in which mixed-layer clay varieties are more important, giving rise to a reduced gamma-ray signature. These outcrop variations can be correlated with similar patterns of gamma-ray values in borehole logs.

The sedimentological reasons for the changes in gamma-ray intensity and clay mineralogy are related to the hydrology of the basins in the Upper Triassic. During the Carnian, extensive incursions of marine-derived waters entered the system of basins, and halite was deposited in the deepest parts of the Devon - Dorset and Somerset basins. The retreat of these marine-derived waters

appears to have been a gradual one and this slow change in the composition of the waters gave rise to the mineralogical and geochemical variations in the mudstones. The more magnesium rich marine-derived waters will supply both  $K^+$  and  $Mg^{2+}$  to the degraded clay material entering the basin, forming a suite of clays including mixed-layer varieties. By contrast the continentally-derived waters supply less  $Mg^{2+}$  to the clays which will regrade to illite. The decrease in the proportion of mixed-layer clays in the upper red mudstones can be attributed to a reduction in the influence of marine-derived waters in the basin. Geochemically the carbonate in the lower red mudstones is relatively enriched in  $^{18}O$  and  $^{13}C$ , which is also indicative of a more marine water type. Nowhere in the mudstones covered in this study were fully marine stable isotopic values found. The waters from which the carbonate formed were of mixed marine-continental or fully continental origin.

The variations in gamma-ray value seen in the borehole logs in the upper Mercia Mudstone Group can thus be related to changes in the clay mineralogy which varies in response to the chemical composition of the depositional waters. Changes in clay mineralogy can be correlated between different sections in Devon and Somerset and give a lithological control to the changes seen in borehole logs throughout southwest Britain.

### 12.3 The Depositional Environment in South Wales

In South Wales a lesser thickness of Mercia Mudstone Group was laid down ( under 120 metres ). The changes in clay mineralogy and geochemistry seen in the sections in Devon and Somerset are not present in the reduced section which overlapped the basement in the late Norian. Only 30 metres of red mudstone underlying the Blue Anchor Formation are exposed. These samples contain carbonates with anomalously enriched  $^{18}O$  values relative to the sections in Devon and Somerset. From evidence at outcrop, the depositional environment of the mudstones in South Wales appears to have been different from that in other areas. There is evidence of a semi-permanent lake in the South Wales area as shown by a series of wave-cut platforms and well developed beach gravels and perilittoral sediments in exposures of marginal deposits southwest of Cardiff. There is also evidence of the fluctuation of the lake shoreline in response to changes in the

input of waters into the area. The enriched  $^{18}\text{O}$  values are indicative of a greater amount of evaporation of the waters in South Wales. They do not show any evidence of input of water from marine sources. There is much evidence in the Sully Island succession for a substantial input of meteoric water into the area. There is no direct evidence in the Somerset section for the presence of a permanent water body. The sedimentary structures which are present indicate that exposure of the beds was the more usual depositional environment. It appears that the lake in South Wales was restricted in area and that the South Wales and Somerset mudstones were laid down in separate subbasins during the Upper Norian.

## References

Note: in the case where more than one article or paper has been taken from a book the full reference for the book is given separately.

## References

- AITKEN, J.D. 1967 Classification and environmental significance of cryptalgal limestones and dolomites with illustrations from the Cambrian and Ordovician of south-west Alberta. *Journal of Sedimentary Petrology* **37**, 1163-1178.
- ALJUBOURI, Z.A. 1972 Geochemistry, Origin and Diagenesis of Some Triassic Gypsum Deposits and Associated Sediments in the East Midlands. Unpublished Ph.D. Thesis, University of Nottingham.
- AL-KATTAN, M.M. 1976 The Geochemistry of Lower Keuper Marl at Lavernock Point, Glamorgan, South Wales. Unpublished M.Sc. Thesis, University of Cardiff.
- ALLEN, J.R.L. 1986 Pedogenic calcretes in the Old Red Sandstone facies ( late Silurian - early Carboniferous ) in the Anglo-Welsh area, Southern Britain. In: Wright, V.P. ( ed. ) *Paleosols: Their Recognition and Interpretation*. Blackwell Scientific Publications, Oxford, 58-86.
- ALLEN, J.R.L. and MATTHEWS, R.K. 1982 Isotopic signatures associated with early meteoric diagenesis. *Sedimentology* **29**, 797-817.
- ANDERSON, T.F. and ARTHUR, M.A. 1983 Stable isotopes of oxygen and carbon and their application to sedimentologic and palaeoenvironmental problems. In: Arthur et al. ( eds. ), 1.1-1.151.
- ANGINO, E.E. and BILLINGS, G.K. 1972 *Atomic Absorption Spectrometry in Geology*, 2nd. Edition. Elsevier, Amsterdam, 191p.
- ARAKEL, A.V. 1982 Genesis of calcrete in Quaternary soil profiles, Hutt and Leman Lagoons, western Australia. *Journal of Sedimentary Petrology* **52**, 109-125.
- ARTHUR, M.A., ANDERSON, T.F., KAPLAN, I.R., VEIZER, J. and LAND, L.S. 1983 *Stable Isotopes in Sedimentary Geology*. S.E.P.M. Short Course No. 10, Dallas, 432pp.

- ARTHURTON, R.S. 1980 Rhythmic sedimentary sequences in the Triassic Keuper Marl ( Mercia Mudstone Group ) of Cheshire, northwest England. *Geological Journal* **15**, 43-58.
- ASSERTO, R.L.A.M. and KENDALL, G.G.St.C. 1977 Nature, origin and classification of peritidal tepee structures and related breccias. *Sedimentology* **24**, 153-210.
- AUDLEY-CHARLES, M.G. 1970a Stratigraphic correlation of the Triassic rocks of the British Isles. *Quarterly Journal of the Geological Society of London* **126**, 19-47.
- AUDLEY-CHARLES, M.G. 1970b Triassic palaeogeography of the British Isles. *Quarterly Journal of the Geological Society of London* **126**, 49-89.
- BAILEY, J. 1976 Trace element technique in the Institute for Petrology, University of Copenhagen. In Bailey, J. and Sorensen, I. X-ray fluorescence analysis. Internal Report, University of Copenhagen.
- BALCHIN, D.A. and RIDD, M.F. 1970 Correlation of the younger Triassic rocks across eastern England. *Quarterly Journal of the Geological Society of London* **126**, 91-101.
- BANNER, F.T., BROOKS, S.M. and WILLIAMS, E. 1971 The geology of the approaches to Barry, Glamorgan. *Proceedings of the Geological Association* **52**, 231-247.
- BARNABY, R.J. and RIMSTIDT, J.D. 1988 Correlation of calcite cathodoluminescence with redox conditions of carbonate cementation. ( Abstract ) Calcite Cements Meeting. The Geological Society, Burlington House.
- BISCAYE, P.E. 1965 Mineralogy and sedimentation of recent deep-sea clay in the Atlantic Ocean and adjacent seas and oceans. *Bulletin of the Geological Society of America* **76**, 803-832.
- BLUCK, B.J. 1965 The sedimentary history of some Triassic conglomerates in the Vale of Glamorgan, South Wales. *Sedimentology* **4**, 225-245.

- BOSWORTH, T.O. 1913 Keuper Marls around Charnwood. Leicester Literary and Philosophical Society. N.D. 129p.
- BOYLE, E.A. 1981 Calcium, zinc, copper and barium in foraminiferal tests. *Earth and Planetary Science Letters* **53**, 111-135.
- BRADSHAW, M.J. 1975 Origin of montmorillonite bands in the Middle Jurassic of Eastern England. *Earth and Planetary Science Letters* **26**, 245-252.
- BRAITHWAITE, C.J.R. 1979 Crystal textures of Recent fluvial pisolites and laminated crystalline crusts in Dyfed, South Wales. *Journal of Sedimentary Petrology* **49**, 181-194
- BROWN, G. and BRINDLEY, G.W. <sup>1980</sup> X-ray diffraction procedures for clay mineral identification. In: Brindley, G.W. and Brown, G. ( eds. ) *Crystal Structures of Clay Minerals and their X-ray Identification*. Mineralogical Society, London, 305-360.
- BROOKS, M. 1987 Geophysical investigations of deep structure in the Bristol Channel area. *Proceedings of the Geological Association* **98**, 397-398.
- BROOKS, M. and AL-SAADY, R.H. 1977 Seismic refraction studies of geologic structures in the inner part of the Bristol Channel. *Journal of the Geological Society of London* **133**, 433-445.
- BUSH, P. 1973 Some aspects of the diagenetic history of the sabkha in Abu Dhabi, Persian Gulf. In: Purser, B.H. ( ed. ) *The Persian Gulf*. Springer-Verlag, New York, 395-409.
- BUTLER, G.P. 1969 Modern evaporite deposition and geochemistry of coexisting brines, the sabkha, Trucial Coast, Arabian Gulf. *Journal of Sedimentary Petrology* **39**, 70-89.
- CASANOVA, J. 1984 Genèse des carbonates d'un travertin Pléistocène: Interprétation paléocéologique du sondage Peyre ( Compregnac Aveyron ). *Geobios Mémoire spécial No. 8*, 219-225.

CURTIS, M.T. 1982 Playa cycles in the Mercia Mudstone ( Keuper Marl ) of Aust Cliff, Avon. Proceedings of the Bristol Naturalists Society **42**, 13-22.

- CASSIDY, J. 1979 Gamma-ray spectrometric surveys of Caledonian granites: method and interpretation. Unpublished Ph.D. Thesis, University of Liverpool.
- CERLING, T.E. 1984 The stable isotopic composition of modern soil carbonates and its relationship to climate. *Earth and Planetary Science Letters* **71**, 229-356.
- CERLING, T.E., QUADE, J., WANG, Y. and BOWMAN, J.R. 1989 Carbon isotopes in soils and palaeosols as ecology and palaeoecology indicators. *Nature* **341**, 138-139.
- CHADWICK, R.A. 1985 Permian, Mesozoic and Cenozoic structural evolution of England and Wales in relation to the principles of extension and inversion tectonics. In: Whittaker ( ed. ), 9-25.
- CHAFETZ, H.S. and BUTLER, J.C. 1980 Petrology of recent caliche pisolites, spherulites and speleothem deposits from central Texas. *Sedimentology* **27**, 497-518.
- CHAFETZ, H.S., RUSH, P.F. and UTECH, N.M. 1989 Carbonate precipitation from moderately to extremely supersaturated waters: an example of significance of microenvironmental parameters. ( abstract ) A.A.P.G. Annual Convention, San Antonio, U.S.A.
- CHOQUETTE, P.W. and JAMES, N.P. 1986 Diagenesis in limestones - 3. The deep burial environment. *Geoscience Canada* **14**, 3-25.
- CONIGLIO, M. and HARRISON, R.S. 1983 Holocene and Pleistocene caliche from Big Pine Key, Florida. *Bulletin of Canadian Petroleum Geology* **31**, 3-13.
- COPE, J.C.W. 1984 The Mesozoic history of Wales. *Proceedings of the Geological Association* **95**, 373-385.
- CRAIG, H. 1957 Isotopic standards for carbon and oxygen and correction factors for mass-spectrometric analysis of carbon dioxide. *Geochimica et Cosmochimica Acta* **12**, 133-149.

- DAVIS, A.G. 1968 The structure of the Keuper Marl. *Quarterly Journal of Engineering Geology* **1**, 145-153.
- DEER, W.A., HOWIE, R.A. and ZUSSMAN, J. 1966 An introduction to the Rock-forming Minerals. Longman, Harlow, 528p.
- DEGENS, E.T. and EPSTEIN, S. 1964 Oxygen and carbon isotope ratios in coexisting calcites and dolomites from recent and ancient sediments. *Geochimica et Cosmochimica Acta* **28**, 23-44.
- DE LANGE, G.J., MIDDLEBURG, J.J. and PRUYERS, P.A. 1989 Middle and Late Quaternary depositional sequences and cycles in the eastern Mediterranean. *Sedimentology* **36**, 151-158.
- DUMBLETON, M.J. and WEST, G. 1966 Studies of the Keuper Marl: Mineralogy. Ministry of Transport Road Research Laboratory Report 40.
- ELLIOTT, R.E. 1961 The stratigraphy of the Keuper facies in southern Nottinghamshire. *Proceedings of the Yorkshire Geological Society* **33**, 197-234.
- EVANS, W.B., WILSON, A.A., TAYLOR, B.J. and PRICE, R.H. 1968 Geology of the country around Macclesfield, Congleton, Crewe and Middlewich. Memoir of the Geological Survey, United Kingdom, 328p.
- FAIRCHILD, I., HENDY, G., QUEST, M. and TUCKER, M.E. 1988 Chemical analysis of sedimentary rocks. In: Tucker ( ed. ), 274-354.
- FERGUSON, J., BURNE, R.V. and CHAMBERS, L.A. 1982 Lithification of peritidal carbonates by continental brines at Fisherman Bay, South Australia, to form a megapolygon / spelean limestone association. *Journal of Sedimentary Petrology* **52**, 1127-1147.
- FERGUSON, J., CHAMBERS, L.A. DONNELLY, T.H. and BURNE, R.V. 1988 Carbon and oxygen isotopic composition of a Recent megapolygon - spelean limestone, Fisherman Bay, South Australia. *Chemical Geology* **72**, 63-76.
- FOLK, R.L. <sup>1974</sup> The natural history of crystalline calcium carbonate: effect of

- magnesium content and salinity. *Journal of Sedimentary Petrology* **44**, 40-53.
- FOLK, R.L., CHAFETZ, H.S. and TIEZZI, P.A. 1985 Bizarre forms of depositional and diagenetic calcite in hot-spring travertines, central Italy. In: Scneideman and Harris ( eds. ), 349-369.
- GEBELEIN, C.D. and HOFFMAN, P. 1971 Algal origin of dolomite in interlaminated limestone-dolomite sedimentary rocks. In: Bricker, O.P. ( ed. ) *Carbonate Cements*. John Hopkins Press, Baltimore, 319-326.
- GIBBS, R.J. 1965 Error due to segregation in quantitative clay mineral x-ray diffraction mounting techniques. *American Mineralogist* **50**, 741-751.
- GIPSON, M. 1966 Preparation of orientated slides for x-ray analysis of clay minerals. *Journal of Sedimentary Petrology* **36**, 1143.
- GLENNIE, K.W. and EVANS, G. 1976 A reconnaissance of the Recent sediments of the Ranns of Kutch, India. *Sedimentology* **23**, 625-647.
- GOLDSMITH, J.R. and GRAF, D.L. 1958 Structural and compositional variations in some natural dolomites. *Geological Journal* **66**, 678-693.
- GREEN, G.W. and MELVILLE, R.V. 1956 The stratigraphy of the Stowell Park Borehole, ( 1949-1951 ). *Bulletin of the Geological Survey of Great Britain* **11**, 1-33.
- GREEN, G.W. and WELCH, F.B.A. 1965 *Geology of the country around Wells and Cheddar*. Memoir of the Geological Survey, United Kingdom, 285p.
- HAMILTON, D. and WHITTAKER, A. 1977 Coastal exposures near Blue Anchor, Watchet and St. Audrie's Bay, North Somerset. In: Savage, R.J.G. ( ed. ) *Geological Excursions in the Bristol District*. University of Bristol, 101-109.
- HANDFORD, C.R., KENDALL, A.C., PREZBINDOWSKI, D.R., DUNHAM, J.B. and LOGAN, B.W. 1984 Salina-margin tepees, pisoliths and aragonite cements, Lake MacLeod, Western Australia; their significance in interpreting

ancient analogues. *Geology* **12**, 523-527.

HARDIE, L.A. 1968 The origin of the recent non marine evaporite deposit of Saline Valley, Inyo County, California. *Geochimica et Cosmochimica Acta* **32**, 1297-1301.

HARRISON, R.K. 1971 The petrology of the Upper Triassic rocks in the Llanbedr ( Mochras Farm ) Borehole. In: Woodland, A.W. The Llanbedr ( Mochras Farm ) Borehole. Institute of Geological Sciences Report 71/18, 37-65.

HARDY, R. and TUCKER, M.E. 1989 X-ray powder diffraction of sediments. In: Tucker ( ed. ), 191-228.

HEIMANN, A. and SASS, E. 1989 Travertines in the northern Hula Valley, Israel. *Sedimentology* **36**, 95-108.

HENSON, M.R. 1973 Clay minerals from the Lower New Red Sandstone of South Devon. *Proceedings of the Geological Association* **84**, 429-445.

HIRD, K. 1985 Petrography and geochemistry of some Carboniferous and Precambrian dolomites. Unpublished Ph.D. Thesis, University of Durham.

HIRD, K. and TUCKER, M.E. 1988 Contrasting diagenesis of two Carboniferous Oolites from South Wales: a tale of climatic influence. *Sedimentology* **35**, 587-602.

HOFMANN, H.J. and JACKSON, G.D. 1987 Proterozoic ministromatolites with radial-fibrous fabric. *Sedimentology* **34**, 963-971.

HOLLOWAY, S. 1985 Triassic: Mercia Mudstone and Penarth Groups. In: Whittaker ( ed. ), 34-36.

HONEYBOURNE, D.B. 1951 The clay mineralogy in the Keuper Marl. *Clay Mineralogy Bulletin* **1**, 150.

HOWER, J. 1981 X-ray diffraction identification of mixed-layer clay minerals. In: Longstaffe, F.J. ( ed. ) Short course in clays and the resource geologist. Mineralogical Association of Canada short course notes. Co-op Press, Edmonton,

39-59.

HUDSON, J.D. 1977 Stable isotopes and limestone lithification. *Quarterly Journal of the Geological Society of London* **133**, 637-660.

HUNT, C.B., ROBINSON, T.W., BOWLES, W.A. and WASHBURN, A.L. 1966 Hydrologic basin, Death Valley, California. Professional Paper, U.S. Geological Survey **494B**.

JAGNOW, D.H. 1989 The geology of Lechuguilla Cave, New Mexico. In: *Subsurface and Outcrop Examination of the Capitan Shelf Margin, Northern Delaware*. S.E.P.M. Core Workshop No. 13, 459-466.

JEANS, C.V. 1978 The origin of the Triassic clay assemblages of Europe with special reference to the Keuper Marl and Rhaetic of parts of England. *Philosophical Transactions of the Royal Society of London* **A.289**, 549-639.

JUKES-BROWN, A.J. 1902 On a deep boring at Lyme Regis. *Quarterly Journal of the Geological Society of London* **63**, 279-289.

KENDALL, A.C. 1985 Radiaxial fibrous calcite: a reappraisal. In: Schneidemann and Harris ( eds. ), 59-78.

KENDALL, A.C. and BROUGHTON, P.L. 1978 Origin of fabrics in speleothems composed of columnar calcite crystals. *Journal of Sedimentary Petrology* **48**, 519-538.

KENDALL, A.C. and TUCKER, M.E. 1973 Radiaxial fibrous calcite: a replacement after acicular carbonate. *Sedimentology* **20**, 365-389.

KENDALL, C.G.St.C. and WARREN, J.K. 1987 A review of the origin and setting of tepees and their associated fabrics. *Sedimentology* **34**, 1007-1027.

KENDALL, C.G.St.C. and WARREN, J.K. 1988 Peritidal evaporites and their sedimentary assemblages. In: Schreiber, B.C. ( ed. ) *Evaporites and Hydrocarbons*. Columbia University Press, New York, 66-138.

- KLEIN, G.V. 1962 Sedimentary structures in the Keuper Marl ( Upper Triassic ). *Geological Magazine* **99**, 137-144.
- KOSTECA, A. and WECLAWICK, S. 1987 Mineral water deposits in vicinity of Tylicz ( Beskid Niski Range, Polish Flysch Carpathians ). *Annales Societatis Geologorum Polonae* **57**, 37-58.
- LAEGER, A.M. and KERR, P.F. 1966 Mojave playa crusts: physical properties and mineral content. *Journal of Sedimentary Petrology* **36**, 377-396.
- LAND, L.S. 1980 The isotopic and trace element geochemistry of dolomite: the state of the art. In: Zenger et al. ( eds. ), 87-110.
- LEAT, P.T., THOMPSON, R.N., MORRISON, M.A., HENDRY, G.L. and DICKIN, A.P. Geochemistry of mafic lavas in the early Rio Grande Rift, Yarmony Mountain, Colorado: lithospheric mantle versus crustal contamination of asthenospheric magmas. *Chemical Geology* in press.
- LIPPMAN, F. 1956 Clay minerals from the Röt Member of the Triassic near Göttingen, Germany. *Journal of Sedimentary Petrology* **2**, 125-139.
- LLOYD, A.J., SAVAGE, R.G.J., STRIDE, A.H. and DONOVAN, D.J. 1973 The geology of the Bristol Channel Floor. *Philosophical Transactions of the Royal Society* **A.274**, 595-626.
- LOGAN, B.W., READ, J.F., HAGAN, G.M., HOFFMAN, P., BROWN, R.G., WOODS, P.J. and GEBELEIN, C.D. 1974<sup>(eds.)</sup> Evolution and Diagenesis of Quaternary Carbonate Sequences, Shark Bay, Western Australia. *A.A.P.G. Memoir* **22** 358p.
- LOGAN, B.W., REZAK, R. and GINSBURG, R.N. 1964 Classification and environmental significance of algal stromatolites. *Journal of Geology* **72**, 68-83.
- LOMAS, J. 1907 Desert conditions and the origin of the British Triass. *Proceedings of the Liverpool Geological Society* **10**, 172-180.
- LOTT, G.K., SOBEY, R.A., WARRINGTON, G. and WHITTAKER, A. 1983

MANN, A.W. and HORWITZ, R.C. 1979 Groundwater calcrete deposits in Australia: some observations from Western Australia. *Journal of the Geological Society of Australia* **26**, 293-303.

MORROW, D.W. 1982 Dolomite - part 2. Dolomitisation models and ancient dolostones. *Geoscience Canada* **9**, 95-107.

The Mercia Mudstone Group ( Triassic ) in the western Wessex Basin. Proceedings of the Ussher Society **5**, 340-346.

LØVBORG, L. and MOSE, E. 1987 Counting statistics in radioelement assaying with a portable spectrometer. Geophysics **52**, 555-563.

LUCAS, J. 1962 La transformation des minéraux argileux dans la sédimentation études sur les argiles du Trias. Mémoires du service de la Carte Géologique d'Alsace et de Lorraine No. 23. Université de Strasbourg, 178p.

LUCAS, J. and ATAMAN, G. 1968 Mineralogical and geochemical study of clay mineral transformations in the sedimentary Triassic Jura Basin ( France ). Clays and Clay Minerals **16**, 365-372.

MACINTYRE, I.G. 1985 Submarine cements - the peloidal question. In: Schneidemann and Harris ( eds. ), 109-116.

McCREA, J.M. 1950 On the isotopic chemistry of carbonates and a palaeotemperature scale. Journal of Chemical Physics **18**, 849-857.

MANFRA, L., MASI, U. and TURI, B. 1976 La composizione isotopica dei travertini del Lazio. Geologica Romana **26**, 293-303.

MAYALL, M.J. 1979 The clay mineralogy of the Rhaetic transgression in Devon and Somerset - environmental and stratigraphic implications. Proceedings of the Ussher Society **4**, 303-311.

MAYALL, M.J. 1981 The Late Triassic Blue Anchor Formation and the initial Rhaetian marine transgression in south-west Britain. Geological Magazine **118**, 377-384.

MILLIKEN, K.L. 1979 The silicified evaporite system - two aspects of silicification history of former evaporite nodules from southern Kentucky and northern Tennessee. Journal of Sedimentary Petrology **49**, 245-256.

MISKIN, F.F. 1919 The Triassic Rocks of South Glamorgan. Transactions of the Cardiff Nature Society **52**, 17-25.

NANSON, G.C., YOUNG, R.W., PRICE, D.M. and RUST, B.R. 1988 Stratigraphy, sedimentology and Late Quaternary chronology of the Channel Country of Western Queensland. In: Warner, R.F. ( ed. ) Fluvial Geomorphology of Australia. Academic Press, Sydney, 151-175.

PURSER, B.H. ( ed. ) 1973 The Persian Gulf: Holocene Carbonate Sedimentation and Diagenesis in a Shallow Epicontinental Sea. Springer-Verlag, Berlin, 471p.

- MUIR, M., LOCK, D. and VON DER BORCH, C. 1980 The Coorong model for penecontemporaneous dolomite formation in the Middle Proterozoic McArthur Group, Northern territories, Australia. In: Zenger et al. ( eds. ), 51-68.
- MYERS, K.J. 1987 Onshore - outcrop gamma-ray spectrometry as a tool in sedimentological studies. Unpublished Ph.D. Thesis, University of London.
- NICKLESS, E.F., BOOTH, S.J. and MOSELEY, P.N. 1975 Celestite deposits of the Bristol area. Transactions of the Institute of Mining and Metallurgy (B) **84**, B62-B64.
- PEARCE, N.J.G. 1988 The petrology and geochemistry of the Igaliko dyke swarm, South Greenland. Unpublished Ph.D. Thesis, University of Durham.
- PENN, I.E. 1987 Geophysical logs in the stratigraphy of Wales and adjacent offshore and onshore areas. Proceedings of the Geological Association **98**, 275-314.
- PILOT, J., RÖSLER, H.J. and MÜLLER, P. 1972 Zur geochwischen entwicklung des meerwassers und mariner sedimente im Phanerozoickum mittels untersuchungen von S-, O- und C- isotopen. Nene Bergbautecknick **2**, 161-168.
- PLATT, N.H. 1989 Lacustrine carbonates and pedogenesis: sedimentology and origin of palustrine deposits from the Early Cretaceous Rupelo Formation, W Cameros Basin, N Spain. Sedimentology **36**, 665-684.
- PLILER, R. and ADAMS, J.A.S. 1962 The distribution of thorium, uranium and potassium in the Mancos Shale. Geochimica et Cosmochimica Acta **26**, 1115-1135.
- REVERDSKY, X., ARGAUD, M. and WALGENITZ, F. 1983 Mineralogical analysis required for log interpretation in complex lithologies. Eighth European Formation Evaluation Symposium Transactions, H1-H24.
- ROBINSON, P. 1980 Determination of calcium, magnesium, manganese, strontium, sodium and iron in the carbonate fraction of limestones and dolomites.

RUST, B.R. and NANSON, G.C. 1989 Bedload transport of mud as pedogenic aggregates in modern and ancient rivers. *Sedimentology* **36**, 291-306.

- Chemical Geology **28**, 135-146.
- ROSEN, M.R., MISER, D.E. and WARREN, J.K. 1988 Sedimentology, mineralogy and isotopic analysis of Pellet Lake, Coorong region, South Australia. *Sedimentology* **35**, 105-122.
- ROSENBAUM, J. and SHEPPARD, S.M.F. 1986 An isotopic study of siderites, dolomites and ankerites at high temperatures. *Geochimica et Cosmochimica Acta* **50**, 1147-1150.
- SCHLUMBERGER 1972 Log Interpretation Volume 1 - Principles. Schlumberger Ltd., New York, 113p.
- SCHNEIDEMANN, N.Z. and HARRIS, P.M. ( eds. ) 1985 Carbonate Cements. S.E.P.M. Special Publication No. 36, 379p.
- SCHULTZ, L.G. 1964 Quantitative interpretation of mineralogical composition from x-ray and chemical data for the Pierre Shale. United States Geological Survey Professional Paper 391-C.
- SHARMA, T. and CLAYTON, R.N. 1965 Measurement of oxygen isotopic ratios of total oxygen of carbonates. *Geochimica et Cosmochimica Acta* **29**, 1347-1353.
- SHEARMAN, D.J. 1966 Origin of marine evaporites by diagenesis. *Transactions of the Institute of Mining and Metallurgy ( B )* **75**, B208-B215.
- SHEPPARD, S.M.F. and SCHWARCZ, H.P. 1970 Fractionation of carbon and oxygen isotopes and magnesium between coexisting metamorphic calcite and dolomite. *Contributions to Mineralogy and Petrology* **26**, 161-198.
- SHERLOCK, R.L. 1928 A correlation of the British Permo-Triassic rocks Part II; England south of the Pennines and Wales. *Proceedings of the Geological Association* **39**, 49-95.
- SOUTHWORTH, C.J. 1987 Lithostratigraphy and depositional history of the Middle Triassic Dowsing Dolomite Formation of the Southern North Sea and

STEINEN, R.P., GRAY, N.H. and MOONEY, J. 1987 A Mesozoic carbonate hot-spring deposit in the Hartford Basin of Connecticut. *Journal of Sedimentary Petrology* 57, 319-326.

- adjoining areas. Unpublished Ph.D. Thesis, University of Oxford.
- SPOLJARIC, N. 1971 Quick preparation of slides of well-orientated clay minerals for x-ray diffraction analysis. *Journal of Sedimentary Petrology* **41**, 588-589.
- STEVENSON, C.R. and WARRINGTON, G. 1971 Jurassic and Cretaceous rocks of Wessex; Highest Keuper deposits. *Proceedings of the Geological Association* **82**, 297.
- STAHAN, A. and CANTRILL, T.C. 1912 The geology of the South Wales Coalfield Part III; The country around Cardiff. *Memoir of the Geological Survey of the United Kingdom*, 100p.
- TAYLOR, S.R. 1982 The Trent, Glen Parva and Blue Anchor Formations ( Upper Triassic ) of the East Midlands and their sulphate deposits. Unpublished Ph.D. Thesis, University of Leicester.
- TAYLOR, S.R. 1983 A stable isotope study of the Mercia Mudstone ( Keuper Marl ) and associated sulphate horizons in the English Midlands. *Sedimentology* **30**, 11-31.
- THOMAS, A.N. 1940 The Triassic rocks of north-west Somerset. *Proceedings of the Geological Association* **51**, 1-43.
- THOMAS, T.M. 1952 Notes on the structure of some minor outlying occurrences of littoral Triass in the Vale of Glamorgan. *Geological Magazine* **89**, 153-162.
- THOMAS, T.M. 1968 The Triassic of the west-central section of the Vale of Glamorgan. *Proceedings of the Geological Association* **79**, 429-439.
- THOMPSON, P., SCHWARTZ, H.P. and FORD, D.C. 1976 Stable isotope geochemistry, geothermometry and geochronology of speleothems from West Virginia. *Bulletin of the Geological Society of America* **87**, 1730-1738.
- THOREZ, J. 1975 *Phyllosilicates and clay minerals*. Editions G. Letotte,

TUCKER, M.E. ( ed. ) 1988 Techniques in Sedimentology. Blackwell, Oxford, 394p.

Belgium, 582p.

TOWE, K.M. 1974 Quantative clay petrology: the trees but not the forest. *Clays and Clay Mineralogy* **22**, 375.

TREWIN, N.H. 1988 Use of the Scanning Electron Microscope in sedimentology. In: Tucker ( ed. ), 229-273.

TUCKER, M.E. 1974 Exfoliated pebbles and sheeting in the Triassic. *Nature* **252**, 375-376.

TUCKER, M.E. 1975 Vadose diagenetic fabrics in Triassic lacustrine limestones from South Wales. Ninth Congres International de Sedimentologie, Nice.

TUCKER, M.E. 1976 Quartz replaced anhydrite nodules ( 'Bristol Diamonds' ) from the Triassic of the Bristol District. *Geological Magazine* **113**, 569-574.

TUCKER, M.E. 1977 The Marginal Triassic deposits of South Wales: Continental facies and palaeogeography. *Geological Journal* **12**, 169-188.

TUCKER, M.E. 1978 The marginal Triassic deposits from South Wales: shore zone clastica, evaporites and carbonates. In: Matter, A. and Tucker, M.E. ( eds. ) *Modern and Ancient Lake Sediments*. Special Publication of the International Association of Sedimentology 2, Blackwell Scientific Publications, 205-224.

TUCKER, M.E. 1981 *Sedimentary Petrology - an Introduction*. Blackwell Scientific Publications, 252p.

TUCKER, M.E. and BURCHETTE, T.P. 1977 Triassic dinosaur footprints from South Wales: their context and preservation. *Palaeogeography, Palaeoecology and palaeoclimatology* **22**, 195-208.

TUCKER, M.E. and LESLIE, A.B. In Press Triassic ( 'Keuper' ) lacustrine stromatolites from South Wales, U.K. ( in press )

TUCKER, R.M. and TUCKER, M.E. 1981 Synsedimentary tectonics in the Cheshire Halite. *Nature* **290**, 495-496.

- VEIZER, J. 1983 Chemical diagenesis of carbonates: theory and application of trace element technique. In: Arthur et al. ( eds. ), 3-1 - 3-100.
- VEIZER, J. and DEMOVIC, R. 1974 Strontium as a tool in facies analysis. *Journal of Sedimentary Petrology* **44**, 93-115.
- VEIZER, J. and HOEFS, J. 1976 The nature of  $O^{18}/O^{16}$  and  $C^{13}/C^{12}$  secular trends in sedimentary carbonate rocks. *Geochimica et Cosmochimica Acta* **40**, 1387-1395.
- VEIZER, J., LEMIEUX, J., JONES, B., GIBLING, M.R. and SAVELLE, J. 1977 Sodium: Palaeosalinity indicator in ancient carbonate rocks. *Geology* **5**, 177-179.
- VON DER BORCH, C.F., BOLTON, B. and WARREN, J.K. 1977 Environmental setting and microstructure of subfossil lithified stromatolites associated with evaporites, Marion Lake, South Australia. *Sedimentology* **24**, 693-708.
- WALKER, T.R. 1975 Diagenetic origin of continental red beds. In: Falke, H. *The continental Permian in central, west and south Europe*. D. Reidel, Dortrecht, Holland, 240-282.
- WARREN, J.K. 1982 The hydrological significance of tepees, stromatolites and boxwork limestones in coastal salinas in South Australia. *Journal of Sedimentary Petrology* **52**, 1171-1201.
- WARRINGTON, G. 1970 The stratigraphy and palaeontology of the 'Keuper' series of the central Midlands of England. *Quarterly Journal of the Geological Society of London* **126**, 183-223.
- WARRINGTON, G. 1974 Les évaporite du Triass britannique. *Bulletin du Société Géologique Francaise* **7**, 708-723.
- WARRINGTON, G. 1976 British Triassic palaeontology *Proceedings of the Ussher Society* **3**, 341-553.
- WARRINGTON, G., AUDLEY-CHARLES, M.G., ELLIOTT, R.E., EVANS,

- W.B., IVEY-COOK, H.C., KENT, P.E., ROBINSON, P.L., SHOTTON, F.W. and TAYLOR, F.M. 1980 A correlation of Triassic rocks in the British Isles. Special Report of the Geological Society of London 13, 78p.
- WATERS, R.A. and LAWRENCE, D.J.D. 1987 Geology of the South Wales Coalfield, Part III, the country around Cardiff. 3rd. edition. Memoir of the British Geological Survey, 114p.
- WEAVER, C.E. 1956 The distribution and identification of mixed-layer clays in sedimentary rocks. *American Mineralogist* 41, 202-221.
- WEIGEL, F. 1986 Uranium. In: Katz, J.J., Seaborg, G.T. and Moss, L.R. ( eds. ) *The chemistry of the actinide elements - 2nd. edition. 1. Actinide elements.* Chapman and Hall, London, 169-442.
- WELTON, J.E. 1984 SEM Petrology Atlas. A.A.P.G., Tulsa, 237p.
- WHITTAKER, A. 1975 A postulated post-Hercynian rift valley system in southern Britain. *Geological Magazine* 112, 137-149.
- WHITTAKER, A. 1980 Triassic salt deposits in southern England. Proceedings of the 5th. Symposium on Salt. Northern Ohio Geological Society, 175-179.
- WHITTAKER, A. ( ed. ) 1985 Atlas of Onshore Sedimentary Basins in England and Wales: Post-Carboniferous Tectonics and Stratigraphy. Blackie, London, 71p.
- WHITTAKER, A. and GREEN, G.W. 1983 Geology of the country around Weston-super-Mare. Memoir of the British Geological Survey, 147p.
- WHITTAKER, A., HOLLIDAY, D.W. and PENN, I.F. 1985 Geophysical logs in British stratigraphy. Special Report of the Geological Society of London 18, 74p.
- WILLS, L.J. 1970 The Triassic succession in the central Midlands, in its regional setting. *Quarterly Journal of the Geological Society of London* 126, 225-283.

WRIGHT, V.P. 1983 A rendzina from the Lower Carboniferous of South Wales. *Sedimentology* **30**, 159-179.

WILLS, L.J. 1976 The Triassic of Worcester and Warwickshire. report of the Institute of Geological Sciences 76/2, 1-211.

WOLLAST, R., MACKENSIE, F.T. and BRICKER, O.P. 1968 Experimental precipitation and genesis of sepiolite at earth-surface conditions. *American Mineralogist* **35**, 1645-1662.

WRIGHT, V.P. 1988 A genetic classification of ancient and modern calcretes based on microstructure. ( abstract ) 9th. I.A.S. Regional Meeting of Sedimentologists, Leuven, Belgium.

WRIGHT, V.P., NORTH, C.P., HANCOCK, P.L. and ROBINSON, D. 1988a Pedofacies variations across an arid alluvial basin: a case-study from the Upper Triassic of S.W. Britain. 9th. ( abstract ) I.A.S. regional Meeting of Sedimentologists, Leuven, Belgium.

WRIGHT, V.P., PLATT, N.H. and WIMBLEDON, W.A. 1988b Biogenic laminar calcretes: evidence of calcified root-mat horizons in palaeosols. *Sedimentology* **35**, 603-620.

YURTZEVER, Y. 1975 Worldwide survey of stable isotopes in precipitation. I.A.E.A. Report of the Section of Isotope Hydrology, 40p.

ZENGER, D.H., DUNHAM, J.B. and ETHINGTON, R.L. ( eds. ) 1980 Concepts and Models for Dolomitisation. S.E.P.M. Special Publication Number 28. Tulsa, Oklahoma, 320p.

## Appendices

## Appendix 1

### Carbonate Cation Chemistry Analytical Techniques

#### A.1.1 Introduction

Trace element analyses were carried out on both the dolomites and limestones of the Sully Island sequence and on the carbonate fraction of the mudstones in the Mercia Mudstone Group. The majority of samples were analysed by Inductively-Coupled Plasma Atomic Emmission Spectrometry ( ICP-AES ). This technique did not provide information on the distribution of sodium in the carbonate fraction and this data were provided by Atomic Absorption Spectrophotometry ( AAS ) analyses.

#### A.1.2 Atomic Absorption Spectrophotometry.

Forty samples taken from the Sully Island succession were analysed by AAS before the problems of stability of the detector became apparent. For this reason the results from the AAS analyses were not used in this study. The data for sodium, however, which were not available by ICP-AES analysis, are used qualitatively and so the technique is here described briefly. The methods used are taken from Angino & Billings ( 1972 ) and Hird ( 1985 ). 0.2 of a gram of oven dried powdered sample were digested in 25 millilitres of acid ( 10% HCl for dolomites put in an oven at 60°C for 4 hours; 3% CH<sub>3</sub>COOH for limestones ) and made up to 50 millilitres with deionised water. Samples were then diluted to the required concentration and measured on the AAS relative to elemental standard solutions. Blanks were prepared in a similar way. Repeatability of the results, in particular for Ca, Mg and Sr, was poor and the data were not of sufficient quality to be used in this study. The Na data were more stable and had a repeatability of  $\pm 10\%$  . The forty Na values used in this study are given in Table A.1.1 .

### A.1.3 Inductively-Coupled Plasma Atomic Emission Spectrometry.

Fifty-five samples from the Sully Island succession and 108 from the three cliff sections of the Mercia Mudstone Group were analysed by ICP-AES . Samples were prepared by the following method. 5 millilitres of HCl were added to 40 milligrams of oven-dried powdered sample and these were placed in an oven at 60°C for 4 hours. Five millilitres of deionised water were then added to the sample. Blanks were prepared in a similar fashion. Contamination of samples by iron leached from clay minerals has been reported ( Robinson, 1980 ). The samples in the Sully Island succession contain little clay material but the samples of Mercia Mudstone Group contain between 20 and 80% of clay minerals. There is no correlation, however, between the percentage of clays in any one sample and the concentration of iron in the carbonate fraction. The contamination of the Mercia Mudstone Group samples by iron, although not discounted, does not appear to have had a significant effect on the variations in Fe content seen in the mudstones.

The ICP-AES provided information on the concentrations of Fe, Mn, Zn and Sr within the carbonate as well as the amounts of Ca and Mg . Repeatability of the results was to within  $\pm 1\%$  . The results of these trace elemental analyses are presented in Tables A.1.2 to A.1.7 .

Table A.1.1 A.A.S. Sodium Analyses, Sully Island Succession. The left hand column contains dolomitic samples from the beds both above and below the Limestone Unit. Only one sample of dolomitised limestone is included. The right hand column contains samples from the Limestone Unit composed of low-Mg calcite.

Description	Na <sub>ppm</sub>
basal dolom	231
basal ferricrete	371
white dolom	882
dolom, qtz nodule	940
carb nodule	574
'sabkha' dolom	684
'sabkha' nodule	2607
carb nodule	554
calcrete	408
calcrete nodule	759
top dolom	2636
dolomitised lst	608
trans bed	944
trans bed	1312
trans bed	773
trans bed	775
trans bed	6047
trans bed	3352
trans bed	1890
trans bed	569

Description	Na <sub>ppm</sub>
fenestral lst	54
fenestral lst	134
microbial lst	140
laminated lst	111
flowstone	54
floe calcite	92
floe calcite sed	301
pisolith	239
pisolith	572
lam pisolith	1059
flowstone	354
flowstone	199
vadose cav	341
vadose cav	93
flowstone	432
flow + microb	229
microb lst	607
peloidal lst	257
calcrete	229
flow dolom	142

Table A.1.2 Trace Elemental Values, Evaporitic Dolomite Unit and the Transitional Beds overlying the Limestone Unit, Sully Island.

Description	Fe <sub>ppm</sub>	Mn <sub>ppm</sub>	Zn <sub>ppm</sub>	Sr <sub>ppm</sub>	% MgCO <sub>3</sub>
ferricrete	5719	1283	27	62	100.1
white dolom	3096	1115	23	136	100.7
'sabkha' nod	1079	462	19	185	86.7
'sabkha' dolom	8230	663	211	291	78.1
carb nod	1722	576	18	94	65.8
calcrete nod	2109	574	26	202	76.0
calcrete dolom	2646	748	26	108	77.3
top dolom	2555	1008	42	71	101.0
trans bed	2975	1207	17	35	100.5
trans bed	5616	1427	33	48	102.1
trans bed	3683	1555	20	36	98.3
trans bed	5763	1494	43	50	100.3
trans bed	2555	1008	42	71	101.0

Table A.1.3 Trace Elemental Values, Clastic Beds, Limestone Unit, Sully Island.

Sample No.	Fe <sub>ppm</sub>	Mn <sub>ppm</sub>	Zn <sub>ppm</sub>	Sr <sub>ppm</sub>	% MgCO <sub>3</sub>
F1	1434	671	22	108	10.1
F4	1044	262	22	144	5.5
F7	1368	2002	16	72	11.8
F10	1024	219	60	131	2.8
F12	1866	183	47	134	2.7
F14	1203	457	50	68	5.7
F18	1304	227	56	85	2.3
F22	2209	134	103	89	3.1
F28	1340	192	110	87	4.3
F33	1281	313	48	82	2.7
F34	1530	185	57	117	2.9
F36	1311	176	75	108	2.7
F40	1512	162	55	84	2.6

Table A.1.4 quad Trace Elemental Values, Limestone Unit, Sully Island and Dinas Powys, ( plus one Carboniferous Limestone sample ).

Description	Fe <sub>ppm</sub>	Mn <sub>ppm</sub>	Zn <sub>ppm</sub>	Sr <sub>ppm</sub>	% MgCO <sub>3</sub>
basal calcrete	1172	564	147	83	2.4
basal calcrete	455	126	75	62	1.4
fenestral lst	2472	1385	24	76	25.1
microbial lst	140	287	212	65	2.0
vad cav	391	159	107	102	2.3
vad sed	1945	438	342	93	3.5
fenestral sed	1878	1102	65	104	3.4
fenestral spar	897	503	19	91	3.6
peloidal lst	630	686	137	75	4.0

Table A.1.4 ( cont. ).

Description	Fe <sub>ppm</sub>	Mn <sub>ppm</sub>	Zn <sub>ppm</sub>	Sr <sub>ppm</sub>	% MgCO <sub>3</sub>
floe calcite	114	188	130	56	1.9
pisolith	214	335	132	60	2.2
pisolith	234	215	176	67	2.5
flowstone A	72	90	164	119	2.7
flowstone B	57	50	230	85	2.2
flowstone sed	1386	308	139	86	2.3
flowstone A	124	487	161	72	2.8
flowstone B	71	225	288	87	2.7
flowstone C	102	267	340	95	2.9
flowst dolom	8708	1744	63	55	77.2
laminated lst	375	852	5	99	1.5
laminated lst	102	174	399	336	7.8
nod calcrete	1236	830	55	72	1.9
nod calcrete	1257	130	153	113	3.6
microbial mounds	183	115	300	147	4.0
fissure fills	486	1123	7	95	5.3
Carb. Lst.	2143	1156	21	58	89.1

Table A.1.5 Trace Elemental Values, Mercia Mudstone Group, Seaton and Brancecombe Cliffs, Devon. Heights quoted are in metres, relative to the base of the Blue Anchor Formation which serves as a datum for the purposes of correlating the three Mercia Mudstone Group sections.

Height	Description	Fe <sub>ppm</sub>	Mn <sub>ppm</sub>	Zn <sub>ppm</sub>	Sr <sub>ppm</sub>	% MgCO <sub>3</sub>
+12.0	Devon 1	5386	719	15	173	100.9
+8.0	green mud	7315	1299	22	234	91.6
+6.0	red mud	6984	1604	21	388	87.3
+4.0	green mud	3851	1271	20	190	91.6
+2.0	green mud	5543	1459	32	271	72.6
-1.0	red mud	5313	1936	32	257	89.6
-2.5	green mud	4755	1486	31	378	52.3
-4.0	red mud	7505	1768	57	431	68.5
-6.5	red mud	6112	1898	40	372	46.1
-7.0	green mud	5348	1300	44	597	28.3
-9.0	red mud	5802	1835	49	355	34.5
-12.0	red mud	5111	1796	49	410	29.2
-16.0	red mud	6089	1667	57	502	23.1
-17.5	green mud	6309	1352	74	644	26.9
-18.0	red mud	8856	1901	65	487	38.7
-19.0	red mud	7630	1821	65	533	36.2
-21.0	red mud	13408	2271	103	465	41.9

Table A.1.5 ( cont. ).

Height	Description	Fe <sub>ppm</sub>	Mn <sub>ppm</sub>	Zn <sub>ppm</sub>	Sr <sub>ppm</sub>	% MgCO <sub>3</sub>
-25.0	red mud	6998	1825	74	535	31.8
-26.0	red mud	8153	1833	93	700	33.2
-28.0	green mud	6385	1623	79	714	25.6
-31.0	red mud	6125	2255	87	426	37.7
-34.0	green mud	7650	2552	99	375	48.7
-37.0	red mud	6244	2456	95	678	49.6
-38.0	red mud	5565	2478	82	866	44.1
-41.0	red mud	10798	2949	101	2470	46.2
-42.0	green mud	14336	2358	448	1478	46.2
-43.0	green mud	5540	2010	70	86682	24.8
-46.0	green mud	13526	2409	135	902	39.1
-46.5	red mud	8531	2464	84	2761	46.8
-65.0	red mud	20638	1530	185	384	86.4
-75.0	red mud	14758	1141	235	499	43.3
-84.0	red mud	21994	2430	149	326	100.2
-100.0	Devon 2	8464	1047	208	98573	73.8
-120.0	Devon 3	3508	1162	63	665	101.3

Table A.1.6 Trace Elemental Values, Mercia Mudstone Group, St. Audrie's Bay, Somerset.

Height	Description	Fe <sub>ppm</sub>	Mn <sub>ppm</sub>	Zn <sub>ppm</sub>	Sr <sub>ppm</sub>	% MgCO <sub>3</sub>
+34.3	green mud	22503	4850	31	6273	90.6
+11.7	green mud	11770	2708	50	399	94.3
+6.7	green mud	11736	1649	53	4395	93.7
+3.0	green mud	4636	815	16	630	19.4
+0.9	green mud	7326	1375	40	410	74.7
+0.5	red mud	12574	1726	55	366	92.5
+0.2	green mud	7844	1791	43	371	93.7
-0.1	red mud	9167	1581	46	42	94.3
-0.5	red mud	13926	1721	64	355	97.2
-1.0	green mud	24810	1521	100	995	59.3
-4.0	red mud	11394	1753	52	534	76.1
-8.0	Somerset 1	8198	1118	55	498	44.9
-8.5	green mud	10058	1542	74	520	61.0
-9.0	red mud	8666	1515	59	607	55.9
-10.0	Somerset 2	12614	1386	72	744	33.1
-10.5	green mud	5333	1823	37	710	46.1
-12.5	green mud	9010	1636	71	820	42.9
-15.0	red mud	9763	1703	86	617	41.5

Table A.1.6 ( cont. ).

Height	Description	Fe <sub>ppm</sub>	Mn <sub>ppm</sub>	Zn <sub>ppm</sub>	Sr <sub>ppm</sub>	% MgCO <sub>3</sub>
-15.7	green mud	7730	1710	79	679	32.3
-19.7	green carb	5563	2305	107	485	33.8
-21.5	red mud	9312	2223	79	677	42.8
-23.1	green mud	4575	1776	63	485	20.7
-24.2	red mud	2808	1968	54	500	13.6
-26.2	red mud	5988	1866	114	639	27.9
-30.8	green mud	5075	4708	74	456	55.8
-32.8	red mud	7689	2090	101	594	34.9
-35.0	red mud	9319	1638	87	602	35.1
-37.0	red mud	11387	2670	112	369	60.8
-39.0	red mud	6394	1781	115	538	23.4
-45.0	red mud	12295	2397	109	308	57.4
-49.0	red mud	12911	2222	201	376	68.2
-51.0	red mud	11248	2635	110	306	64.9
-53.0	red mud	9184	2246	131	444	42.1
-55.4	green mud	13282	2428	102	375	24.1

Table A.1.6 ( cont. ).

Height	Description	Fe <sub>ppm</sub>	Mn <sub>ppm</sub>	Zn <sub>ppm</sub>	Sr <sub>ppm</sub>	% MgCO <sub>3</sub>
-57.0	red mud	9557	2562	119	319	55.4
-61.0	red mud	15755	2207	156	225	100.0
-73.0	red mud	15495	3212	130	156	101.4
-79.7	red mud	13924	1062	186	144	40.3
-86.7	red mud	12417	1416	99	133	22.0
-92.7	red mud	12800	1338	84	111	20.0
-102.0	Somerset 3	9025	2467	299	117	0.0
-111.0	red mud	24682	2921	135	178	102.0
-121.0	red mud	21571	2803	168	294	76.4
-123.0	red mud	14580	3297	110	249	94.5
-128.4	green mud	4571	2680	45	287	37.4
-129.4	red mud	18103	3054	126	213	89.6
-133.4	red mud	12188	2744	111	265	74.0
-138.4	red mud	10784	1874	112	395	44.7
-146.5	red mud	5514	1714	71	305	53.7

Table A.1.7 Trace Elemental Values, Mercia Mudstone Group, Penarth Cliffs, South Wales.

Height	Description	Fe <sub>ppm</sub>	Mn <sub>ppm</sub>	Zn <sub>ppm</sub>	Sr <sub>ppm</sub>	% MgCO <sub>3</sub>
+14.6	green mud	15634	1167	55	415	74.7
+10.9	green mud	6260	2000	13	4122	45.6
+5.6	green mud	15510	1383	47	771	91.6
+5.0	green mud	16174	1229	91	33850	69.2
+4.8	red mud	11124	1809	28	1876	95.5
+2.0	Wales 1	6720	1023	24	346	99.5
+1.1	green mud	10596	1392	32	934	95.5
+0.1	green mud	998	630	40	29101	5.3
-0.2	green mud	4256	1845	45	11307	97.3
-0.8	green mud	71791	1362	392	1985	101.3
-2.4	red mud	11788	2074	87	1116	98.2
-5.4	red mud	8075	2399	90	11550	95.6
-5.8	Wales 2	6175	1706	40	31096	103.6
-7.3	green mud	5638	1997	86	478	96.5
-10.4	red mud	13715	2200	163	519	97.4
-12.2	red mud	11314	2236	163	2491	90.8
-14.2	red mud	10990	2781	135	2837	97.8
-16.7	Wales 3	12220	2092	143	292	100.3
-30.0	red mud	6460	2232	115	211	103.6

## Appendix 2

### Stable Isotopic Analyses

#### A.2.1 Notation

Stable isotopic compositions are reported in the  $\delta$  notation as follows:

$$\delta_{(x)} = \frac{R_{(x)} - R_{(std)}}{R_{(std)}} \times 10^3 \quad A.2.1$$

where  $R_{(x)}$  is the isotopic ratio  $^{13}\text{C} / ^{12}\text{C}$ ,  $^{18}\text{O} / ^{16}\text{O}$  of the sample and  $R_{(std)}$  is the corresponding ratio of the standard.

Isotopic fractionation between two substances A and B, which occurs during any chemical process, is expressed as a fractionation factor:

$$\alpha_{(A-B)} = \frac{R_{(A)}}{R_{(B)}} = \frac{1000 + \delta_{(A)}}{1000 + \delta_{(B)}} \quad A.2.2$$

All samples are reported in permil ( ‰ ) relative to an internationally accepted standard, PDB.

#### A.2.2 Methods

Sample preparation and analytical methods are standard and are based on those given in McCrea ( 1950 ) and Craig ( 1957 ). The techniques involve the extraction of  $\text{CO}_2$  from carbonate samples and measurement of its isotopic composition using a mass spectrometer.

Sampling of the carbonates from South Wales was carried out after petrographic study. Between 5 and 15 milligrams of sample were removed using a hand-held rotary drill with a 0.8 millimetre diameter burr. In the case of analysis of the Mercia Mudstone Group, whole-rock samples between 10 and 80 milligrams were used depending on the proportion of non-carbonate in the rock. Samples were reacted under vacuum with 4 millilitres of 100% phosphoric acid at 25°C for

the samples composed of calcite, and 55°C in the case of dolomitic or mixed-carbonate samples. The samples were reacted for up to 24 hours, until the reaction was complete.

The evolved CO<sub>2</sub> gas was then analysed on a V.G. Isogas Sira 12 and V.G. Micromass 903 triple collector mass spectrometer. Raw data as  $\delta 45$  and  $\delta 46$  ratios were converted to  $\delta$  notation relative to the PDB standard by on-line computer.

In the case of the samples reacted at 55°C, additional corrections were necessary to take account of the temperature dependant fractionation of oxygen (Sharma & Clayton, 1965; Rosenbaum & Sheppard, 1986). The  $\delta^{18}O$  value obtained from the mass spectrometer is calculated assuming a reaction temperature of 25°C, and the computer uses an appropriate fractionation factor. In order to correct the  $\delta^{18}O$  values in carbonate samples run at 55°C, a fractionation factor for reactions at the elevated temperature was calculated by reacting the laboratory standard (TDS,  $^{18}O = -10.797$  at 25°C) at both temperatures.

Using the equation:

$$\delta^{18}O = \frac{\delta^{18}O_{meas} + 1000}{\alpha_{25}} - 1000 \quad A.2.3$$

The fractionation factor for the reaction of dolomite at 55°C ( $\alpha_{55}$ ) can be calculated and the data from samples reacted at the higher temperature adjusted manually. In practice the TDS standard was included in every batch of samples reacted at the higher temperature and a fractionation factor was calculated for each batch. This was necessary since it was found that the  $\delta^{18}O$  of the standard tended to drift during the time spent in the laboratory. The value of  $\alpha_{55}$  varied between 1.0095 and 1.0098. Duplicate dolomite standards run at 25°C differed by  $\pm 0.3\%$  from the calculated 55°C results. These values are similar to those reported by Hird (1985). All of the dolomitic samples taken from the Mercia Mudstone Group in this study were reacted at the higher temperature.

Duplicate analyses of at least one sample in each batch of 16 were carried out in order to ensure precision of the results. The laboratory calcite standard (MCS) was also analysed in each run. The following data were obtained (n=38).

isotope	value	$\sigma$	$\frac{2\sigma}{\sqrt{n}}$
$\delta^{18}O$	-9.177	$\pm 0.110$	0.043
$\delta^{13}C$	-0.700	$\pm 0.211$	0.080

Average sample reproducibility based on 30 samples, is  $\delta^{18}O \pm 0.144\text{‰}$  and  $\delta^{13}C \pm 0.102\text{‰}$ . Stable isotopic data are listed in tables A.2.1 to A.2.6 in parts per thousand on the PDB scale. Mineralogy is described as calcite ( C ) or dolomite ( D ).

Table A.2.1 Stable Isotopic Results, Evaporitic Dolomite Unit and mudstones overlying the Limestone Unit.

Sample No.	Description	Mineralogy	$\delta^{13}C$	$\delta^{18}O$
1	basal dolomite	D	-0.6	-6.4
2	basal ferricrete	D	-1.3	+0.9
3	sediment, 'sabkha band'	D	+0.4	-4.3
4	'sabkha' nodule	C	-1.3	-2.1
5	'sabkha' nodule	C/D	-1.2	-0.7
6	g.w. calcrete	D	-2.2	+0.8
7	sediment, in 6	D	-1.8	-0.5
8	sediment, top unit	D	-3.4	-3.6
9	0.1 m. above lst.	D	-2.7	-1.4
10	1.0 m. above lst.	D	-2.1	-1.6
11	4.0 m. above lst.	D	-0.4	-0.7

Table A.2.2 Stable Isotopic Results, Limestone Unit ( not travertines ).

Sample No.	Description	Mineralogy	$\delta^{13}C$	$\delta^{18}O$
1	basal calcrete	C	-6.4	-4.6
2	basal calcrete	C	-4.3	-4.0
3	vein in calcrete	C	-5.1	-4.4
4	nodular calcrete	C	-2.3	-3.8
5	sediment, in 4	C	-1.7	-3.2
6	intrapelsparite	C	-4.1	-5.3
7	intrapelsparite	C	-5.4	-4.1
8	intrapelsparite	C	-5.8	-4.8
9	clastic lst.	C	-1.5	-4.8
10	pelleted lst.	C	-2.9	-3.9
11	laminated lst.	C	-3.6	-3.8
12	microbial beds	C	-4.1	-3.6
13	microbial beds	C	-3.8	-3.8
14	spar, microbial beds	C	-4.0	-4.0
15	spar, fenestral lst.	C	-4.8	-5.5
16	spar, fenestral lst.	C	-7.8	-5.7
17	dolomitised lst.	D	-2.2	-4.7
18	dolomitised lst.	D	-3.5	-1.8
19	Carb. Lst.	C/D	-0.9	-3.7

Table A.2.3 Stable Isotopic Results, Travertine Deposits. Samples taken from Dinas Powys are labelled ( DP ). The flowstones marked A to D represent successive bands within one sheet, sampled on a millimetric scale. The dolomitic flowstones are interlaminated on a fine scale and not the result of dolomitisation of the Limestone Unit by waters from the overlying mudstones.

Sample No.	Description	Mineralogy	$\delta^{18}O$	$\delta^{13}C$
1	fissure fill	C	-3.6	-6.4
2	fissure fill	C	-3.5	-7.8
3	fissure fill	D/C	-1.9	-4.8
4	flowstone	C	-5.6	-2.3
5	flowstone	C	-4.9	-2.4
6	flowstone	D	-2.9	-3.0
7	flowstone A	C	-5.2	-2.1
8	flowstone B	C	-5.9	-3.8
9	flowstone C	C	-5.6	-2.4
10	flowstone A (DP)	C	-4.4	-3.4
11	flowstone B (DP)	C	-3.3	-2.3
12	flowstone C (DP)	C	-3.6	-2.5
13	flowstone D (DP)	C	-3.6	-3.0
14	flowstone	C	-7.4	-6.2

Table A.2.3 ( cont. )

Sample No.	Description	Mineralogy	$\delta^{13}C$	$\delta^{18}O$
15	micrite, in 14	C	-8.0	-6.5
16	spar A, cavity	C	-7.5	-4.6
17	spar B, cavity	C	-7.7	-5.4
18	sediment, cavity	C	-5.5	-5.3
19	pisolith (DP)	C	-2.2	-2.1
20	sediment, in 19	C	-3.7	-3.1
21	floe calcite	C	-5.0	-5.2
22	floe calcite	C	-3.8	-3.5
23	micrite	C	-6.1	-7.2
24	cement in 23	C	-6.5	-4.9
25	cement	C	-3.9	-2.2
26	cement	C	-2.9	-3.1
27	late spar	C	-6.4	-4.9

The stable isotopic results for the three studies of the Mercia Mudstone Group are given in vertical sections. The heights are the distance above or below the base of the Blue Anchor Formation, in metres, which is used as a datum in all of the measurements of the Mercia Mudstone Group used in this study.

Table A.2.4 Stable Isotopic Results, Mercia Mudstone Group, Devon.

Sample No.	Height	Description	Mineralogy	$\delta^{13}C$	$\delta^{18}O$
1	+8.0	green mud	D	+1.4	+1.5
2	+2.0	green mud	D	+1.0	+1.6
3	-1.0	red mud	D	+1.8	+1.2
4	-4.0	red mud	D/C	+1.6	-0.0
5	-9.0	red mud	C/D	+0.3	-3.0
6	-16.0	red mud	C	+1.3	-2.7
7	-21.0	red mud	C/D	+0.6	-2.9
8	-25.0	red mud	C/D	+0.2	-3.1
9	-27.0	red mud	D	+0.8	-3.6
10	-33.0	red mud	C/D	+0.5	-0.1
11	-37.0	red mud	C/D	+1.2	-2.1
12	-41.0	red mud	C/D	+0.9	-2.7
13	-55.0	red mud	C	-1.4	-3.8
14	-65.0	red mud	C/D	-2.4	-3.8
15	-75.0	red mud	D/C	-1.9	-3.4
16	-100.0	Devon 2	C/D	-0.1	+0.1
17	-120.0	Devon 3	D	-2.3	+2.1

Table A.2.5 Stable Isotopic Results, Mercia Mudstone Group, Somerset. The final three results given in this table were taken from one of the calcrete cycles in the cliffs at Watchet, not the section at St. Audrie's Bay.

Sample No.	Height	Description	Mineralogy	$\delta^{13}C$	$\delta^{18}O$
1	+34.3	green mud	D	-4.9	-0.5
2	+11.7	green mud	D	-1.1	-2.1
3	+4.7	green mud	D	+2.2	+1.2
4	+3.0	green mud	D	+1.5	+1.1
5	-0.1	red mud	D	+2.1	+1.4
6	-9.0	red mud	D	+1.4	-1.7
7	-10.5	green mud	D/C	+1.2	-0.8
8	-18.7	red mud	C/D	+1.2	-3.1
9	-21.0	green carb.	C/D	+1.1	-4.0
10	-21.5	red mud	C/D	+1.3	-2.8
11	-24.0	green carb.	C/D	+1.8	-4.8
12	-28.2	red mud	C	+0.9	-3.7
13	-30.8	green mud	C/D	-0.9	-5.1
14	-41.0	red mud	C	+1.9	-3.4

Table A.2.5 ( cont. )

Sample No.	Height	Description	Mineralogy	$\delta^{13}C$	$\delta^{18}O$
15	-53.0	red mud	C/D	+1.2	-2.8
16	-53.7	green mud	C/D	+1.7	-4.0
17	-61.0	red mud	D	+1.3	+1.2
18	-68.0	red mud	C	-3.8	-4.6
19	-86.7	red mud	C	-0.7	-1.5
20	-104.0	red mud	D	-0.5	-1.7
21	-115.0	red mud	D	+0.5	-1.0
22	-121.4	green mud	C/D	-0.3	-4.7
23	-123.0	red mud	D	+0.9	-0.9
24	-130.2	red mud	C/D	-0.3	-2.8
25	-138.4	red mud	D/C	+0.4	-1.6
26	PED 1	nodule	D	-0.1	-2.1
27	PED 2	red marl	D	-0.1	-0.6
28	PED 3	marl / sulphate	D	-1.8	-4.7

Table A.2.6 Stable Isotopic Results, South Wales.

Sample No.	Height	Description	Mineralogy	$\delta^{13}C$	$\delta^{18}O$
1	+14.6	green mud	D/C	+1.1	+1.6
2	+10.9	green mud	D	-1.1	-0.1
3	+4.8	red mud	D	-0.5	-0.0
4	-0.2	green mud	D	+0.9	+0.7
5	-2.4	red mud	D	+0.9	+0.6
6	-4.1	red mud	D	+0.8	+0.3
7	-7.3	green mud	D	+1.9	+0.5
8	-10.4	red mud	D	+1.2	+0.6
9	-12.2	red mud	D	+1.0	+0.6
10	-14.2	red mud	D	+1.6	+0.7

## Appendix 3

### Clay Mineralogy Analyses Techniques

#### A.3.1 Sample Preparation

X-ray diffraction analyses of mudstone samples were carried out in order to identify the clay mineral species present and to provide a semi-quantitative estimate of the proportions of the different clay types.

Roughly 100 grams of calcareous mudstone were crushed to pass through a  $61\mu\text{m}$  mesh. 25 grams of this powder was then placed in a beaker containing 400 millilitres of distilled water and stirred vigorously. The beaker was then placed in an ultrasonic bath at  $20^{\circ}\text{C}$ . After one hour the beaker was removed and the sample stirred and left for six hours, after which the topmost 200 millilitres containing the under  $2\mu\text{m}$  fraction ( Gipson, 1966 ) was removed. From this fraction two 50 millilitre samples were taken and placed in containers in which a glass slide had been placed. Three grams of flocculent (  $\text{CaCl}$  ) were then added to the containers which were shaken and immediately placed in a centrifuge which was spun at 3000 rpm. for 15 minutes. After this the clear liquid was carefully pipetted off and the glass slide coated in the under  $2\mu\text{m}$  fraction was removed and allowed to dry slowly. Two such slides were prepared for most of the samples.

Some discussion has taken place as to the validity of any preparation technique which involves the settling of clays through a water column. Gibbs ( 1965 ) and Towe ( 1974 ) have both stated that smectites, which form much smaller particles than either illite or chlorite, will have a slower settling velocity and will therefore be concentrated on the topmost surface of the slide. By contrast Spoljaric ( 1971 ) using SEM techniques showed that the top layer of a settled clay sample did not preferentially contain one particular clay species. In his experiments Spoljaric used centrifuge speeds of 2100 rpm. and did not use any flocculent. With the addition of the flocculent recommended by Taylor ( 1982 ) it was found that the entire clay fraction settled in 30 minutes if the sample was left to stand. This suggests that there will have been no chance for the individual

clay species to have settled at different speeds. To ensure that no differential settling took place and that the clay particles were parallel to the plane of the glass slide the centrifuge was used. Taylor ( 1982 ) used smear mounts of the settled clays in his XRD analyses. In this study it was found that the settled mounts gave a far better peak to background ratio. Since there was no evidence for the differential settling of the clays in the settled mounts, these were used in the XRD analyses.

### A.3.2 Clay Mineral Analyses

Analyses were carried out on a Phillips PW 1130 generator / diffractometer assembly using iron filtered Co K $\alpha$  radiation. Operating conditions were as follows ( unless otherwise stated ): 40 kV, 20 mA; range  $4 \times 10^4 - 4 \times 10^2$  counts per second; divergence and receiving slits  $0.5^\circ$ , scatter slit  $1^\circ$ ; scan speed  $1^\circ 2\theta \text{min}^{-1}$  and chart speed 10 millimetres per minute. Preliminary scans of selected samples were run over a range of  $2-70^\circ 2\theta$  to identify bulk mineralogy.

The orientated clay mounts were then analysed before and after various treatments.

- 1) Air-dried.
- 2) After 4 hours in an ethylene glycol saturated atmosphere at  $60^\circ\text{C}$ .
- 3) After 2 hours in a furnace heated to  $550^\circ\text{C}$ .

After each treatment the clay mounts were analysed over a range of  $3-17^\circ 2\theta$  and the various peaks were identified and their peak areas measured ( Biscaye, 1965 ). Where two clay mounts were made both were analysed in the air-dried condition and one was further treated by glycolation and heating. 10% of the samples were rerun in order to ensure reproducibility of results.

### A.3.3 Scanning Electron Microscopic Studies

Scanning electron microscopy was carried out in the Department of Engineering, University of Durham using a Stereoscan 600 instrument with a magnification range of 20 to 5000 and a working distance of 15 -30 millimetres. Scanning electron microscope ( SEM ) studies were carried out with two main objectives:

- 1) To study in detail the structure of the cements and flowstones within the limestones in South Wales in order to identify any evidence of replacement textures.
- 2) To identify if possible the clay components within the mudstones of the Mercia Mudstone Group and to make an estimate of the relative crystallinities of the various clay types.

The methods of preparation of the limestone and mudstone samples is quite different ( Trewin, 1988 ). In the case of the limestone a plug of finely polished sample 5 millimetres in diameter and between 2 and 8 millimetres in thickness was etched in 0.5% formic acid for one minute. The sample was then attached to the SEM stub using a paste of colloidal silver in amyl acetate ( Fig. A.3.1a ) and then coated with a thin ( 200Å ) layer of gold.

In the case of samples of mudstone a fractured surface of the appropriate size was prepared and attached to the SEM stub in a similar fashion to that for the carbonate samples ( Fig A.3.1b ). No etching was employed in the preparation of the mudstone samples.

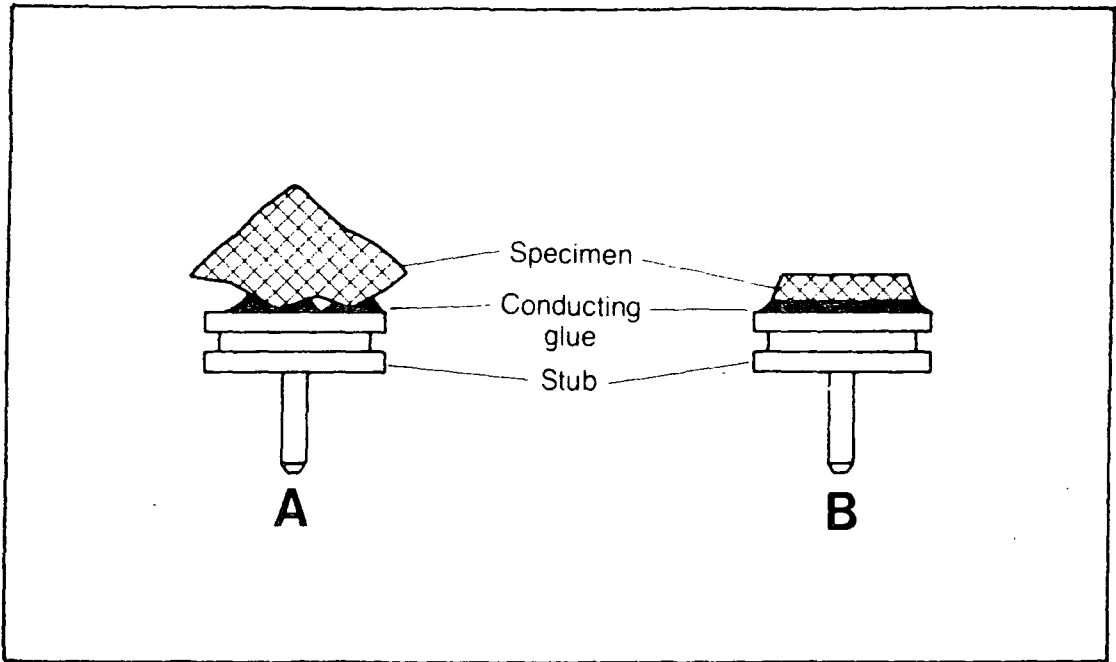


**Fig. A.3.1** Mounting of samples for SEM examination. A - fractured sample of mudstone. B - polished and etched face of carbonate. ( after Trewin, 1988 ).

## Appendix 4

### Outcrop Gamma-ray Correlation

#### A.4.1 Instrumentation

The instrument used was a geometrics G410A Spectrometer with a GPX 21 NaI ( Tl ) detector which was carried in an adapted frame rucksac ( Fig. A.4.1 ). The principles of gamma-ray spectrometry and the counting statistics used are given in Chapters 2 and 3 of Myers ( 1987 ). A brief outline is given here along with information on the data reduction and instrument calibration.

The spectrometer counts gamma-rays of particular wavelength and processes them so as to display four readings, each of which corresponds to the intensity of gamma-rays of one particular wavelength, for every count period ( Fig. A.4.2 ). During operation an internal reference source (  $^{133}\text{Ba}$  ) is used to monitor drifts in the sensitivity of the detector. The four channels in the spectrometer used give a total gamma-ray count and individual readings for the elements potassium, uranium and thorium. The total count readings, minus background, can be directly compared with borehole data in terms of the relative variations in gamma-ray value.

Details of selection of sample sites and the necessary outcrop geometry are given in Chapter 10 . To ensure that the sensitivity of the detector crystal had not decayed since the last regular use of the machine ( Cassidy, 1979 ), a number of outcrops of granite used as control stations by Cassidy were measured. The outcrops used by Cassidy were those with good surface geometry and had been calibrated using XRF and neutron activation analyses. Two of the stations in the Loch Doon Granite in the Southern Uplands were used and six measurements of two minutes duration were taken at each and the results reduced using Cassidy's equations. The results are shown in Tables A.4.1 and A.4.2. The elemental data are given in parts per million ( U and Th ) and % ( K ).



**Fig. A.4.1** Portable gamma-ray spectrometer. The detector to the left is sitting on a sub-horizontal surface of red mudstones with poor planar geometry relative to the faces used in the cliff sections. Length of detector 50 centimetres.

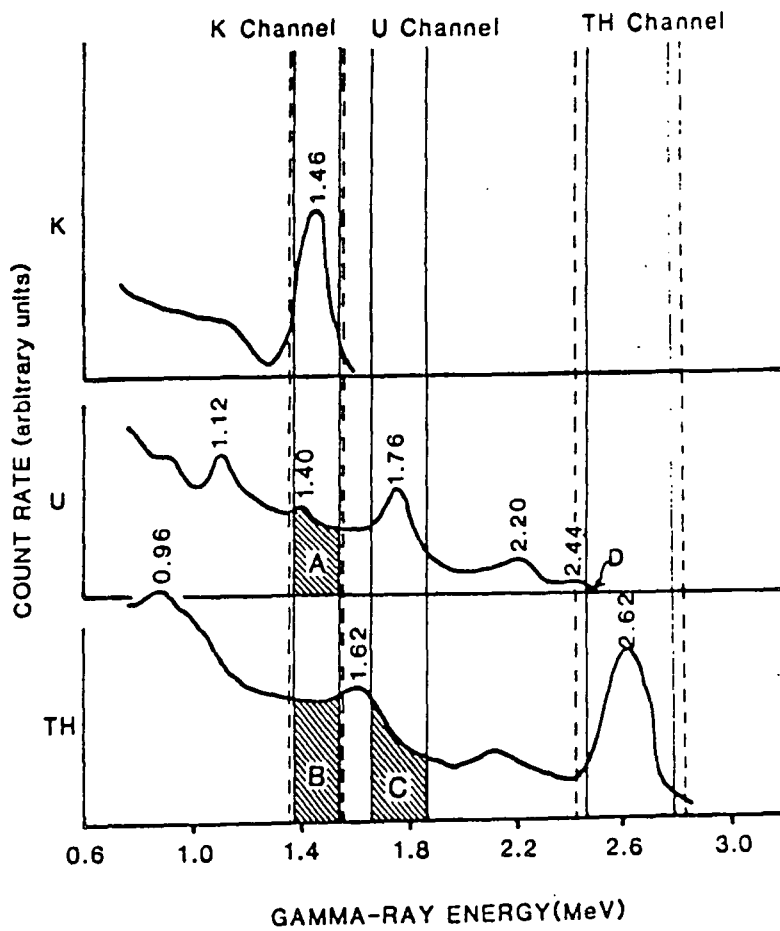


**Fig. A.4.2** Gamma-ray spectra of K, U and Th showing the energy windows used in the GR410 Spectrometer.

Table A.4.1 Station Grid. Ref. NX445786

	K	U	Th
Cassidy ( 1979 )	3.49	4.22	15.06
This study	2.83	5.45	13.81

Table A.4.2 Station Grid. Ref. NX547753

	K	U	Th
Cassidy ( 1979 )	5.05	7.63	30.47
This study	4.22	7.68	29.03

From this it was decided that the uranium and thorium channels were stable within acceptable limits and needed no adjustment. The sensitivity of the potassium channel had decayed through time and needed to be corrected before field work could take place. This was in agreement with work carried out at the Open University in 1988 ( G. Brown, pers comm. ). The equations used in the reduction of the raw data, given in Section A.4.2, were adjusted accordingly. Other than the adjustment of the K channel, the equations used are taken directly from Cassidy ( 1979 ).

#### A.4.2 Reduction of Gamma-Ray Data

The elemental counts given by the gamma-ray spectrometer in the field must be reduced to give % K<sub>2</sub>O and ppm U and Th information. The following equations were used:

$$ppmTh = \frac{C_{Th} - B_{Th}}{15.9} \quad A.4.1$$

$$ppmU = \frac{C_U - B_U - 0.63C_{Th}}{31.5} \quad A.4.2$$

$$\%K_2O = \frac{C_K - B_K - 0.71C_U - 0.13C_{Th}}{300} \quad A.4.3$$

Where  $C_x$  is the number of counts per two minutes in the Th, U and K channels; and  $B_x$  is the background count for similar time in each channel. The denominator in equation A.4.3 ( 300 ) is the adjusted value which in Cassidy's study was quoted as 361. The adjustment was made on the basis of the variations in the values for the two control stations in the Loch Doon Granite measured as part of this study.

Background counts were extrapolated from the field data and had the following values:

$$B_{Th} = 0 \qquad B_U = 40 \qquad B_K = -14$$

This is comparable with the background counts given in Cassidy ( 1979 ). Once the background values were established, the raw data were reduced using an adaptation of a programme written in BASIC and included in Myers ( 1987 ). This was adapted for a Texas Instruments TI-66 calculator and provided % K<sub>2</sub>O and ppm U and Th .

### A.4.3 Calibration of Field Data

#### A.4.3.1 Introduction

As well as initial calibration of the spectrometer using established field stations set up previously by other workers, control stations were used as part of this study to ensure that the spectrometric values obtained could be directly related to elemental values in the rock. Nine control stations were established, three in each field area. For each, care was taken to ensure good outcrop geometry and an unweathered face. At each station, six or more readings were taken and the following results found:-

Table A.4.3 Elemental values at the control stations.

Station	%K <sub>2</sub> O	U <sub>ppm</sub>	Th <sub>ppm</sub>
Wales 1	1.33	4.48	4.52
Wales 2	1.68	6.27	6.93
Wales 3	2.07	6.81	8.39
Somerset 1	1.71	4.63	5.53
Somerset 2	1.80	5.67	7.77
Somerset 3	2.26	5.74	7.82
Devon 1	1.79	3.35	5.40
Devon 2	1.92	4.41	11.60
Devon 3	2.35	2.53	8.97

Since readings in each area were taken over a period of several days, long term drift of the sensitivity of the detector could not be assessed. The internal <sup>133</sup>Ba calibration of the instrument required little readjustment during the three week period that the machine was being used, and repeat readings taken at the beginning and end of one day did not suggest that there was significant drift over short periods of time. The readings taken at outcrop and the reduced data are presented in Tables A.4.5 to A.4.12 .

After readings had been taken at the nine control stations, between 1 and 2 kilograms of sample were collected, roughly following the geometry of the effective sample of the detector ( Fig. 9.1 ). This whole rock sample was then crushed to pass through a 61 $\mu$ m mesh and analysed as follows by neutron activation and x-ray fluorescence methods.

#### A.4.3.2 Neutron Activation Analyses

Absolute values of U and Th were determined by neutron activation ( NA ) analysis at the University of London Reactor Centre at Sellwood Park. Analytical procedures were the same as those in Leat et al. ( in press ). 0.2 of a gram of

each control sample, including one duplicate, were irradiated in one batch for 5 consecutive days, interspersed with 3 standard samples of known composition to correct for variations in neutron flux. Gamma-ray photons were collected by a EG+G ORTEC low energy photon detector. Gamma-rays were collected in the range 50 to 900KeV and processed as 4096 channel spectra. Two separate counts of the elemental concentrations were made, 5 and then 8 days after irradiation for 90 minutes per sample. The results of the two counts are given in Table A.4.4 . In both elements the subscripts A and B refer to the first and second counts respectively.

Table A.4.4 Neutron Activation Results

Station	U <sub>A</sub>	U <sub>B</sub>	Th <sub>A</sub>	Th <sub>B</sub>
Wales 1	1.88	2.61	6.67	5.94
Wales 2	2.30	3.15	10.81	9.55
Wales 3	2.96	2.08	15.68	12.28
Somerset 1	5.66	5.16	6.96	6.74
Somerset 2	3.44	2.95	11.34	10.00
Somerset 3	2.75	1.62	10.76	9.32
Devon 1	2.77	1.91	3.00	2.91
Devon 2	2.40	2.74	14.73	13.32
Devon 3	2.08	1.46	8.14	7.99

The results of the NA analyses and comparison with the gamma-ray and XRF techniques are discussed in Chapter 9 .

#### A.4.3.3 X-Ray Fluorescence Analyses

In order to calibrate potassium as well as the uranium and thorium values, x-ray fluorescence ( XRF ) was used. The 9 control samples were made into pressed pellets according to the method described in Fairchild et al. ( 1988 ).

The XRF analyses were carried out using a Phillips PW1400 X-ray spectrometer.

Operating conditions for major and trace elements are given in Pearce ( 1988, appendix 3 ). Major element data were processed using the computer programme XRF CBI written by Dave Stevenson and Colin Watson of Durham University. Trace element analyses were processed using the programme K-FACTOR modified from the Greenland Geological Union programme ( Bailey, 1976 ). Sedimentary carbonate, shale and soil NBS standards were used in calibration to have as near as possible equivalent standard / sample types.

The results of the XRF analyses for K, U and Th are given in Table 9.1 , along with a discussion of results. The heights given refer to the distance in metres above or below the base of the Blue Anchor Formation which is used as a datum in the study. In all cases the control station samples are composed of green mudstone ( Station 1 ) and red mudstone ( Stations 2 and 3 ).

Table A.4.9 Gamma-ray Raw Count Data, Penarth Cliffs, South Wales.

Height	Description	Total	K raw	U raw	Th raw
+15.5	red mud	1520	964	294	141
+14.5	grey mud	821	414	177	81
+13.5	green mud	1281	777	302	95
+12.5	green mud	1005	632	226	72
+9.5	green mud	1150	708	227	119
+8.5	green mud	1123	666	199	78
+6.5	greem mud	1203	689	257	109
+6.0	green mud	984	545	228	85
+5.0	green mud	1127	612	242	105
+3.0	green mud	1126	675	213	87
+2.0	Wales 1	1072	567	243	78
0.0	green mud	1169	722	228	100

Table A.4.9 ( cont. )

Height	Description	Total	K raw	U raw	Th raw
-0.8	red mud	1322	933	302	144
-1.8	red mud	1229	935	273	138
-2.8	red mud	1407	976	313	133
-4.1	red mud	1348	893	296	176
-5.1	red mud	1484	888	312	139
-5.9	Wales 2	1311	726	312	118
-7.0	red mud	1038	492	233	92
-8.0	red mud	1513	867	332	128
-10.0	red mud	1647	999	385	142
-14.0	red mud	1414	860	313	112
-16.7	Wales 3	1598	869	344	142
-20.4	red mud	1563	898	358	155
-22.4	red mud	1326	778	271	142
-30.0	red mud	1204	1021	249	152

Table A.4.6 Gamma-ray Raw Count Data, St. Audrie's Bay, Somerset.

Height	Description	Total	K raw	U raw	Th raw
+37.0	green shale	1609	930	356	156
+35.3	green dolom	1160	602	259	107
+34.3	green mud	1087	620	212	86
+32.8	green dolom	1114	686	207	114
+31.8	green mud	1037	603	252	78
+14.8	green mud	1263	728	318	105
+13.4	green mud	1701	982	465	126
+12.4	green mud	1839	1075	524	135
+11.6	green mud	1507	884	399	126
+10.7	green mud	1193	647	294	116
+9.5	green mud	1255	631	296	105
+8.8	green mud	1184	551	297	76
+7.9	green mud	1133	540	291	72
+7.5	green mud	1101	540	260	82
+6.7	green mud	1299	666	302	74
+4.6	green mud	1327	672	338	94
+3.6	green mud	1519	813	304	89
+1.5	red mud	1144	571	255	103
+1.1	green mud	1339	755	313	119
+0.1	green mud	1320	860	284	111

Table A.4.6 ( cont. )

Height	Description	Total	K raw	U raw	Th raw
-1.0	green mud	1278	873	266	145
-1.6	red mud	1284	795	282	145
-2.2	red mud	1392	863	324	129
-4.0	green mud	1325	761	283	126
-5.6	red mud	1134	600	231	113
-7.6	red mud	1184	696	299	107
-9.8	red mud	1409	820	303	129
-12.0	red mud	1135	600	232	114
-13.5	green mud	1275	740	266	110
-14.9	green mud	1363	740	281	99
-17.5	green mud	1345	1016	272	140
-17.8	red mud	1286	874	263	137
-18.8	red mud	1337	862	292	163
-21.2	green mud	1287	747	308	123
-22.7	red mud	1388	788	314	150
-24.1	green mud	1158	704	228	121
-25.2	green mud	1103	717	277	122
-26.6	red mud	1198	774	235	118

Table A.4.6 ( cont. )

Height	Description	Total	K raw	U raw	Th raw
-27.8	red mud	1271	791	266	133
-29.5	green mud	1272	787	300	126
-31.2	red mud	1284	813	283	150
-33.2	green mud	1351	930	296	151
-34.3	red mud	1349	1037	307	162
-35.6	red mud	1323	942	301	166
-37.6	red mud	1469	973	326	149
-40.9	red mud	1422	868	302	163
-42.8	green mud	1365	915	293	154
-44.6	red mud	1422	959	323	159
-48.4	red mud	1356	847	315	161
-50.4	red mud	1551	947	342	194
-53.6	red mud	1280	754	273	149
-54.8	red mud	1326	812	317	141
-57.9	green mud	1470	938	338	158

Table A.4.6 ( cont. )

Height	Description	Total	K raw	U raw	Th raw
-60.3	red mud	1386	840	323	145
-63.0	red mud	1474	920	297	153
-66.0	red mud	1476	916	324	174
-76.0	red mud	1485	889	343	142
-78.0	red mud	1211	693	238	130
-81.0	red mud	1127	575	271	103
-83.7	red mud	949	472	237	93
-85.0	red mud	1097	654	215	122
-88.0	red mud	1275	770	272	115
-94.0	red mud	1357	774	266	141
-99.0	red mud	1234	838	281	138
-101.0	Somerset 1	1371	898	304	132
-105.0	red mud	1335	1042	242	161
-109.0	green mud	1245	961	237	149
-113.0	red mud	1018	688	190	119

Table A.4.6 ( cont. )

Height	Description	Total	K raw	U raw	Th raw
-123.0	red mud	1188	889	305	170
-124.0	red mud	1149	733	258	147
-131.0	red mud	1383	1006	280	202
-135.0	red mud	1186	755	260	127
-137.0	red mud	1386	830	305	156
-138.4	red mud	1176	671	277	145
-139.4	red mud	1307	775	273	167
-141.4	green mud	1279	764	306	139
-143.4	red mud	1235	708	271	127
-146.2	red mud	1316	817	280	139
-150.4	red mud	1155	712	251	101
-152.4	red mud	1219	794	228	133
-156.4	red mud	1190	645	279	115

Table A.4.7 Gamma-ray Raw Count Data, Calcrete Profiles, West Watchet, Somerset.

Sample No.	Description	Total	K raw	U raw	Th raw
1	mudst some gyp	1503	892	346	136
2	gyp anticlines	1156	652	245	126
3	mudst	1217	681	271	135
4	nodular calcrete	1225	567	260	140
5	gyp anticlines	1245	712	263	132
6	mudst	1248	730	286	114
7	nodular gyp	1315	804	305	135

Table A.4.8 Gamma-ray Raw Count Data, Control Stations, East Watchet, Somerset.

Station No.	Total	K raw	U raw	Th raw
Somerset 1	1138	686	245	94
Somerset 2	1360	757	301	131

Table A.4.5 Gamma-ray Raw Count Data, Seaton and Brang combe Cliffs, Devon.

Height	Description	Total	K raw	U raw	Th raw
+12.0	Devon 1	1028	679	203	91
+10.0	green mud	702	380	155	53
+8.0	green mud	970	503	228	87
+6.0	green mud	966	451	241	80
+4.0	green mud	1139	560	241	84
+2.0	green mud	935	505	187	96
-1.3	red mud	1098	759	230	93
-4.8	red mud	1123	842	213	123
-6.4	red mud	1112	737	237	107
-8.4	red mud	1161	800	240	137
-10.0	red mud	1125	803	242	135
-12.0	red mud	1087	689	198	110
-14.0	red mud	1179	762	247	120
-16.0	red mud	1386	828	316	131
-18.0	red mud	1373	831	282	157
-21.5	red mud	1185	712	261	129
-31.0	red mud	1244	875	252	132
-33.0	red mud	1174	732	243	120

Table A.4.5 ( cont. )

Height	Description	Total	Kraw	U raw	Th raw
-35.0	red mud	1322	839	295	148
-37.0	red mud	1312	963	247	157
-40.0	red mud	1357	1028	266	173
-63.0	red mud	1172	625	272	175
-65.0	red mud	1144	640	228	176
-73.0	red mud	1048	519	214	165
-75.0	red mud	1182	671	248	163
-77.0	red mud	1379	853	245	181
-79.0	red mud	1385	805	299	181
-84.0	red mud	1488	876	300	192
-120.0	Devon 2	1089	862	213	148
-125.0	Devon 3	1081	780	228	134
-140.0	gyp mud	521	317	101	45

The reduced data are presented in %K and ppm U and Th as calculated by the programme adapted from Myers ( 1987 ). The data points are listed in the same order as those for the raw data and therefore the descriptions of the lithologies are not included in these tables. Heights are in metres above or below the base of the Blue Anchor Formation.

Table A.4.10 Gamma-ray Corrected Values, Seaton and Branscombe Cliffs, Devon.

Height	% K	U <sub>ppm</sub>	Th <sub>ppm</sub>
+12.0	1.79	3.35	5.40
+10.0	0.92	2.59	3.09
+8.0	1.14	4.23	5.11
+6.0	0.94	4.78	4.65
+4.0	1.31	4.70	4.90
+2.0	1.25	2.75	5.74
-1.3	1.99	4.17	5.49
-4.8	2.30	3.03	7.40
-6.4	1.90	4.11	6.36
-8.4	2.09	3.61	8.24
-10.0	2.09	3.61	8.24
-12.0	1.83	3.71	6.61
-14.0	1.95	4.17	7.16
-16.0	2.00	6.14	7.74
-18.0	2.08	4.54	9.43
-21.5	1.75	4.44	7.70
-31.0	2.31	4.09	7.91
-33.0	1.86	4.04	7.17

Table A.4.10 ( cont. )

Height	% K	$U_{ppm}$	$Th_{ppm}$
-35.0	2.08	5.14	8.84
-37.0	2.60	3.43	9.49
-40.0	2.77	3.71	10.46
-63.0	1.65	3.87	10.58
-65.0	1.89	2.45	10.71
-73.0	2.01	2.22	10.04
-75.0	1.66	3.34	9.86
-77.0	2.25	2.89	11.00
-79.0	1.59	4.60	10.91
-84.0	1.92	4.41	11.60
-100.0	2.35	2.53	8.97
-120.0	2.05	3.29	8.07
-140.0	0.78	1.03	2.35

Table A.4.11 Gamma-ray Corrected Data, St. Audrie's Bay, Somerset.

Height	% K	U <sub>ppm</sub>	Th <sub>ppm</sub>
+37.0	2.24	6.91	9.25
+35.3	1.39	4.81	6.32
+34.3	1.57	3.74	5.08
+32.8	1.79	3.02	6.84
+31.8	1.42	5.17	4.51
+14.8	1.68	6.73	6.10
+13.4	2.16	10.97	7.19
+12.4	2.33	12.67	7.67
+11.6	1.99	8.88	7.30
+10.7	1.46	5.74	6.83
+9.5	1.40	6.03	6.14
+8.7	1.15	6.64	4.31
+7.9	1.13	6.53	4.07
+7.5	1.20	5.34	4.75
+6.6	1.52	6.84	1.18
+4.6	1.45	7.58	5.38
+3.5	2.00	6.60	5.12
+1.5	1.30	4.77	6.07
+1.1	1.77	6.29	6.99
+0.1	2.19	5.53	6.53

Table A.4.11 ( cont. )

Height	% K	$U_{ppm}$	$Th_{ppm}$
-1.0	2.26	4.27	8.70
-1.6	1.99	5.70	5.78
-2.2	2.10	6.44	7.60
-4.0	1.86	5.19	7.48
-5.6	1.45	3.80	6.74
-7.6	1.61	6.08	6.26
-9.8	2.01	5.77	7.64
-12.0	1.45	3.82	6.81
-13.5	1.84	4.97	6.50
-14.9	1.81	5.67	5.78
-17.5	2.73	4.57	8.38
-17.8	2.28	4.34	8.20
-18.8	2.16	4.74	9.79
-21.2	1.75	6.05	7.25
-22.7	1.87	5.70	8.94
-24.1	1.80	3.55	7.25
-25.2	1.73	5.08	7.23
-26.5	2.05	3.83	7.05

Table A.4.11 ( cont. )

Height	% K	$U_{ppm}$	$Th_{ppm}$
-26.5	2.05	3.83	7.05
-27.7	2.00	4.51	7.95
-29.5	1.91	5.73	7.45
-31.2	2.02	4.71	8.99
-33.2	2.38	5.11	9.03
-34.3	2.71	5.24	9.71
-35.6	2.40	4.97	9.97
-37.6	2.45	6.10	8.86
-40.9	2.15	5.06	9.78
-42.8	2.34	4.95	9.22
-44.6	2.41	5.80	9.49
-46.6	1.98	6.89	8.14
-48.4	2.05	5.51	9.63
-50.4	2.31	5.71	11.66
-53.6	1.85	4.42	8.94
-54.8	1.94	5.97	8.37
-57.9	2.30	6.30	9.41

Table A.4.11 ( cont. )

Height	% K	$U_{ppm}$	$Th_{ppm}$
-60.3	2.02	6.08	8.61
-63.0	2.34	5.10	9.16
-66.0	2.26	5.54	10.43
-76.0	2.14	6.78	8.39
-78.0	1.74	3.69	7.80
-81.0	1.28	5.27	6.05
-83.7	1.02	4.39	5.48
-85.0	1.66	3.12	7.33
-88.0	1.92	5.07	6.81
-94.0	1.94	4.35	8.45
-99.0	2.12	4.89	8.24
-101.0	2.26	5.74	7.82
-105.0	2.88	3.19	9.75
-109.0	2.62	3.27	9.00
-113.0	1.84	2.38	7.19

Table A.4.11 ( cont. )

Height	% K	$U_{ppm}$	$Th_{ppm}$
-123.0	2.21	5.01	10.21
-124.0	1.82	3.98	8.84
-131.0	2.65	3.58	12.26
-135.0	1.89	4.44	7.58
-137.0	2.02	5.29	9.33
-138.4	1.56	4.62	8.68
-139.4	1.91	4.06	10.07
-143.4	1.81	5.66	8.26
-146.2	2.05	4.84	8.30
-150.2	1.78	4.68	5.96
-152.2	2.10	3.31	8.01
-156.2	1.49	5.29	6.79

Table A.4.12 Gamma-ray Corrected Values, Calcrete Profiles, West Watchet, Somerset.

Sample No.	% K	$U_{ppm}$	$Th_{ppm}$
1	2.14	6.99	8.01
2	1.59	3.99	7.54
3	1.62	4.63	8.06
4	1.26	4.18	8.40
5	1.74	4.44	7.89
6	1.75	5.53	6.72
7	1.95	5.71	8.01

Table A.4.13 Gamma-ray Corrected Data, Control Stations, East Watchet, Somerset.

Sample No.	% K	$U_{ppm}$	$Th_{ppm}$
Somerset 1	1.71	4.63	5.53
Somerset 2	1.80	5.67	7.77

Table A.4.14 Gamma-ray Corrected Values, Penarth Cliffs, South Wales.

Height	% K	U <sub>ppm</sub>	Th <sub>ppm</sub>
+15.5	2.50	5.24	8.41
+14.5	0.97	2.73	4.82
+13.5	1.88	6.42	5.50
+12.5	1.59	4.46	4.17
+9.5	1.82	3.56	7.13
+8.5	1.76	3.49	4.59
+6.5	1.69	4.71	6.45
+6.0	1.29	4.27	4.99
+5.0	1.47	4.31	6.22
+3.0	1.75	3.75	5.14
+2.0	1.33	4.88	4.52
+0.1	1.87	3.97	5.93

Table A.4.14 ( cont. )

Height	% K	$U_{ppm}$	$Th_{ppm}$
-0.8	2.38	5.44	8.58
-1.8	2.46	4.64	8.25
-2.8	2.50	6.00	7.87
-4.1	2.24	4.61	10.60
-5.1	1.67	5.85	8.25
-5.9	1.68	6.27	6.93
-7.0	1.10	4.29	5.42
-8.0	2.10	6.71	7.53
-10.0	2.40	8.11	8.33
-14.0	2.12	6.42	6.55
-16.7	2.07	6.81	8.39
-18.4	2.13	7.00	9.19
-20.4	2.37	5.74	9.31
-22.4	1.94	4.49	8.50
-30.0	2.79	3.59	9.17

## **Appendix 5**

### **Insoluble Residue and Dolomite Stoichiometry Methods**

#### **A.5.1 Insoluble Residue Methods**

Insoluble residue analyses were carried out in order to determine the weight % of the carbonate fraction within the mudstones of the Mercia Mudstone Group. The following methods were used.

Between 0.5 and 1.0 grams of oven dried mudstone powder was placed in a beaker and 75 millilitres of HCl were added. The beaker was then placed on a hot plate at 60°C in a fume-cupboard for 4 hours and stirred occasionally. After reaction was complete and the carbonate was fully digested the beaker was removed and the acid filtered off. The remaining non-soluble residue was collected on a pre-weighed filter paper and placed in an oven at 110°C for one hour. The dried paper and residue were then weighed and the weight of the non-soluble fraction calculated as a percentage of the whole rock weight. The insoluble residue values do not show any correlation with the other variables calculated in the Mercia Mudstone Group and have not been discussed in the study. For this reason the results are not presented in the appendix.

#### **A.5.2 Dolomite Stoichiometry and Ordering Calculations**

##### **A.5.2.1 Introduction**

X-ray diffraction analyses were carried out on dolomitic samples in order to find the molar % CaCO<sub>3</sub> within the dolomite and the ordering of cations in the crystal structure. The following methods were used.

##### **A.5.2.2 Dolomite Stoichiometry Calculations**

Powdered samples of dolomite containing an internal standard ( Cerium Oxide ) were analysed by XRD in order to find the % CaCO<sub>3</sub> in the dolomite structure.

A scan speed of  $0.25^{\circ}2\theta$  per minute was used. The dolomite peak used in the calculation of ordering is  $d_{104}$  and the distance between this peak and an adjacent cerium oxide peak is measured on the XRD chart ( Fig. A.5.1 ). The spacing between the two peaks reflects the difference in lattice spacing which in dolomite is dependent on the amount of  $\text{CaCO}_3$  in the structure ( Goldsmith & Graf, 1958 ). A stoichiometric dolomite with 50%  $\text{CaCO}_3$  in its structure will have a lattice spacing of  $2.886\text{\AA}$  while 55% of  $\text{CaCO}_3$  will alter the lattice spacing to  $2.901\text{\AA}$  . The substitution of iron into the dolomite structure can also affect lattice spacing but the dolomites analysed in this study contain under 1% Fe , which does not affect the calculation of %  $\text{CaCO}_3$  . Once this spacing is established the molar %  $\text{CaCO}_3$  can be calculated to within  $\pm 0.25\%$  .

### A.5.2.3 Ordering Ratios

The relative ordering of dolomite, or the extent of mixing of the cations ( Ca and Mg ) in the c-axis direction ( Goldsmith & Graf, 1958 ), is found by measuring the ratios of the 015 and 110 peak areas ( Fig. A.5.1 ). The 015 diffraction peak is the result of the segregation of Ca and Mg into separate sheets in the crystal and is thus a measure of the order of the structure relative to the 110 diffraction peak which is of constant intensity. The peak areas were calculated by multiplying peak height by peak width at half peak height.

In mudstone samples from the Mercia Mudstone Group the calculation of order in the dolomite was not possible because the ordering peaks used by Goldsmith & Graf were obscured by minor illite peaks. The illite could not be completely removed from the sample since it often occurs as a coating on the surfaces of coarse clastic grains. For this reason the ordering of the dolomite in the Mercia Mudstone Group could not be measured.

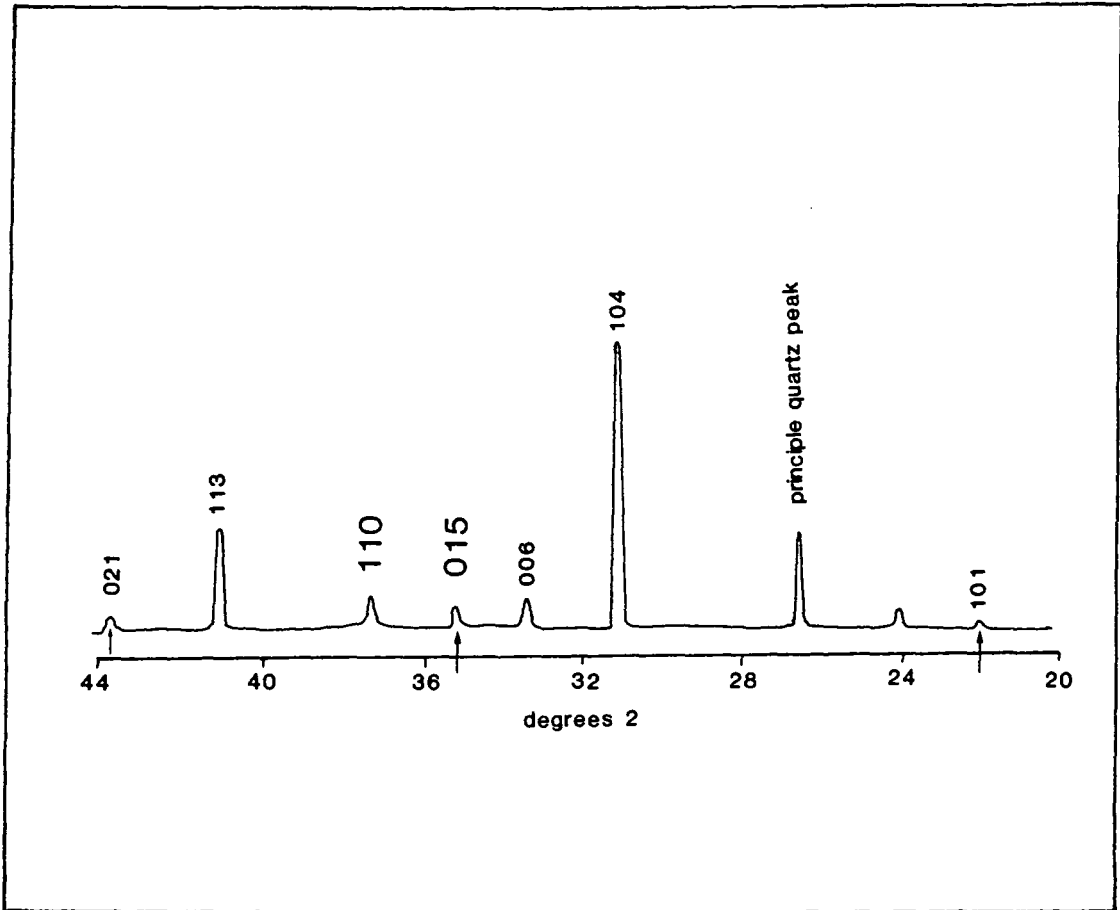


**Fig. A.5.1** The diffraction peaks of dolomite showing ordering reflections ( arrowed ). Peaks are identified in hexagonal indices. Cu  $K\alpha$  radiation. ( after Hardy & Tucker, 1988 ).

